AD-A041 891 CALSPAN CORP BUFFALO N Y F/G 17/7
MULTIPATH AND PERFORMANCE TESTS OF TRSB RECEIVERS.(U)
MAR 77 J BENEKE, C W WIGHTMAN, C B VALLONE DOT-FA74WA-3445
UNCLASSIFIED CALSPAN-AG-5580-E-1 FAA-RD-77-66 NL

1 OF 3
ADA041891

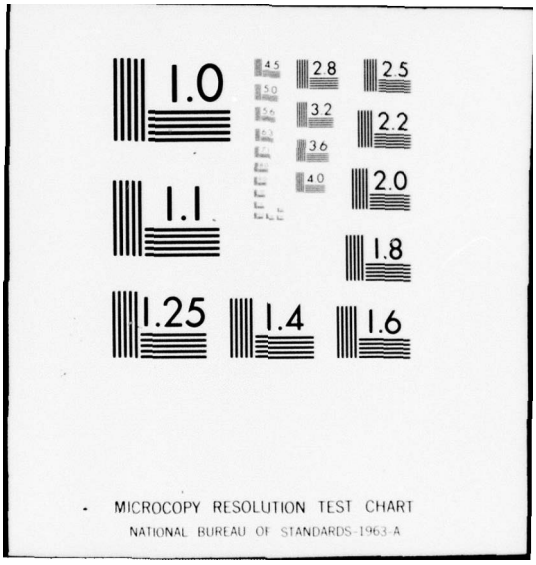
1.0
1.1
1.25
1.4
1.6
1.8
2.0
2.2
2.5
2.8
3.2
3.6
4.0
4.5
5.0
5.6
MICROCOPY RESOLUTION TEST CHART
NATIONAL BUREAU OF STANDARDS-1963-A

Report No. FAA-RD-77-66

(12)

MULTIPATH AND PERFORMANCE TESTS OF TRSB RECEIVERS

J. Beneke, C.W. Wightman, A.M. Offt
C. B. Vallone

Calspan Corporation
4455 Genesee Street
Buffalo, New York 14221

MARCH 1977
INTERIM REPORT

Prepared for

U.S. DEPARTMENT OF TRANSPORTATION
FEDERAL AVIATION ADMINISTRATION
Systems Research & Development Service
Washington, D.C. 20590

NOTICE

This document is disseminated under the sponsorship of the Department of Transportation in the interest of information exchange. The United States Government assumes no liability for its contents or use thereof.

TECHNICAL REPORT STANDARD TITLE PAGE

1. Report No.	2. Government Accession No.	3. Recipient's Catalog No.
FAA-RD-77-66		

4. Title and Subtitle	5. Report Date
MULTIPATH AND PERFORMANCE TESTS OF TRSB RECEIVERS	March 1977
	6. Performing Organization Code

7. Author(s)	8. Performing Organization Report No.
J. Beneke, C.W. Wightman, C.B. Vallone A.M. Offt	AG-5580-E-1

9. Performing Organization Name and Address	10. Work Unit No.
Calspan Corporation 4455 Genesee Street Buffalo, NY 14221	11. Contract or Grant No. DOT-FA 74 WA-3445
	13. Type of Report and Period Covered Interim Report 1974 to Mar 1977
12. Sponsoring Agency Name and Address Department of Transportation Federal Aviation Administration Systems Research & Development Service Washington, DC 20590	14. Sponsoring Agency Code ARD-722

15. Supplementary Notes

16. Abstract

A landing system simulation program has been carried out in support of the Microwave Landing System (MLS) program of the Federal Aviation Administration. Both scanning beam and doppler scan techniques were simulated and several angle processors were tested with each technique. This report contains the results of extensive simulation evaluations on the time reference scanning beam (TRSB) system. The results of the doppler simulation tests are published in the Calspan Technical notes referenced in this report.

A representative set of multipath parameters was selected and used to explore the dynamic characteristics of the TRSB technique. Tests were run to determine the multipath error magnitude as a function of separation angle, amplitude, scalloping frequency and different processor parameters. These tests were conducted on a TRSB simulator that uses a computer to control the multipath parameters for each scan. Typical multipath scenarios were programed that represented the signals an aircraft would receive when flying through a multipath interference region. Some of the multipath scenarios used in the ICAO AWOP evaluations were simulated.

The receivers used in the ICAO flight test program were evaluated in the simulator. A breadboard processor was developed that operates as a dwell gate processor, similar to the flight test receivers, or as a single edge processor (SEP) to evaluate the flare system.

A closed loop simulation, including aircraft and autopilot characteristics, MLS signals with dynamic multipath characteristics and the MLS processor, was used to determine the aircraft perturbations resulting from hangar multipath reflections. The effectiveness of MLS rate derived data in compensating for wind shear effects was demonstrated.

17. Key Words	18. Distribution Statement
Microwave Landing System (MLS) Time Reference Scanning Beam (TRSB) Multipath Scalloping Frequency Doppler Microwave Landing System (DMLS)	Document is available to the U.S. public through the National Technical Information Service, Springfield, Virginia 22161.

19. Security Classif. (of this report)	20. Security Classif. (of this page)	21. No. of Pages	22. Price
Unclassifed	Unclassified	~~204~~ 218	

Form DOT F 1700.7 (8-69)

407 727

METRIC CONVERSION FACTORS

Approximate Conversions to Metric Measures

Symbol	When You Know	Multiply by	To Find	Symbol
		LENGTH		
in	inches	*2.5	centimeters	cm
ft	feet	30	centimeters	cm
yd	yards	0.9	meters	m
mi	miles	1.6	kilometers	km
		AREA		
in^2	square inches	6.5	square centimeters	cm^2
ft^2	square feet	0.09	square meters	m^2
yd^2	square yards	0.8	square meters	m^2
mi^2	square miles	2.6	square kilometers	km^2
	acres	0.4	hectares	ha
		MASS (weight)		
oz	ounces	28	grams	g
lb	pounds	0.45	kilograms	kg
	short tons (2000 lb)	0.9	tonnes	t
		VOLUME		
tsp	teaspoons	5	milliliters	ml
Tbsp	tablespoons	15	milliliters	ml
fl oz	fluid ounces	30	milliliters	ml
c	cups	0.24	liters	l
pt	pints	0.47	liters	l
qt	quarts	0.95	liters	l
gal	gallons	3.8	liters	l
ft^3	cubic feet	0.03	cubic meters	m^3
yd^3	cubic yards	0.76	cubic meters	m^3
		TEMPERATURE (exact)		
°F	Fahrenheit temperature	5/9 (after subtracting 32)	Celsius temperature	°C

*1 in = 2.54 (exactly). For other exact conversions and more detailed tables, see NBS Misc. Publ. 286, Units of Weights and Measures, Price $2.25, SD Catalog No. C13.10:286.

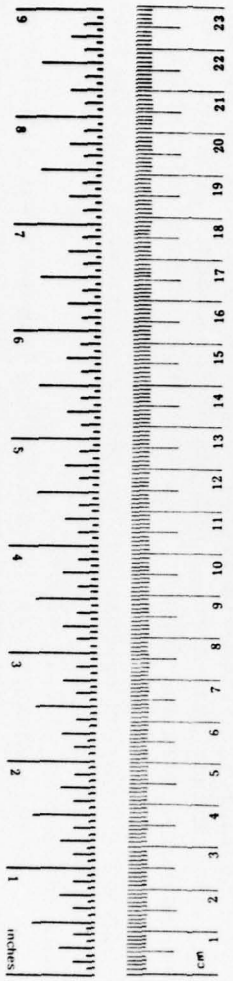

Approximate Conversions from Metric Measures

Symbol	When You Know	Multiply by	To Find	Symbol
		LENGTH		
mm	millimeters	0.04	inches	in
cm	centimeters	0.4	inches	in
m	meters	3.3	feet	ft
m	meters	1.1	yards	yd
km	kilometers	0.6	miles	mi
		AREA		
cm^2	square centimeters	0.16	square inches	in^2
m^2	square meters	1.2	square yards	yd^2
km^2	square kilometers	0.4	square miles	mi^2
ha	hectares (10,000 m^2)	2.5	acres	
		MASS (weight)		
g	grams	0.035	ounces	oz
kg	kilograms	2.2	pounds	lb
t	tonnes (1000 kg)	1.1	short tons	
		VOLUME		
ml	milliliters	0.03	fluid ounces	fl oz
l	liters	2.1	pints	pt
l	liters	1.06	quarts	qt
l	liters	0.26	gallons	gal
m^3	cubic meters	35	cubic feet	ft^3
m^3	cubic meters	1.3	cubic yards	yd^3
		TEMPERATURE (exact)		
°C	Celsius temperature	9/5 (then add 32)	Fahrenheit temperature	°F

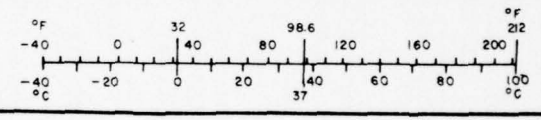

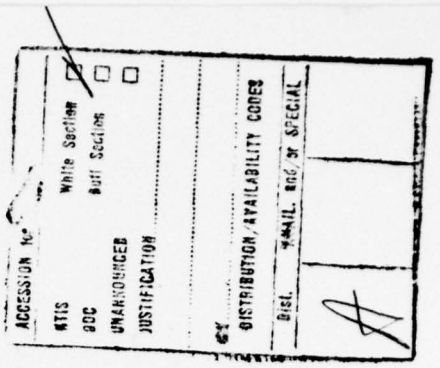

TABLE OF CONTENTS

TABLE OF CONTENTS (Cont.)

Section 1.0
INTRODUCTION

The material in this report is prepared in support of the Microwave Landing System (MLS) program for the Federal Aviation Administration. This report contains the results of simulator evaluations of the TRSB receivers.

Analyses and simulation evaluations were conducted on the scanning beam and doppler techniques in support of the selection process to determine the technique to be proposed by the U.S. as the common international MLS. After the selection of the time reference scanning beam (TRSB) system as the candidate system for submission to the International Civil Aviation Organization (ICAO) the analyses and simulations concentrated on the TRSB system.

The Calspan simulator was modified to represent the proposed TRSB signal format. Simulations were conducted to measure the performance characteristics of the TRSB system in a multipath environment. The flight test receivers were tested in the TRSB simulator. Performance data on the flight test receivers was used in the ICAO evaluations of the systems proposed for MLS. The hardware simulations provided measurements of the multipath errors, interference effects and low signal level capabilities of the TRSB system. Data developed in the simulator evaluations of the flight test receivers provided a measure of how well the Lincoln Laboratory computer model approximated the performance of the TRSB receivers.

1.1 Background Information

Twelve technical notes (References 1 through 12) have been prepared under this contract. The first two provided technical data and suggested specifications for the preliminary functional requirements document. Technical Note 3 presented comparative performance data of simulator tests on the multipath performance of the two proposed FM encoded scanning beam systems, the time reference scanning beam (TRSB) system and the two competing doppler systems. These simulator tests showed the TRSB and doppler system will have comparable multipath errors providing the grating lobe frequencies inherent in the doppler azimuth and elevation data systems are sufficiently high so that motion averaging is effective in reducing the errors from hangar reflections.

Calspan TN-4, TN-5 and TN-6 contain the results of simulator tests on the Phase 2 1/2 and Phase 3 receivers and the breadboard single edge processor. These tests included multipath errors, low signal level tests and the effects of propeller modulation. The tests provided a data base for the ICAO submissions.

Technical Notes 7 and 10 provided information on simulator evaluations of the doppler system. TN-7 includes data on tests run with the ITT Gilfillan processor at multipath levels near 0 dB and showed a significant increase in the errors for these high levels of multipath. The AGC design in this processor appeared to be susceptible to multipath levels above -2 dB. Tests were also run to measure the out-of-beam azimuth multipath error as a function of scalloping frequency to verify the results of the Lincoln Laboratories doppler computer model that showed significant errors occurring at subharmonics of the grating lobe frequency for the U.K. correlation processor. The effectiveness of center line emphasis and higher reference signal levels was evaluated.

In TN-10 a breadboard of the U.K. doppler AGC system was tested under various multipath situations. Large amplitude variations during a doppler scan period were noted that could have a significant effect upon the digital correlator in the airborne processor.

Calspan Technical Note 8 includes the results of simulation tests on TRSB processors when subject to weather radar and CW signal interference. In TN-11 tests results are included on the effects of high levels of multipath that exceed the processor thresholds. The performance of the single edge processing (SEP) technique when subject to multipath interference on the single edge used for thresholding are shown in TN-9 and 12. TN-12 also shows the performance advantages of using the SEP as the elevation processor.

In addition to the twelve technical notes a simulation study was conducted under subcontract by Bendix Flight Systems Division using the DC-10 simulation to determine DME accuracy requirements. A coupled approach was simulated using MLS elevation guidance up to the flare initiation point that was determined from the DME and elevation data. The autoland was accomplished using radio altimeter and MLS flare data. The results of this study are reported in Reference 13.

1.2 Scope of Report

This report summarizes the results of the simulation evaluations reported in the technical notes on the TRSB system. The conclusions resulting from the simulation tests are summarized in Section 2 of this report. These tests measured the performance characteristics, errors when subject to multipath signals and the effects of interference such as the weather radars or CW signals and propeller modulation on the TRSB receivers. The TRSB simulation facility used in evaluating the MLS receivers is described in Section 3.

Section 4 summarizes the significant test results on the performance of the Phase 2 1/2 and Phase 3 receivers that utilize thresholds for determining beam centroids to measure the time interval between the TO-FRO scanning beams that decodes the angle information. This processing technique is referred to as the dwell gate processing. The data in Section 4 is taken from Calspan Technical Notes 4, 5, 6 and 11. These data cover the performance of the receiver when subject to various multipath situations and when operating at low signal levels.

The single edge processing (SEP) technique is described in Section 5 and includes the results reported in TN-4, TN-6, TN-9 and TN-12. The SEP technique has been proposed for the flare processor since it determines the beam threshold using only the one edge of the beam that is least affected by the ground multipath reflections. Data are presented that show the SEP technique will be equally effective in reducing the multipath errors when used to process the elevation data.

Section 6 reports the results of a limited number of closed loop simulations that show the effects of hangar multipath reflections on an aircraft making a automatic approach using the MLS elevation data. An available analog computer simulation of the 707 aircraft was used in the simulations.

The results of simulations to determine the effects of propeller modulations on the MLS receiver are included in Appendix A. These results were reported in the first edition of Calspan TN-4. The combined effect of multipath hangar reflections and propeller modulations were evaluated.

The results of tests to determine the effects of interferring signals such as a weather radar or CW signals on the TRSB processors were reported in Calspan TN-8. These data are included in Appendix B.

Section 2.0
CONCLUSIONS

The following conclusions and observations are made from the test results. They are numbered the same as the sections that follow to facilitate examination of the detailed discussions and graphs.

(3.0) Simulation Facility

- The simulator has proven very useful, not only for multipath tests but for a variety of interference, propeller modulation and processor performance tests as well. Tests were carried out with flight test receivers and a breadboard receiver with two different angle processing techniques.
- Since the hybrid simulation uses the actual RF receiver and processor components all the receiver nonlinearities, dynamic range effects and noise effects and their interactions are realistically represented and included so that the performance data is representative of flight test results.
- Simulator tests with actual hardware are essential on all new processing techniques and can reduce the amount of flight testing required on new processors.
- This simulation facility permits evaluating the receivers over a large number and range of parameters within a very short test period.
- Simulator evaluations are more effective than flight tests for measuring processor multipath performance since the multipath parameters can be precisely controlled.

(4.0) Dwell Gate Processors

(4.2) Receiver Characteristics

- The acquisition, confidence, and flag circuitry worked well in the flight test receivers. In the Phase 2 1/2 receiver the time period for acquisition was about 2 seconds and 7 seconds for track confidence. In the Phase 3 receiver acquisition occurs in 1.5 seconds or less for azimuth and elevation data down to signal levels between -104 dBm and -106.5 dBm for the four receivers tested. For -65 dBm signal

levels acquisition requires about 1 second. This receiver uses a 15 second track confidence counter.

- The Phase 3 receiver α,β data filter exhibited reduced average errors in the baseline tests but higher noise errors at the lower scalloping frequencies (0.3 Hz used in baseline tests where the filter has a 2 dB overshoot) and slightly improved filtering at the higher scalloping frequencies compared to the Phase 2 1/2 receiver 10 radian/second filter. The digital implementation of this receiver was very stable in contrast to instabilities in dwell gate thresholding of the Phase 2 1/2 receiver.

(4.3) Characteristics of Multipath Effects

- The baseline tests confirm the previous tests and analytical derivations of multipath error. Motion averaging reduces the multipath errors significantly. In case the multipath reaches the level of the dwell gate threshold, the errors can become large. The single edge processors for elevation data show a dramatic reduction in the multipath error.

- The data rate jitter incorporated into the signal format eliminates the error peaks that are associated with the grating lobes of a regular data rate. However, the averaging between grating lobes becomes less effective so the overall motion averaging improvement is somewhat reduced.

- Receiver threshold level setting in the dwell gate processor has a pronounced effect on multipath errors. The error becomes large when the multipath level reaches the threshold so low thresholds are undesirable. The -3 dB threshold used in the flight test receiver is a good compromise between multipath susceptibility and noise disturbance requirements.

- The Phase 2 1/2 and Phase 3 receivers did not exhibit any significant difference in the scalloping frequency tests. The elevation errors tended to be reduced at higher scalloping frequencies as the phase difference between the DOWN-UP beams approached 180°. For azimuth the errors are a minimum for scalloping frequencies at odd multiples of the time difference between the TO and FRO beams.

- Beamwidth Effects

  A wider beamwidth illuminates proportionately more reflectors thus increasing the amount of multipath that may occur. The errors that may be caused by multipath are also increased proportionately to the beamwidth. However, for small multipath-to-direct separation angles that would be typical of many hangar reflections in elevation, the wider beamwidth errors are only moderately greater than those for the narrower beamwidth. Narrow beamwidth (0.4°) baselines tests with the Phase 3 receiver showed reduced peak errors approximately proportional to the beamwidth reduction and the smaller range of separation angles for in-beam multipath errors.

- Sidelobe Effects

  Sidelobe multipath can cause appreciable errors if it is not kept small. The errors are particularly large for the wider beamwidth antennas. In order to keep these errors within limits, it will be necessary to ensure that the multipath sidelobes immediately adjacent to the main beam do not exceed -20 dB from the direct beam level.

- Out-of-Beam Multipath

  Out-of-beam multipath is effectively eliminated by the tracking gate. If it exceeds the tracked signal and persists long enough, depending on the receiver confidence circuitry, it may cause the receiver to drop track and return to the acquisition mode. The confidence limits (times) are readily varied parameters of the receiver design. When two equal (within ±1 dB) signals were applied to the flight test receiver in the acquisition mode, it would not acquire either signal. Otherwise, it always acquires the larger of the signals presented to it. The signal validation logic in the Phase 3 receiver maintains track for 15 seconds before acquiring a multipath signal that is 1 dB greater than the tracked signal. This only occurs in 15 seconds if the multipath signal always exceeds the tracked signal by 1 dB.

- High Level Multipath Tests

  Multipath levels of -2 dB and higher will cause noisy performance in the Phase 3 receiver for multipath separation angles between 1.0 and 1.75 degrees when the multipath phase is near 180 degrees. The -2 dB and higher multipath at separation angles between 1.0 and 1.75 degrees has not been a design consideration in TRSB since it is difficult to postulate a realistic scenario. Modifications can be made in the tracking gate control logic of the Phase 3 receiver that should result in normal errors even at -1 dB multipath levels.

(4.4) Results of Multipath Scenario Tests

- Hangar Reflections in Elevation

  The Phase 3 receiver exhibited a significant improvement for the AWOP hangar multipath scenarios as compared in the Phase 2 1/2 receiver. Building B-2 in the AWOP scenario was the only hangar elevation multipath to cause significant errors. This error reduction is a result of the α,β data filter and the narrow tracking gates.

- Effects of Aircraft Speed

  Tests were run at 40, 80 and 120 (some 128) knots. There was no simple relationship of error to speed but the maximum errors occurred at the lower speeds. The duration of the errors is, of course, inversely proportional to the speed.

- Aircraft Reflections

  At the likely multipath amplitudes of -10 dB and below, aircraft reflections cause only small errors. If the multipath should reach -6 dB, significant errors can occur but their effect is alleviated in any case by the short duration (<1 second) of the exposure.

- Azimuth Ground Reflections

  An irregular reflecting surface in front of the azimuth antenna can introduce significant errors if it is strongly illuminated. As the scalloping frequency is very low, the errors would tend to show up as a bend in the beam that actually divert the aircraft from the desired track. Every effort must be made to keep the multipath level low or the separation angle small by considerations of antenna design and surface configuration (including snow cover).

- Errors similar to those found in the flight tests for threshold screen multipath were produced with the Phase 2 1/2 receiver and a screen simulation scenario. It was necessary to increase the separation angle to 0.6° (by tilting the screen) in the simulated scenario to make the errors as large as the field tests.

For the other screen tests the uneven surface and unknown tilt of the screens made it impossible to reproduce flight test recordings by the screen simulation with a single flat surface. However, the error magnitudes could be bounded by proper selection of multipath amplitudes and screen tilts.

(5.0) Single Edge Processing (SEP)

(5.2) SEP for Flare

- In the case of elevation data, the multipath distortion occurs principally on the inside beam edges for typical hangar reflections for elevation and the surface in front of the flare antenna. Single edge processing greatly reduces the effect of this elevation multipath.

- The SEP angles have a bias since they are derived from measurements on one side of the beams. A beamwidth measurement is needed to correct this bias and an average dwell gate measurement appears to be adequate. Accurate beamwidth measurements for the SEP can be made with a digital dwell gate processor. If the beamwidth

measurement is averaged 10 to 20 seconds the effects of hangar multipath will be insignificant for elevation. The effects of ground reflections for flare can be made insignificant if the beamwidth measurement is averaged for a period of about 25 seconds before touchdown. The effects of beam broadening from a focused flare antenna must be evaluated.

- Nonlinearities in the logarithmic IF amplifier can cause beamwidth variations as a function of signal level. If adequate linearity of the log characteristic can not be assured, it will be necessary to calibrate the receiver as a function of signal level. This can be done by comparing simultaneously the SEP and dwell gate processor outputs in the absence of multipath.

- The simulator tests have shown that the variation in dwell gate width can be used to reduce the SEP flare multipath error to less than 2 feet with -25 dB sidelobes at the worst case touchdown tested (8 ft aircraft antenna height and touchdown at 4000 ft from the flare antenna). The correction results in a modest reduction in the rate error. If the sidelobe levels can be kept to -30 dB these corrections will not be necessary.

- The SEP was found to be more effective in reducing the errors from surface reflections in the flare scenarios than the multipath control technique (MCT). MCT was evaluated with power programing on the ground transmissions and an airborne correction that is a function of the indicated angle.

- Closed loop simulation tests of the SEP with aircraft dynamics and autopilot control to touchdown are required to determine the accuracy requirements on the flare angle and angle rate data. In many flare couplers the rate-of-descent command is derived from the altitude and altitude rate measurements so that errors in these measurements can interact in the closed loop system.

(5.3) SEP for Elevation

- The SEP can be used for elevation as well as flare data to significantly reduce errors from hangar reflections.
- Single edge processing is especially effective for slow moving helicopters in heliport scenarios.
- The SEP technique will result in larger errors for multipath occuring at a higher elevation angle (position multipath) than the direct signal.
- Elevation hangar scenarios that generate significant levels of multipath result in rather large negative multipath separation angles. Thus, the "tilted" hangars can not generate positive multipath separation angles that could interfere with SEP thresholding.
- Multipath can occur at positive separation angles from hangar edge diffraction but its amplitude is too low to significantly affect the SEP.
- Dual mode single edge and beam centroid processing only requires additional algorithms in the microprocessor and is feasible for future TRSB processors.

(6.0) Aircraft Closed Loop Tests

- The aircraft flight path deviations and control motions resulting from the AWOP B2 hangar multipath are insignificant for aircraft making an automatic approach.
- Autopilots deriving rate data from MLS elevation angle signals would be effective in reducing flight path displacements caused by vertical wind shears.
- It may be desirable to use single edge processor when a rate type autopilot is used to minimize control motions induced by hangar multipath.

- The SEP produces insignificant flight path deviations and control motions as a result of hangar multipath.

(Appendix A) Propeller Modulation Effects

- Propeller modulation has no appreciable effect at high signal levels in the absence of multipath for both elevation and azimuth. At low azimuth signal levels near acquisition, propeller modulation causes a slight increase in angle errors but principally it increases the number of missed scans when it eclipses an angle beam or DPSK signal. Even so, at the required acquisition level of less than 50% missed scans, random propeller modulation at the 8 dB eclipsing level causes less than 2 dB equivalent reduction in signal level. Worst case propeller modulation causes more losses (6 dB) in the azimuth case but this requires a propeller speed locked to the data rate and phase shifted for maximum number of eclipses which is only likely to occur with an aircraft propeller for a few seconds. The acquisition level for elevation is almost independent of propeller modulation.

- Propeller modulation increases the susceptibility of the receiver to the multipath errors. The largest error increases occur when the multipath by-passes the propeller. Hangar scenarios were run with the propeller modulation on the direct beam only. Worst case propeller modulations will cause a significant increase in the multipath errors when the depth of modulation reaches -8 dB. Below -8 dB only moderate increases in the error standard deviation and mean shift occurred. With a -12 dB modulation the errors will more than double in some hangar scenarios.

- Propeller modulation effects on multipath errors will be insignificant if the aircraft antenna is located so that the modulation amplitude does not exceed 4 to 6 dB.

(Appendix B) Weather Radar and CW Pulse Interference Tests

Pulse Interference Effects

- A 20 dB pulse-interference/angle ratio lasting for at least fifteen seconds is required to decrement the confidence counter and cause system flags. This ratio is relatively independent of the pulse train and the angle signal strength.
- The intermittent interference from a weather radar should not cause system flags or prevent signal acquisition.
- At high pulse-interference/DPSK ratios the missed decodes approach 10% for the 6 microsecond, 200 PPS radar and 20% for the 2 microsecond, 400 PPS radar. At a pulse-interference/DPSK ratio of 20 dB the percent of missed decodes is about 7 to 8% for continuous pulse interference.
- The sensitivity of DPSK to pulse interference increases at signal levels below -90 dBm.
- Missed data or decodes do not significantly affect the accuracy of the data and are only significant if they reach the 50% required for a system flag.
- The NAFEC test data show that the duration of the peak levels of weather radar interference are less than 0.4 seconds over a 4 second radar scan period and thus cannot significantly affect the accuracy or signal acquisition. Also, a measured peak level of -70 dBm would primarily result in missed DPSK decodes.
- The single edge processor (SEP) showed pulse interference characteristics similar to the dwell gate processors.
- The out-of-beam multipath logic should include symmetry checks to prevent radar pulses from decrementing the confidence counter.

CW Interference

Tests showed the TRSB angle data has a CW interference threshold of -6 dB to -8 dB relative to the angle data. This threshold can be several dB lower because of the effect of CW interference on the DPSK signals. At low signal levels the interference thresholds may be significant in a severe CW interference environment.

Section 3.0
TRSB HARDWARE SIMULATION FACILITY

Block diagrams of the TRSB Signal Simulator are shown in Figures 3-1 and 3-2. The simulator provides an output waveshape equivalent to that received in the aircraft from a TO-FRO or DOWN-UP scanning beam transmitter. In addition, the multipath from a single reflecting surface is simulated. The simulator variable parameters are controlled by a digital computer for each scan. An analog computer simulation of aircraft-autopilot dynamics can be connected to the TRSB signal simulator for closed loop simulations.

In the TRSB simulation the beam shapes are controlled by counters that address PROM's (programmable read only memories). Beamwidth is controlled by selecting the clock frequency for the PROM address counters. The PROM outputs drive double balanced mixers to the desired signal shape by means of digital to analog converters. The multipath beams include first and second sidelobes on each side. The RF phase of the first sidelobe is 180° shifted from the main beam and second sidelobe by inverting the drive to the double balanced mixer beam shaper. At present, PROM's have been programmed for -20, -25, and -30 dB sidelobes (both equal). This beam generation is directed by a digital word from the computer which thus sets the angles (TO-FRO beam separation time) for both the direct and multipath beams.

The multipath beams are further controlled by the computer to offset the carrier frequency (scalloping frequency difference) and to set the multipath amplitude. These changes are made between scans as desired. The direct beam and multipath beam are then summed and the composite signal is translated to C-band for application to the receiver. Provision for synchronization, and function identification DPSK transmissions are made in the simulator.

The receiver under test produces an indicated output angle that is made available to the control computer by the interface unit. A normal test consists of 5 seconds with direct signal only, up to 20 seconds of multipath and terminates with 2 seconds of direct signal. The indicated angle is stored in the computer and also provided to the chart recorder for a visual indication

of test progress. Following the end of the test, the stored data may be filtered by a 10 radian/second cutoff low pass filter or by an α,β filter with variable parameters as well as by other digital filters (path following, control motion, rate) as specified in the "ICAO Test Plan for U.S. Microwave Landing System". In each case, the mean shift in angle from the 5 seconds before multipath application and the standard deviation during the multipath are computed. The filtered outputs are also available for chart recording.

Operational control of the computer is centered in the teletypewriter with control indications and statistics printouts. The paper tape reader is used for program loading and also for loading the multipath amplitude profiles. When an amplitude profile has been loaded into the computer, it can be used for a series of tests in which other parameters are varied. The other parameters, which are introduced from the teletype keyboard, include: the direct angle, direct angle increment (added to the direct angle each data period), the multipath angle, multipath angle increment, scalloping frequency, frequency increment, multipath duration and function (elevation or azimuth). The test run is started from the keyboard. Selection of the data processing filters is made following completion of the test run. When analysis of the data is completed, including angle printouts and plots of filtered data if desired, a return to the start for test repetition or parameter modification is made.

The interface unit can accommodate the TRSB Phase 2 1/2 receiver, Phase 3 receiver and the ITT Doppler processor that operates with a separate Doppler simulator. It is easily modified to interface other units with digital outputs.

Calspan is extending the capabilities of this simulator by the addition of several items to permit using the PDP-11 as the MLS digital processor in addition to controlling the simulators. A direct memory access (DMA) board and a hardware multiply-divide board are being added to the computer. A high speed analog-digital converter will be added to provide an input of the receiver log video signal into the PDP-11.

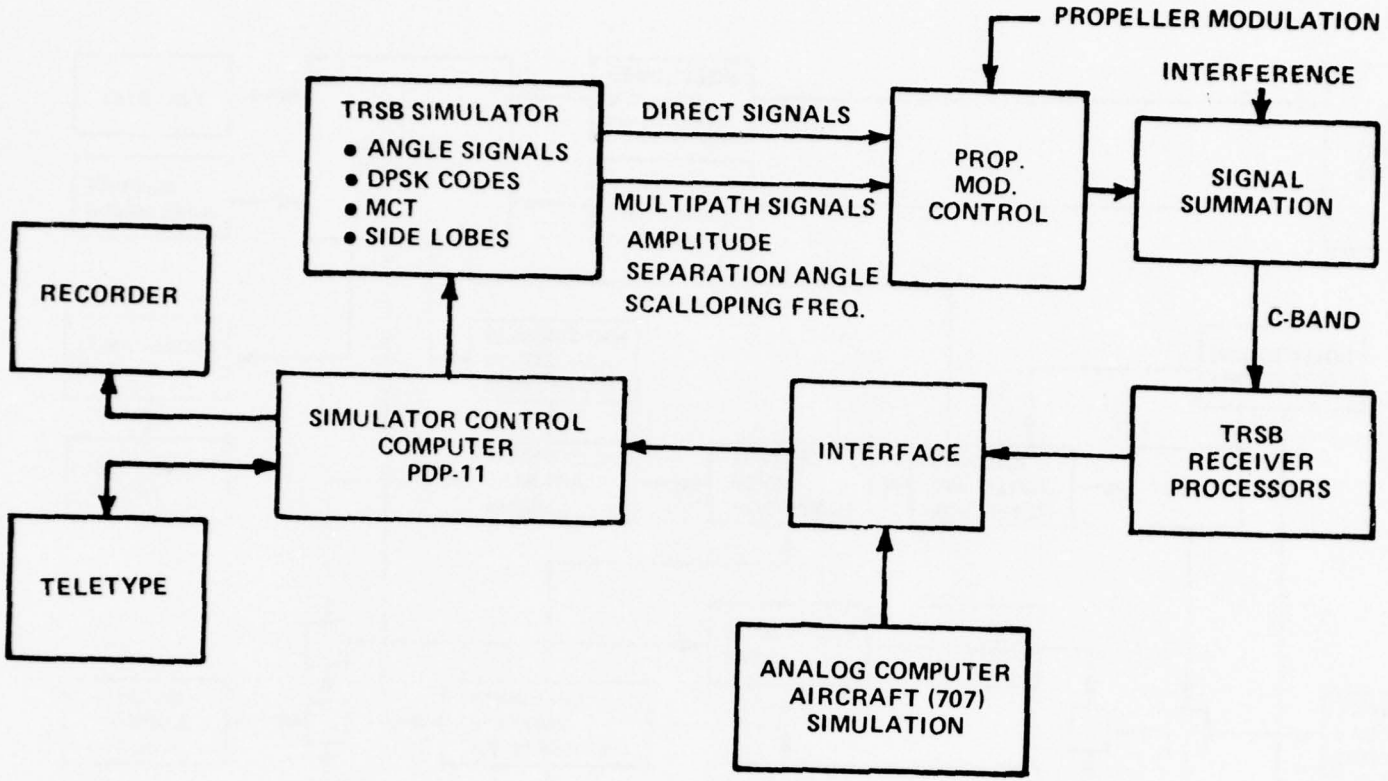

Figure 3-1 TRSB HARDWARE SIMULATION FACILITY

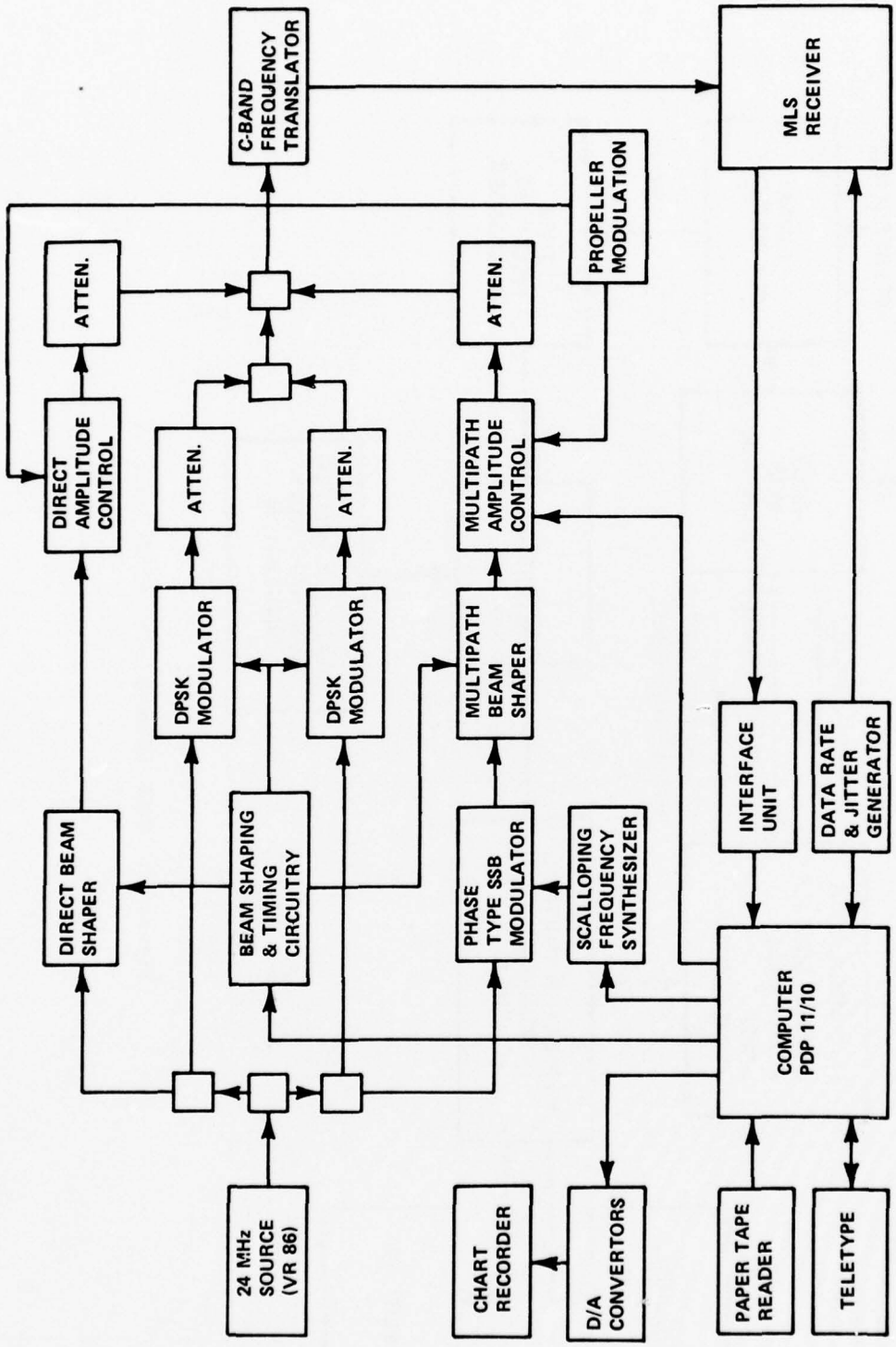

Figure 3-2 CALSPAN TRSB SIMULATOR

and -106.5 dBm for the four receivers tested. For -65 dBm signal

Section 4.0
DWELL GATE PROCESSORS

An extensive series of tests has been carried out using the TRSB hardware simulator with Phase 2 1/2 and Phase 3 flight test receivers and a breadboard receiver. The breadboard receiver has two operating modes for elevation data to permit a comparative performance evaluation of single edge processing with the dwell gate processing technique. The results of the single edge processor tests are described in Section 5.

4.1 Description of Tests

The simulator produces TO-FRO (DOWN-UP for elevation) pulses that are the same as those an airplane would receive from an MLS ground station. In addition, a single multipath signal is simulated with a wide range of variable parameters. Special provisions were made for adding other interferring signals, including pulse and CW interference, adjacent channel signals and propeller modulation. Interference and propeller modulation test results are included in Appendices A and B.

The simulated signal parameters were designed to match the selected format. The time reference coding was 100 microseconds per degree, except for a simulated flare screen test at 200 microseconds per degree, so that the 3 dB beamwidths were 50, 100 and 150 microseconds for 1, 2, and 3 degree beamwidths respectively*. Antenna sidelobes were not generated for the early tests with the Phase 2 1/2 receiver but were added for subsequent tests. Sidelobes of -20 dB, -25 dB and -30 dB are used in the tests. The jittered data rate had a repetition period of 592 milliseconds, resulting in averaging data rates of 40.5 Hz and 13.5 Hz for elevation and azimuth signals respectively. The raw angle data was collected at these rates and processed by a low-pass digital filter (10 radian/second cutoff) or an α,β filter before evaluation of the test results. The error statistics are, therefore, restricted to those frequency components that can cause perturbations to the aircraft or its control surfaces. Some comparative elevation tests were run between the 10 radian/second filter and a

*All tests were run with 1 degree beamwidths except as noted.

5 Hz zero order hold using an 8 point average. The error statistics are quite comparable although the 10 radian/second filter in the Phase 2 1/2 receiver was slightly less effective than the 5 Hz zero order hold filtering.

Baseline multipath tests were carried out on the receivers in which the test parameters were varied independently so their effects could be isolated. These tests do not represent any real multipath situation. The tests were used to determine the effects of the following variables:

Multipath separation angle
Multipath amplitude
Scalloping frequency
Jittered data rate
Transmitter beamwidth

The results of these tests are measured by their effect on the angle errors produced in the receiver. The mean angle shift and standard deviation of error are the principal statistics compared but number of missed scans is also indicated where it is significant. Peak-to-peak errors are about three times the standard deviation since the error distribution is not Gaussian. Plots of the error statistics are provided for evaluation of the effects.

Several airport situations were postulated that could produce large in-beam multipath during the landing phase. These were simulated with several levels of multipath to represent the signal reflected from various types of hangars. The error for a zero dB hangar (reflection coefficient = 1) that includes the M/D reduction from antenna pattern shaping is marked on the graphs. Errors for other hangar reflection levels can be read from these curves by shifting above or below the 0 dB hangar. Later hangar scenario tests used the AWOP scenarios and multipath parameters prescribed for the ICAO multipath performance evaluations.

Other variables from the list above were incorporated into some of these tests to ascertain their effect in the multi-variable environment. The mean shift and error standard deviation were also used to indicate the relative effects of these multipath situations. It must be noted that many of these tests are of short duration, or low scalloping frequency, or both so that

there is a certain amount of instability in the test statistics. That is, the test results would differ from run to run depending on the scalloping frequency phase (random) at initiation. Some of the irregularities in the curves, particularly the mean values, are due to this randomness.

4.2 Receiver Characteristics

The MLS Phase 2 1/2 and Phase 3 receivers and the Calspan breadboard receiver were run through a series of tests on the MLS signal simulator. The receivers are briefly described in Table 1.

Table 1 - TEST RECEIVER CHARACTERISTICS

Phase 2 1/2 Receiver
- Bendix Serial No. E-104
- Used in Flight Test Program
- One RF Channel (5189.4 MHz)
- Analog Angle Processing
- (α, β = 0) Angle Filter with 1°/Second Rate
- Limiter Preceding Filter

Phase 3 Receiver
- Bendix Serial No. P101
- 200 RF Channels (Channel 190, 5088 MHz Tested)
- All Digital Angle Processing
- (α, β) Angle Filter with Rate Limiter Following Filter

Breadboard Receiver
- Similar to Phase 2 1/2 Receiver
- Filters and Rate Limiters Selectable in PDP-11 Computer
- No DPSK Decoder
- No Confidence Counter or Flag Circuitry

The Phase 3 receiver has tracking gates that adapt to the beamwidth of the received signal. The video signal is digitized before signal thresholding. An Advanced Micro Devices 9080A μprocessor chip is used. The Phase 2 1/2 receiver uses a fixed tracking gate width of about 250 μsec. Analog circuits are used in determining the 3 dB beam threshold. The flag circuits in the Phase 2 1/2 and Phase 3 receivers are activated by the following:

- Frame Flag - Any frame in which the receiver fails to make a valid angle measurement. The acquisition counter is decremented at the clock rate when this occurs. This failure may be caused by an invalid function identity decode or by detection of an improper number of dwell gates during a scan. The receiver output from the previous frame is held during a frame flag.
- Slew Rate - An angle measurement that represents a change exceeding one degree per second. This check occurs before the data filtering in the Phase 2 1/2 receiver and after the α-β filter in the Phase 3 receiver.
- Confidence - The "inside-the-tracking-gate" peak detector output exceeds the "outside-the-gate" peak detector on the FRO scan. If the reverse is true, confidence is low and the confidence counter is decremented. When the counter is fully decremented, or reset, a system flag occurs - receiver output is inhibited.

4.2.1 Data Filter Responses

The receiver angle errors in these plots, and throughout this report except where noted, have been passed through either a low-pass filter with 10 radian/second cutoff or the α-β filter. The frequency response characteristics of the azimuth and elevation filters are compared in Figures 4-1 and 4-2 for the Phase 2 1/2, Phase 3 and breadboard receivers.

Tests were run to measure the frequency, step and ramp responses of the TRSB receivers. These data were taken to assist the AWOP Performance Sub-Group in evaluating the effects of processor filters on TRSB performance data. The tests were run on a Phase 2 1/2 receiver that was used in taking the flight test data. Identical tests were run on the Phase 3 receiver since the filter was changed from an α type to an α-β filter. The Phase 3 receiver includes the processing techniques recommended for the TRSB system. The rate limiter follows the smoothing filter in the Phase 3 receiver instead of operating directly on the raw data as was done in the Phase 2 1/2 receiver.

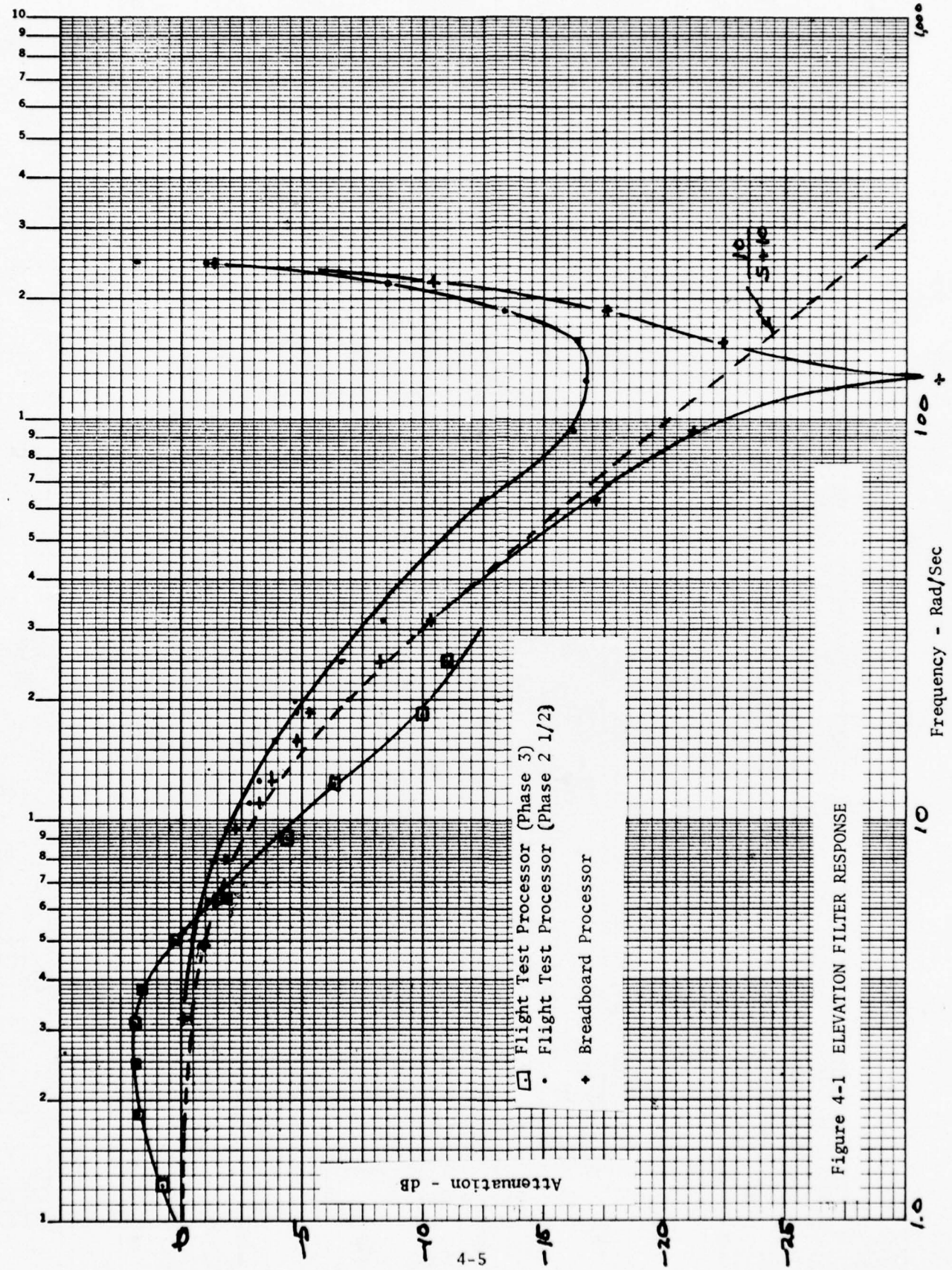

Figure 4-1 ELEVATION FILTER RESPONSE

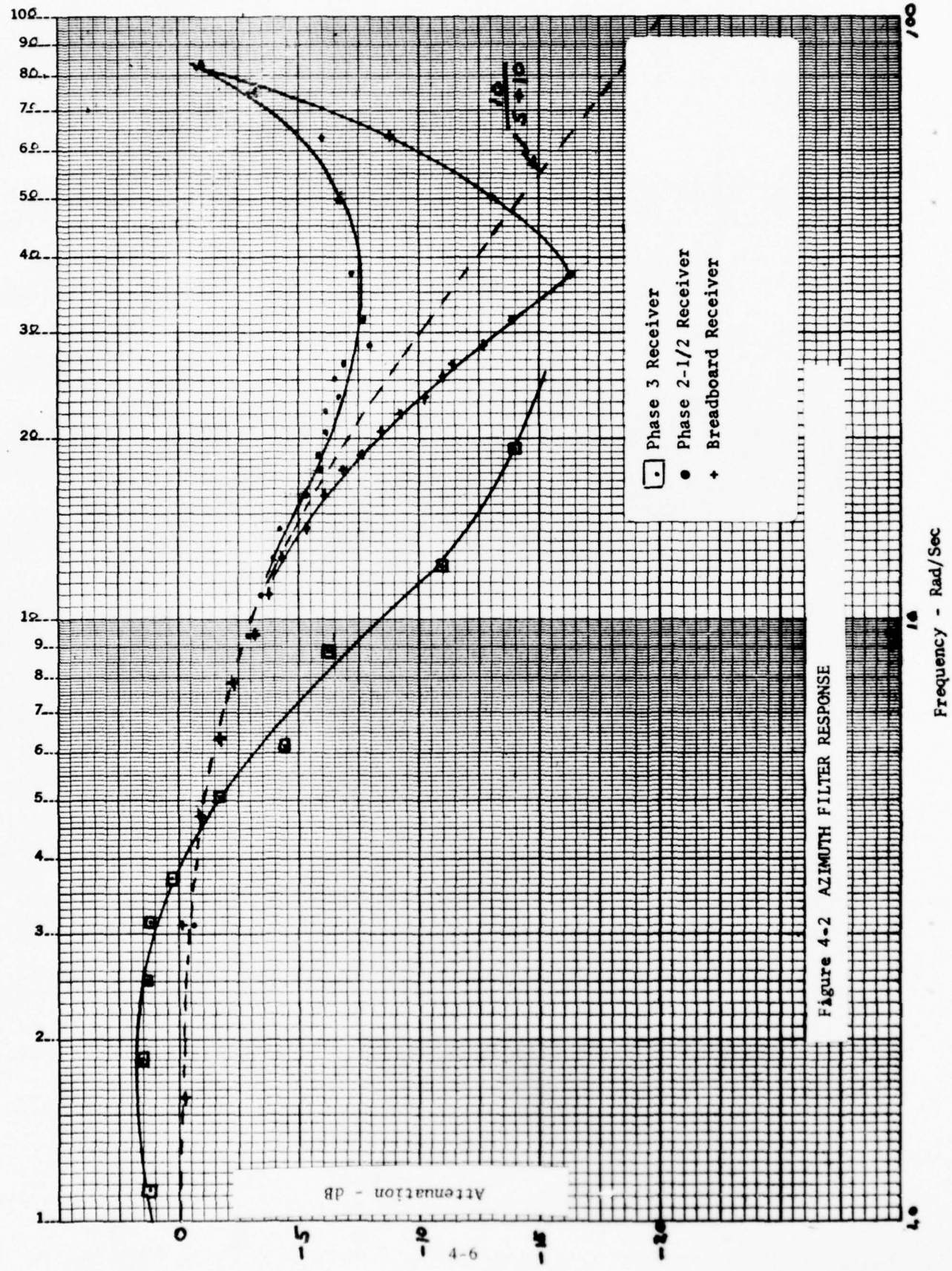

Figure 4-2 AZIMUTH FILTER RESPONSE

These tests were run on the multipath simulator. The step and ramp inputs were generated by a program in the PDP 11/10 computer that controls the TRSB simulator parameters and test scenarios. For the frequency response tests a low frequency generator, HP 203A, was fed into an analog-to-digital converter and input to the simulator control computer.

4.2.1.1 Phase 2 1/2 Receiver Test Results

Figure 4-3 shows the elevation channel amplitude and phase responses versus frequency. The 3 dB point for this filter occurs at 11 radians/sec. It should be noted that for these tests the 1 degree/sec rate limiter restricts the amplitude response above 14 Hz or 90 radians/sec.

The azimuth channel frequency response curves are shown in Figure 4-4. Phase shift was not plotted beyond 10 radians/second because the 13.5 Hz data rate prevented an accurate phase measurement. The 3 dB point for this filter occurs at 10 radians/second.

Step responses are plotted in Figures 4-5 and 4-6. A one data period delay is apparent in these plots. The delay is a result of the filter implementation required in the test bed processor that had a limited data processing capacity.

Figure 4-7 shows the elevation channel ramp response for this processor. An "α" type filter was used with $\alpha = 0.25$. By the use of z transforms it can be shown that a delay of $(\frac{1-\alpha}{\alpha})$ T seconds will result from a ramp input, where T is the sample period. A delay of 0.075 seconds results from the 40 Hz data rate. An additional delay of 0.025 seconds results from the 40 Hz quantization of the ramp input for a total delay of 0.1 seconds.

The azimuth channel ramp response shown in Figure 4-8 has a time lag of 0.15 seconds as would be expected from an "α" = 0.5, a 13.5 Hz data rate and the quantization of the ramp input. The jittered data rate requires an estimate of the average lag as is indicated by the dashed line passing through an average updated data point.

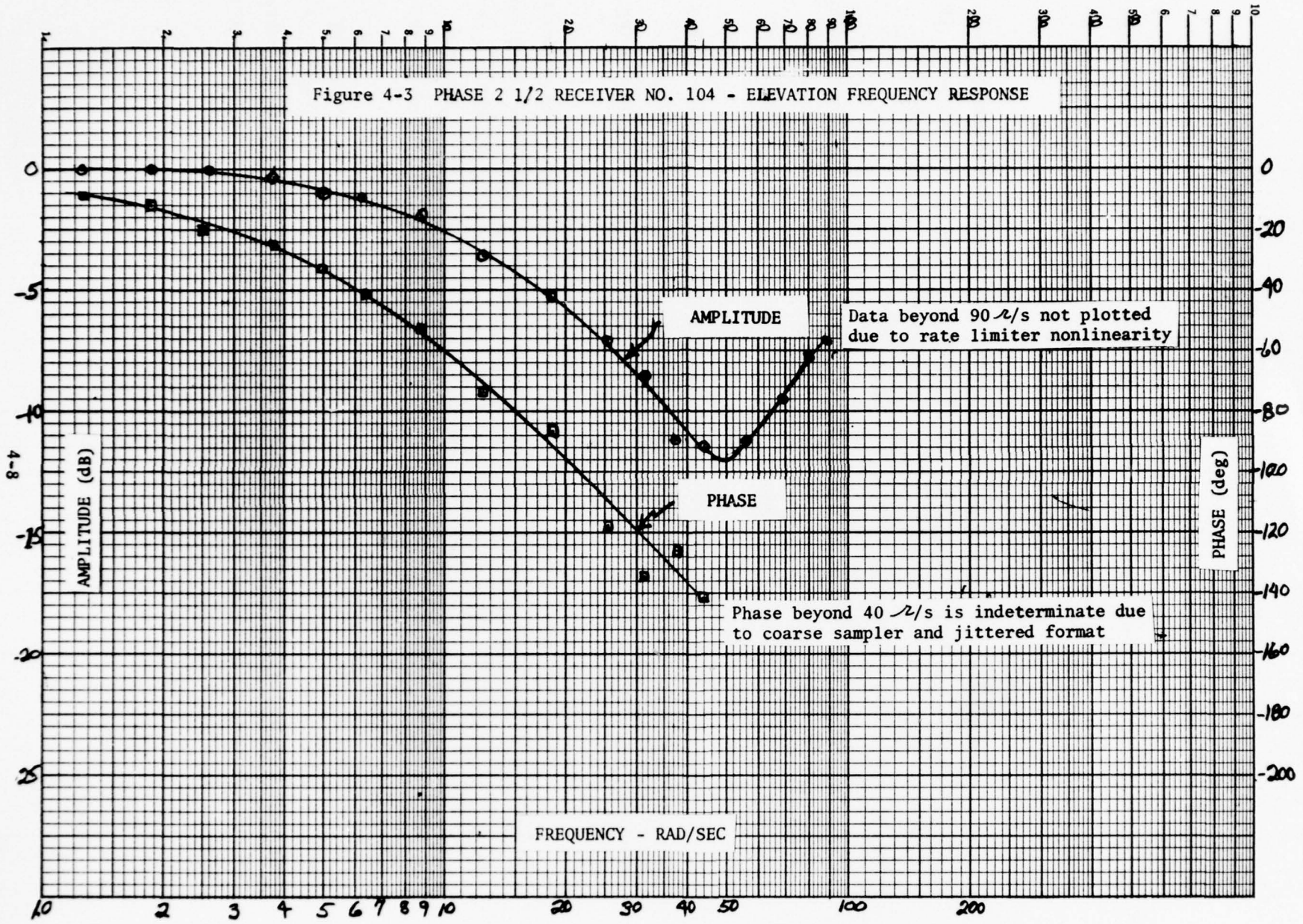
Figure 4-3 PHASE 2 1/2 RECEIVER NO. 104 - ELEVATION FREQUENCY RESPONSE
AMPLITUDE
PHASE
Data beyond 90 r/s not plotted due to rate limiter nonlinearity
Phase beyond 40 r/s is indeterminate due to coarse sampler and jittered format
AMPLITUDE (dB)
PHASE (deg)
FREQUENCY - RAD/SEC
0
-5
-10
-15
-20
-25
0
-20
-40
-60
-80
-100
-120
-140
-160
-180
-200
1
2
3
4
5
6
7
8
9
10
20
30
40
50
100
200

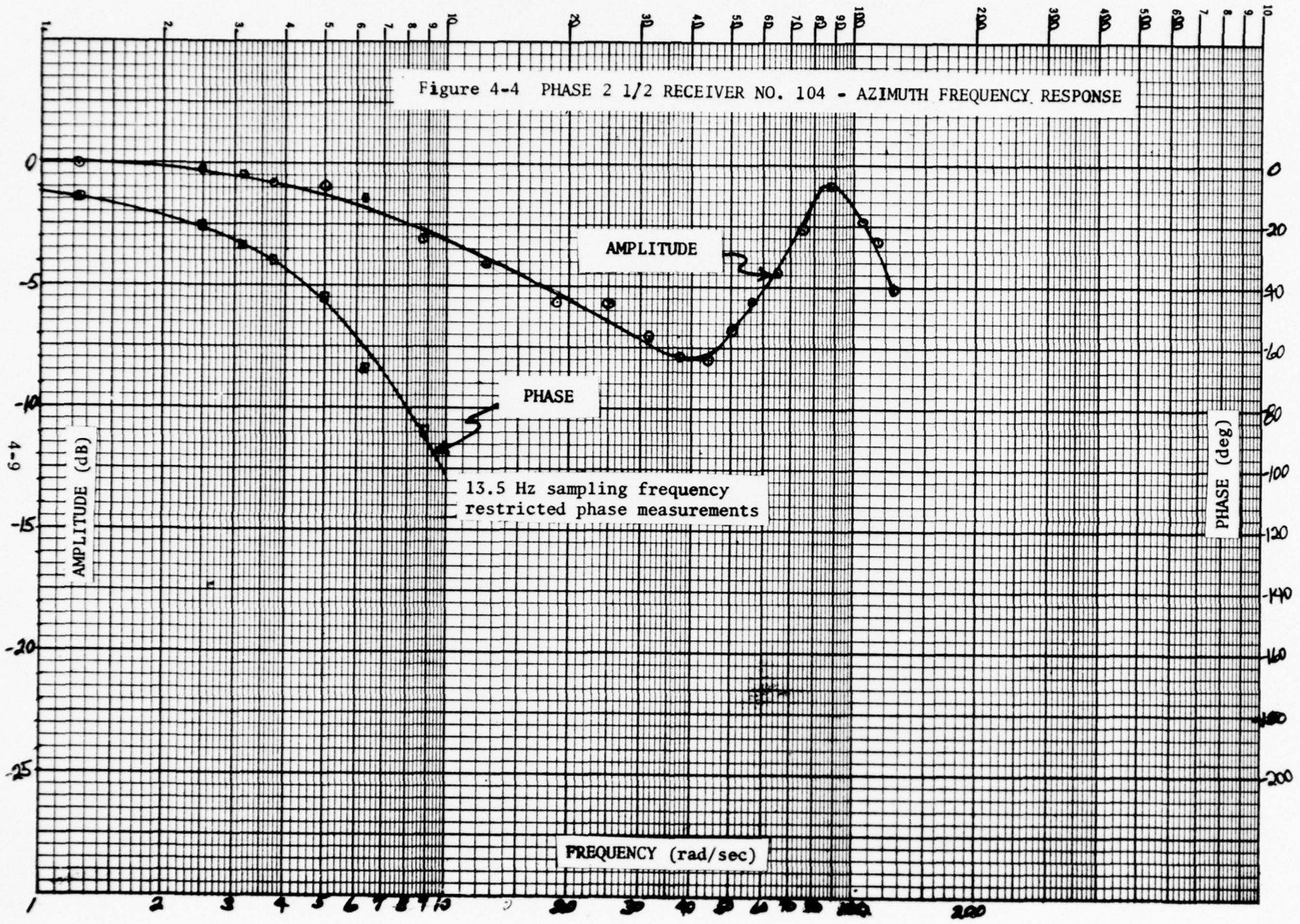
Figure 4-4 PHASE 2 1/2 RECEIVER NO. 104 - AZIMUTH FREQUENCY RESPONSE
AMPLITUDE
PHASE
13.5 Hz sampling frequency
restricted phase measurements
AMPLITUDE (dB)
PHASE (deg)
FREQUENCY (rad/sec)
0
-5
-10
-15
-20
-25
0
-20
-40
-60
-80
-100
-120
-140
-160
-180
-200
1
2
3
4
5
6
7
8
9
10
20
30
40
50
60
70
80
90
100
200

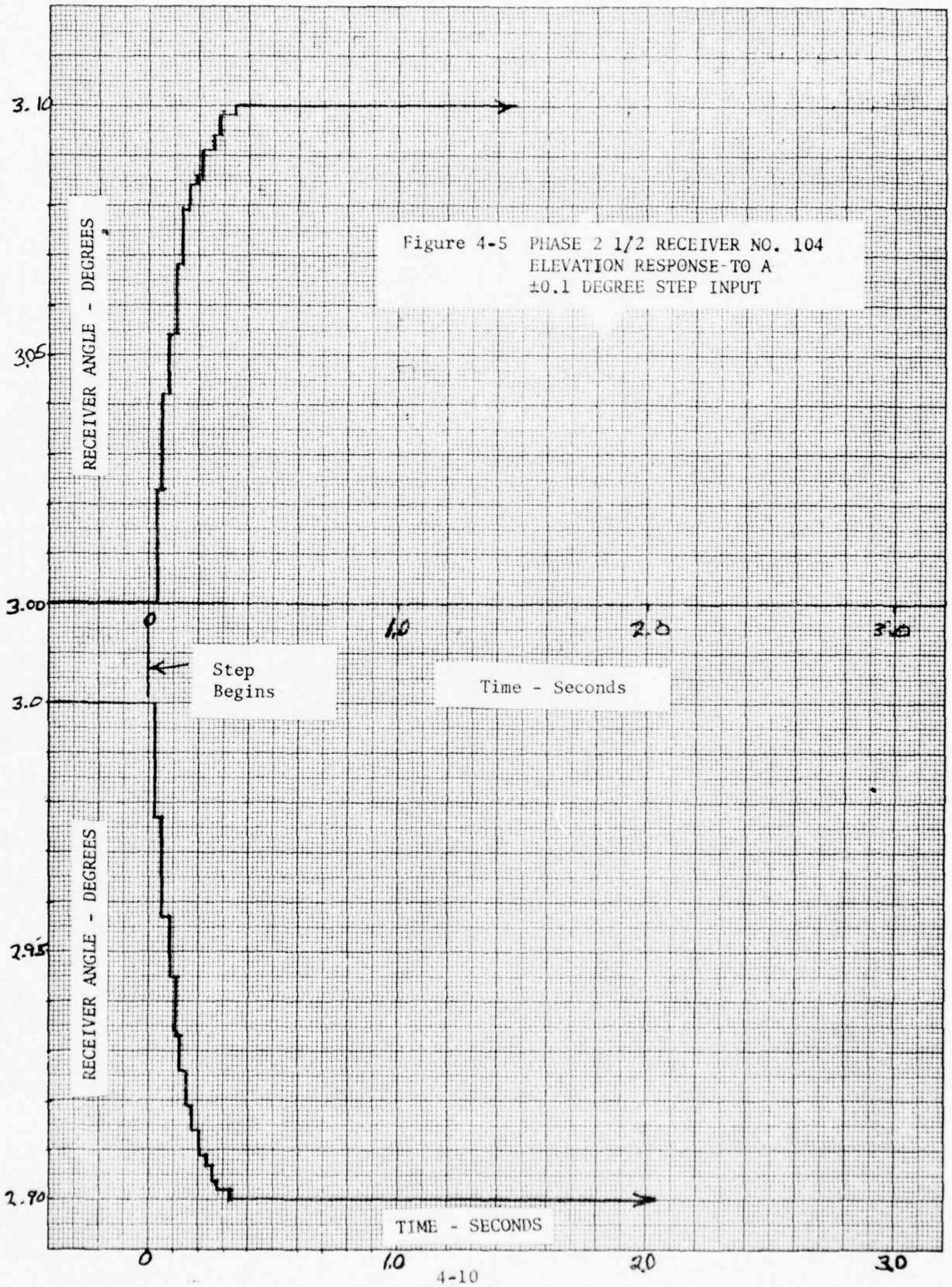

Figure 4-5 PHASE 2 1/2 RECEIVER NO. 104
ELEVATION RESPONSE TO A
±0.1 DEGREE STEP INPUT

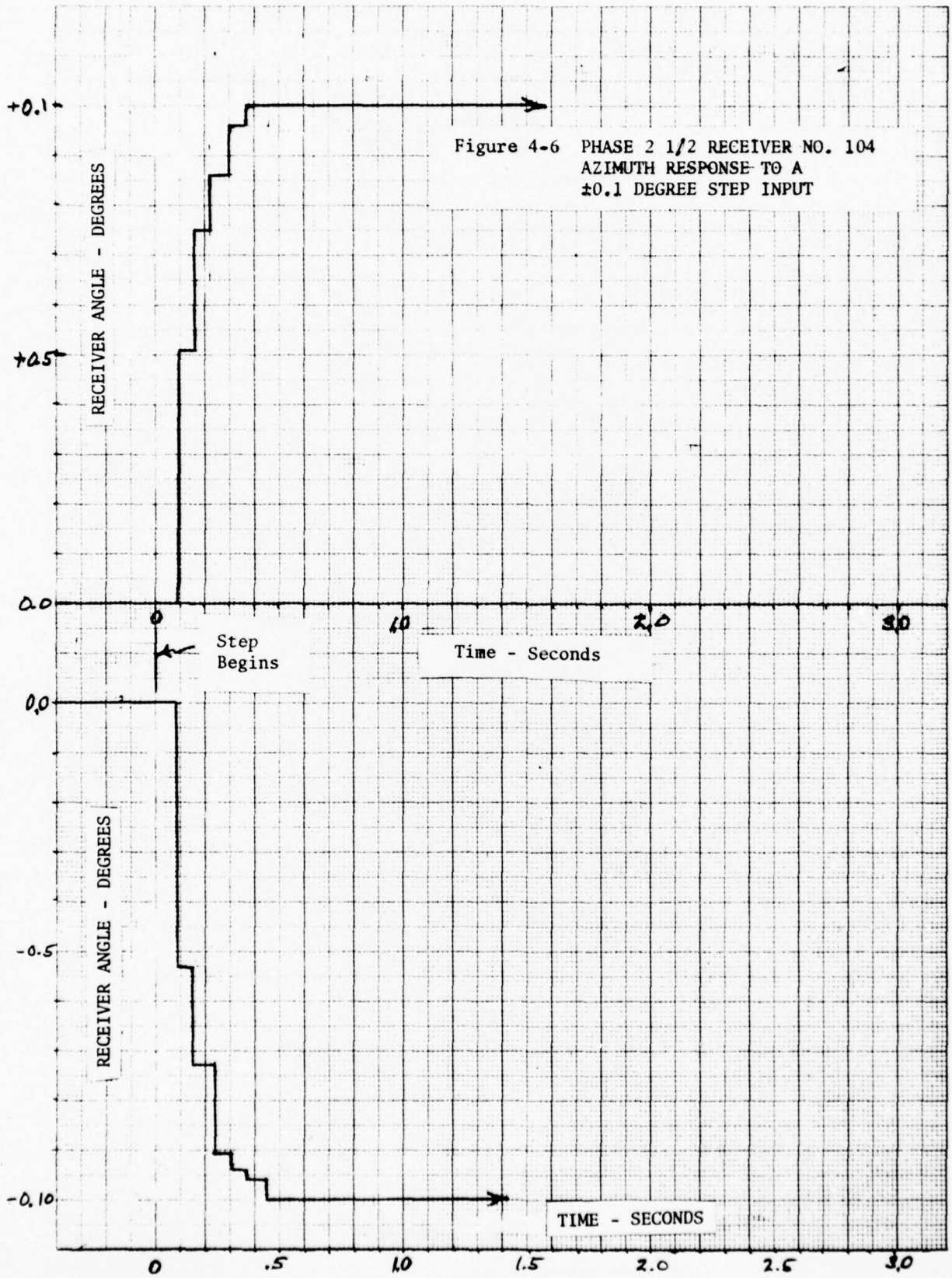

Figure 4-6 PHASE 2 1/2 RECEIVER NO. 104
AZIMUTH RESPONSE TO A
±0.1 DEGREE STEP INPUT

Figure 4-7 PHASE 2 1/2 RECEIVER NO. 104
ELEVATION RESPONSE TO A
+0.5 DEG/SEC RAMP

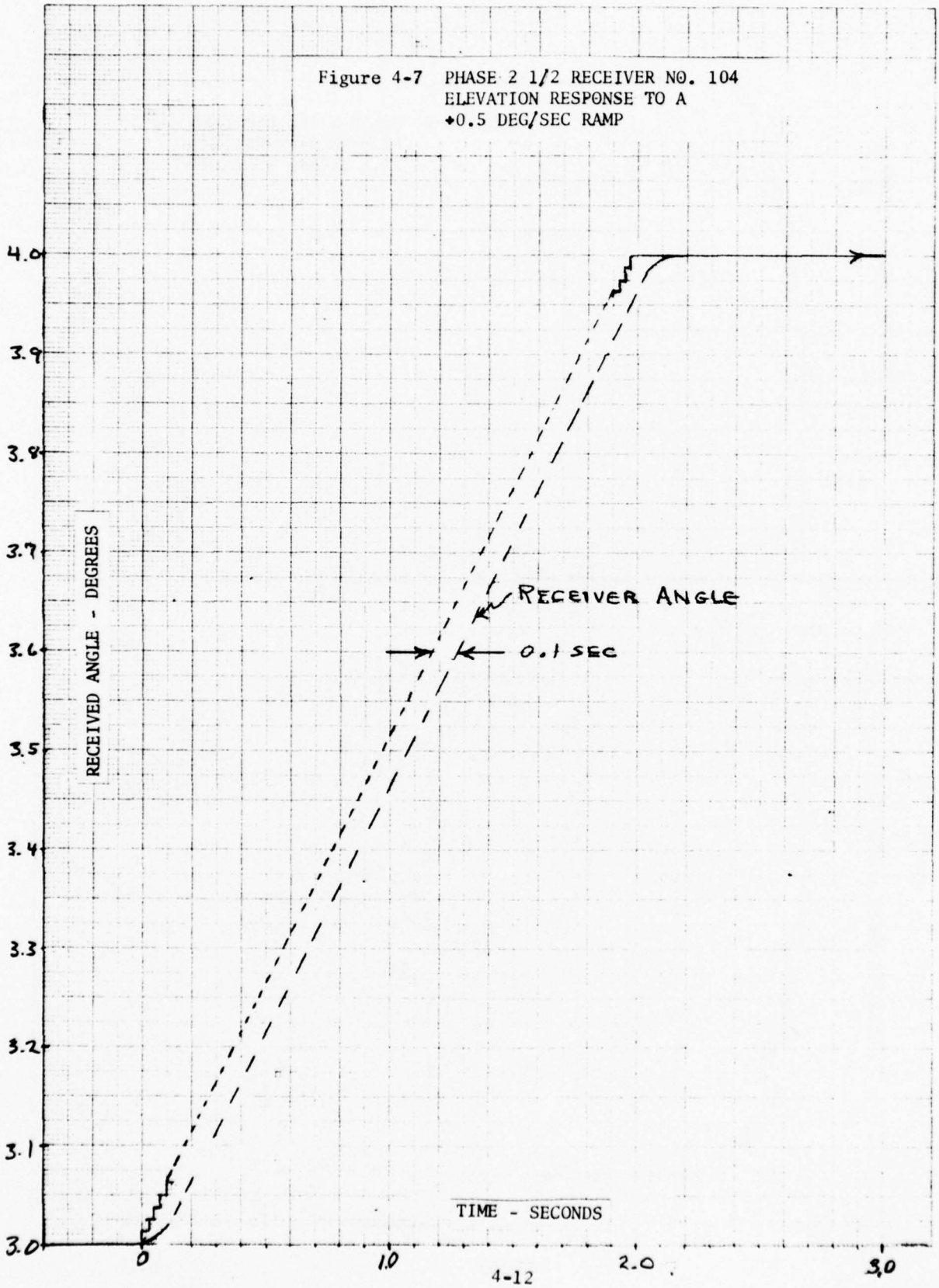

Figure 4-8 PHASE 2 1/2 RECEIVER NO. 104
AZIMUTH RESPONSE TO A
+0.5 DEG/SEC RAMP INPUT

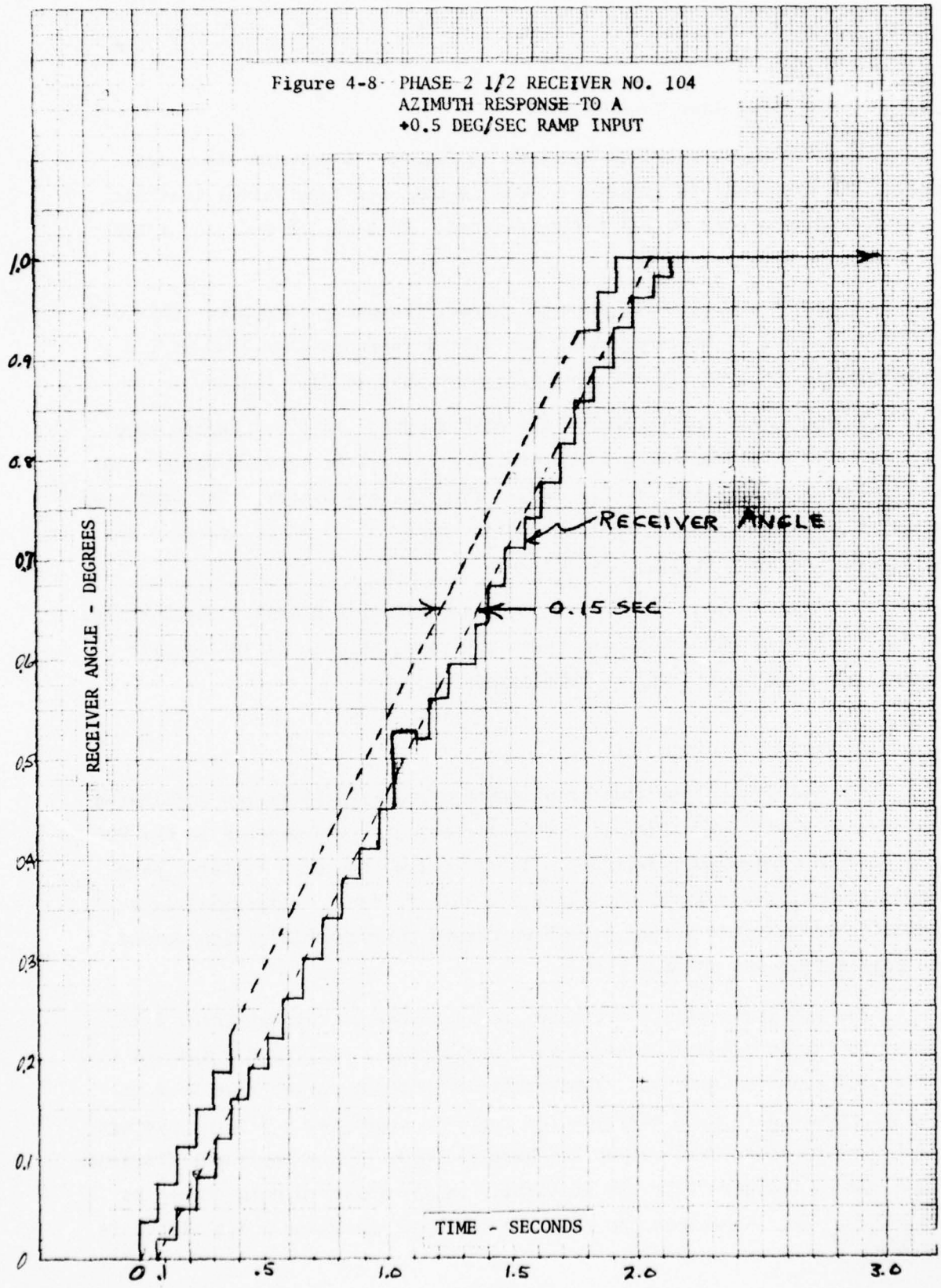

4.2.1.2 Phase 3 Receiver Test Results

The frequency response is shown in Figure 4-9 for the elevation channel. The overshoot is apparent (2 dB) in this α-β type filter that has a 3 dB cut-off frequency at 7.8 radians/second. An α of 1/8 and β of 1/128 were used in this filter.

Figure 4-10 shows the azimuth channel frequency response. This α-β type filter has a 2 dB overshoot with the filter response down 3 dB at 5.8 radians/second. An α of 1/4 and β of 1/32 were used in this filter.

Figures 4-11 and 4-12 show the step response to a 0.1 degree step input. The one data sample lag is a result of the filter implementation that uses the predicted position for the output from the α-β filter. The predicted position is computed from the (n-1) position and velocity which are zero for the initiation of this test.

The ramp responses are shown in Figures 4-13 and 4-14. These curves show that the filter output catches up to the ramp, then leads and finally overshoots when the input ramp is terminated.

4.2.1.3 Comparison of Data Filters

The results of the simulation tests are available as raw unfiltered data and after filtering. Several filter algorithms are programed in the PDP-11 computer and are keyboard selectable. These include the data filters, path following filter, control motion filter and rate filter. Statistical data presented in the various graphs have been passed through a 10 radian/second single pole filter and the α,β filter.

The amplitude versus frequency response curves for the Phase 2 1/2 receiver and the breadboard receiver were presented in Figures 4-3 and 4-4 for elevation and azimuth channels. The elevation response curves have been re-plotted in Figure 4-15. In addition the response curve for a 8-point average with a 5 Hz zero order hold output has been plotted. These amplitude frequency response curves indicate that the statistics on the filtered data should be very similar. For comparison the response curve of the Phase 3 α,β filter is included.

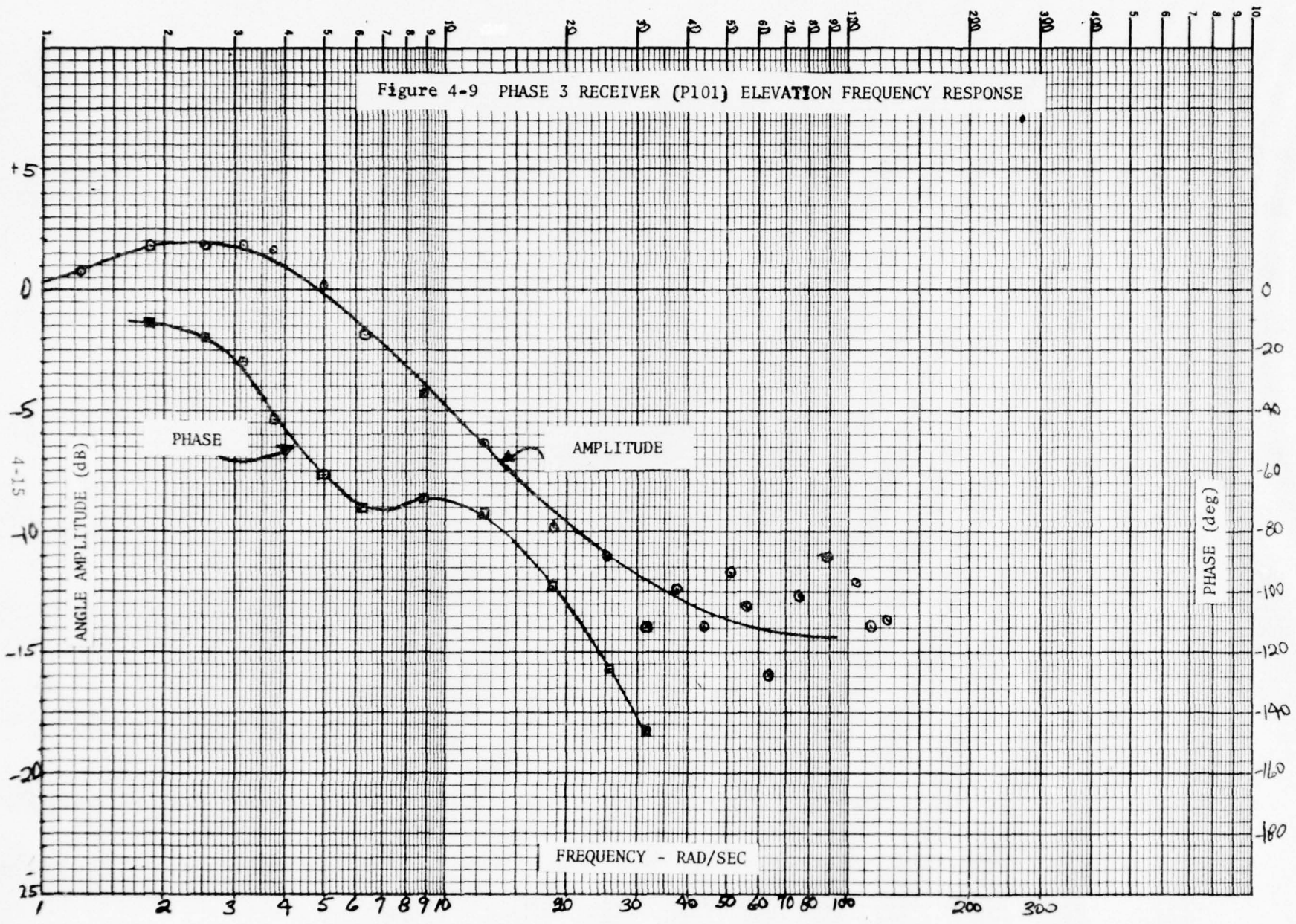

Figure 4-9 PHASE 3 RECEIVER (P101) ELEVATION FREQUENCY RESPONSE

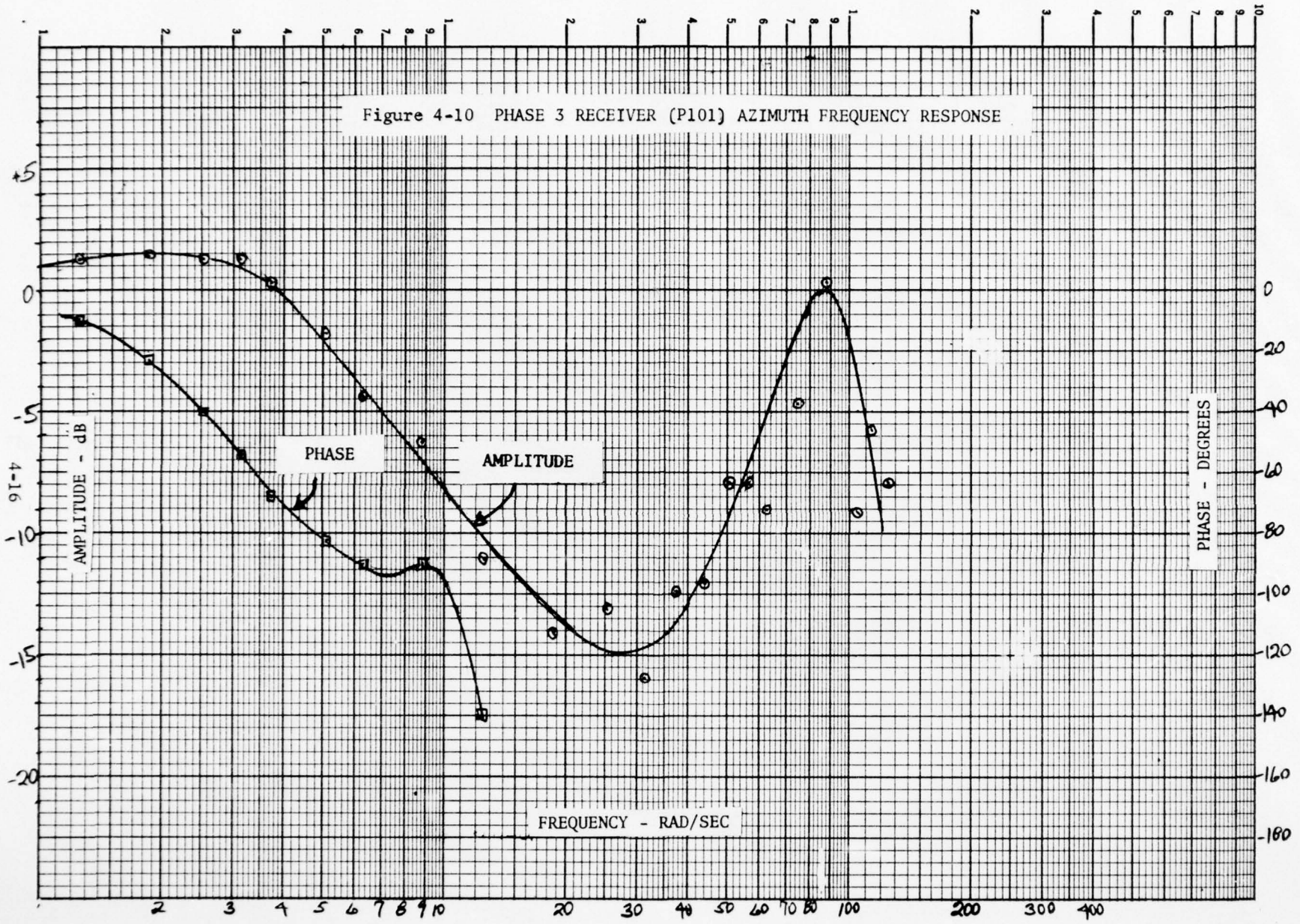
Figure 4-10 PHASE 3 RECEIVER (P101) AZIMUTH FREQUENCY RESPONSE
AMPLITUDE - dB
PHASE - DEGREES
PHASE
AMPLITUDE
FREQUENCY - RAD/SEC
+5
0
-5
-10
-15
-20
0
-20
-40
-60
-80
-100
-120
-140
-160
-180
2 3 4 5 6 7 8 9 10 20 30 40 50 60 70 80 100 200 300 400

Figure 4-11 PHASE 3 RECEIVER (P101) ELEVATION RESPONSE TO A +0.1 DEG STEP

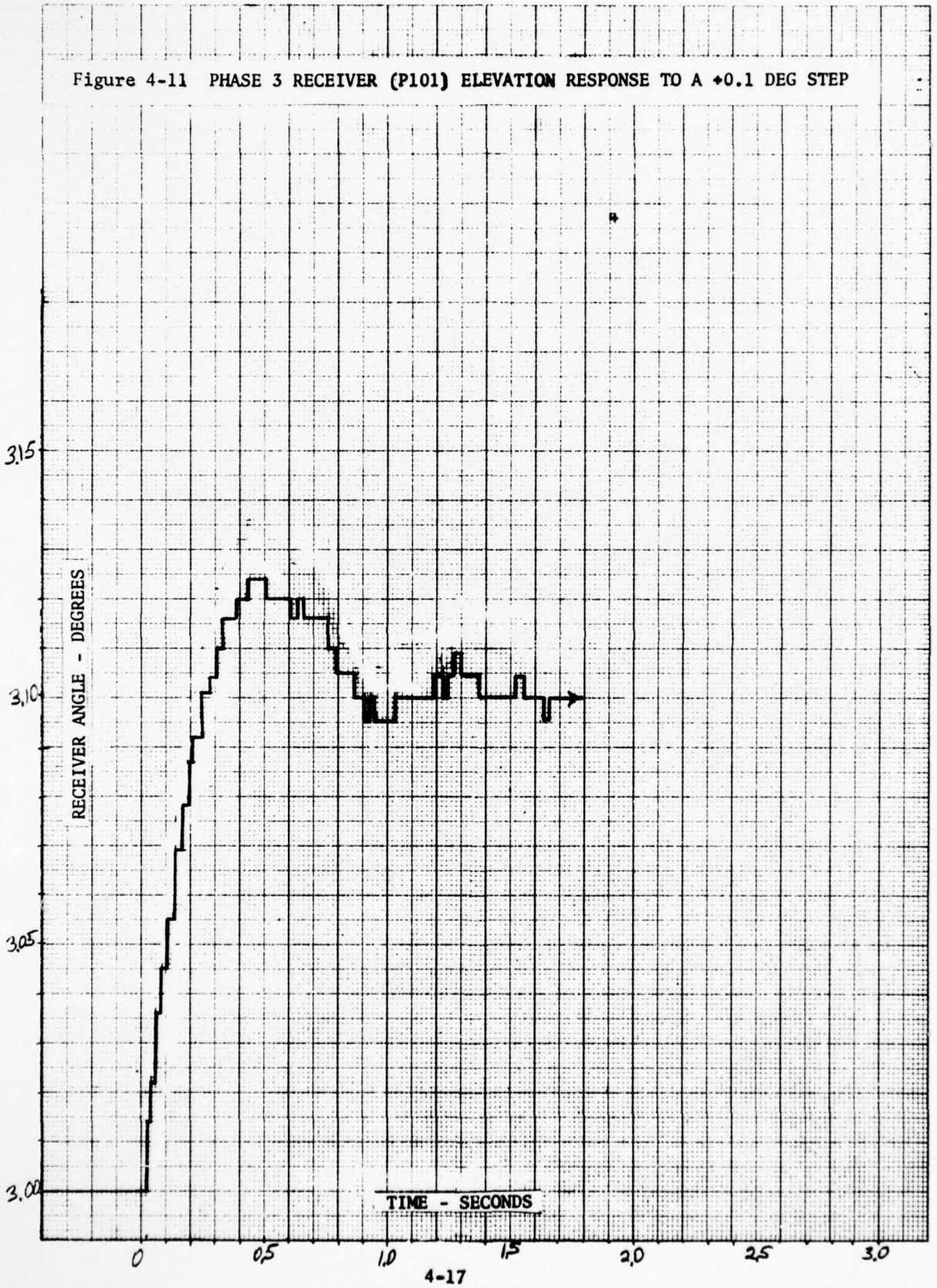

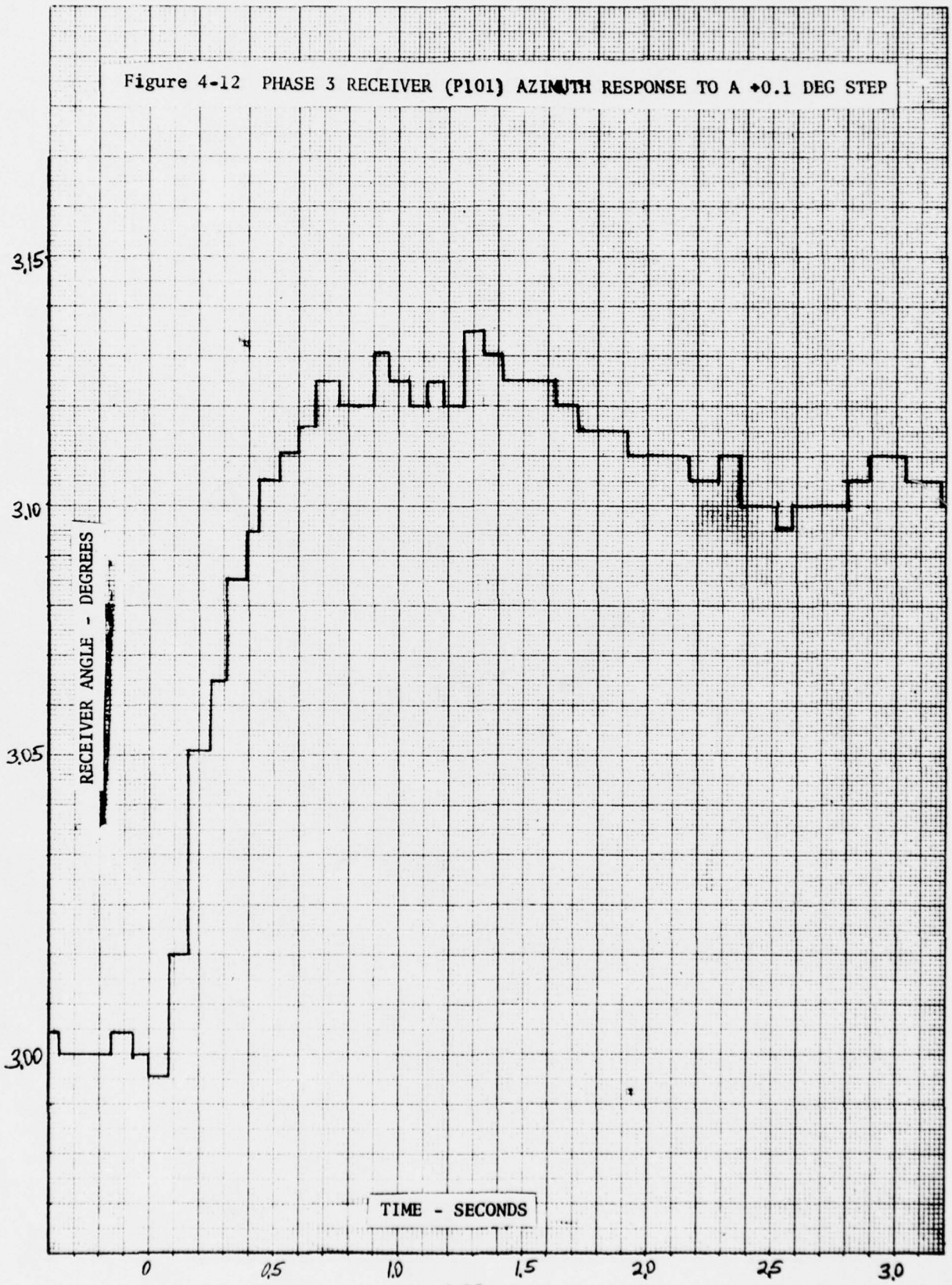
Figure 4-12 PHASE 3 RECEIVER (P101) AZIMUTH RESPONSE TO A +0.1 DEG STEP
3.15
3.10
3.05
3.00
RECEIVER ANGLE - DEGREES
TIME - SECONDS
0
0.5
1.0
1.5
2.0
2.5
3.0

Figure 4-13 PHASE 3 RECEIVER (P101) ELEVATION RESPONSE TO A ◆0.5 DEG/SEC RAMP

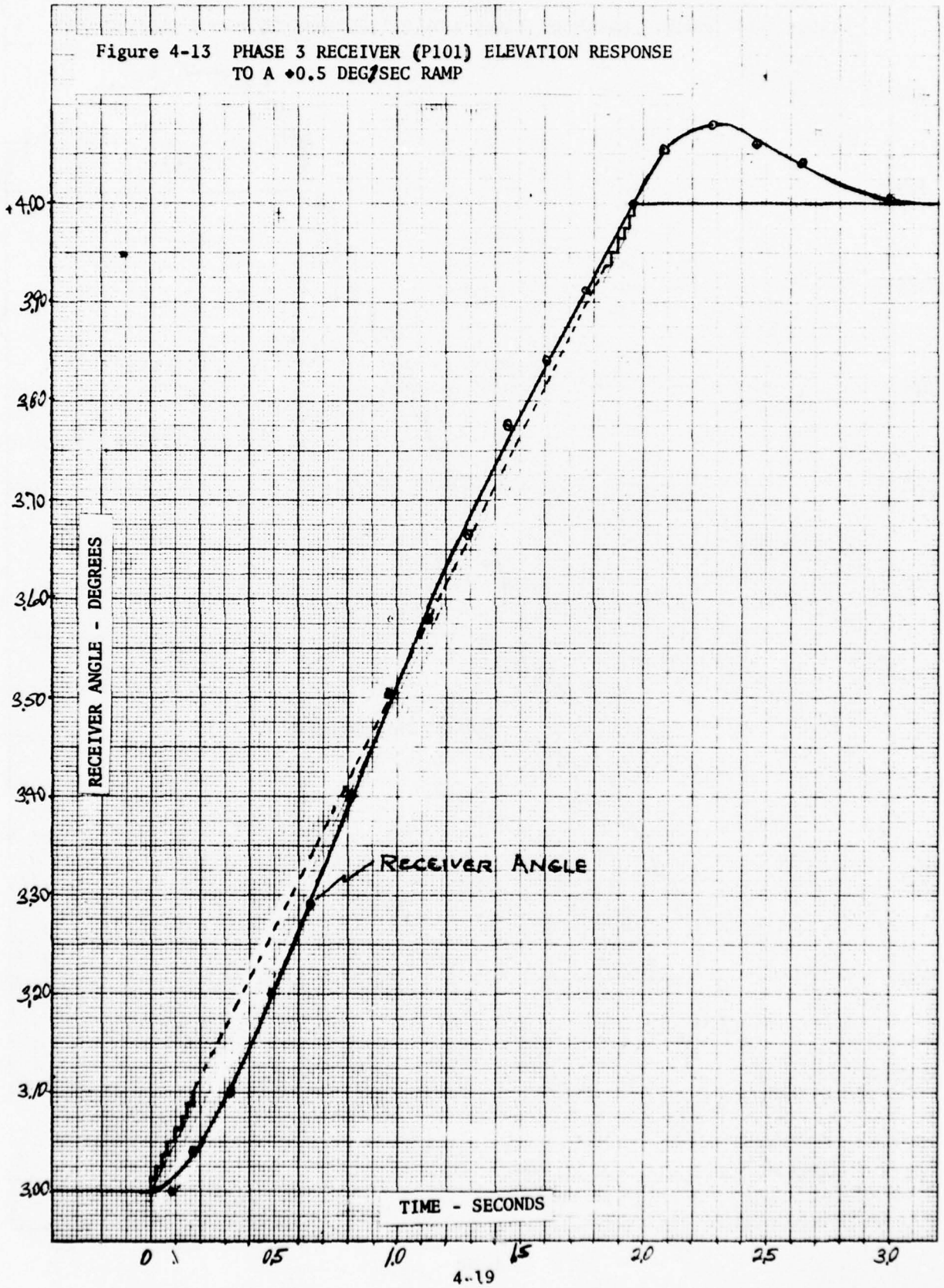

Figure 4-14 PHASE 3 RECEIVER (P101) AZIMUTH RESPONSE TO A ±0.5 DEG/SEC STEP

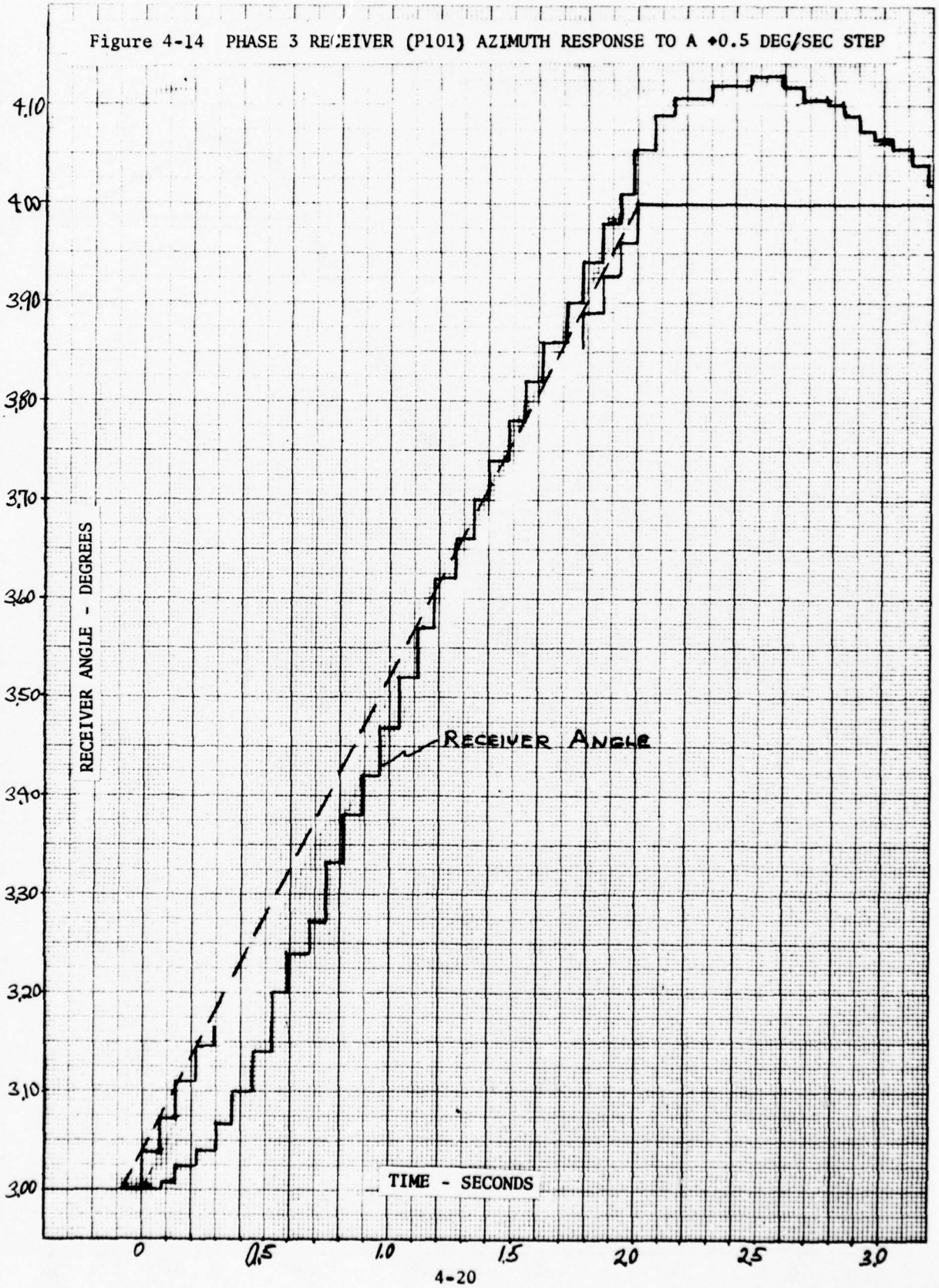

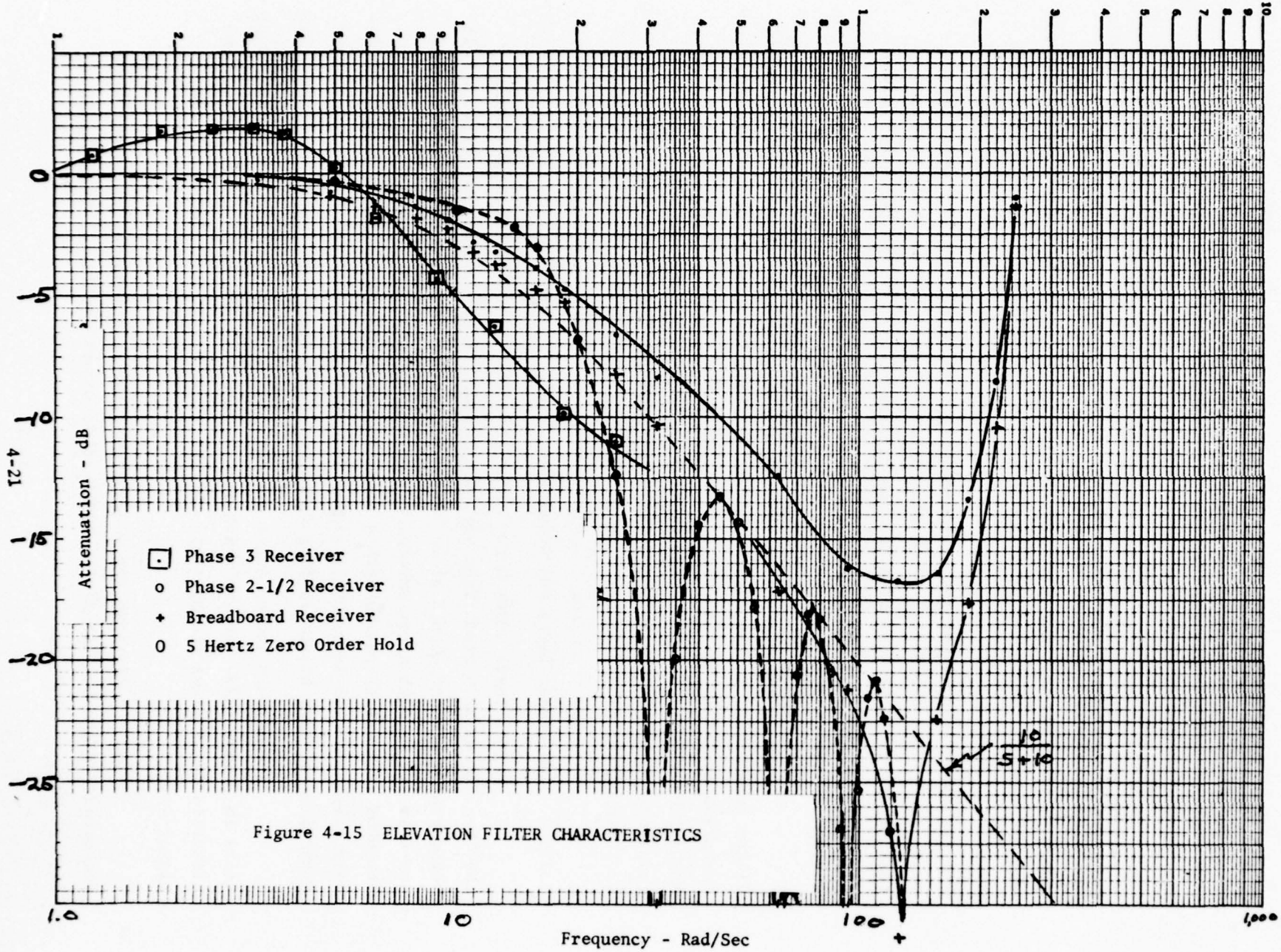

Figure 4-15 ELEVATION FILTER CHARACTERISTICS

Figure 4-16 shows the results of statistical plots for the AWOP B2 elevation multipath scenario described in Section 4.4.1. These data were taken with the breadboard receiver and the raw data for each run was stored in the computer and then filtered with the Phase 2 1/2 receiver 10 radian/second filter and the 8-point average, 5 Hz data rate. The statistics on the mean shift are identical, however, the rms error is less when filtered for th, 5 Hz data rate. The α,β filter algorithms were not available when these data were taken so no test results are available. From the filter response curves it is apparent that errors would be less with the α,β filter.

4.2.2 Slew Rate Limiter

A rate limiter of 1 deg/sec operating on the data before the 10 radian filter is included in the Phase 2 1/2 flight test receiver. For certain multipath scenarios it was found that the slew rate limiter significantly increases the mean error. See the screen test results in Section 4.4.2. In the Phase 3 receivers the rate limiter operates on the data after the 10 radian filter where it has no significant effect on the mean error.

4.2.3 Low Signal Level and Acquisition Tests

Signal level tests were run on four Phase 3 receivers to determine the level at which system flags were displayed. Flags occurred at signal levels between -104 dBm and -106.5 dBm. These results are shown in Figures 4-17, 4-18 and 4-19 for azimuth angle errors, missed angle frames and missed DPSK decodes. The DPSK data are by-passed with a simulator synchronization pulse for the angle-only tests. A high level angle signal is used for the DPSK missed decodes tests. Typical error time histories from these tests are shown in Figures 4-20 and 4-21.

The azimuth coding angle was varied from 0° to 40° for the signal level tests in Figure 4-22. No variation is apparent with the angle code. Error time histories for various coding angles are shown in Figure 4-23 for a -65 dBm signal level.

Figure 4-24 shows the acquisition time as a function of signal level for elevation and azimuth data. Acquisition occurs within 1.5 seconds for signals down to -100 dBm.

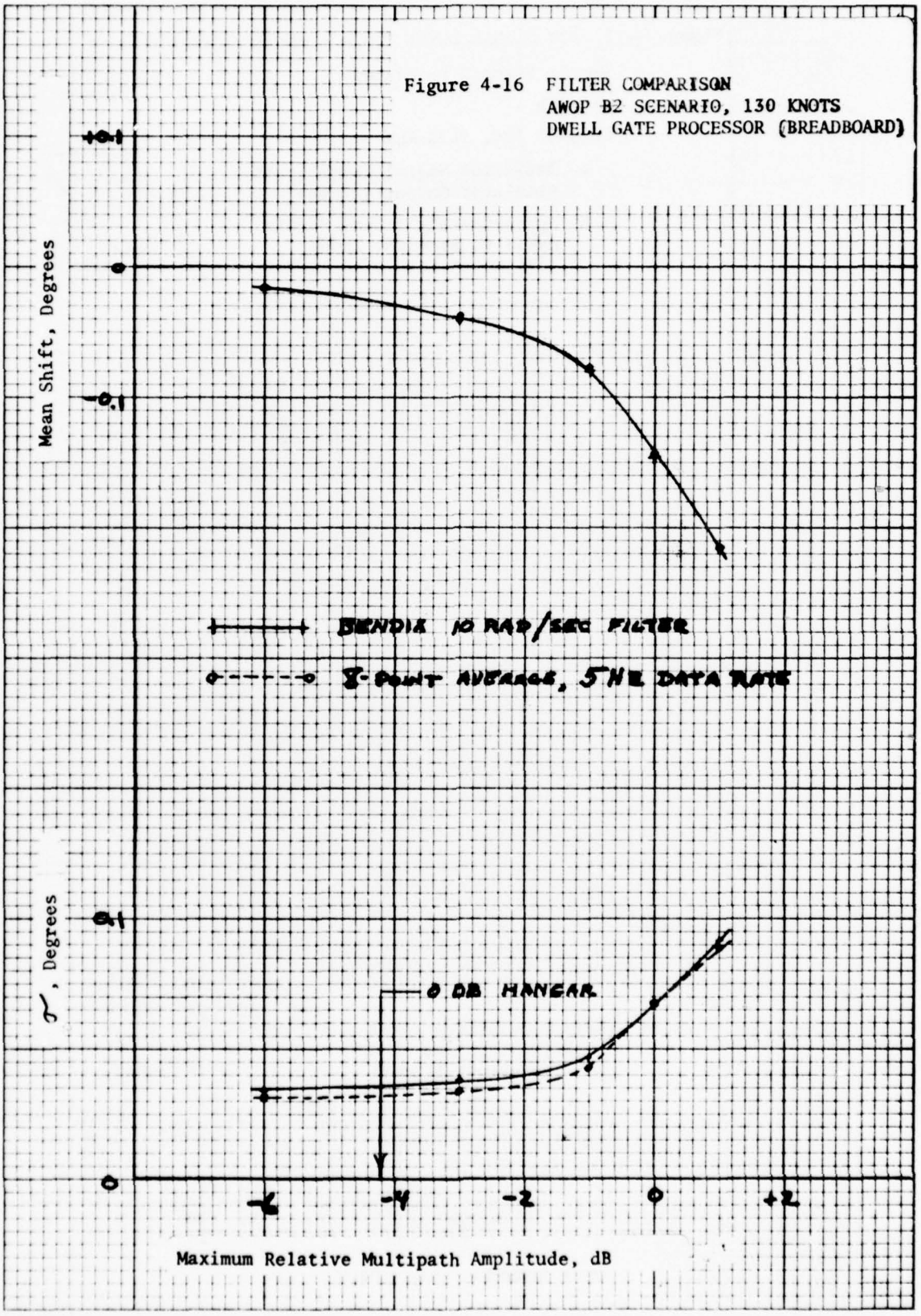

Figure 4-16 FILTER COMPARISON
AWOP B2 SCENARIO, 130 KNOTS
DWELL GATE PROCESSOR (BREADBOARD)

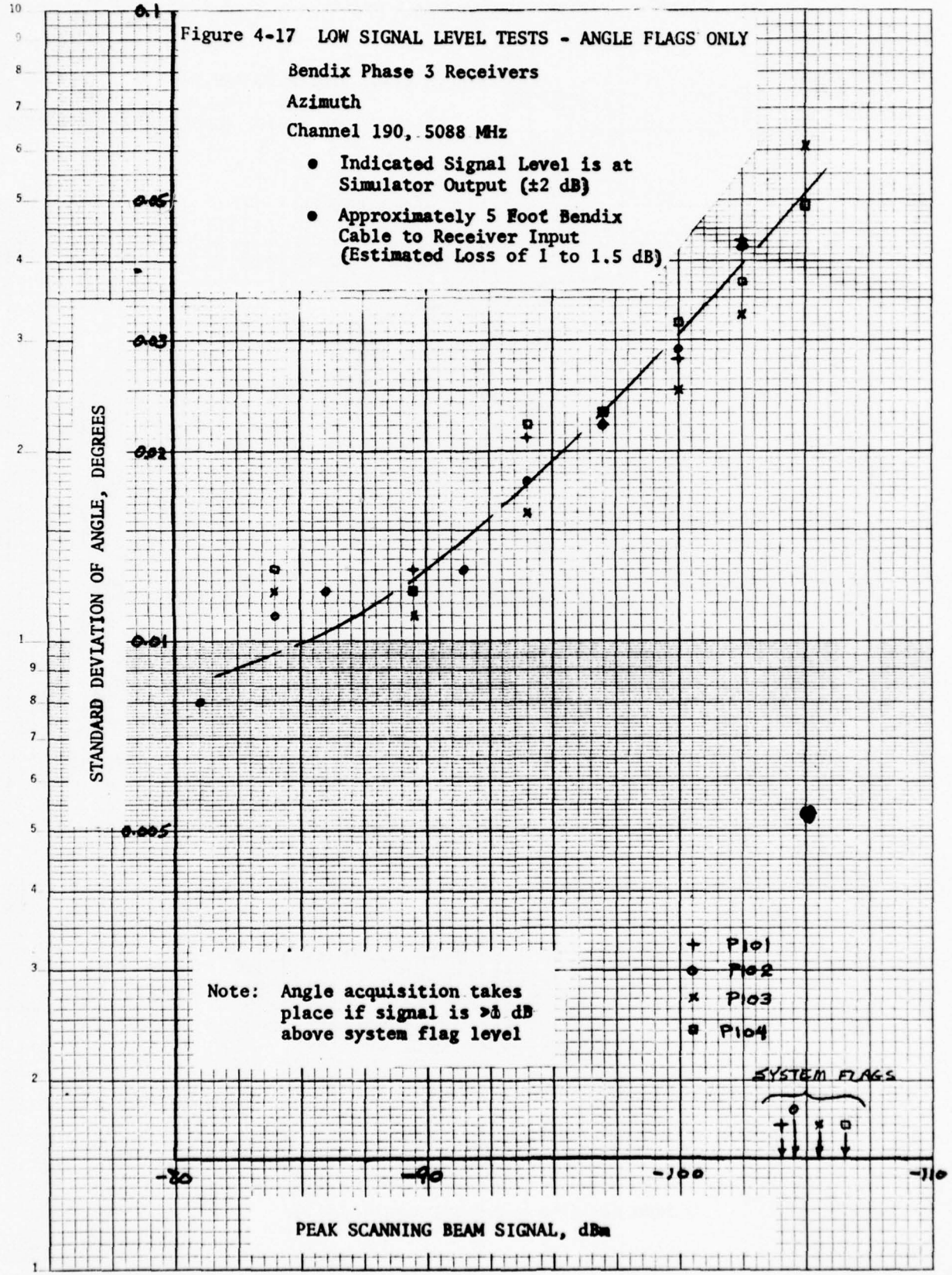
Figure 4-17 LOW SIGNAL LEVEL TESTS - ANGLE FLAGS ONLY
Bendix Phase 3 Receivers
Azimuth
Channel 190, 5088 MHz
• Indicated Signal Level is at Simulator Output (±2 dB)
• Approximately 5 Foot Bendix Cable to Receiver Input (Estimated Loss of 1 to 1.5 dB)
STANDARD DEVIATION OF ANGLE, DEGREES
0.1
0.05
0.03
0.02
0.01
0.005
Note: Angle acquisition takes place if signal is >8 dB above system flag level
P101
P102
P103
P104
SYSTEM FLAGS
-80
-90
-100
-110
PEAK SCANNING BEAM SIGNAL, dBm

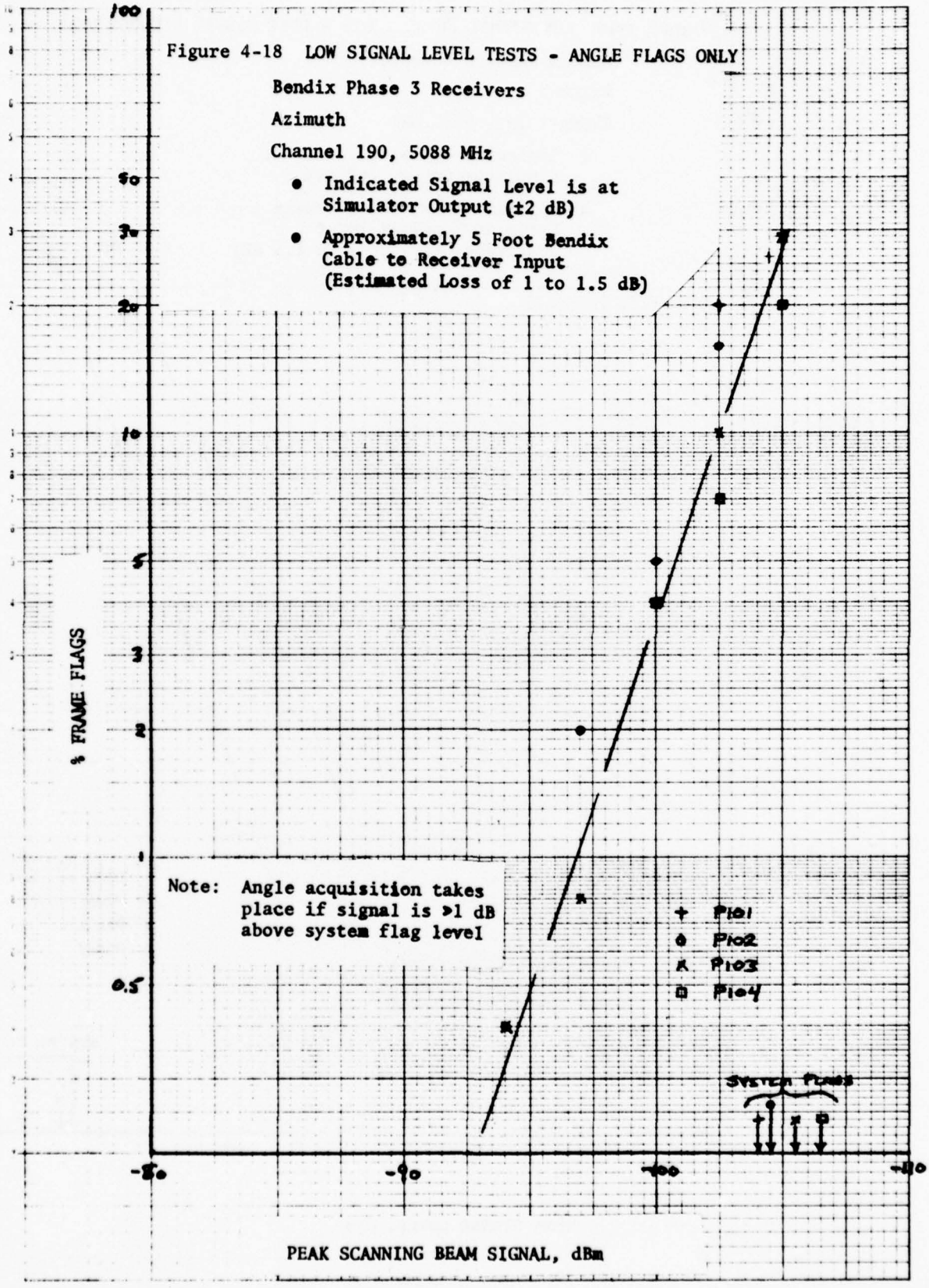

Figure 4-18 LOW SIGNAL LEVEL TESTS - ANGLE FLAGS ONLY

Bendix Phase 3 Receivers

Azimuth

Channel 190, 5088 MHz

- Indicated Signal Level is at Simulator Output (±2 dB)
- Approximately 5 Foot Bendix Cable to Receiver Input (Estimated Loss of 1 to 1.5 dB)

Figure 4-19 LOW SIGNAL LEVEL TESTS - DPSK MISSED DECODES ONLY

Bendix Phase 3 Receivers

Azimuth

Channel 190, 5088 MHz

- Indicated Signal Level is at Simulator Output (±2 dB)
- Approximately 5 Foot Bendix Cable to Receiver Input (Estimated Loss of 1 to 1.5 dB)

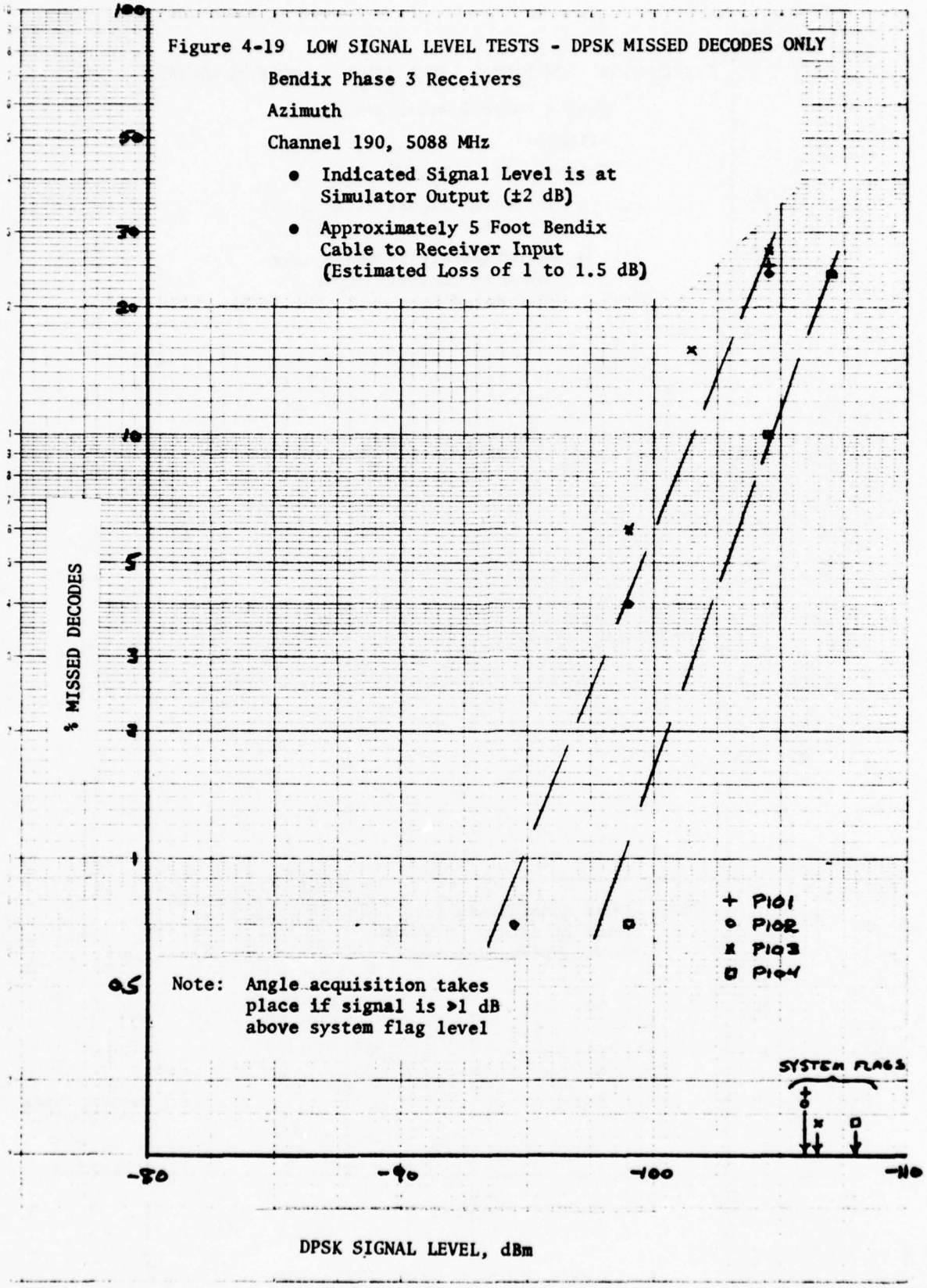

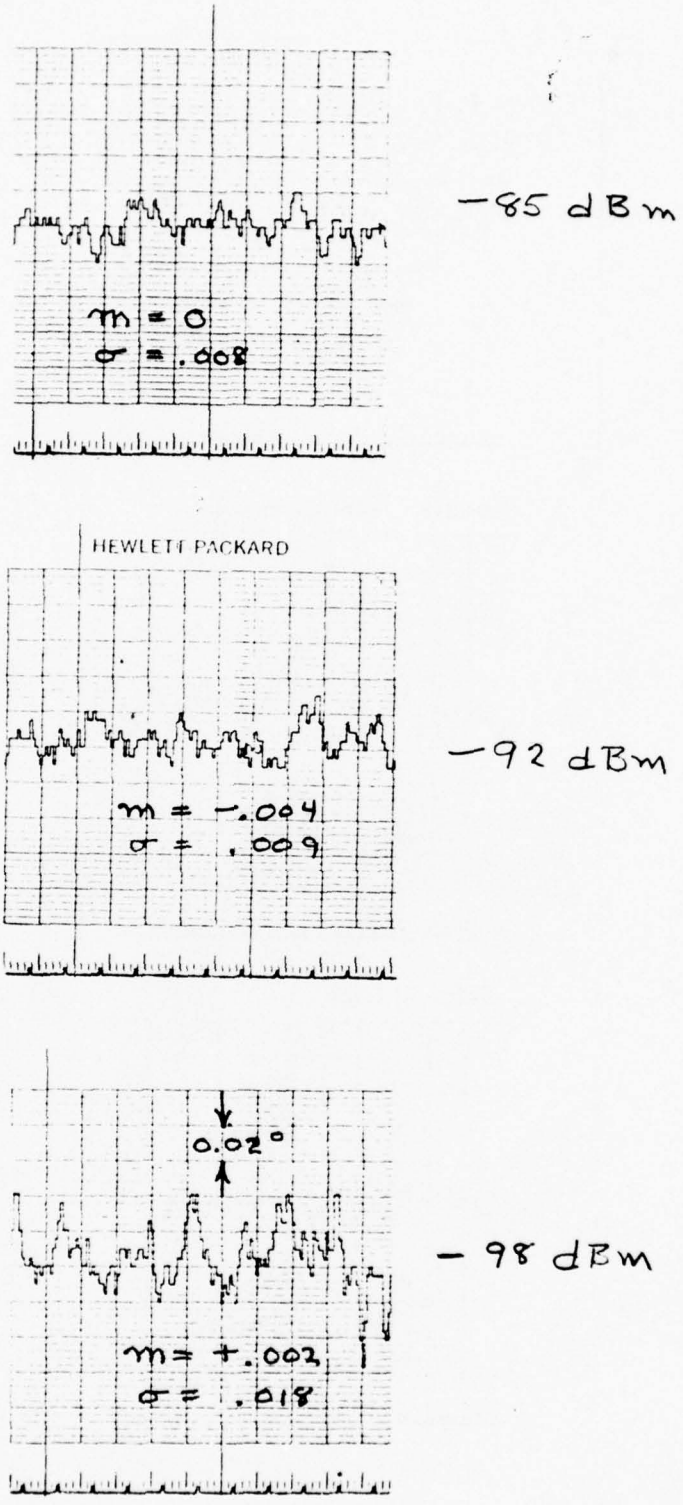

Figure 4-20 AZIMUTH 0° ERROR TIME HISTORIES
Phase 3 RECEIVER

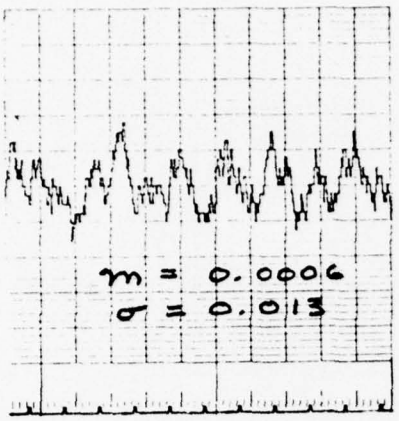

-99 dBm

'80-0258 PRINTED IN U.S.A.

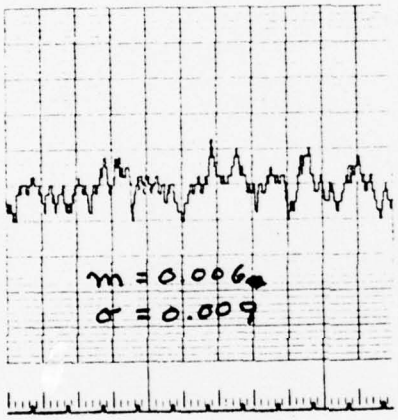

-93 dBm

RINTED IN U.S.A.

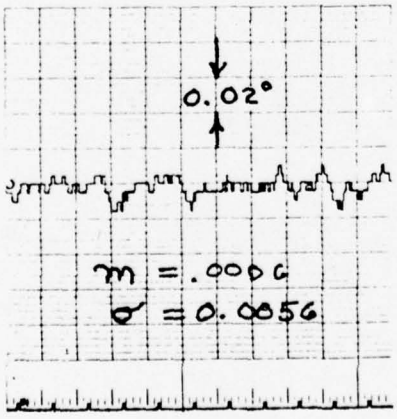

-65 dBm

Figure 4-21 ELEVATION ERROR TIME HISTORIES
PHASE 3 RECEIVER

Figure 4-22 STANDARD DEVIATION OF ERROR VS. SIGNAL LEVEL
PHASE 3 RECEIVER P102
AZIMUTH - ANGLE VARIED

Note: Statistics were not acquired for azimuth angles or 30° and 40° but plots were indistinguishable from those at smaller angles.

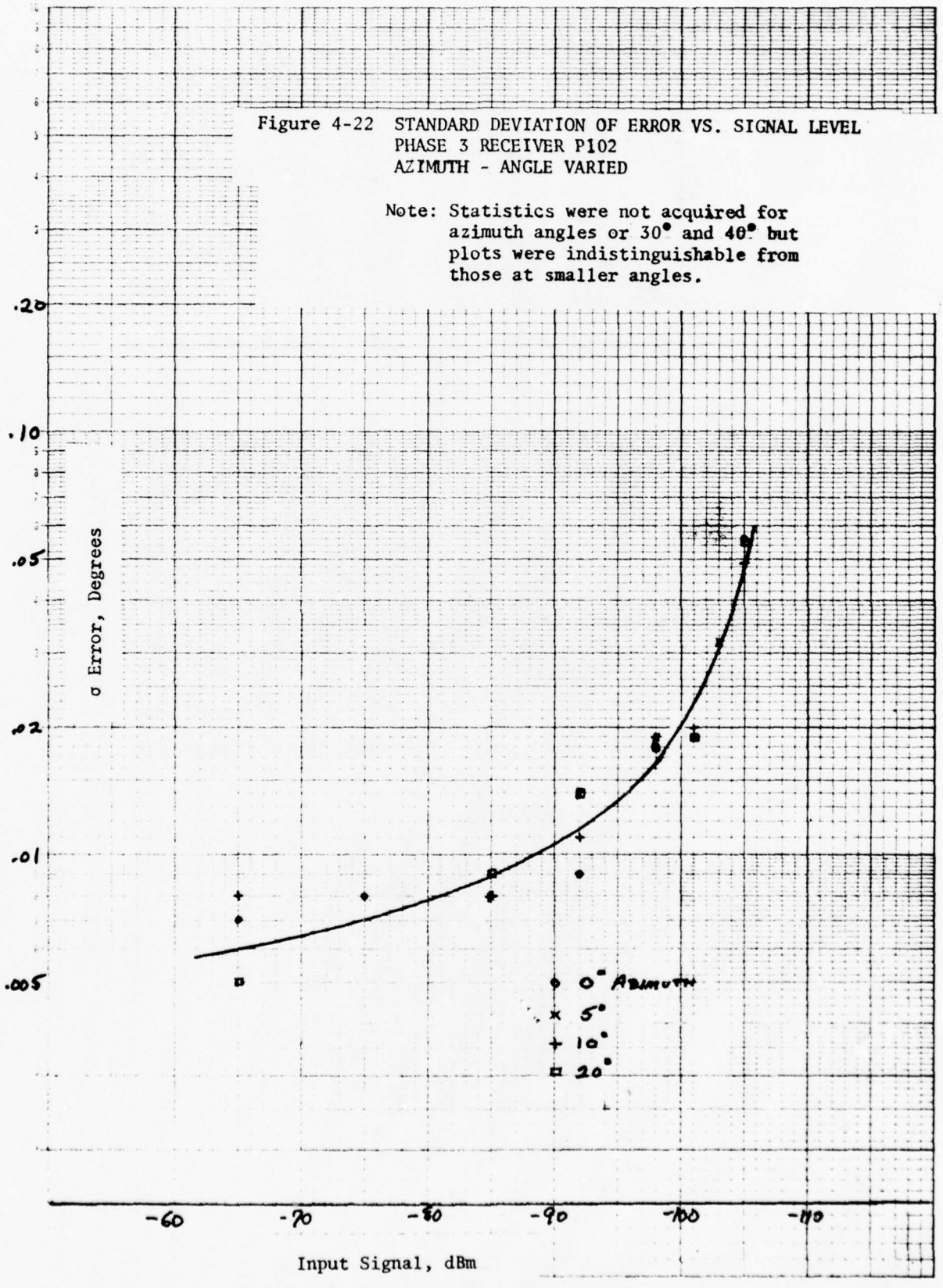

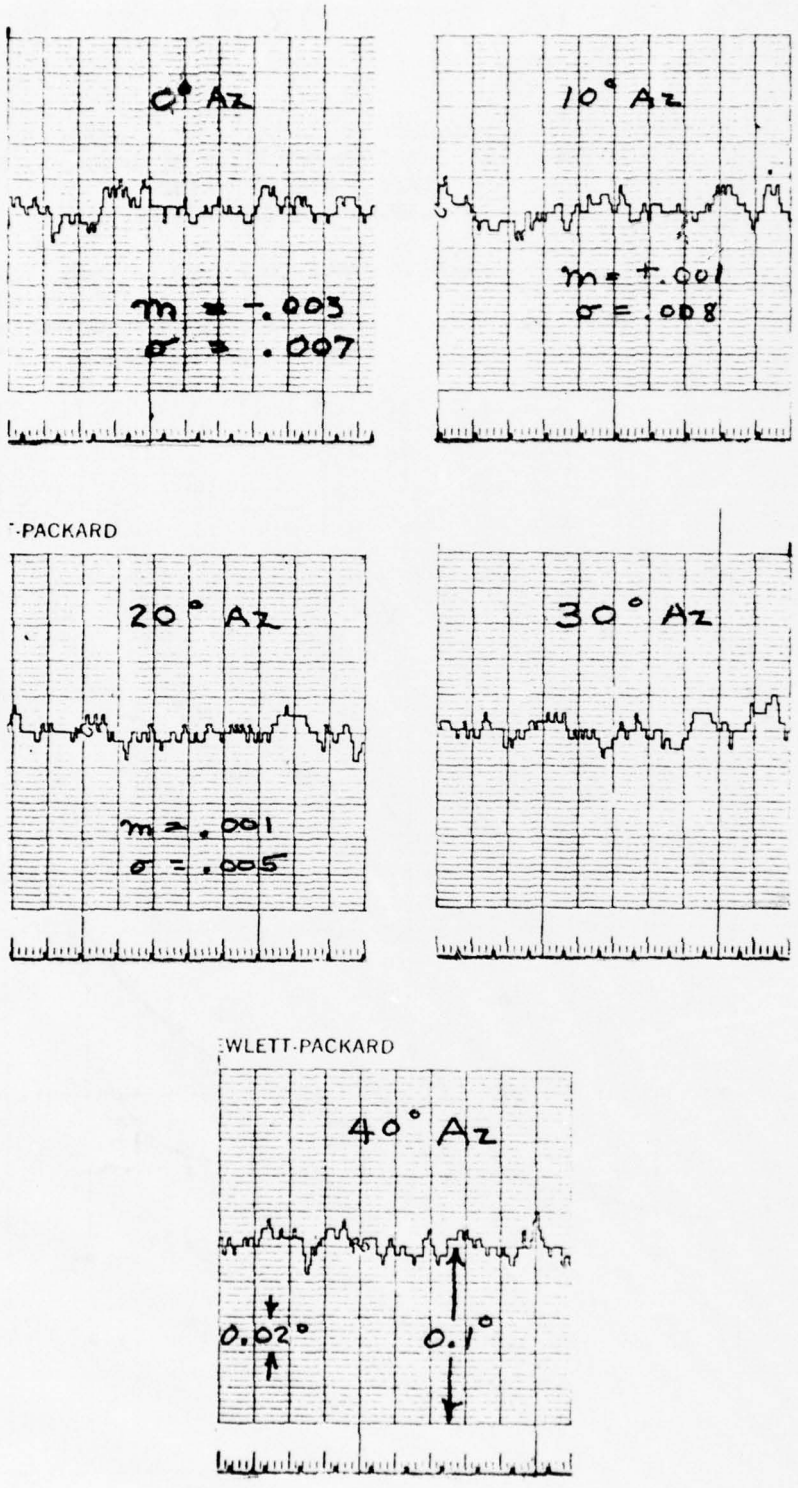

Figure 4-23 AZIMUTH ERROR TIME HISTORIES
-65 dBm SIGNAL, PHASE 3 RECEIVER

Figure 4-24 ACQUISITION TIME, PHASE 3 RECEIVER P102
o AZIMUTH
+ ELEVATION

DPSK was 12 dB above Signal (no missed decodes)

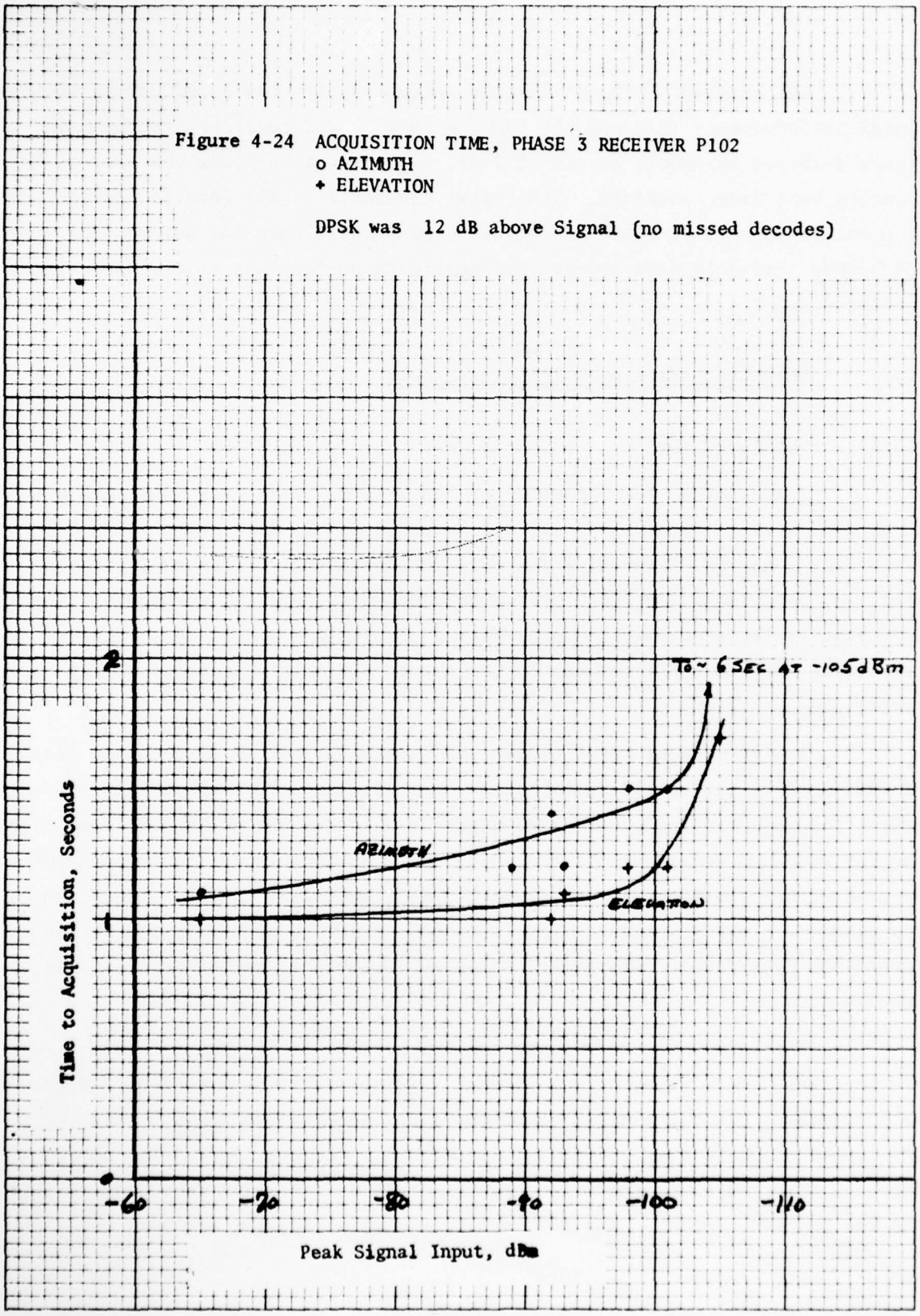

The setting of the dwell gate threshold also has an effect on the low signal performance. Test results for the Phase 2 1/2 receiver are shown in Figure 4-25 for threshold levels of 2 dB, 3 dB, and 4 dB below the peak of the scanning beam video waveform. The higher threshold (2 dB) results in receiver drop out (system flag) at a 2 dB higher signal level than the normal 3 dB setting. The higher threshold does improve the multipath performance as discussed in Section 4.3.3.

4.3 Characteristics of Multipath Effects

4.3.1 Baseline Tests

The baseline tests consist of ten seconds of in-beam multipath with fixed parameters. These tests are not intended to simulate any multipath situation. They do, however, illustrate the dependence of the multipath induced errors on individual multipath parameters and processor configurations. These dependencies are generally obscured during simulations of actual multipath situations (or during flight tests) because of the multiplicity of simultaneous variations occurring.

The results of these tests, the multipath induced errors, are plotted as functions of the varied multipath parameters. The error is plotted as two parts; the mean (10 second average) angle change when the multipath is applied, and the standard deviation (or rms value) of the error about the mean. Peak-to-peak errors are typically about three times the standard deviation. The raw data, on a scan-by-scan basis, is passed through a 10 radian per second cutoff low-pass single pole filter or an α-β filter before the error statistics are computed.

The baseline test results are illustrated in Figures 4-26 and 4-27 for the Phase 2 1/2 receiver and Figures 4-28 and 4-29 for the Phase 3 receiver. Both receivers exhibit similar error characteristics. The Phase 3 receiver has larger standard deviations at low scalloping frequencies due to the overshoot in the data smoothing filter at 0.3 Hz (the scalloping frequency selected for the baseline tests). The mean errors for this receiver are smaller,

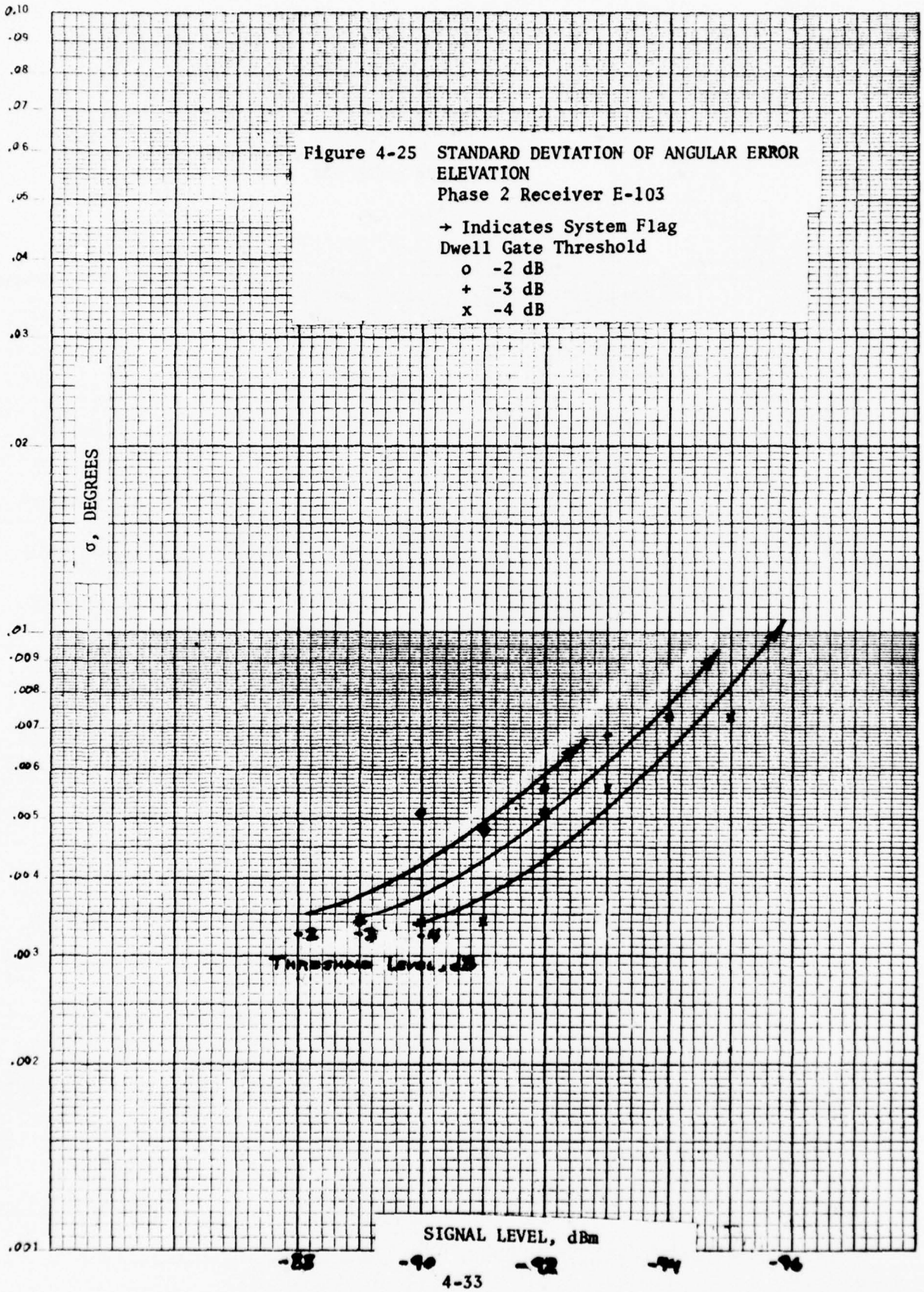

Figure 4-25 STANDARD DEVIATION OF ANGULAR ERROR ELEVATION
Phase 2 Receiver E-103

→ Indicates System Flag
Dwell Gate Threshold
o -2 dB
+ -3 dB
x -4 dB

Figure 4-26 ELEVATION BASELINE TESTS
Bendix Receiver E-104, Phase 2 1/2
-3 dB Threshold
0.32 Hz Scalloping Frequency
-20 dB Sidelobes

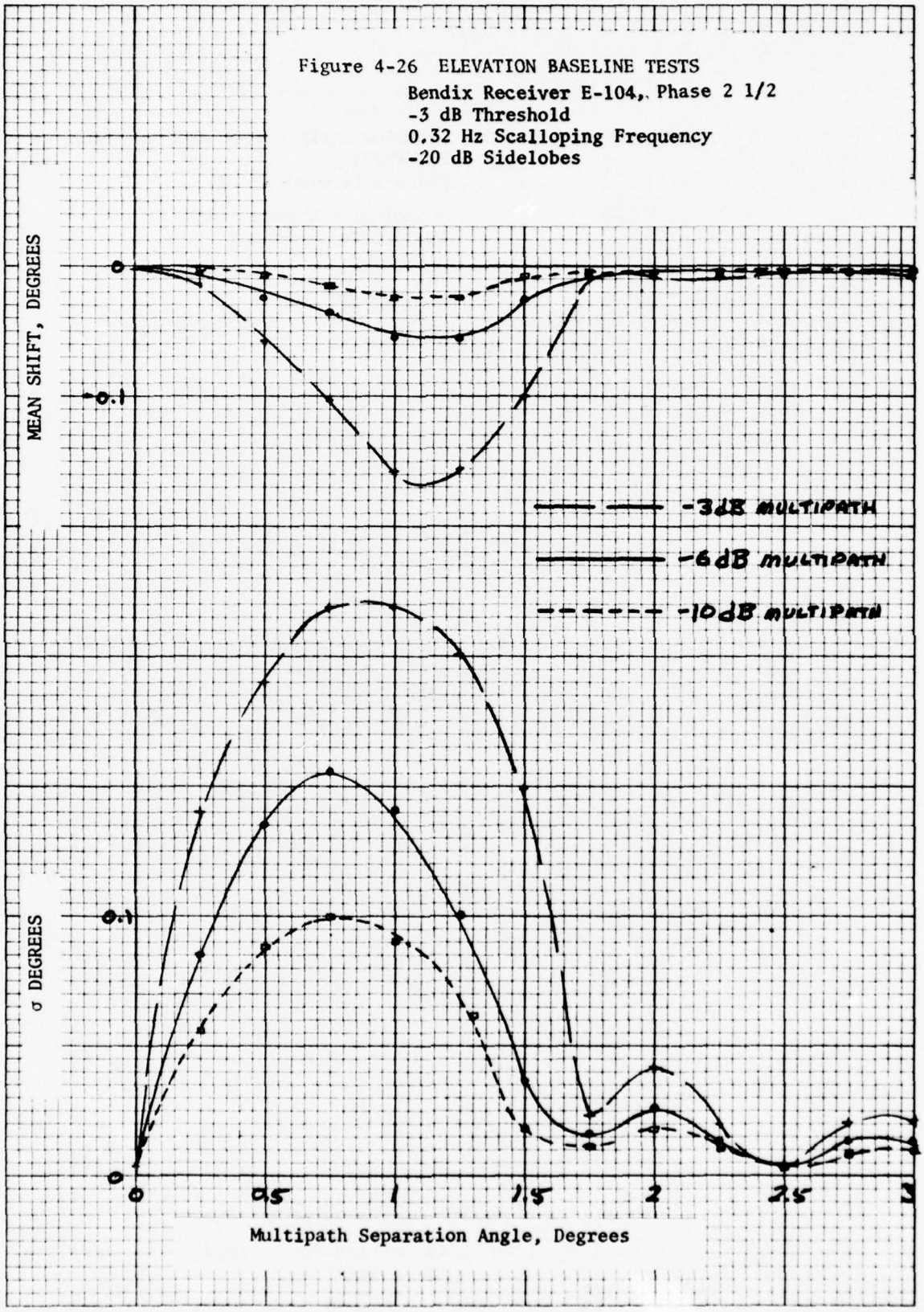

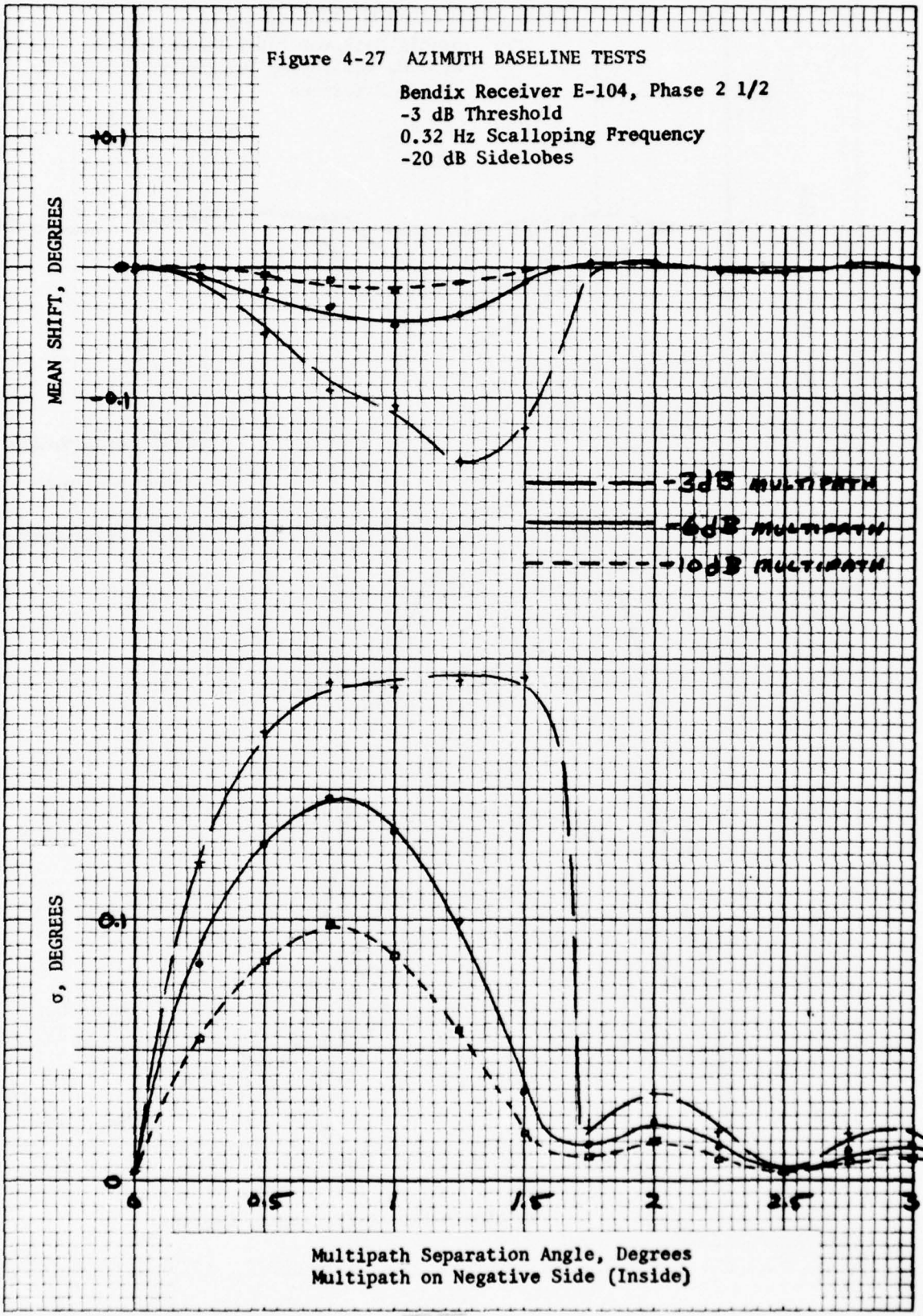
Figure 4-27 AZIMUTH BASELINE TESTS
Bendix Receiver E-104, Phase 2 1/2
-3 dB Threshold
0.32 Hz Scalloping Frequency
-20 dB Sidelobes
MEAN SHIFT, DEGREES
+0.1
-0.1
-3dB MULTIPATH
-6dB MULTIPATH
-10dB MULTIPATH
σ, DEGREES
0.1
0
0
0.5
1
1.5
2
2.5
3
Multipath Separation Angle, Degrees
Multipath on Negative Side (Inside)

Figure 4-28 ELEVATION BASELINE TESTS
Bendix Receiver P101, Phase 3
0.32 Hz Scalloping Frequency
-20 dB Sidelobes

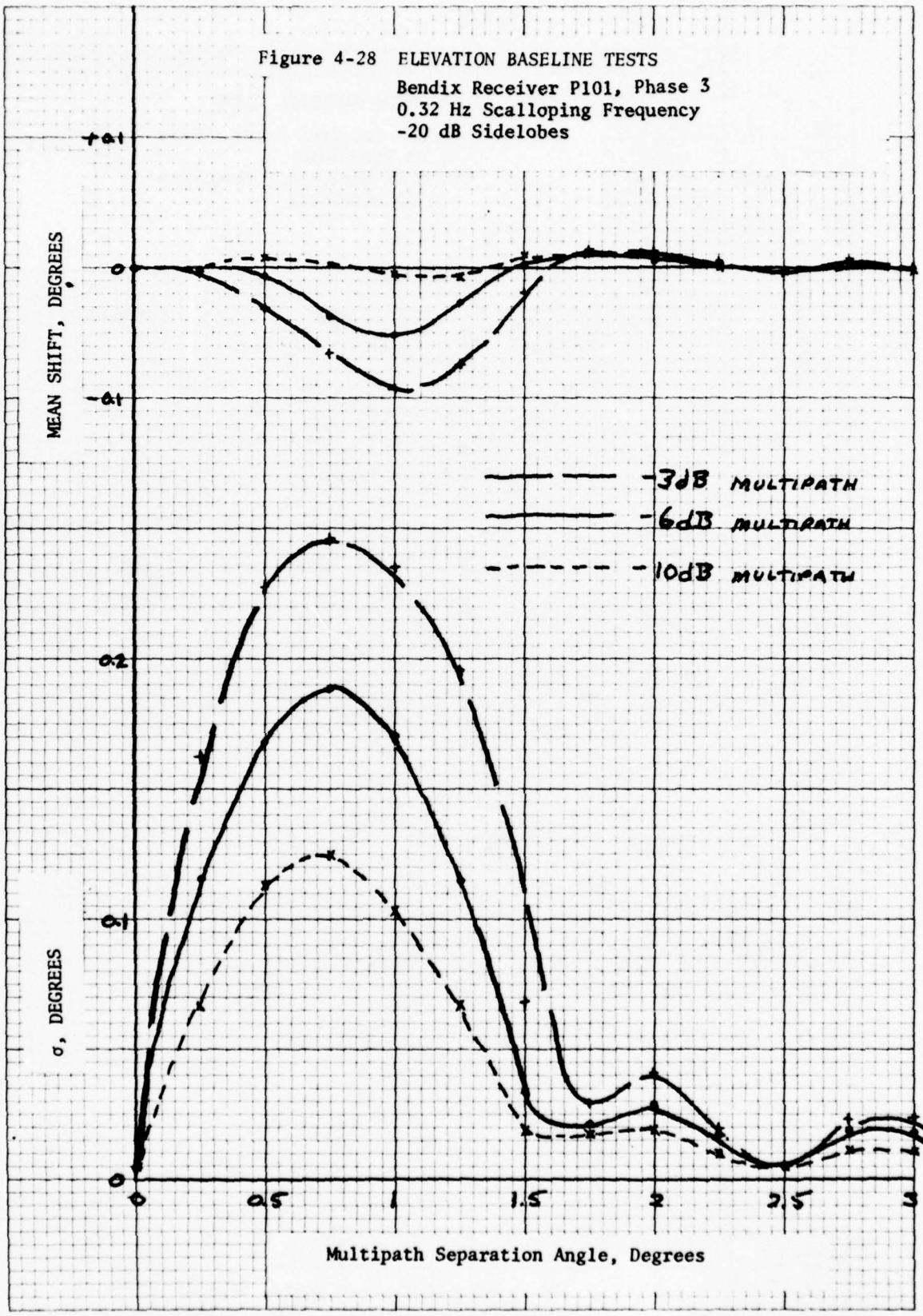

Figure 4-29 AZIMUTH BASELINE TESTS

Bendix Receiver P101, Phase 3
0.32 Hz Scalloping Frequency
-20 dB Sidelobes

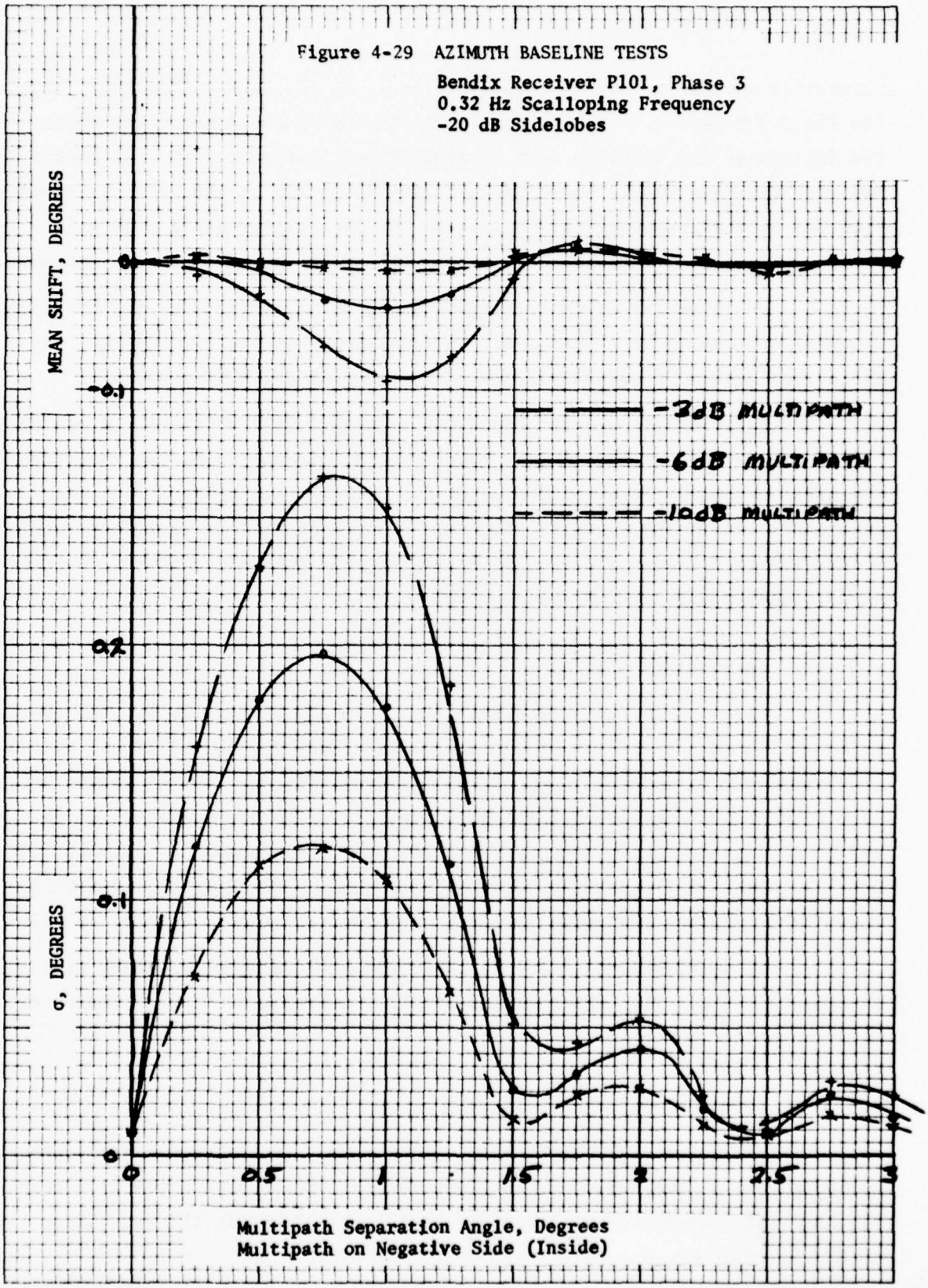

apparently due to the narrow tracking gates. At the higher scalloping frequencies the Phase 3 receiver exhibits improved filtering of the error. The effect of the two filters on the baseline test is illustrated in Figure 4-30. In Figure 4-31 the elevation errors are shown for baseline tests run at the 0.32 Hz normally used and at the frequency (0.8 Hz) where the data filter has a 0 dB gain. The effects of the filter overshoot are apparent on the noise error measurements.

The symmetry of the multipath error is illustrated by the baseline azimuth tests shown in Figure 4-32. The multipath is placed on both sides of the direct beam with complete symmetry in the bias and noise errors.

Early baseline tests reported in Calspan TN-4 of a Phase 2 1/2 receiver showed smaller errors than those reported here. It was felt that variation in the dwell gate threshold could account for the discrepancy so a test was run that bears out this hypothesis (Figure 4-33). When this receiver arrived for tests, the threshold was over 2 dB lower than the nominal -3 dB but this was adjusted and monitored for these tests.

4.3.1.1 Resolution of Tests

Figure 4-34 shows that the resolution capability of the TRSB simulator is about 1/2 dB for the baseline tests. The curves for the -2 dB and -2 1/2 dB are based upon the average value of several repetitions. The 10 second baseline test with the rate limiter does show a sensitivity to the multipath phase. This effect plus the error in setting the multipath levels causes a maximum shift in both the mean and the standard deviation of about 0.02 degrees over a series of runs. The computer controlled multipath amplitude has a resolution of 0.25 dB.

These tests were run with the breadboard receiver modified as described in Section 4.3.8. This modification permits operation at 0 dB multipath with well controlled errors.

4.3.2 Effect of Data Rate Jitter

The actual data rate is not regular, but is jittered for azimuth and elevation data. The time between elevation functions varies from 11.2 to 31.2 milliseconds. Twenty-four elevation scans are included in the repetition interval of 592 milliseconds for an average data rate of 40.5 Hz.

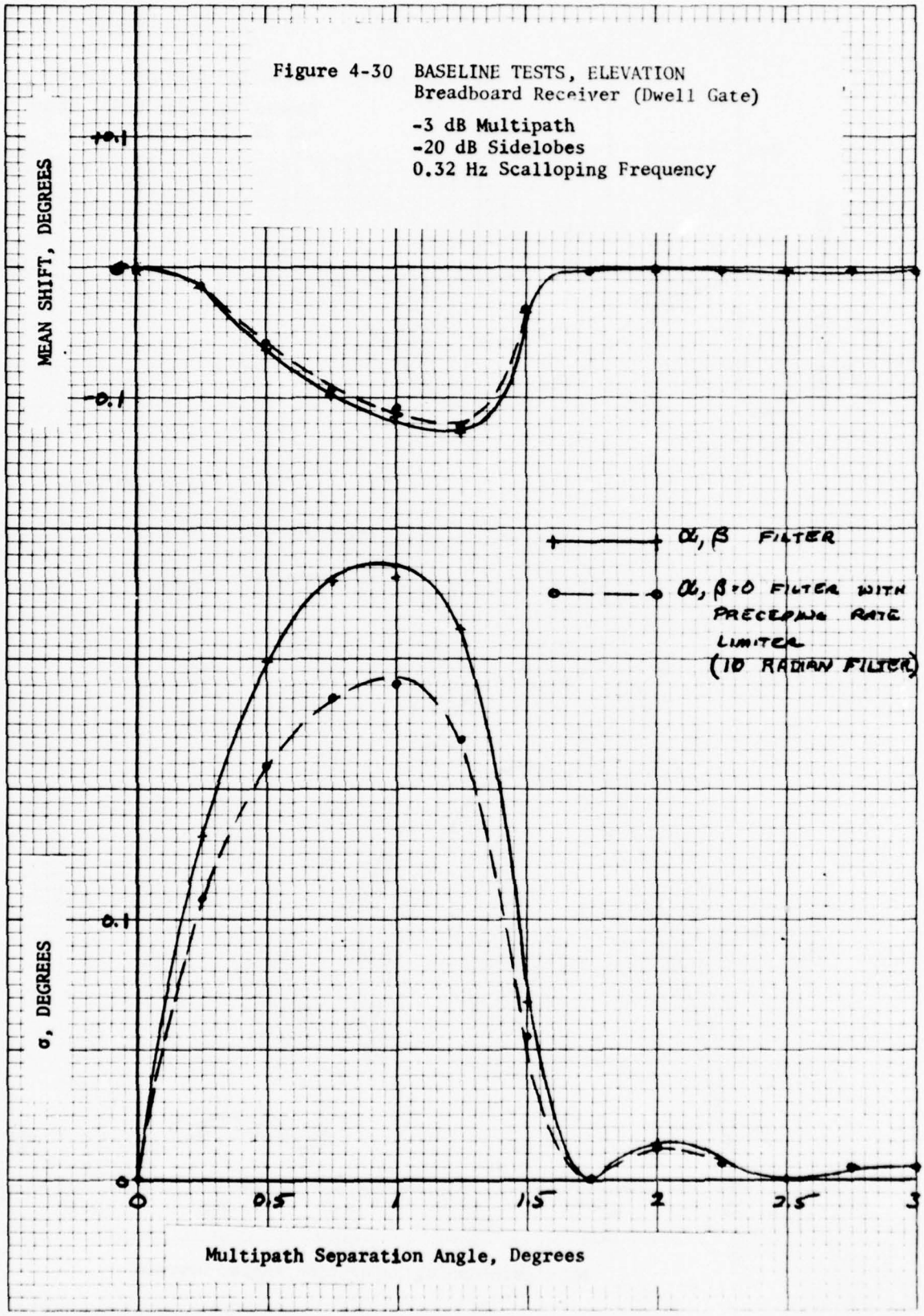

Figure 4-30 BASELINE TESTS, ELEVATION
Breadboard Receiver (Dwell Gate)

-3 dB Multipath
-20 dB Sidelobes
0.32 Hz Scalloping Frequency

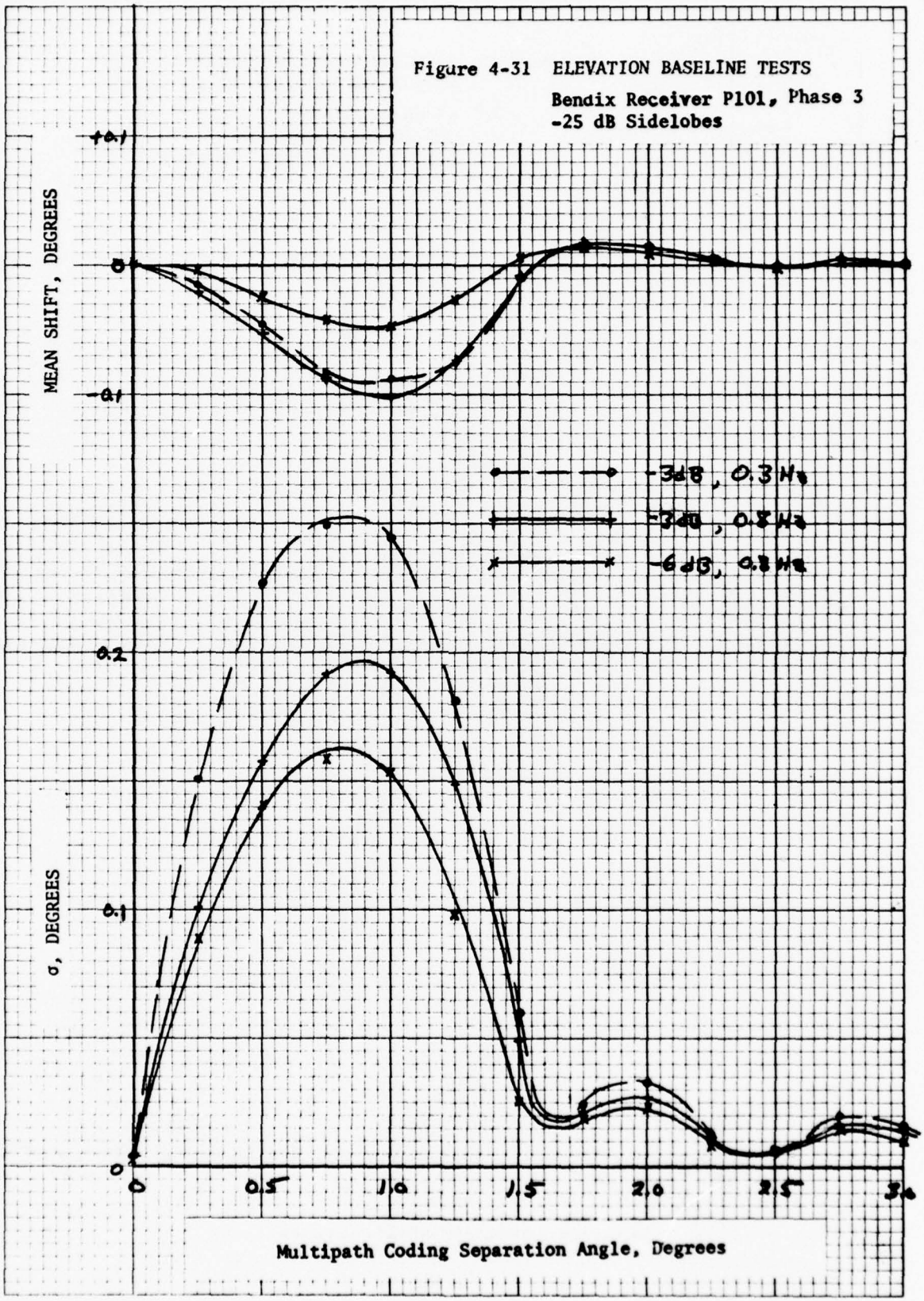
Figure 4-31 ELEVATION BASELINE TESTS
Bendix Receiver P101, Phase 3
-25 dB Sidelobes
MEAN SHIFT, DEGREES
+0.1
0
-0.1
-3dB, 0.3 Hz
-3dB, 0.8 Hz
-6dB, 0.8 Hz
σ, DEGREES
0.2
0.1
0
0
0.5
1.0
1.5
2.0
2.5
3.0
Multipath Coding Separation Angle, Degrees

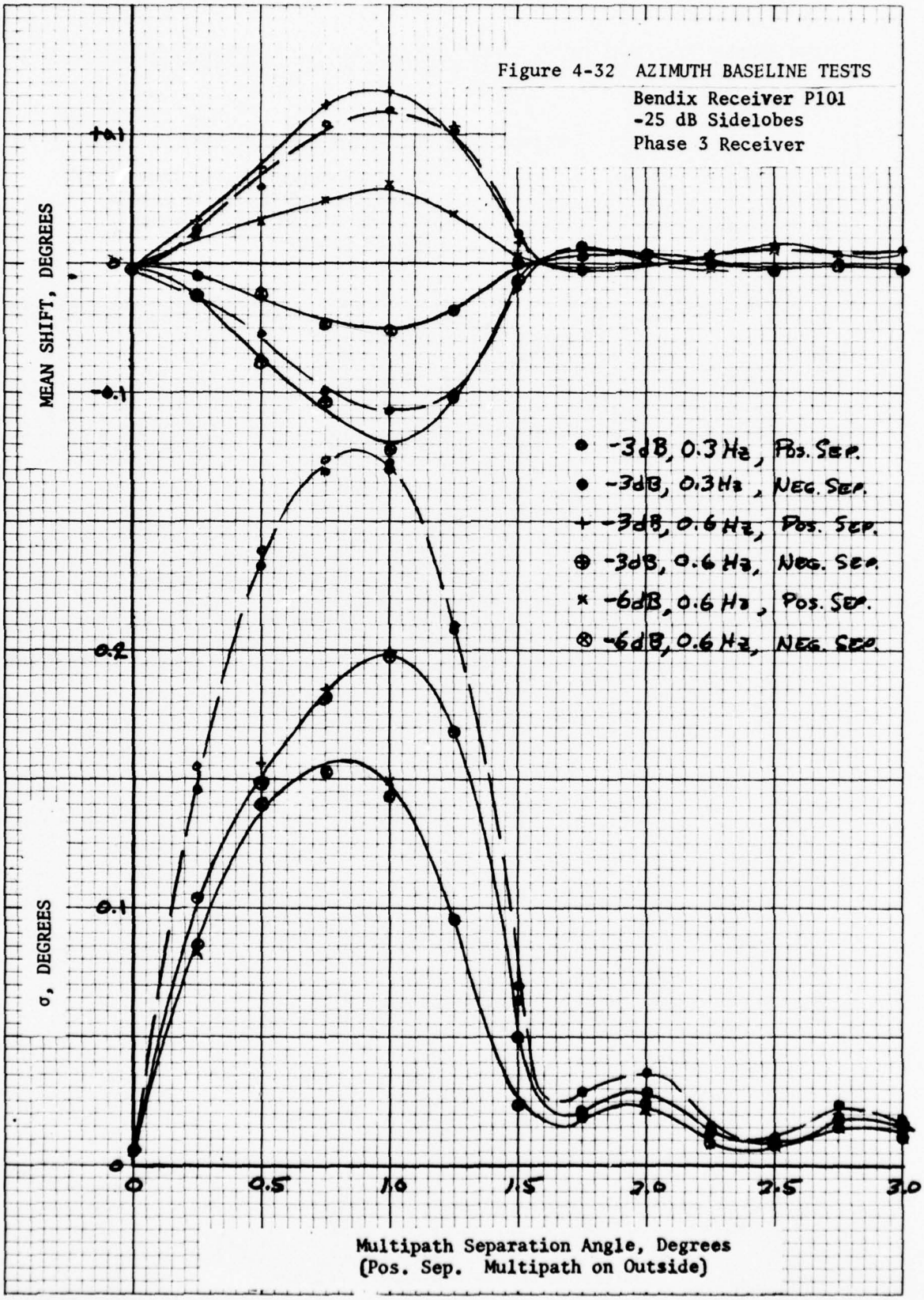
Figure 4-32 AZIMUTH BASELINE TESTS
Bendix Receiver P101
-25 dB Sidelobes
Phase 3 Receiver
MEAN SHIFT, DEGREES
+0.1
0
-0.1
● -3dB, 0.3 Hz, Pos. Sep.
● -3dB, 0.3 Hz, Neg. Sep.
+ -3dB, 0.6 Hz, Pos. Sep.
⊕ -3dB, 0.6 Hz, Neg. Sep.
× -6dB, 0.6 Hz, Pos. Sep.
⊗ -6dB, 0.6 Hz, Neg. Sep.
σ, DEGREES
0.2
0.1
0
0
0.5
1.0
1.5
2.0
2.5
3.0
Multipath Separation Angle, Degrees
(Pos. Sep. Multipath on Outside)

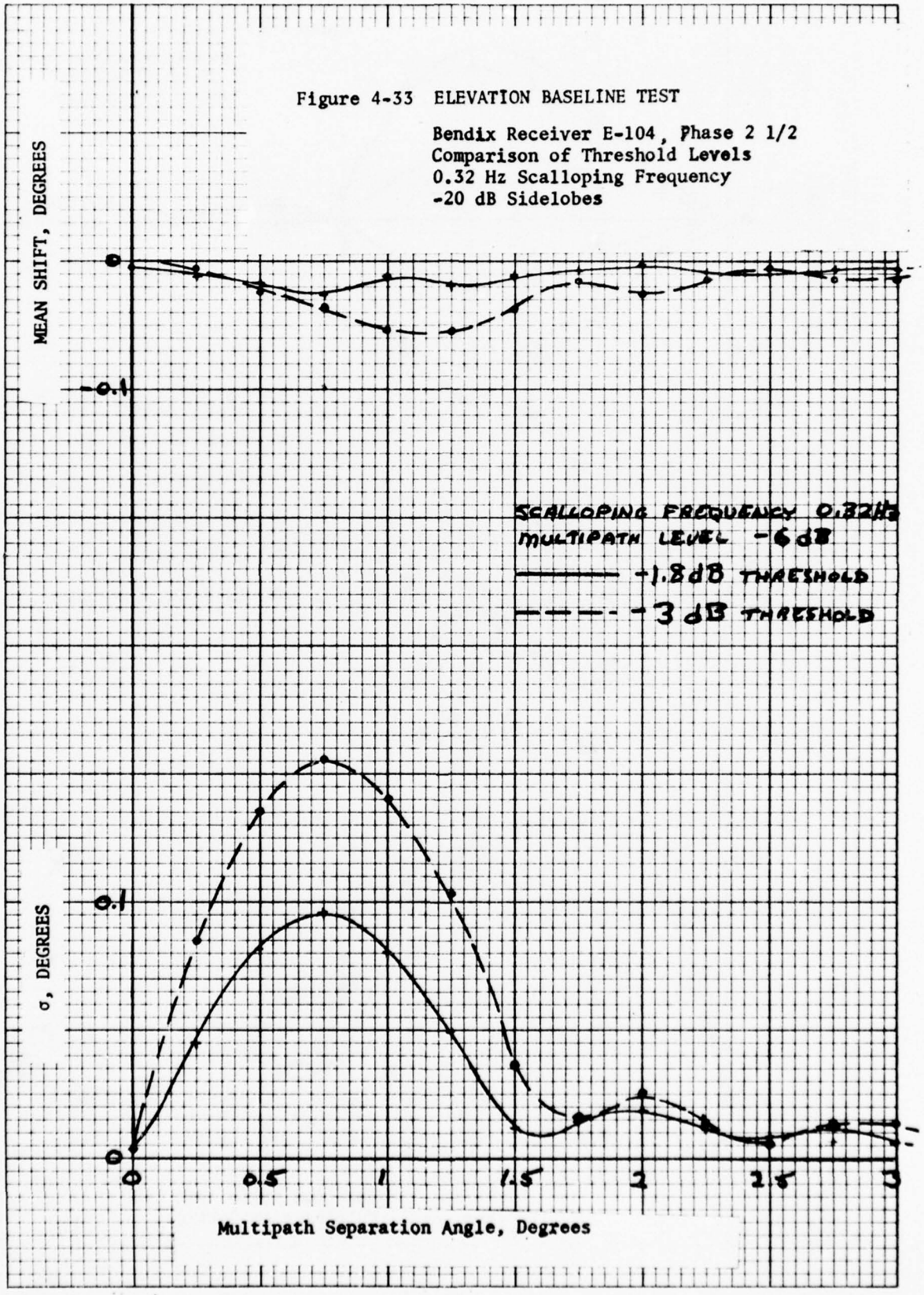

Figure 4-33 ELEVATION BASELINE TEST

Bendix Receiver E-104, Phase 2 1/2
Comparison of Threshold Levels
0.32 Hz Scalloping Frequency
-20 dB Sidelobes

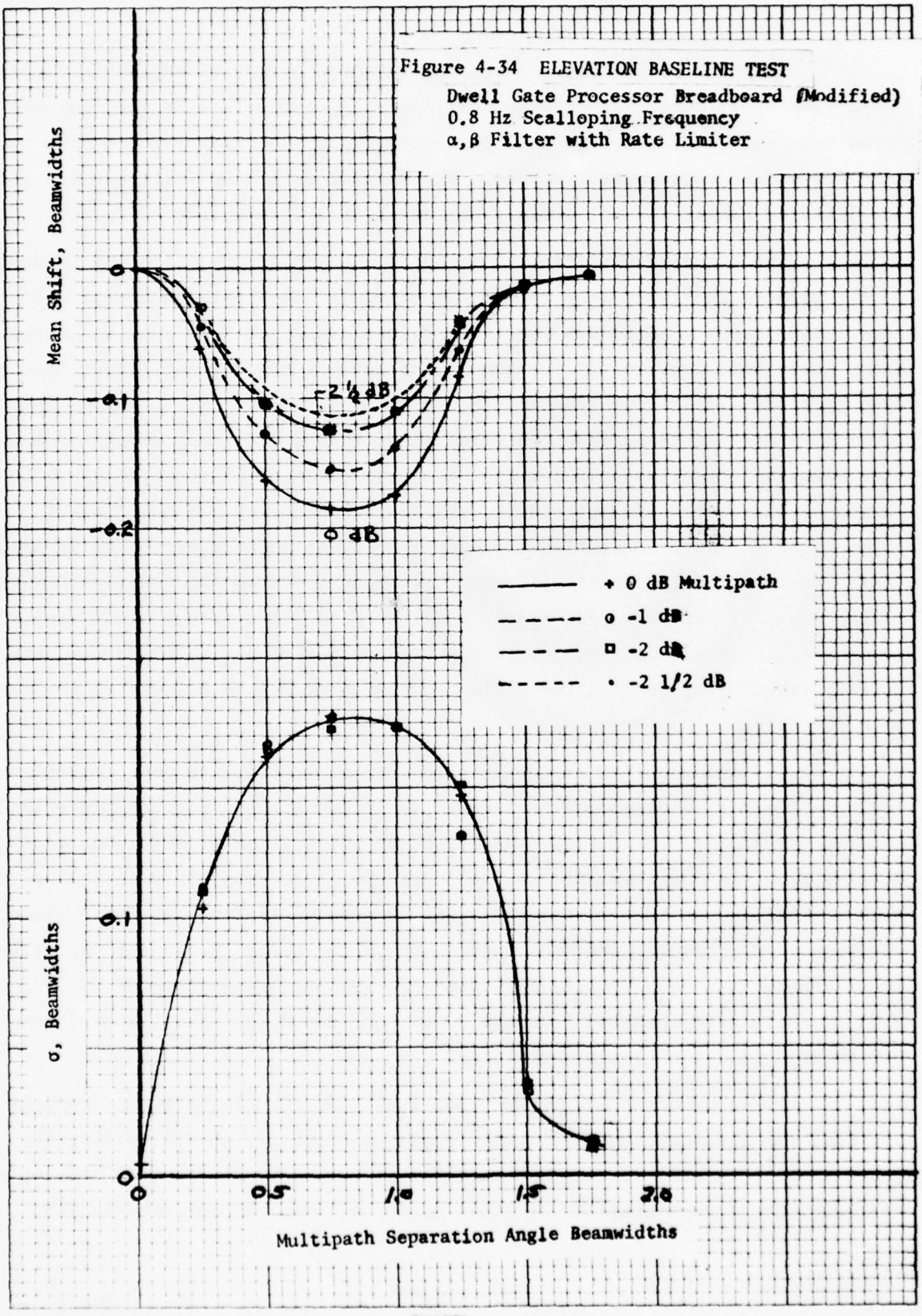
Figure 4-34 ELEVATION BASELINE TEST
Dwell Gate Processor Breadboard (Modified)
0.8 Hz Scalloping Frequency
α,β Filter with Rate Limiter
Mean Shift, Beamwidths
0
-0.1
-0.2
-2 1/2 dB
0 dB
+ 0 dB Multipath
o -1 dB
□ -2 dB
• -2 1/2 dB
σ, Beamwidths
0.1
0
0
0.5
1.0
1.5
2.0
Multipath Separation Angle Beamwidths

Examples of the errors with the jittered data rate appear in Figure 4-35. The error curve for the low scalloping frequency is like that for the fixed data rate. At the high scalloping frequency the error is much more noise-like for a fixed data rate. However, the statistics of the filtered data for the jittered format are not greatly different from the unjittered format.

The standard deviation of error as a function of scalloping frequency is illustrated in Figure 4-36 for both the regular and jittered format. The data rate jitter tends to suppress the grating lobe effect at some cost in increased error where motion averaging is normally effective. The average error has not been plotted. It is approximately the same for both formats. However, this average is only achieved when the duration of the test is long enough to make the averaging effective. That is, if the test duration is short compared to a period of the difference between the scalloping frequency and the closest harmonic of the data repetition frequency, then the mean error may be large or small depending on the phase difference between the direct and multipath signals. In the non-jittered 40 Hz data rate case, the difference frequency is zero at 40 Hz and its harmonics. At scalloping frequencies of 40 Hz, 80 Hz ---, the error is a constant lying between the maximum and minimum values allowed by the multipath parameters.

The frame period of the jittered format is 0.592 seconds corresponding to a repetition frequency of 1.689 Hz. An example showing the variation in mean values appears in Figure 4-37. Here, the scalloping frequency of 76 Hz differs from the 45th harmonic of the repetition frequency, 76.0135 Hz, by such a small amount that little averaging is possible in the test of 5 seconds duration. As a result, the mean values vary from -0.018° to -0.101° on different runs. There is a much smaller variation in the standard deviations (0.028° to 0.043°) which were computed from the 10 radian/second low pass filtered data rather than from the raw data shown.

In an airborne environment scalloping frequencies are continuously varying. As a result, the averaging should be effective in controlling the mean error. However, if the multipath situation should result in a scalloping frequency close to a harmonic of 1.689 Hz for a time long compared to the

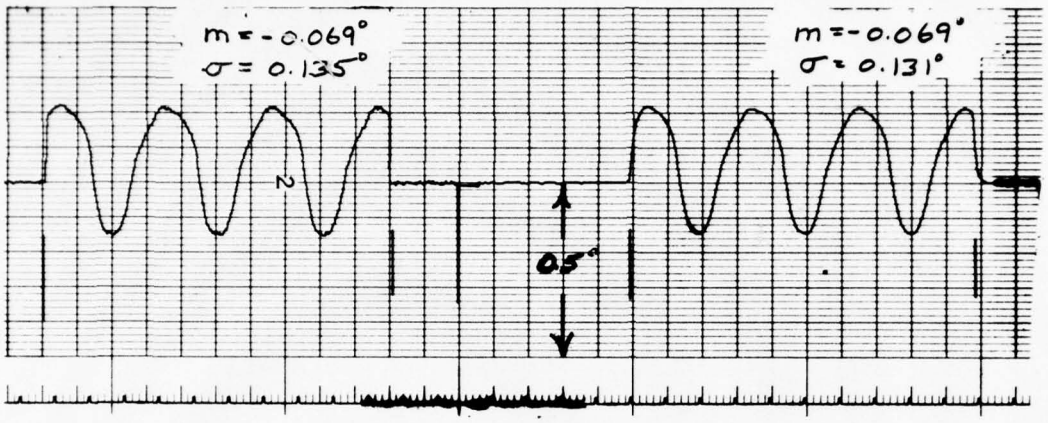

0.32 Hz Scalloping Frequency

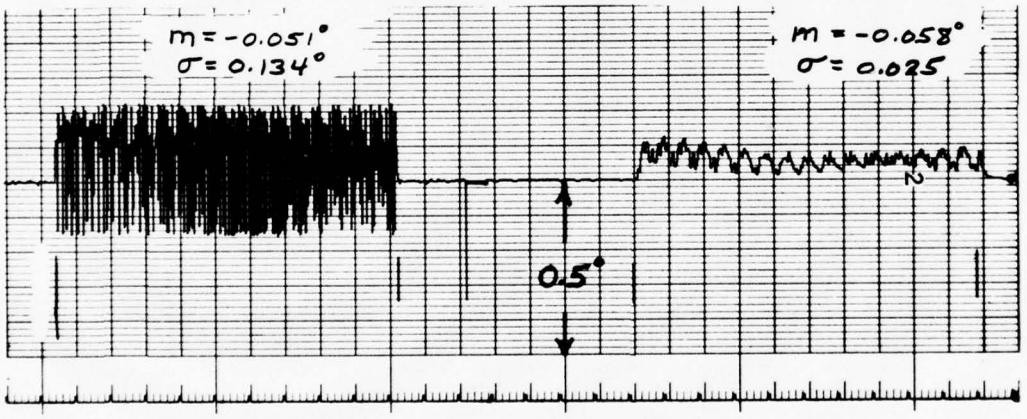

20.32 Hz Scalloping Frequency

Raw Data

Filtered Data

Multipath Separation Angle 0.75°
Multipath Relative Amplitude -6 dB
Breadboard Receiver

Figure 4-35 JITTERED DATA RATE, ELEVATION

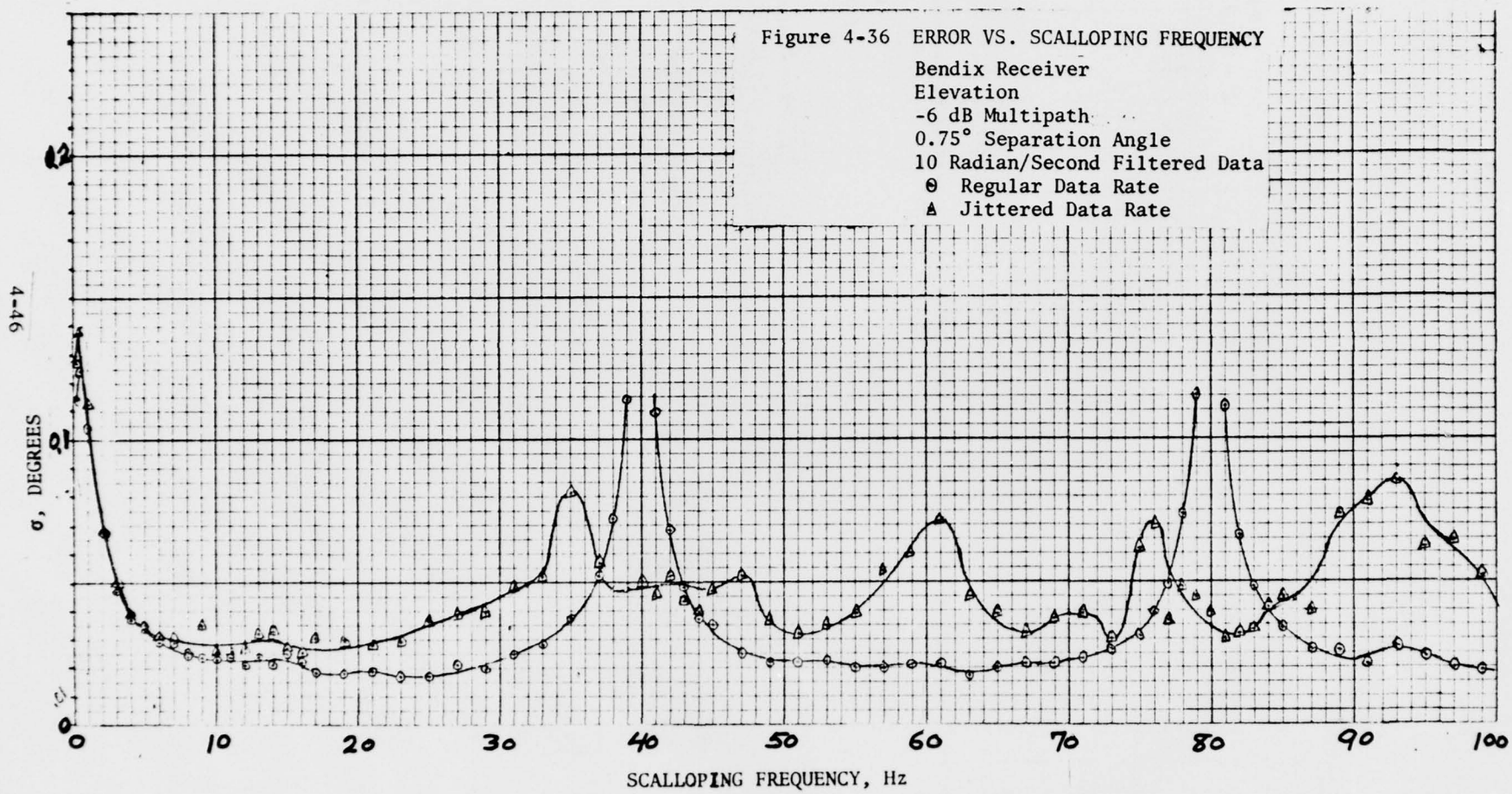
Figure 4-36 ERROR VS. SCALLOPING FREQUENCY
Bendix Receiver
Elevation
-6 dB Multipath
0.75° Separation Angle
10 Radian/Second Filtered Data
Θ Regular Data Rate
Δ Jittered Data Rate
σ, DEGREES
SCALLOPING FREQUENCY, Hz
0
10
20
30
40
50
60
70
80
90
100

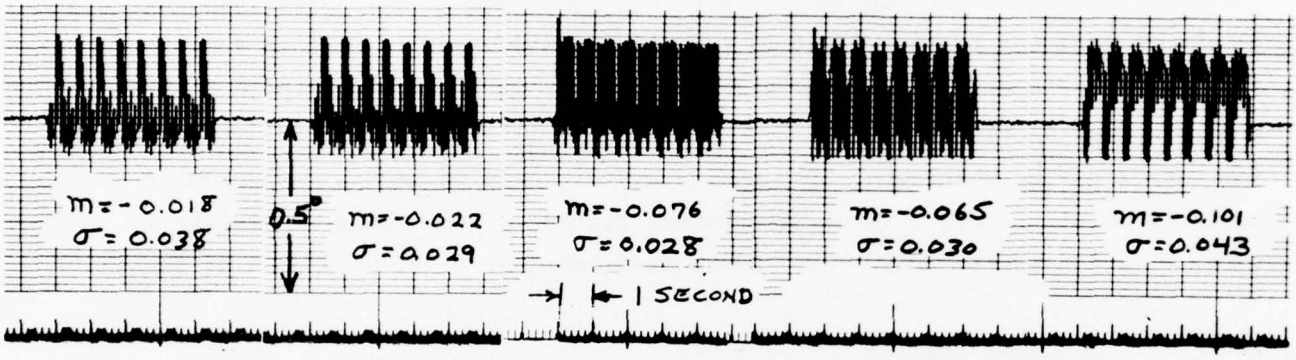

Note: Mean and standard deviation are for 10 radian/second filtered data (not shown).

Figure 4-37 REPETITIVE RUNS, ELEVATION

Raw Data Records
Jittered Data Rate
Separation Angle 1°
Multipath Amplitude -6 dB
Scalloping Frequency 76 Hz

difference period, then the mean error will be a function of the random phases of the direct and multipath signals. The error may be very small or large but could certainly vary greatly from run to run thus complicating any attempt to evaluate the multipath effect.

4.3.3 Threshold Level Effects

The dwell gate threshold level has an effect on multipath induced errors in addition to its effect on sensitivity discussed in Section 4.2.3. The results of a test of the Phase 2 1/2 receiver with fixed multipath parameters appear in Figure 4-38. Higher thresholds (less negative) tend to reduce the effect of the multipath. The choice of threshold to use is a compromise with the receiver sensitivity. The normal setting of the Phase 3 receiver is -3 dB relative to the beam peak. Breadboard receiver tests used a -4 dB threshold.

4.3.4 Beamwidth Effects

Most of the multipath tests were run with a simulated one degree beamwidth signal. This would be typical of the elevation and azimuth beams at the highest category ground stations. At lower category ground stations, wider beamwidth antennas would be used in the interest of size and economy. Baseline tests were run with representative wide beamwidth signals of 2° for elevation.

Figure 4-39 illustrates the results of the Phase 2 1/2 receiver tests using a 2° beamwidth and parameters. Also plotted are the results of elevation tests with 1° beamwidth for comparison. It is apparent that the peak errors and the range of multipath angles for which errors occur are both increased by a factor of two when the beamwidth is doubled.

It should be noted that the multipath error is very similar for the 1° and 2° beamwidths for multipath separation angles up to 0.5°. Thus, in many hangar scenarios the resulting elevation multipath errors are relatively insensitive to beamwidth.

Multipath performance tests were run on the simulator to determine the error reduction resulting from a 0.4 degree beamwidth with a processor designed for the nominal 1 degree beamwidth. The Phase 3 receiver was used

Figure 4-38 BASELINE ELEVATION TEST

Threshold Level Effects
Bendix Receiver
-6 dB Multipath
0.32 Hz Scalloping Frequency
Jittered Data Rate

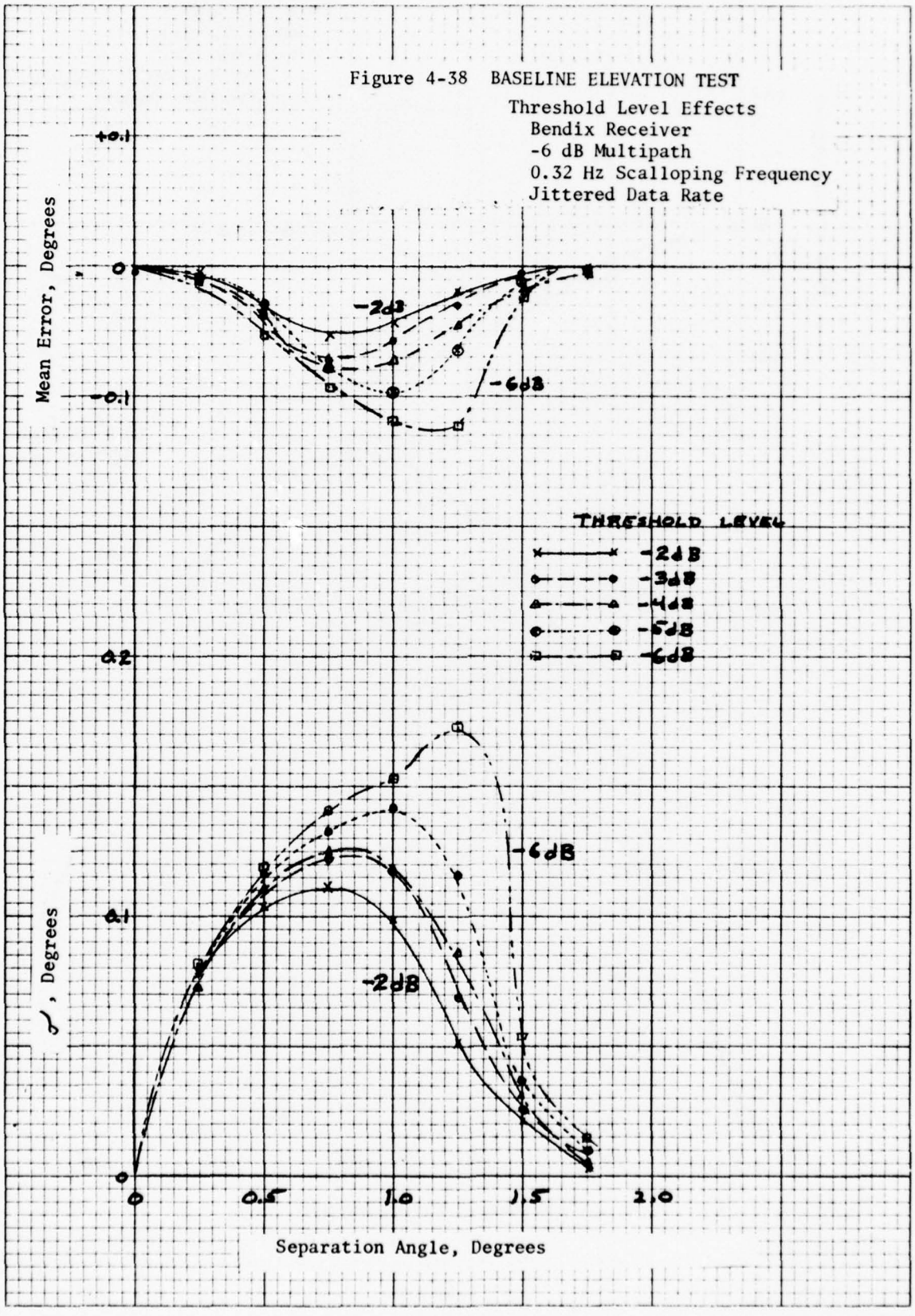

Figure 4-39 BASELINE ELEVATION TEST

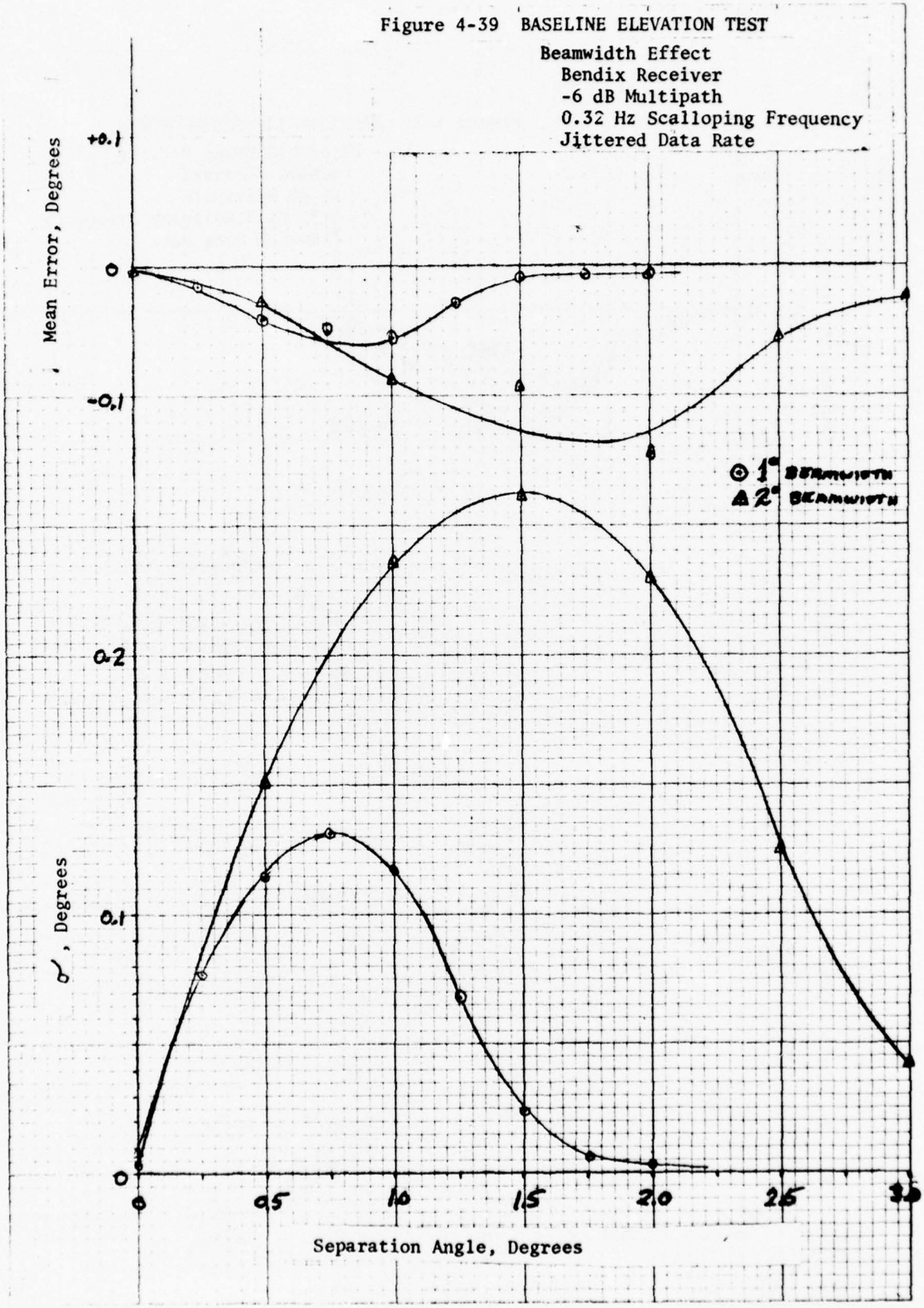

in these tests since it has an adaptive tracking gate width that is set according to the received beamwidth. A fixed video filter bandwidth of 26 kHz is used in this receiver.

Baseline tests were run to measure the error versus multipath separation angle. The results of the azimuth tests with the 0.4 degree beamwidth are shown in Figure 4-40. The -3 dB error curve for the 1.0 degree beamwidth is plotted for comparison. It can be seen from this comparison that the noise errors are reduced by about the ratio of the beamwidths of 1.0 degree versus 0.4 degrees (20 μsec dwell gates).

4.3.5 Multipath Scalloping Frequency Effects

Figures 4-41 through 4-44 illustrate the effect of varying the scalloping frequency for a fixed elevation multipath level (-6 dB) and separation angle (0.75°) for the Phase 2 1/2 and Phase 3 receivers. The errors are reduced as the scalloping frequency approaches a condition of 180° phase difference between the DOWN-UP scans. At 3° elevation angle, this corresponds to about 700 Hz. Azimuth scalloping frequency tests have minimum errors at those scalloping frequencies that are at odd multiples of the time difference between the TO-FRO beams. For azimuth on centerline the error nulls occur at odd multiples of about 75 Hz (time interval between the TO-FRO beams is 6.6 milliseconds). Figure 4-45 shows azimuth scalloping frequency tests for the breadboard receiver.

The Phase 3 receiver showed greater variability on these tests but the average standard deviations are similar. The greater variability may be a result of the aliasing effects from the high scalloping frequencies in combination with the overshoot characteristic of the α, β filter at the low frequencies.

4.3.6 DPSK Multipath

The foregoing tests were carried out with scanning beam multipath only. The DPSK signal will also be subject to multipath, particularly since it is transmitted from an omnidirectional antenna that illuminates potential reflectors throughout the MLS coverage region. A test of DPSK multipath

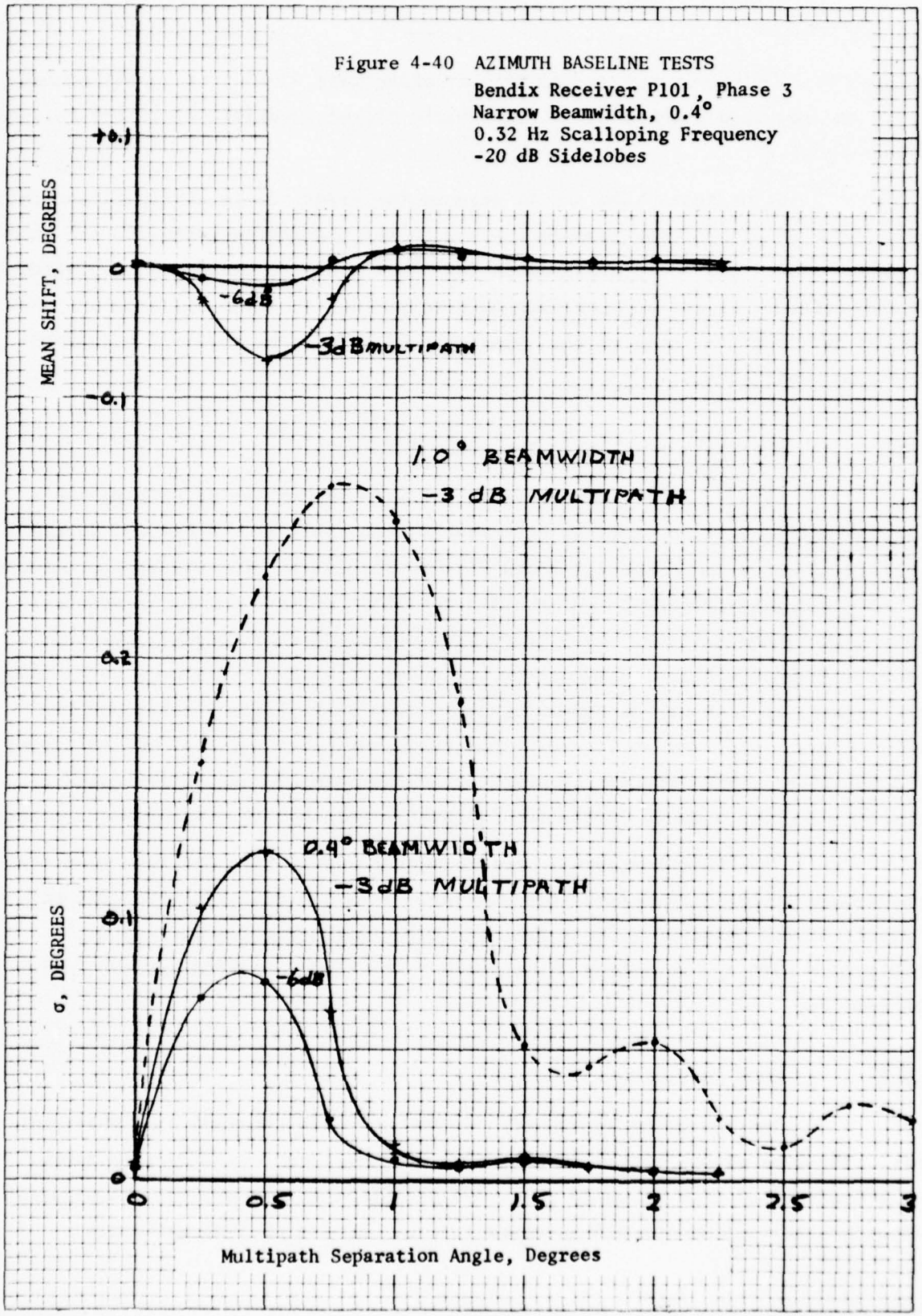

Figure 4-40 AZIMUTH BASELINE TESTS
Bendix Receiver P101, Phase 3
Narrow Beamwidth, 0.4°
0.32 Hz Scalloping Frequency
-20 dB Sidelobes

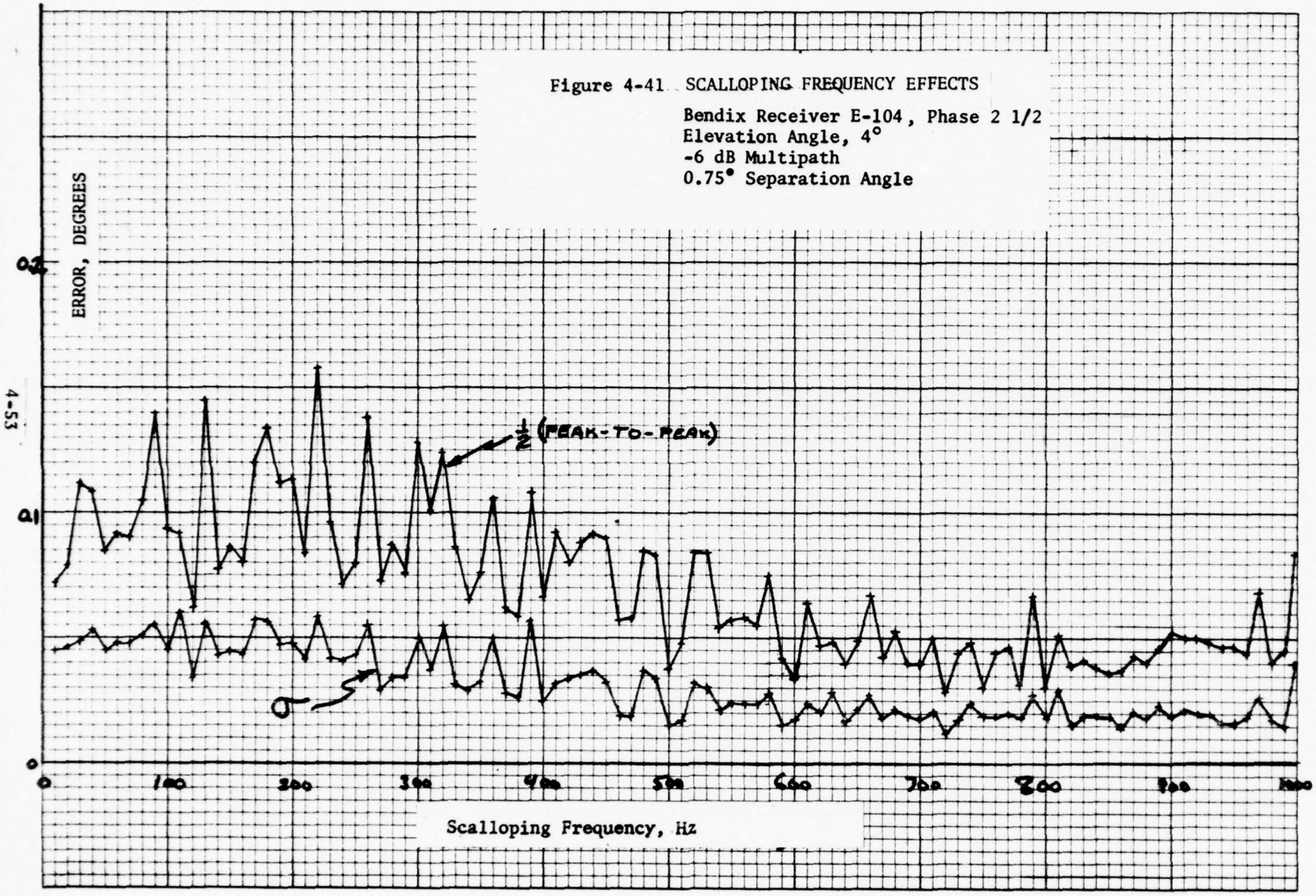
Figure 4-41 SCALLOPING FREQUENCY EFFECTS
Bendix Receiver E-104, Phase 2 1/2
Elevation Angle, 4°
-6 dB Multipath
0.75° Separation Angle
ERROR, DEGREES
0.2
0.1
0
½ (PEAK-TO-PEAK)
σ
0
100
200
300
400
500
600
700
800
900
1000
Scalloping Frequency, Hz

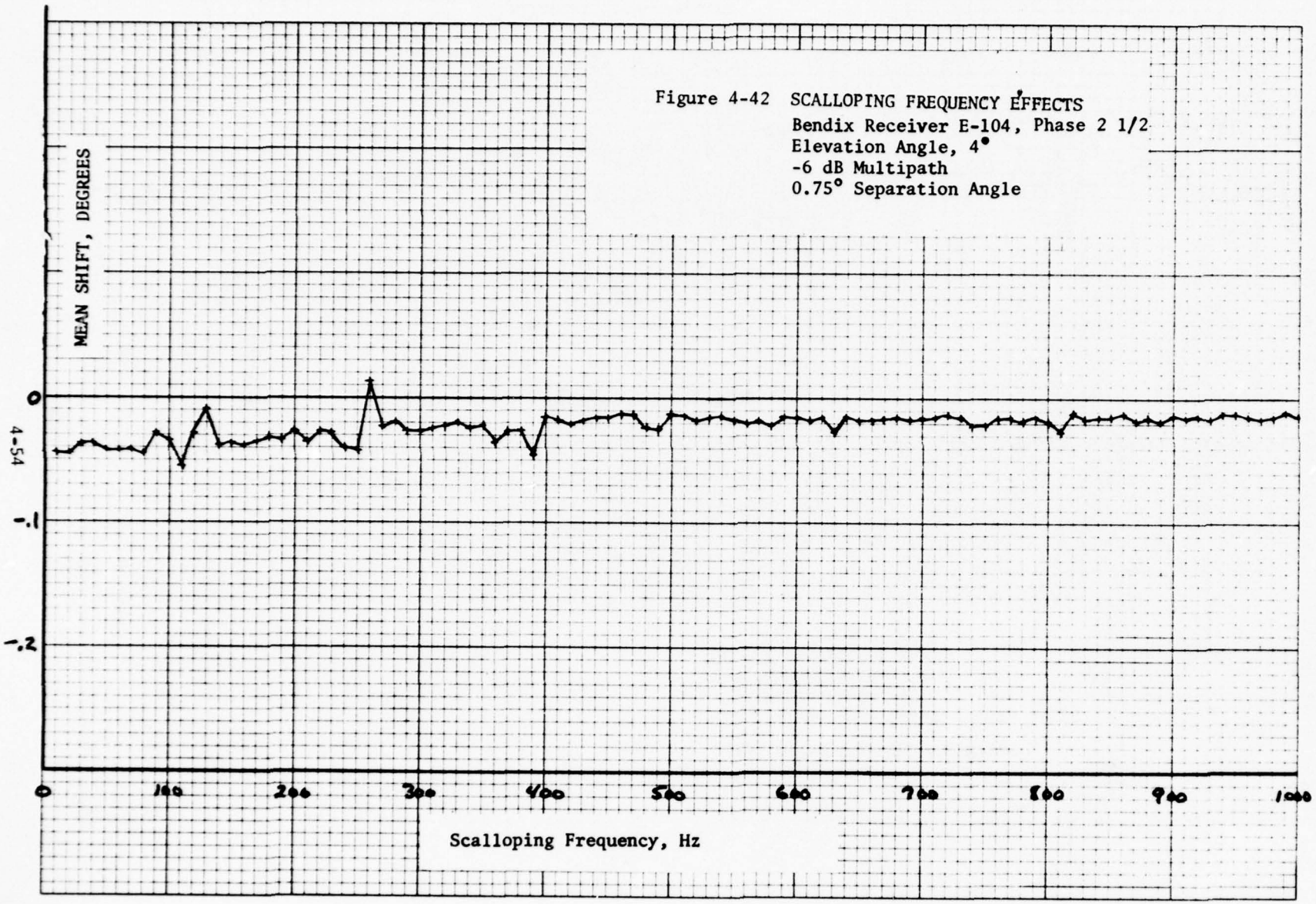

Figure 4-42 SCALLOPING FREQUENCY EFFECTS
Bendix Receiver E-104, Phase 2 1/2
Elevation Angle, 4°
-6 dB Multipath
0.75° Separation Angle

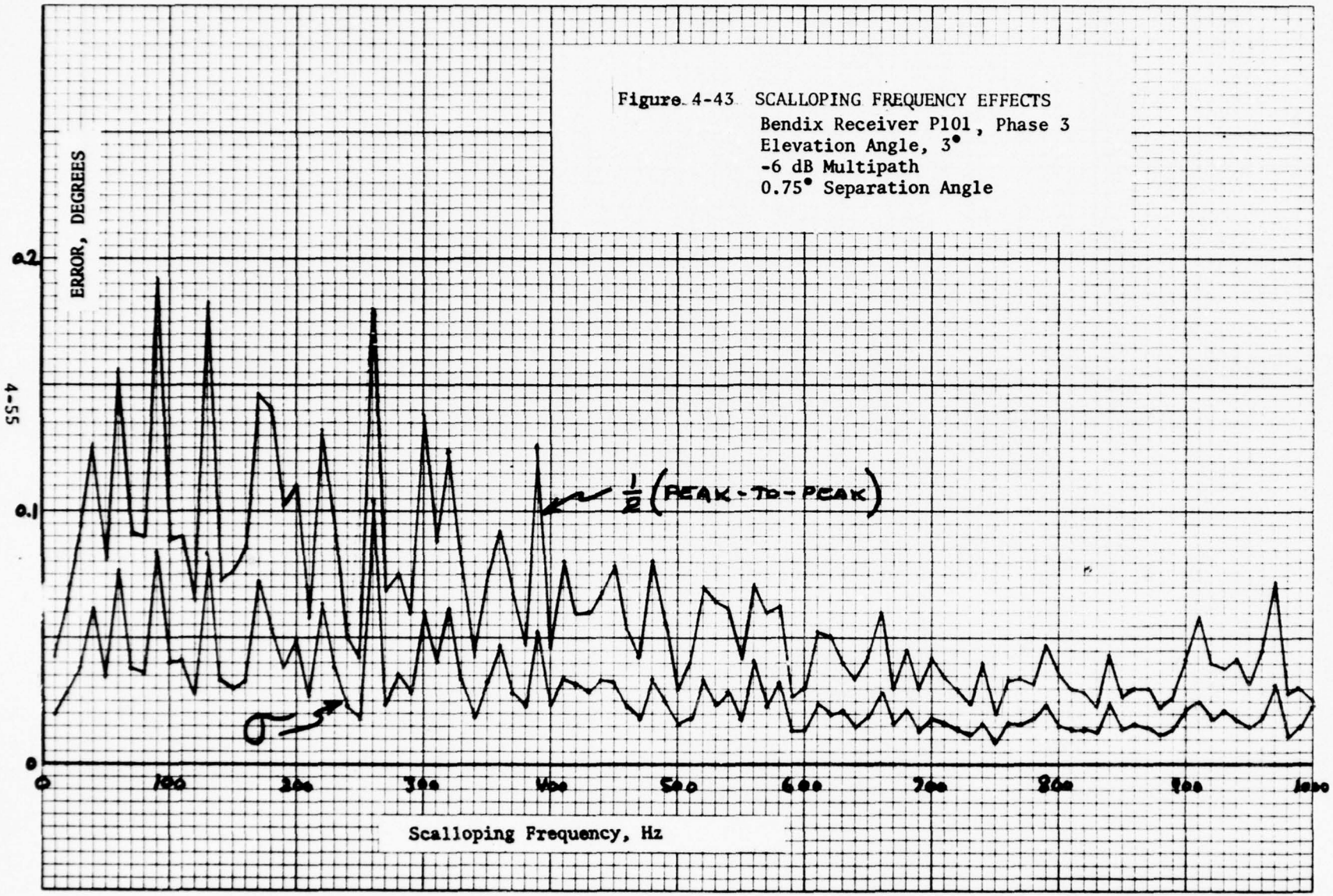

Figure 4-43 SCALLOPING FREQUENCY EFFECTS
Bendix Receiver P101, Phase 3
Elevation Angle, 3°
-6 dB Multipath
0.75° Separation Angle

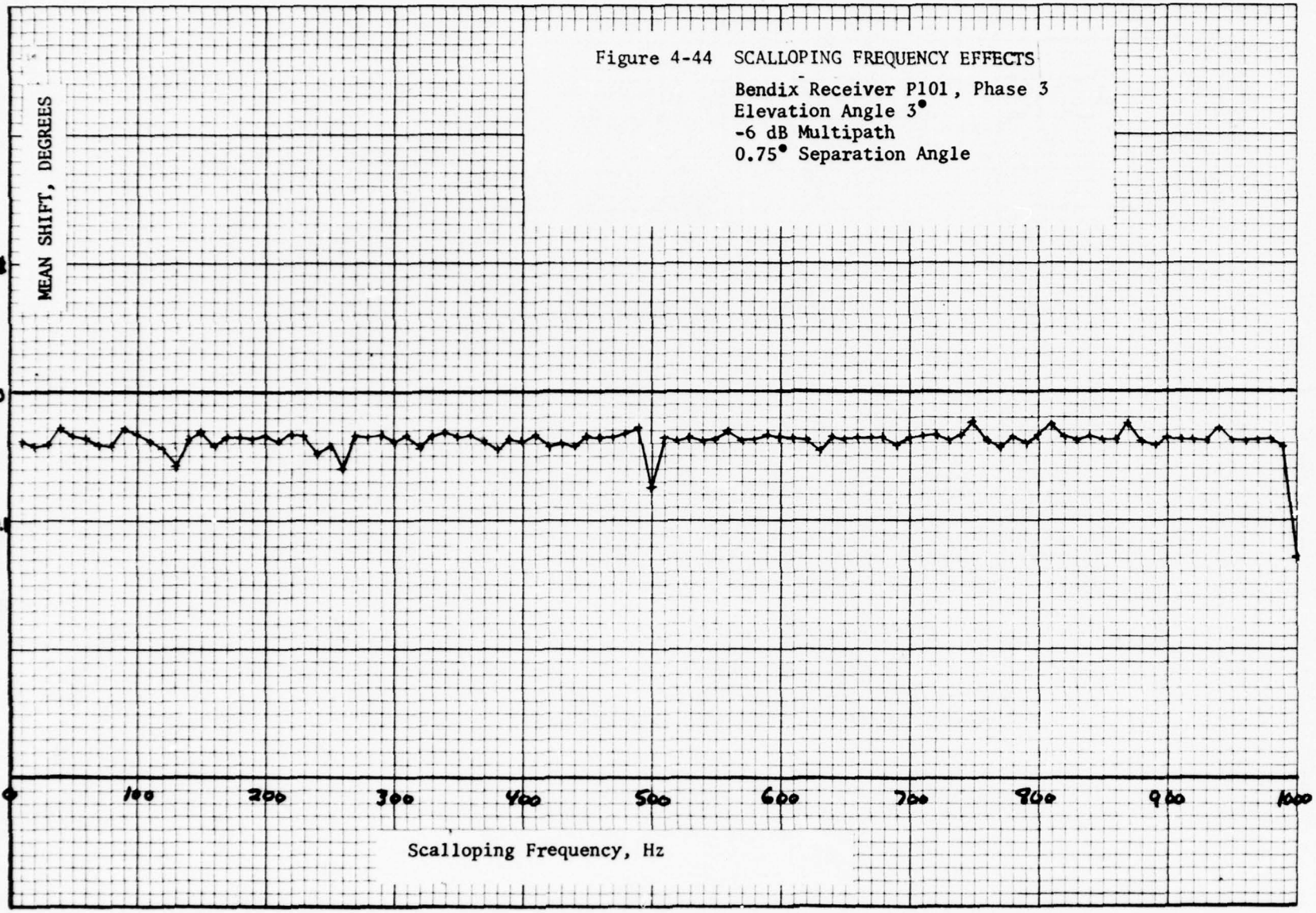
Figure 4-44 SCALLOPING FREQUENCY EFFECTS
Bendix Receiver P101, Phase 3
Elevation Angle 3°
-6 dB Multipath
0.75° Separation Angle
MEAN SHIFT, DEGREES
+0.1
0
-0.1
0
100
200
300
400
500
600
700
800
900
1000
Scalloping Frequency, Hz

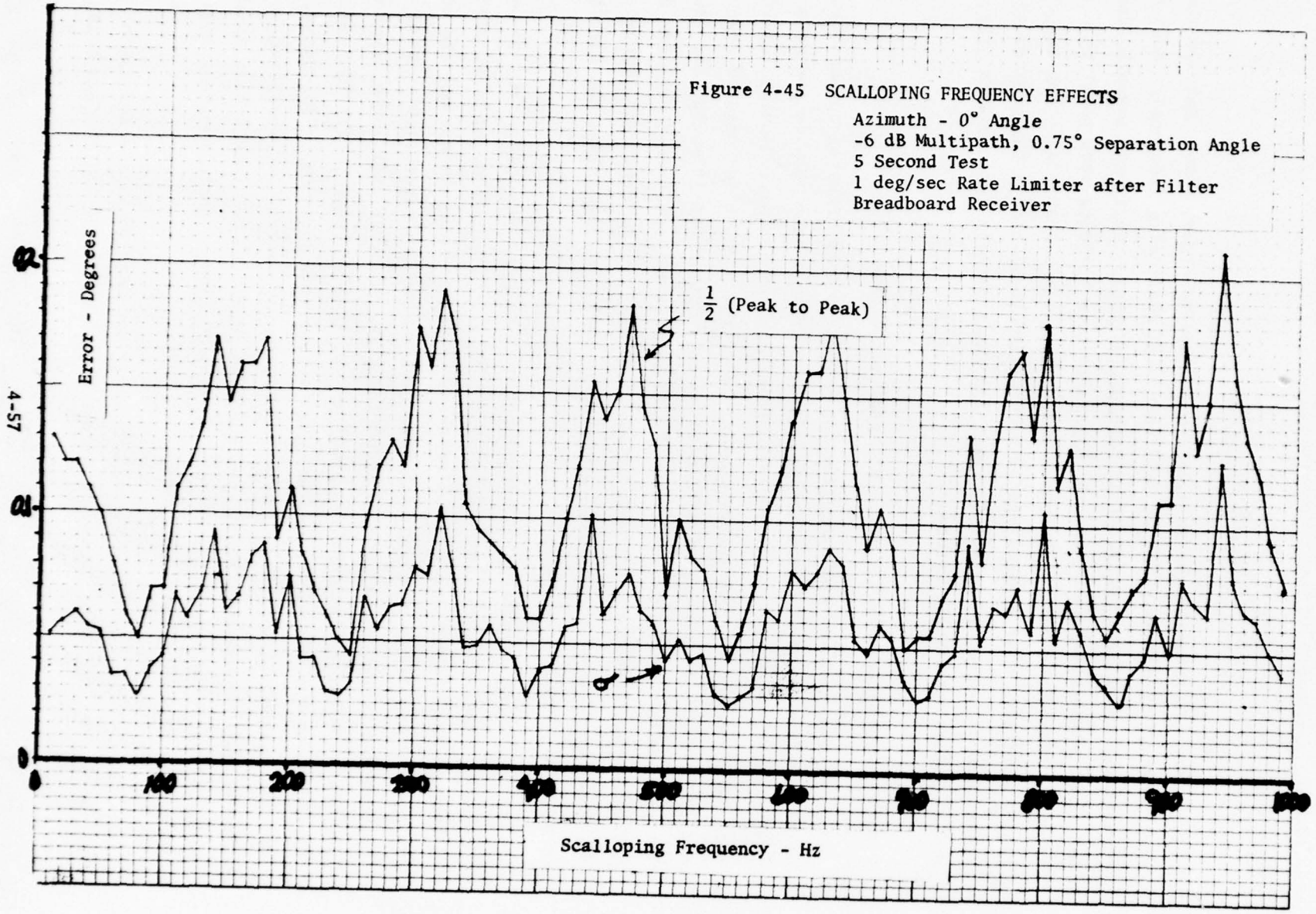

Figure 4-45 SCALLOPING FREQUENCY EFFECTS

Azimuth - 0° Angle
-6 dB Multipath, 0.75° Separation Angle
5 Second Test
1 deg/sec Rate Limiter after Filter
Breadboard Receiver

sensitivity was run with the results illustrated in Figure 4-46. Only in the case of equal amplitude multipath and very high scalloping frequencies does a significant error rate occur. This combination could occur, for example, during the final phase of approach if a highly reflective building were positioned and oriented to produce multipath from a wide angle (for a high scalloping frequency) to the aircraft. The probability of such multipath with duration greater than a fraction of second is extremely small and the effect is to introduce missed frames rather than angle errors.

4.3.7 Out-of-Beam Multipath and Signal Validation

The receiver tracking gate for azimuth data eliminates out-of-beam multipath from the angle computation. A comparison of the outside the gate peak detector with the inside the gate peak detector is carried out following each FRO scan and the confidence counter is incremented or decremented depending on the result. When a signal has built up full confidence it would take seven seconds in the Phase 2 1/2 receiver and 15 seconds in the Phase 3 receiver of continuously greater out-of-beam signal to reinstate the acquisition cycle. It is unlikely that multipath could prevail for such a period unless the direct signal was shadowed throughout.

At the time of signal acquisition it is possible that an out-of-beam multipath signal of the same magnitude as the direct signal could be present. A test of the acquisition time in the presence of two signals was carried out with the Phase 2 1/2 receiver with the results shown in Figure 4-47. When the signals are nearly equal (within about 1 dB) the receiver will not acquire either signal. Otherwise, the receiver acquires the larger signal in 1.7 to 3 seconds depending on the signal level. The acquisition time seems to be independent of which signal is positive (clockwise from runway centerline, resulting in greater TO-FRO beam separation). There does appear to be a small bias of the acquisition failure region such that the inside beams tend to suppress acquisition more than equivalent outside beams.

The P101 receiver validation logic was checked with a multipath signal in the following tests. A direct signal at 0° and -65 dBm was being

Figure 4-46 DPSK MULTIPATH PERFORMANCE
Bendix Receiver
DPSK Level -80 dBm
No Scanning Beam Interference

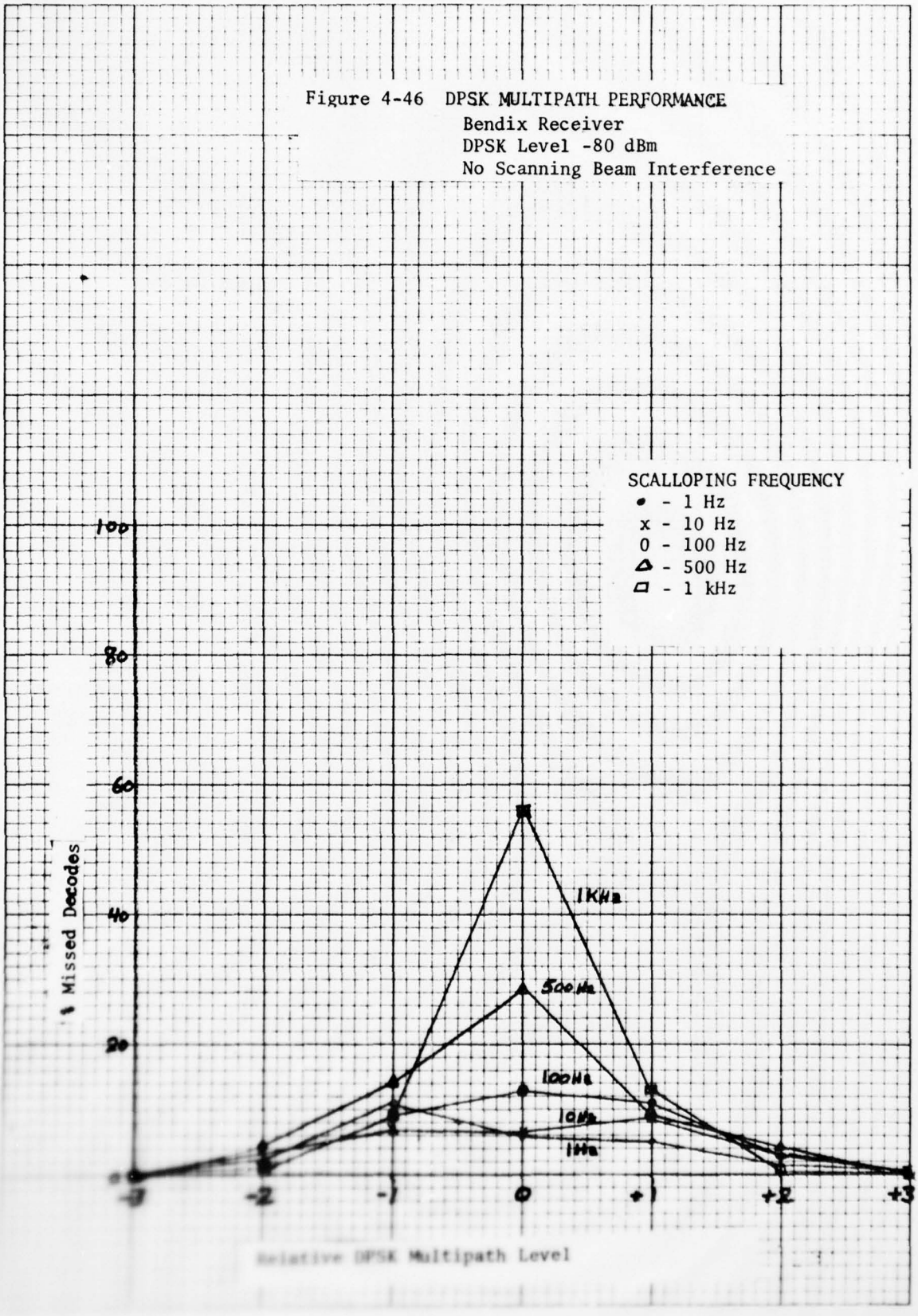

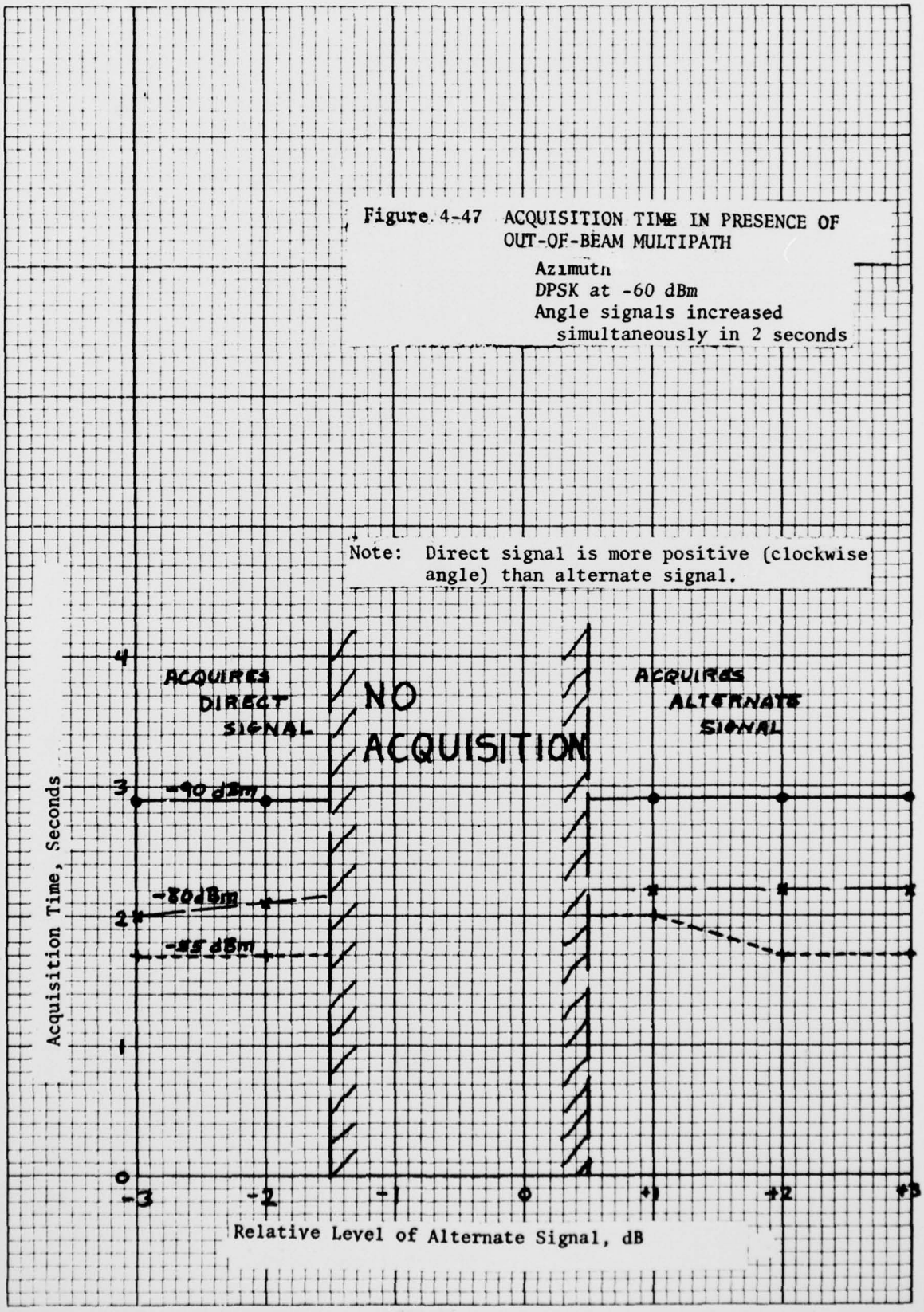

Figure 4-47 ACQUISITION TIME IN PRESENCE OF OUT-OF-BEAM MULTIPATH

Azimuth
DPSK at -60 dBm
Angle signals increased simultaneously in 2 seconds

tracked by the receiver. An alternate signal (a constant amplitude multipath) at -8° and +1 dB relative level was applied. The direct signal was dropped in 15 seconds and a track on the alternate signal was started one second later.

The alternate signal was then reduced by 2 dB so that it was 1 dB below the original direct signal. In 15 seconds the alternate signal was dropped and the direct signal was reacquired in one second more. This test was repeated with the direct signal at -85 dBm with exactly the same results.

4.3.8 Effects of High Level Multipath

Simulation tests were run to determine the Phase 3 receiver error characteristics at multipath levels above -3 dB and as a function of signal level. Previous azimuth and elevation multipath tests of error versus separation angle (baseline tests) had been limited to -3 dB multipath levels. Antenna pattern shaping and path length attenuation make it very unlikely that multipath-to-direct (M/D) signal ratios will ever exceed -3 dB in the scanning beam system except during the flare. However, questions were raised in the ICAO meetings as to what the TRSB error characteristics are at high M/D ratios.

The results of a 0 dB baseline test are shown in Figure 4-48. These error statistics are computed over a 10 second test period so the effect of the multipath phase is averaged. A 0.8 Hz scalloping frequency was used so the α-β smoothing filter in the Phase 3 receiver would operate at a gain of 0 dB. The peak errors occur at multipath separation angles between 1.0° and 1.75°.

Tests were run at a very low scalloping frequency (1/16 Hz) to show the multipath phase effect. Figures 4-49 through 4-52 show these curves for various separation angles and M/D ratios of -3 dB, -2 dB, -1 dB and 0 dB. The erratic performance at M/D ratios above -2 dB and near the 180° phase angle is apparent for separation angles of 1° and 1.5°.

Figure 4-53 shows the elevation peak error for a multipath phase of 0° and 180° for the Phase 3 receiver at M/D ratios of -3 dB and -1 dB. Because of the erratic performance at 180° multipath phase the curve for -1 dB could not be completed between separation angles of 1 and 1.5 beamwidths. A -1 dB curve is shown for the modified breadboard receiver which is similar to the

Figure 4-48 ELEVATION BASELINE TESTS - PHASE 3 RECEIVER P-102

0.8 Hz Scalloping Frequency
0 dB Multipath
-25 dB Sidelobes

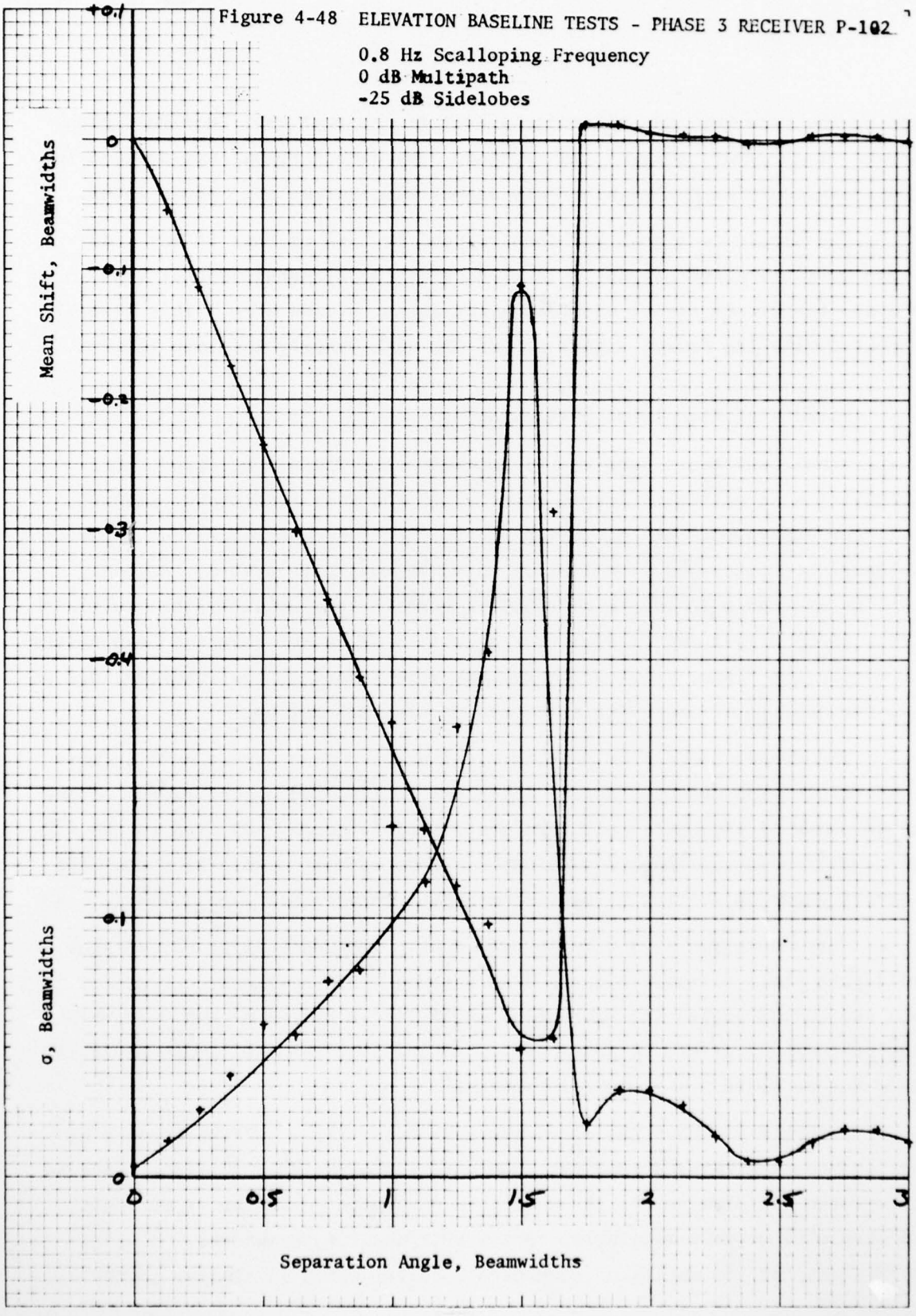

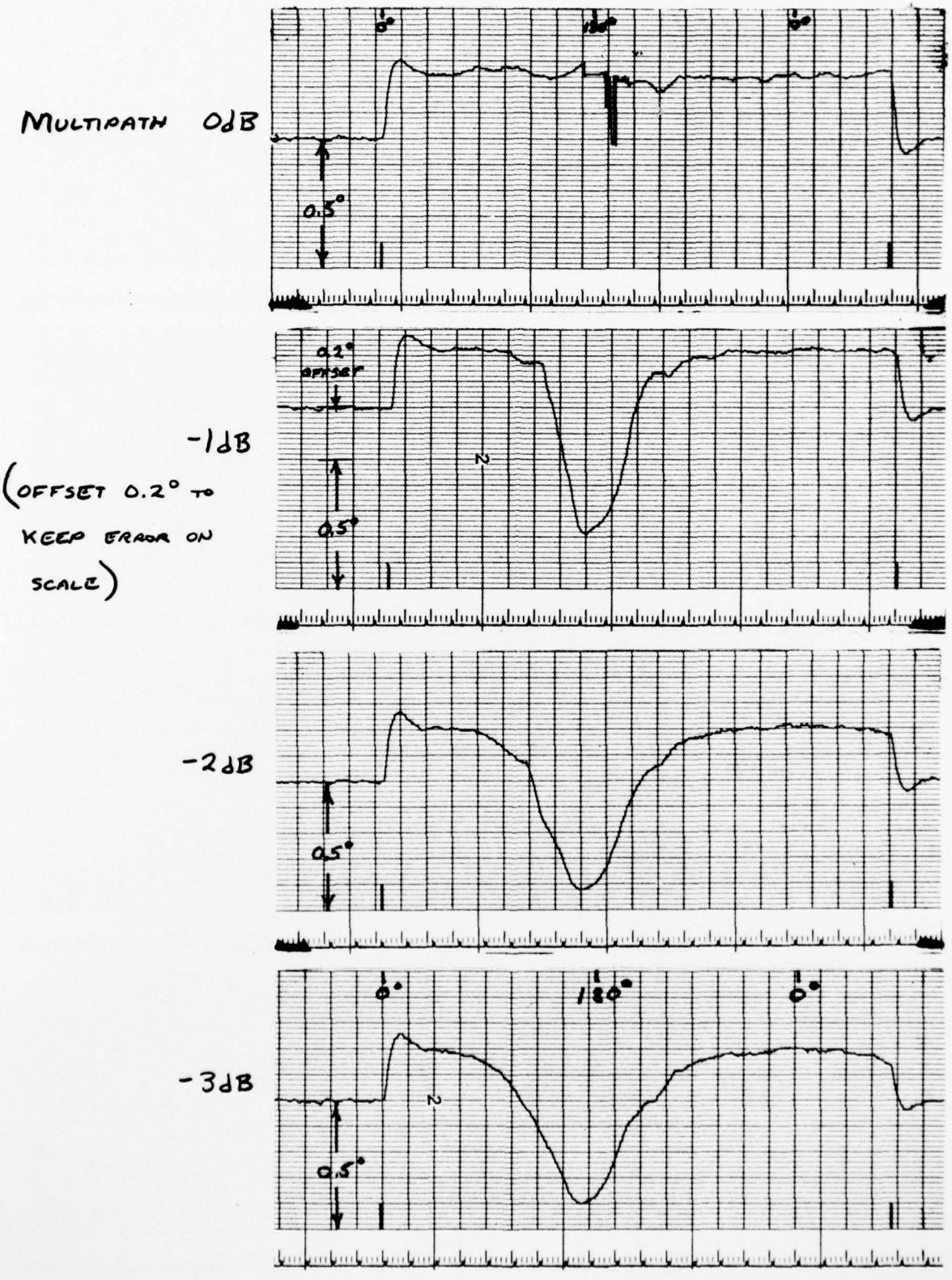

Figure 4-49 ELEVATION PHASE ERROR PLOTS, PHASE 3 RECEIVER P-102
1/2 BEAMWIDTH SEPARATION ANGLE, 1/16 Hz SCALLOPING FREQUENCY

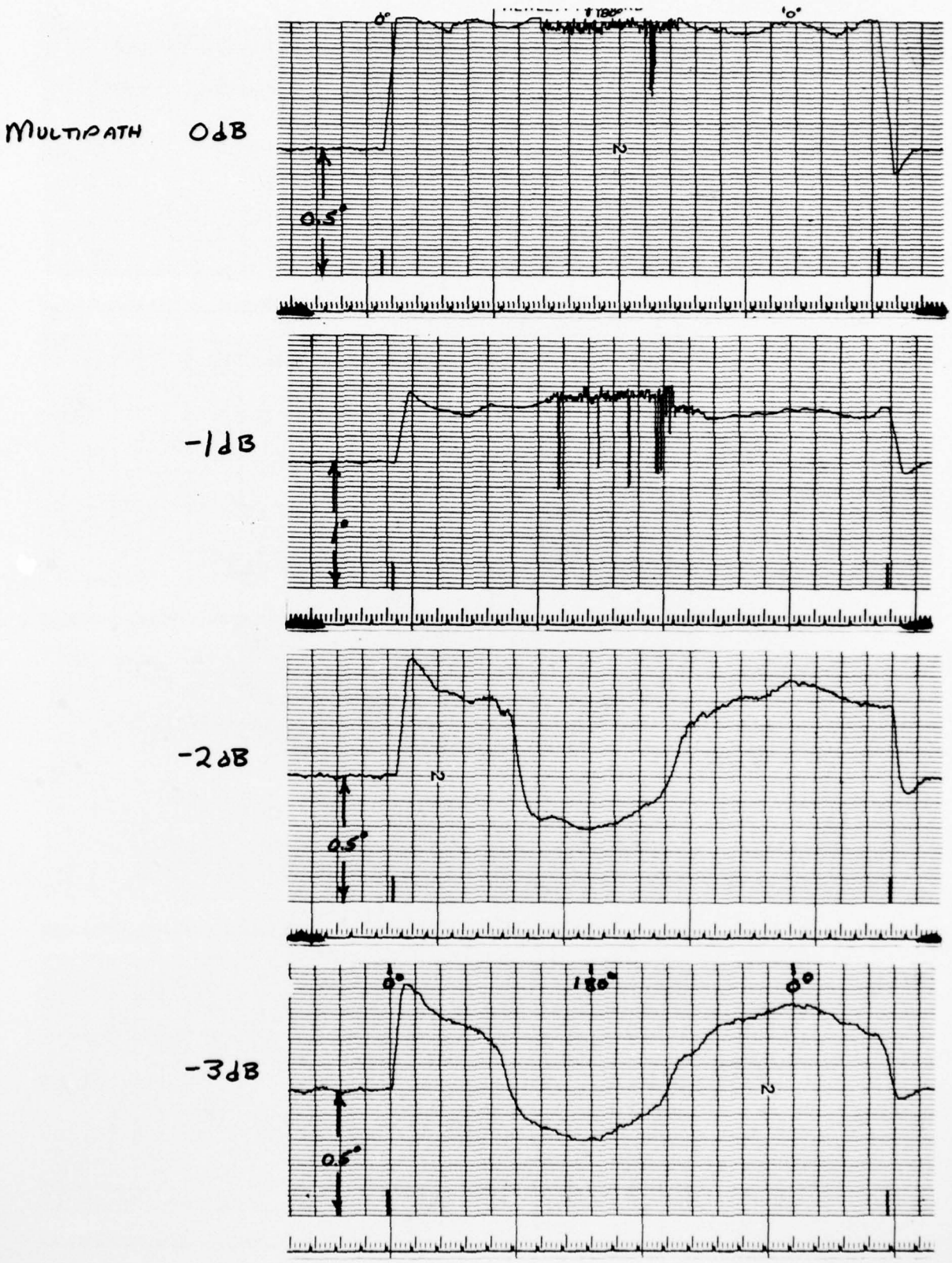

Figure 4-50 ELEVATION PHASE ERROR PLOTS, PHASE 3 RECEIVER P-102, 1 BEAMWIDTH SEPARATION ANGLE, 1/16 Hz SCALLOPING FREQUENCY

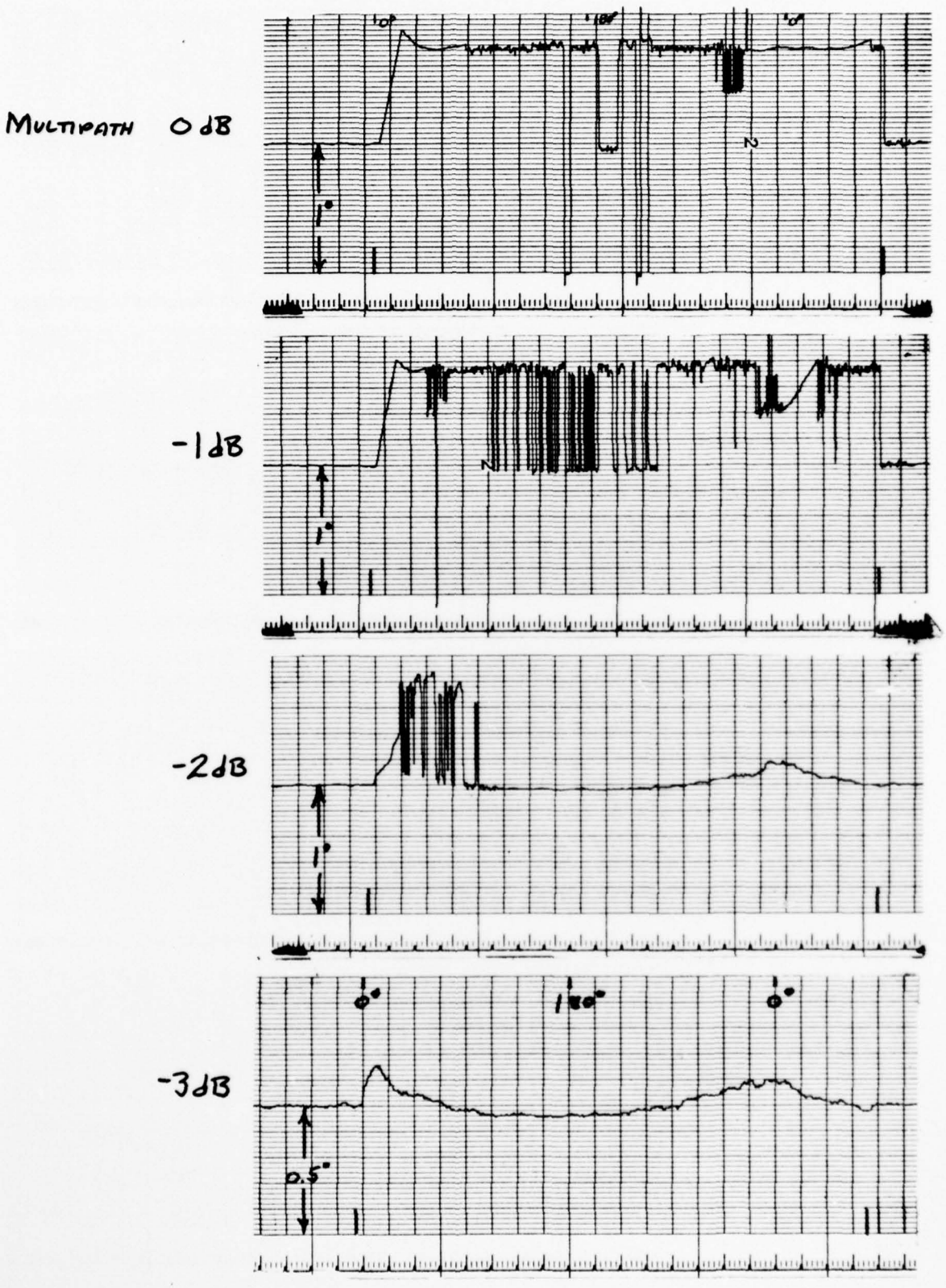

Figure 4-5. ELEVATION PHASE ERROR PLOTS, PHASE 3 RECEIVER P-102
1 1/2 BEAMWIDTHS SEPARATION ANGLE, 1/16 Hz SCALLOPING FREQUENCY

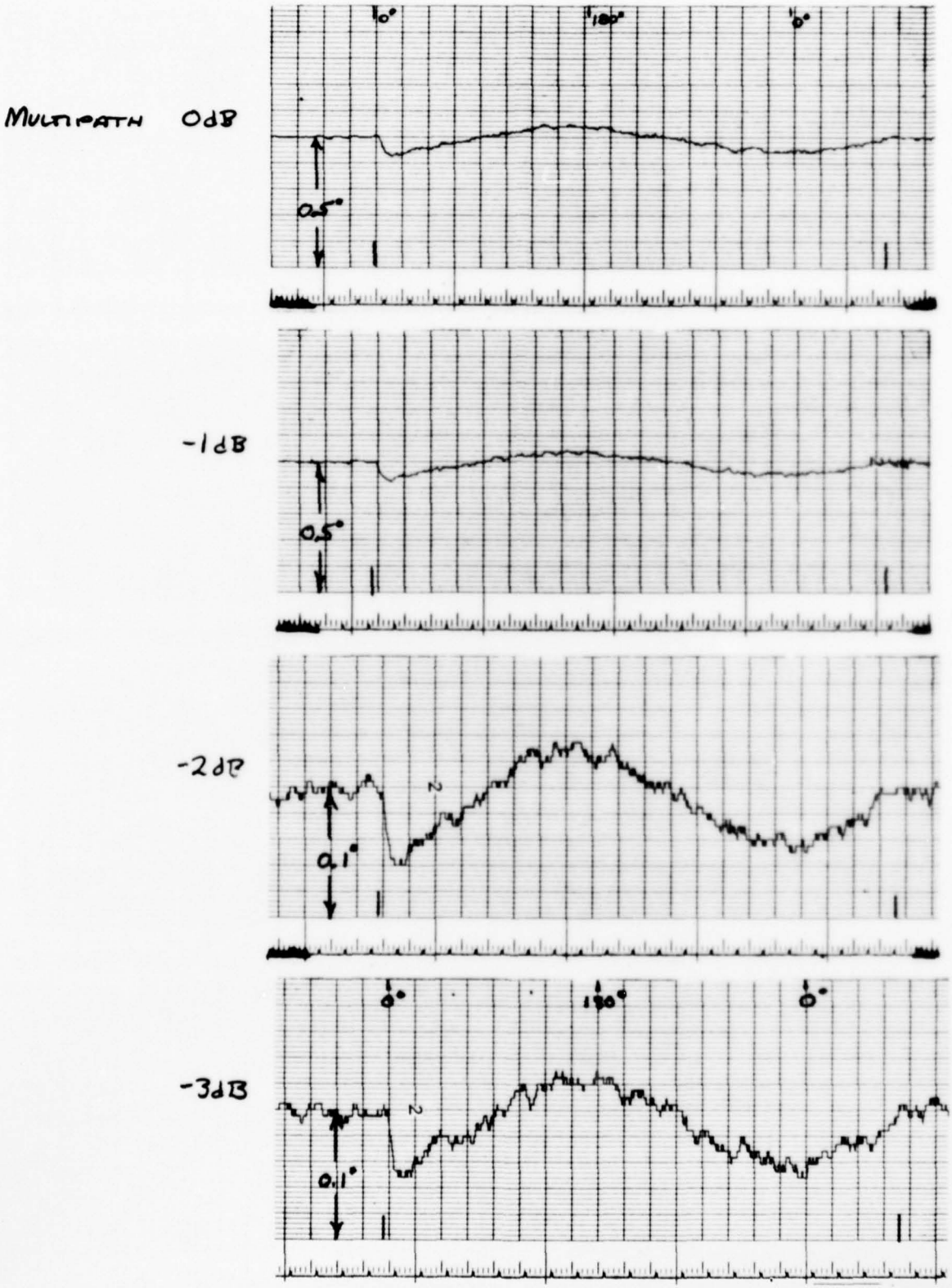

Figure 4-52 ELEVATION PHASE ERROR PLOTS, PHASE 3 RECEIVER P-102, 2 BEAMWIDTHS SEPARATION ANGLE, 1/16 Hz SCALLOPING FREQUENCY

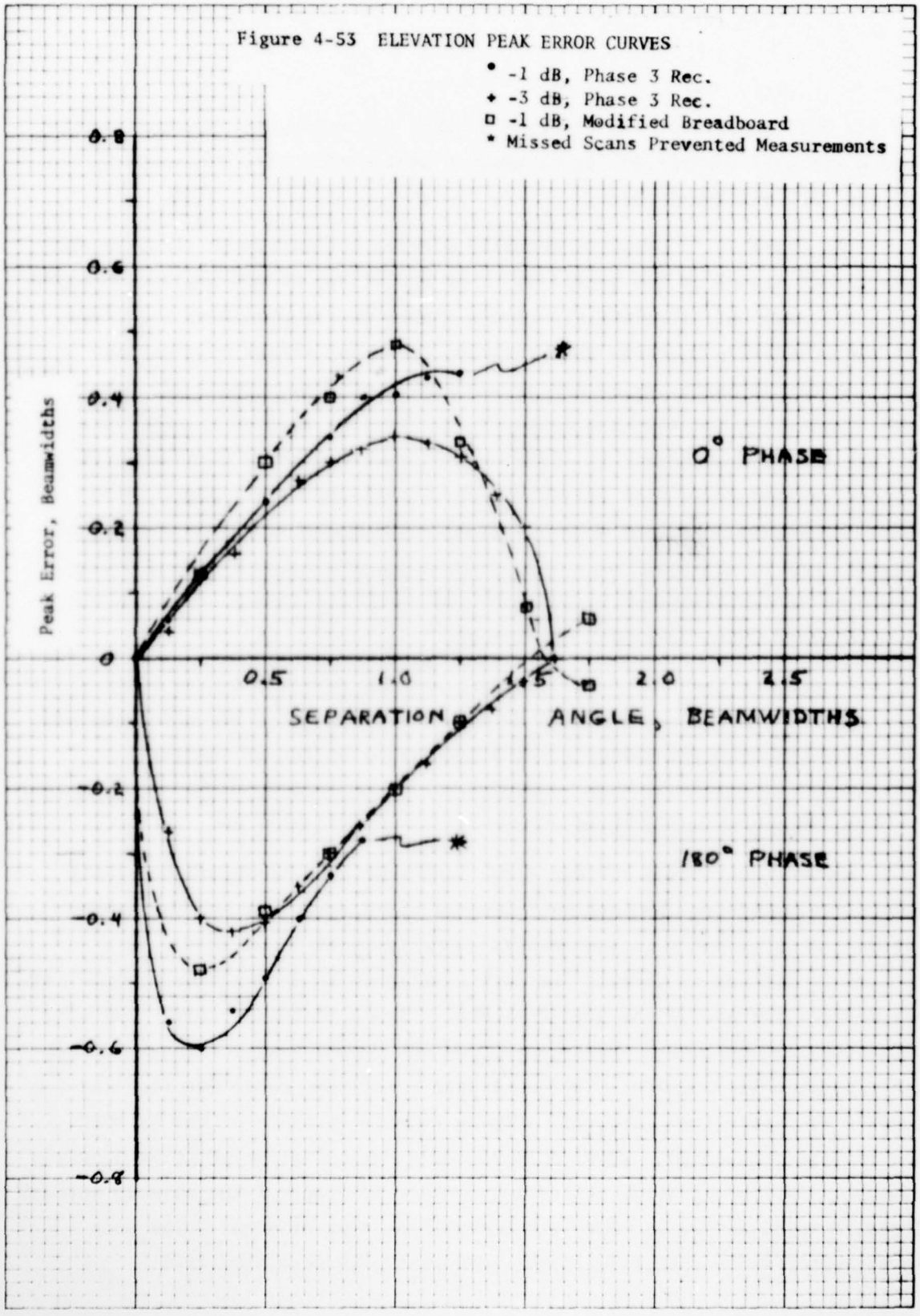
Figure 4-53 ELEVATION PEAK ERROR CURVES
• -1 dB, Phase 3 Rec.
+ -3 dB, Phase 3 Rec.
□ -1 dB, Modified Breadboard
* Missed Scans Prevented Measurements
Peak Error, Beamwidths
0.8
0.6
0.4
0.2
0
-0.2
-0.4
-0.6
-0.8
0.5
1.0
1.5
2.0
2.5
SEPARATION ANGLE, BEAMWIDTHS
0° PHASE
180° PHASE

Phase 2 1/2 TRSB receiver. The curves show that the errors for the modified breadboard are well controlled for separation angles of 1 to 1.5 beamwidths for both 0° and 180° multipath phases.

The Phase 2 1/2 receiver normally decodes the multipath signal rather than the direct signal at M/D levels of -2 dB and higher as the separation angle reaches one beamwidth. A relatively simple change in the processor logic was made in the breadboard receiver that resulted in normal errors even in the critical separation angle region and at M/D ratios of 0 dB. The logic was modified to position the tracking gates on the trailing edge of the FRO beam rather than the leading edge. In addition a narrower tracking gate was used. Logic modifications could also be made in the Phase 3 processor that should provide similar performance at 0 dB multipath. It should be noted that multipath above -3 dB at a separation angle of one beamwidth has not been a design consideration in TRSB since it is difficult to postulate a realistic scenario that can generate these multipath conditions.

A baseline test for 0 dB multipath was run on the modified Phase 2 1/2 receiver and the results are shown in Figures 4-54 and 4-55. The noise and bias curves are well controlled throughout the separation angles of interest.

4.4 Multipath Scenario Tests

Several postulated airport situations were used to derive multipath parameters for realistic simulations. Five of these scenarios are for hangar reflections in elevation with the results reported in TN-4 and TN-6. Such hangars are considered to present the most likely source of troublesome multipath. Typical results for one of the scenarios are included in this report. Two of the situations are multipath from aircraft on the ground near the runway threshold for elevation and azimuth. This multipath is of very short duration and low amplitude. Multipath from laterally sloping terrain in front of the azimuth antenna is also considered. This could be actual ground slope or drifted snow, for example. An inhomogeneous reflecting surface in front of the azimuth antenna could result in an analogous, but less controlled, type of error. The four screen reflector tests specified in the ICAO test plan were simulated.

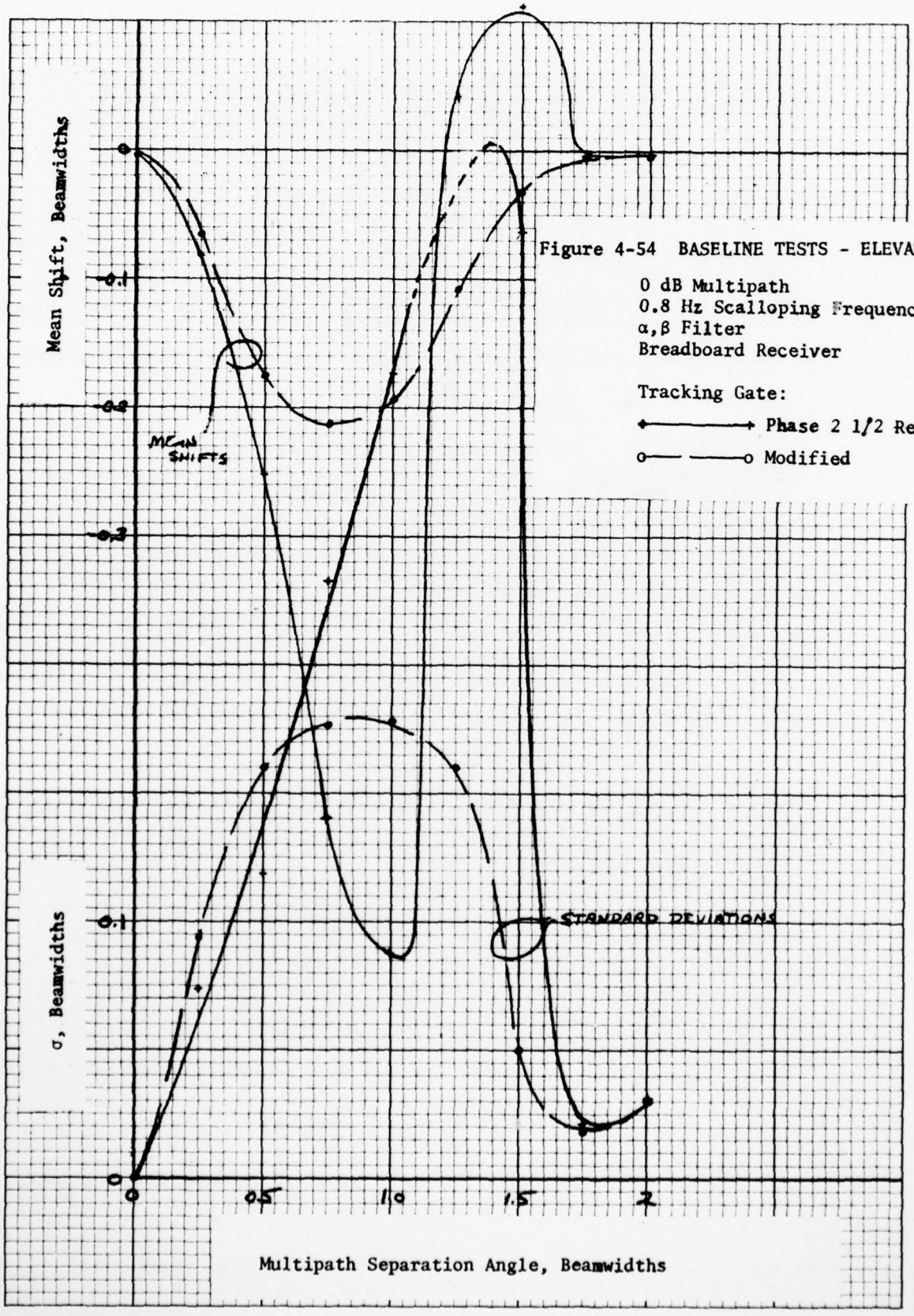

Figure 4-54 BASELINE TESTS - ELEVATION

0 dB Multipath
0.8 Hz Scalloping Frequency
α,β Filter
Breadboard Receiver

Tracking Gate:

Phase 2 1/2 Rec.

Modified

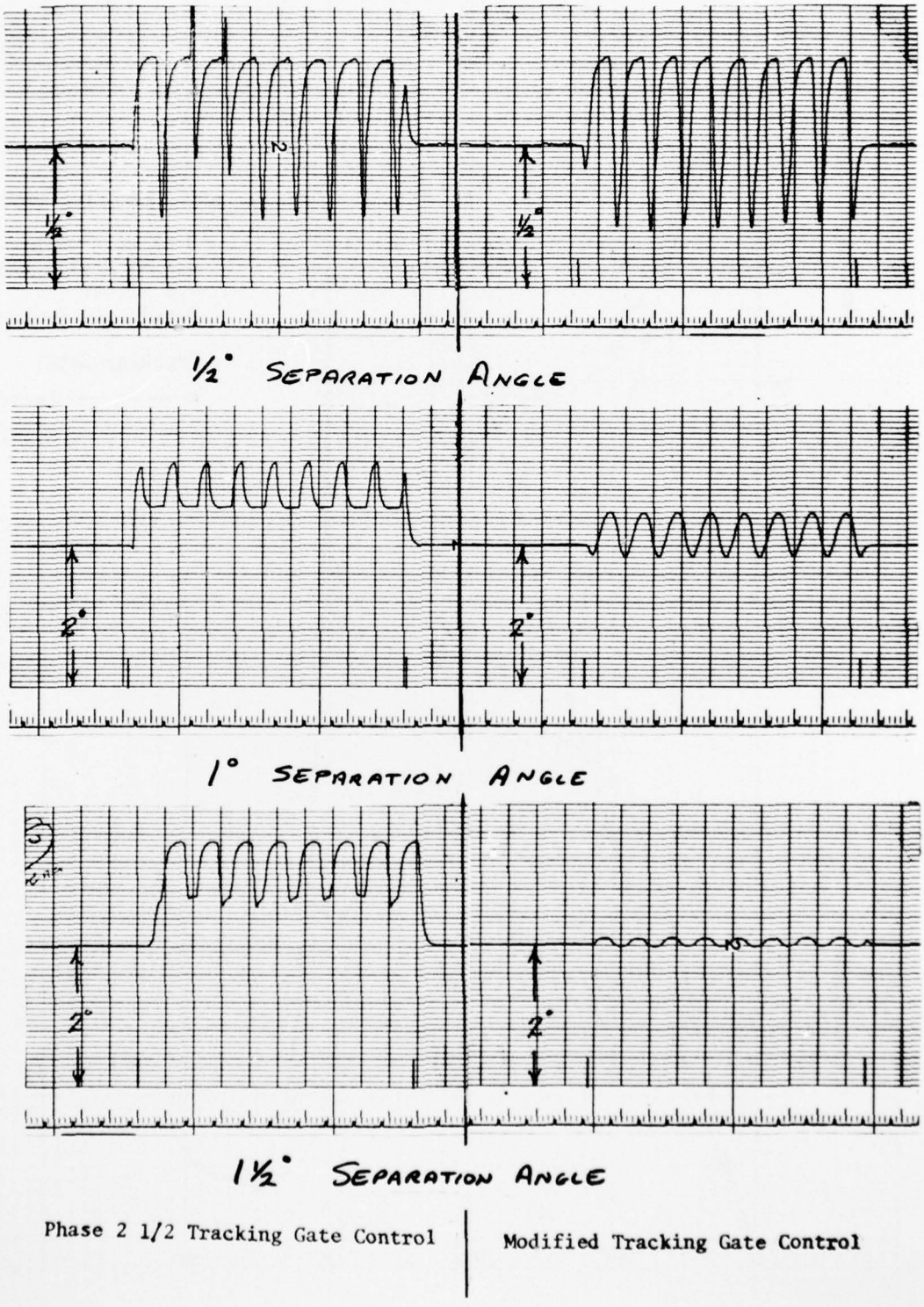

Figure 4-55 ELEVATION BASELINE TESTS - EFFECT OF MODIFIED TRACKING GATES
0 dB MULTIPATH, 0.8 Hz SCALLOPING FREQUENCY, 1° BEAMWIDTH

The geometry of the AWOP scenario 1, Building B2 (Reference 14) is shown in Figure 4-56 with the multipath parameters for an aircraft approaching at 130 knots. In the computer simulations of this scenario the multipath region was extended to occur from 3300 feet to 1350 feet to approximate the passage of the first Fresnel zone over the reflector edge.

The other scenarios tested used different hangar orientations and antenna locations which resulted in different multipath parameters. At lower approach speeds the multipath durations are proportionately longer and the scalloping frequencies lower. Some of the slow speed runs had to be truncated because of data storage limits in the computer program.

4.4.1 Results of Multipath Scenario Tests

The representative multipath situations were tested at several peak multipath levels and at different aircraft speeds. The actual multipath levels are dependent on a number of parameters but the values chosen for test are presumed to be worst case values. Errors are plotted versus the multipath amplitude that is the peak multipath/direct (M/D) ratio occurring at the receiver for this scenario. The results of the tests are determined by scalloping frequencies and multipath separation angles as well as amplitude so these parameters must be considered in comparing results.

In evaluating the results of the hangar scenarios it is necessary to consider the effects of antenna pattern shaping normally used in the horizontal pattern of the elevation antenna. For those hangar orientations producing multipath interference near runway threshold the pattern shaping reduces the M/D ratio at the receiver by -3 to -5 dB for "worst case" hangar locations. For elevation installations on the opposite side of the runway the reduction in the M/D ratio would be greater.

A typical pattern shape of gain versus angle off boresight is flat out to 10°, drops to -4 dB at 20° and -7 dB at 60°. The effect of this type of pattern shaping is noted on the graphs by a "0 dB hangar" index. The 0 dB hangar index is located by considering a hangar reflection coefficient of one (ρ=1), the path length attenuation for the scenario and the M/D reduction due

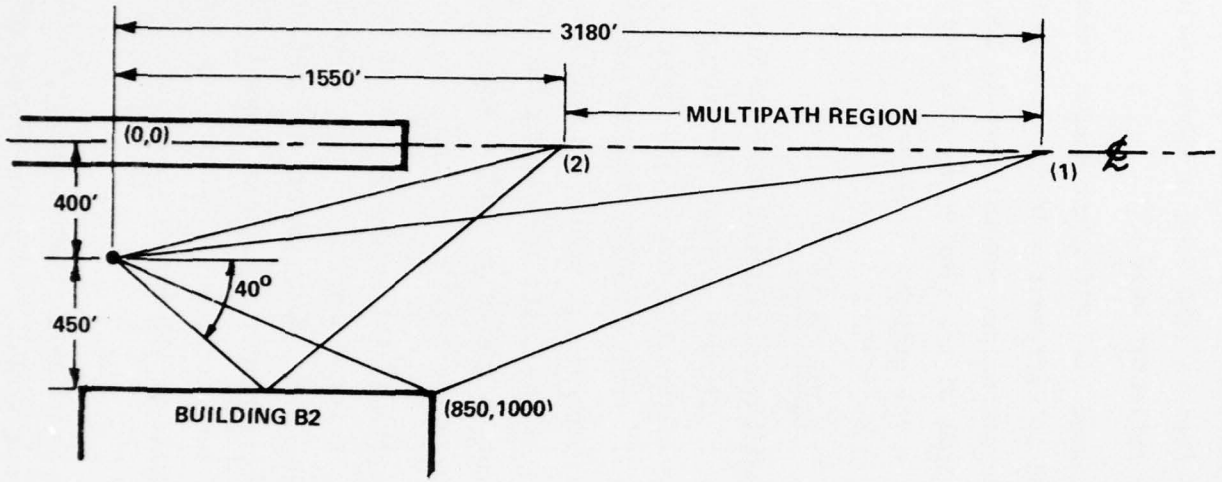

	POINT 1	POINT 2	
RANGE	3180	1550	FEET
SCALL. FREQ.*	75	228	Hz
A/C HEIGHT	159	77	FEET
REFL. HT. (GEOM.)	55	27	FEET
SEPARATION ANGLE	0.19	0.58	DEG.
GLIDE SLOPE	2.86	2.86	DEG.
PATH ATTEN	0.2	2.4	DB

*AT 130 KNOTS

Figure 4-56 AWOP SCENARIO ⊥ BUILDING 52

AD-A041 891 CALSPAN CORP BUFFALO N Y F/G 17/7
MULTIPATH AND PERFORMANCE TESTS OF TRSB RECEIVERS.(U)
MAR 77 J BENEKE, C W WIGHTMAN, C B VALLONE DOT-FA74WA-3445
UNCLASSIFIED CALSPAN-AG-5580-E-1 FAA-RD-77-66 NL

2 OF 3
ADA041891

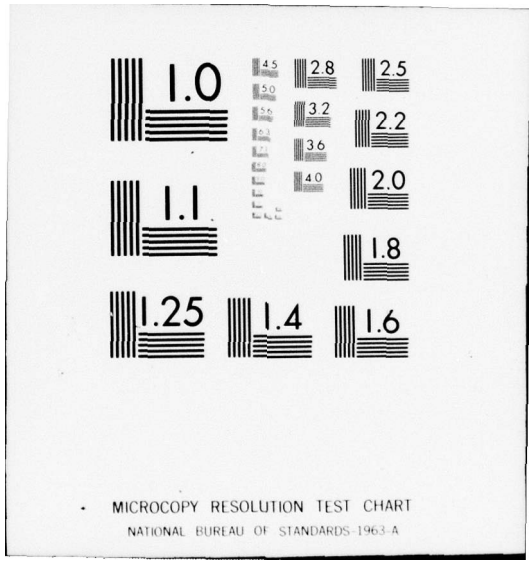
1.0
1.1
1.25
1.4
1.6
1.8
2.0
2.2
2.5
2.8
3.2
3.6
4.0
4.5
5.0
MICROCOPY RESOLUTION TEST CHART
NATIONAL BUREAU OF STANDARDS-1963-A

to pattern shaping. On Figure 4-57 a -1 dB hangar index (ρ=0.9) is also shown. Typical hangar situations would be -1 dB or less. Peak multipath amplitudes at and above the 0 dB hangar index could only occur if the airborne antenna had a large null in the direction of the direct signal.

Figure 4-57 shows the performance of the breadboard processor in the AWOP B-2 scenario when operating as a dwell gate and single edge processor (SEP). The dwell gate processing mode is representative of the Phase 2 1/2 receiver performance. The SEP is described in Section 5.

Table 1 shows the multipath parameters used in aircraft and ground reflection scenarios. Scenarios C-1 and D-1 were run at lower levels of multipath signal since they represent reflections from aircraft. The difference angle in elevation scenario (C-1) was chosen large to provide a worst case error for a tilted reflecting surface on an aircraft. As shown in Figure 4-58 the error is significant at the -6 dB multipath level but this high a level is unrealistic. The multipath separation angle in azimuth (Scenario D-1) was chosen as large as physically likely but did not result in appreciable error at any multipath level (Figure 4-59). The multipath duration is very short for both of these scenarios (0.85 sec and 0.7 sec).

If the surface in front of the azimuth antenna is flat and homogeneous, the reflected beam will be symmetrical with the direct beam and the errors will be negligible. However, if the azimuth antenna is allowed to illuminate the ground, there will be vertical lobing of the pattern with possible signal loss in the pattern nulls as well as increased susceptibility to multipath from other reflectors. When the surface is tilted laterally, the reflected beam will be displaced from the direct beam and the resultant distortion will cause errors. Any reflection variability caused, for example, by vegetation, snow cover or drifting snow, or an obstruction can cause similar errors. Scenario E-1 consists of a lateral slope of 5 degrees throughout the reflecting region. This results in a very small multipath difference angle and scalloping frequency.

The results of the E-1 tests are shown in Figure 4-60. The errors tend to become large at high multipath levels. Normally, the azimuth antenna would be designed with sufficient aperture to prevent much ground illumination. Snow drifts may still present a problem.

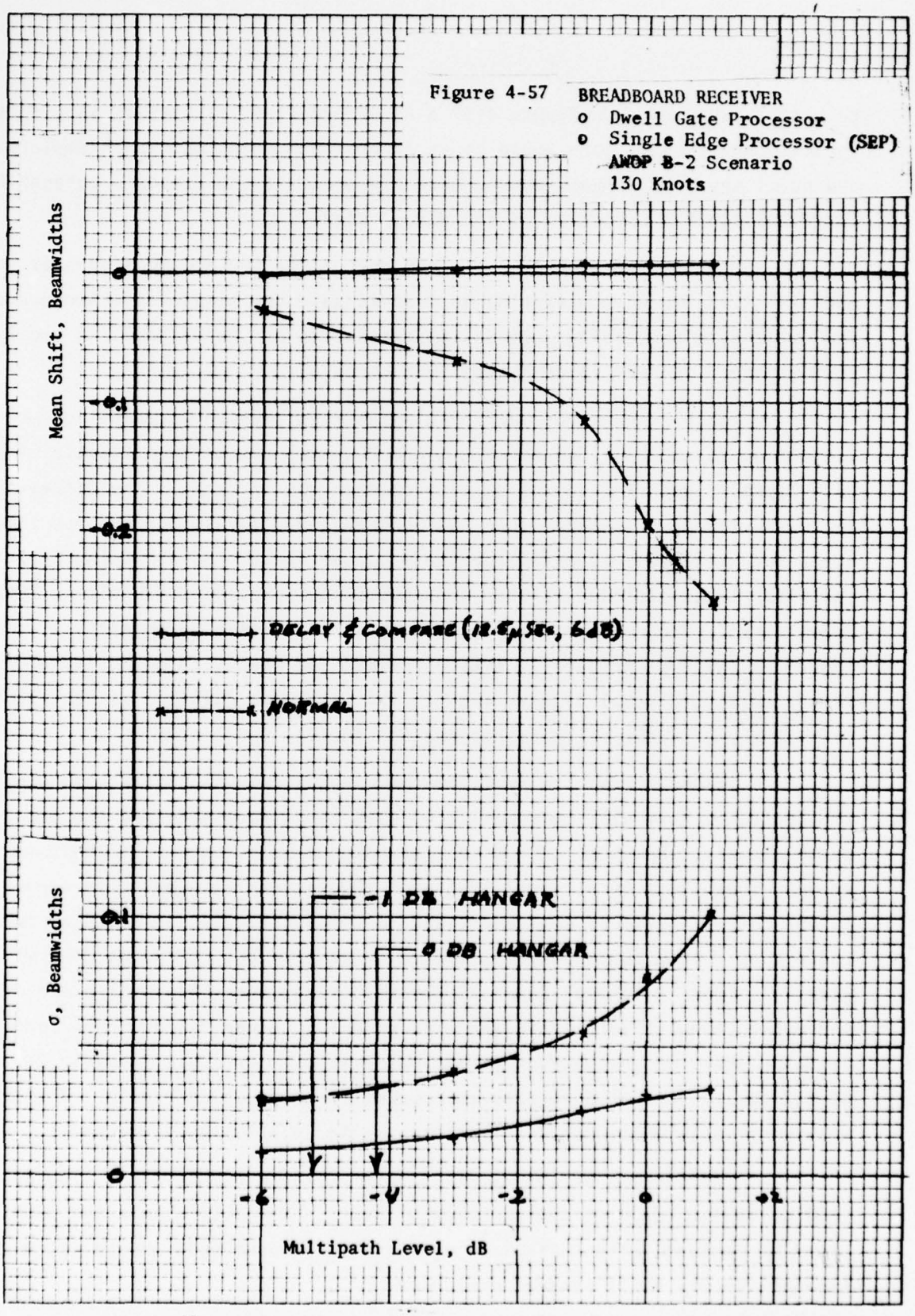

Figure 4-57 BREADBOARD RECEIVER
- o Dwell Gate Processor
- o Single Edge Processor (SEP)

AWOP B-2 Scenario
130 Knots

Table 2 AIRCRAFT AND GROUND REFLECTION MULTIPATH TEST PARAMETERS

Code	Transmitter Position*	Reflector	Multipath Ranges	Duration Seconds	Difference Angle		Scalloping Freq.		Aircraft Height	
					Start	Finish	Start	Finish	Start	Finish
					Degrees		Feet		Feet	
C1	400 Ft Offset	Large Aircraft at 400 Ft from ℄ (Non-Vertical Reflector)	1200 to 1050 Ft	0.85	1.00°	1.12°	244	284	63	55
D1	12000 Ft from EL-1	Large Aircraft at 300 Ft from ℄	1480 to 1350 Ft	0.7	1.28°	1.58°	136	139	78	71
E1	12000 Ft from EL-1	Ground (or Snow) Surface, Tilted 5° Laterally	5000 to 1000 Ft	20.0	0.18°	0.02°	0.06	0.06	262	52

*Aircraft on 3° Glide Slope

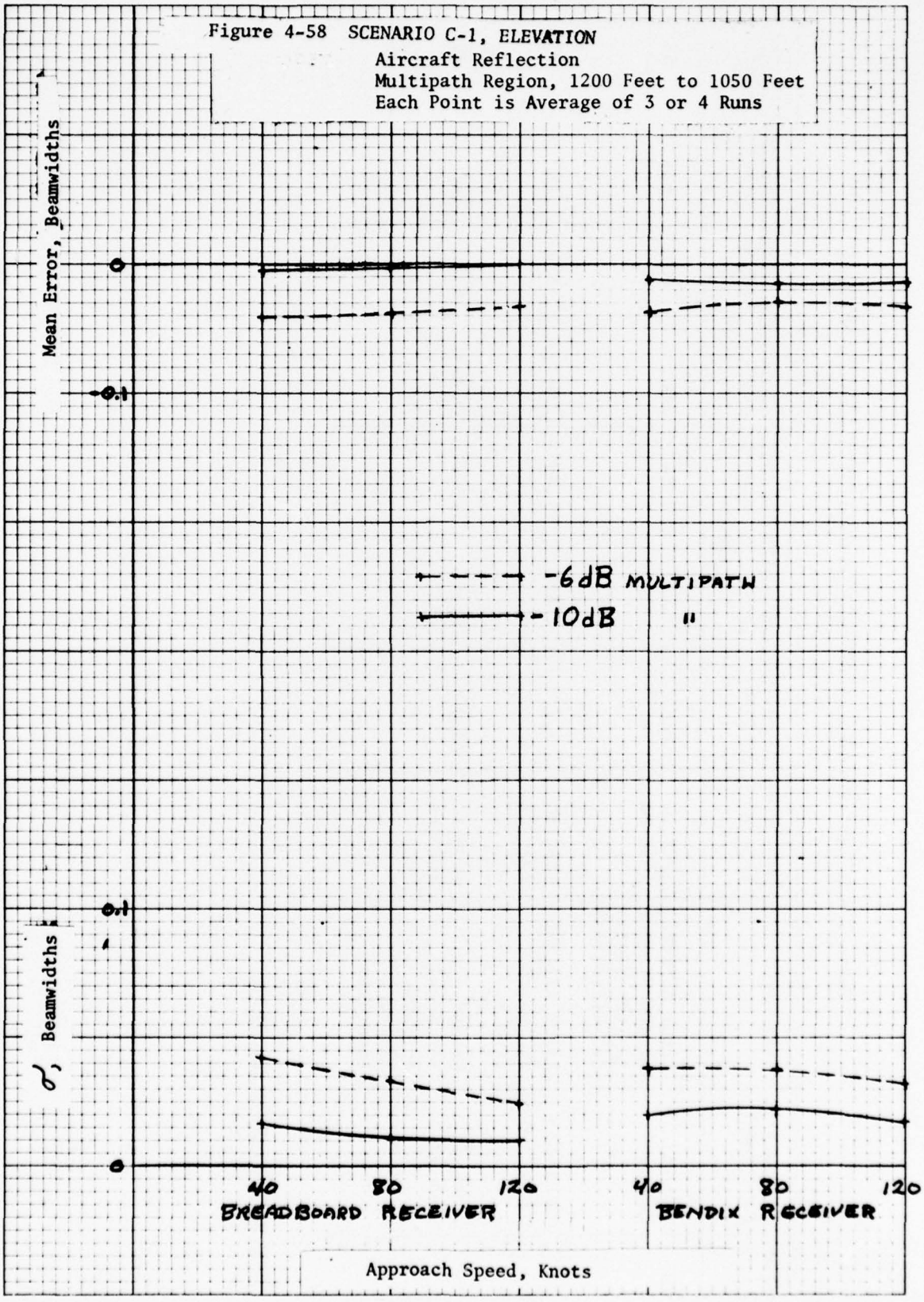
Figure 4-58 SCENARIO C-1, ELEVATION
Aircraft Reflection
Multipath Region, 1200 Feet to 1050 Feet
Each Point is Average of 3 or 4 Runs
Mean Error, Beamwidths
0
-0.1
-6dB MULTIPATH
-10dB "
σ, Beamwidths
0.1
0
40
80
120
BREADBOARD RECEIVER
40
80
120
BENDIX RECEIVER
Approach Speed, Knots

Figure 4-59 SCENARIO D-1, AZIMUTH
Aircraft Reflection
Multipath Region, 1480 feet to 1350 Feet
from Elevation Reference

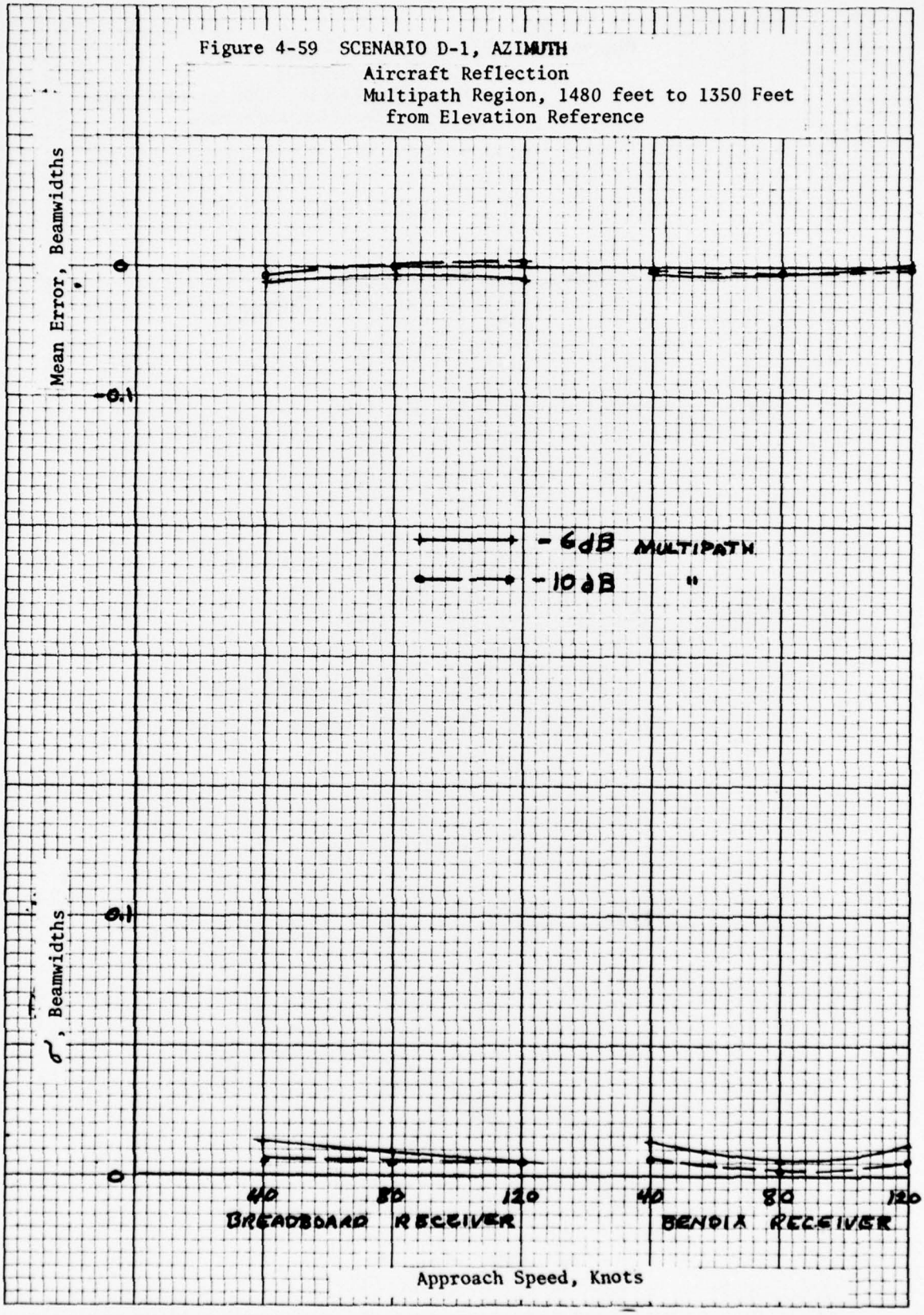

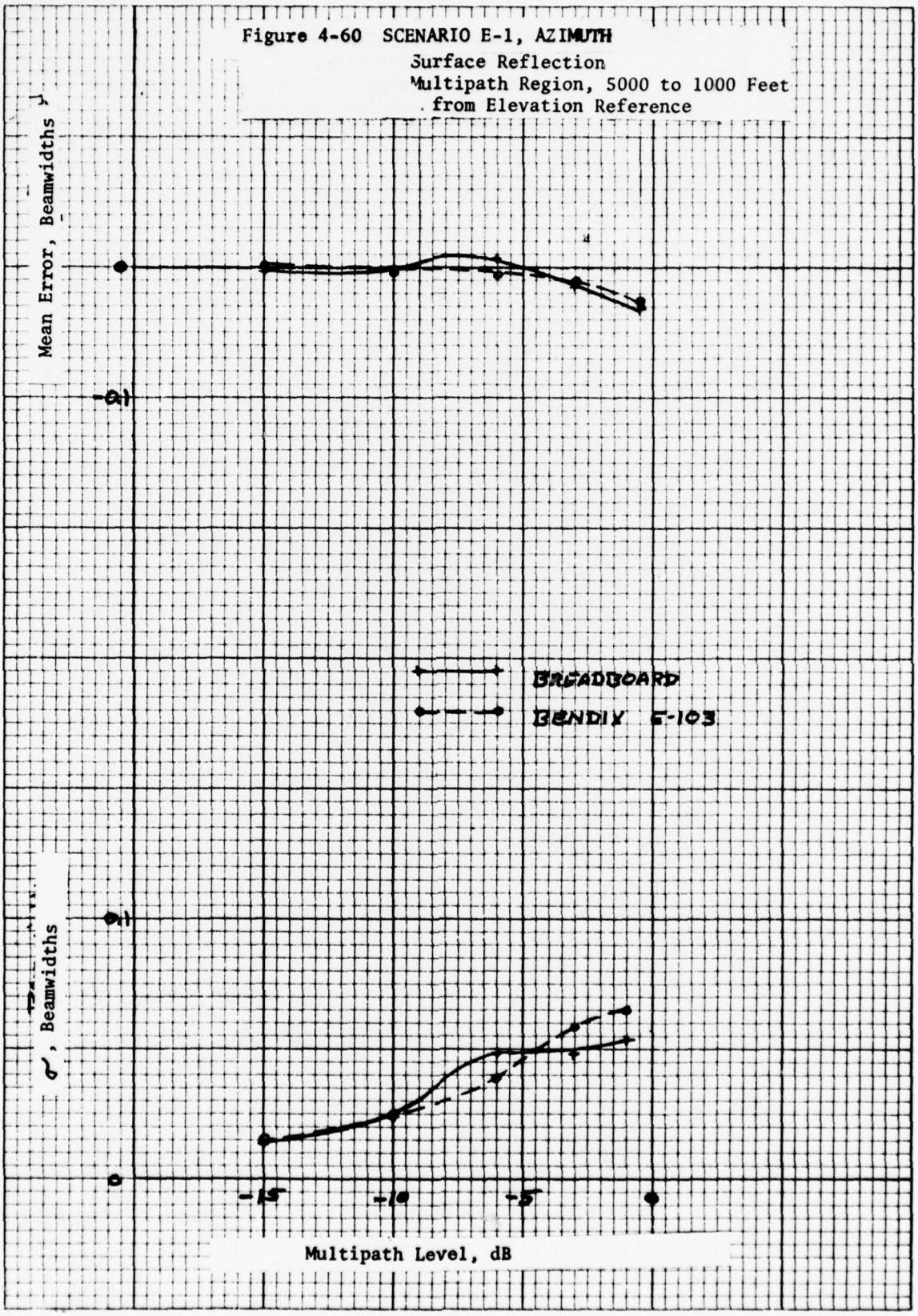
Figure 4-60 SCENARIO E-1, AZIMUTH
Surface Reflection
Multipath Region, 5000 to 1000 Feet
from Elevation Reference
Mean Error, Beamwidths
-.01
BROADBOARD
BENDIX E-103
σ, Beamwidths
.01
0
-15
-10
-5
Multipath Level, dB

The multipath parameters of the AWOP scenario B2 simulation shown in Figure 4-56 were modified to represent the same multipath interference region as that used in the digital simulation at Lincoln Laboratories (14). Edge diffraction multipath was included that extended the multipath region to 3800 feet although at a very low level. The antenna pattern was extended beyond the nominal 40° shown in Figure 4-56 resulting in multipath interference up to 1000 feet from the antenna.

Figures 4-61 and 4-62 show three repetitive runs of the breadboard receiver and the Phase 3 receiver with the modified AWOP B2 scenario. The breadboard receiver has very similar performance characteristics to the Phase 2 1/2 receiver. The rms error with the Phase 3 receiver is less than the breadboard receiver due to the sharper cutoff characteristics of the α,β filter. Comparison of the breadboard and Phase 3 receiver errors indicates that the adaptive narrow tracker gates in the Phase 3 implementation were effective in reducing the average angle error. Variations between runs in the mean error were a result of the random multipath phase for the start of each run.

4.4.2 Screen Tests

The screen tests specified in the ICAO test plan were simulated as flat plates. The actual screens use a wire mesh surface that is somewhat flexible and the flexing of the 25 ft by 50 ft frame made its reflectivity somewhat unpredictable in field tests. In addition a slight screen tilt, changes in the screen orientation and aircraft heading changes greatly affected the characteristics of the resulting multipath observed in flight tests. Thus, in the simulations a range of multipath amplitudes and screen tilt angles were used with the resulting errors bracketing the flight test results. These data are reported in Calspan TN-4.

It was found that screen test A could be reasonably well simulated by the single flat plate used in these scenarios. The screen A multipath tests generate an interference region near runway threshold. This scenario was run on the Calspan simulator using the screen location and orientation specified for the ICAO tests. The multipath interference was represented by a flat rectangle

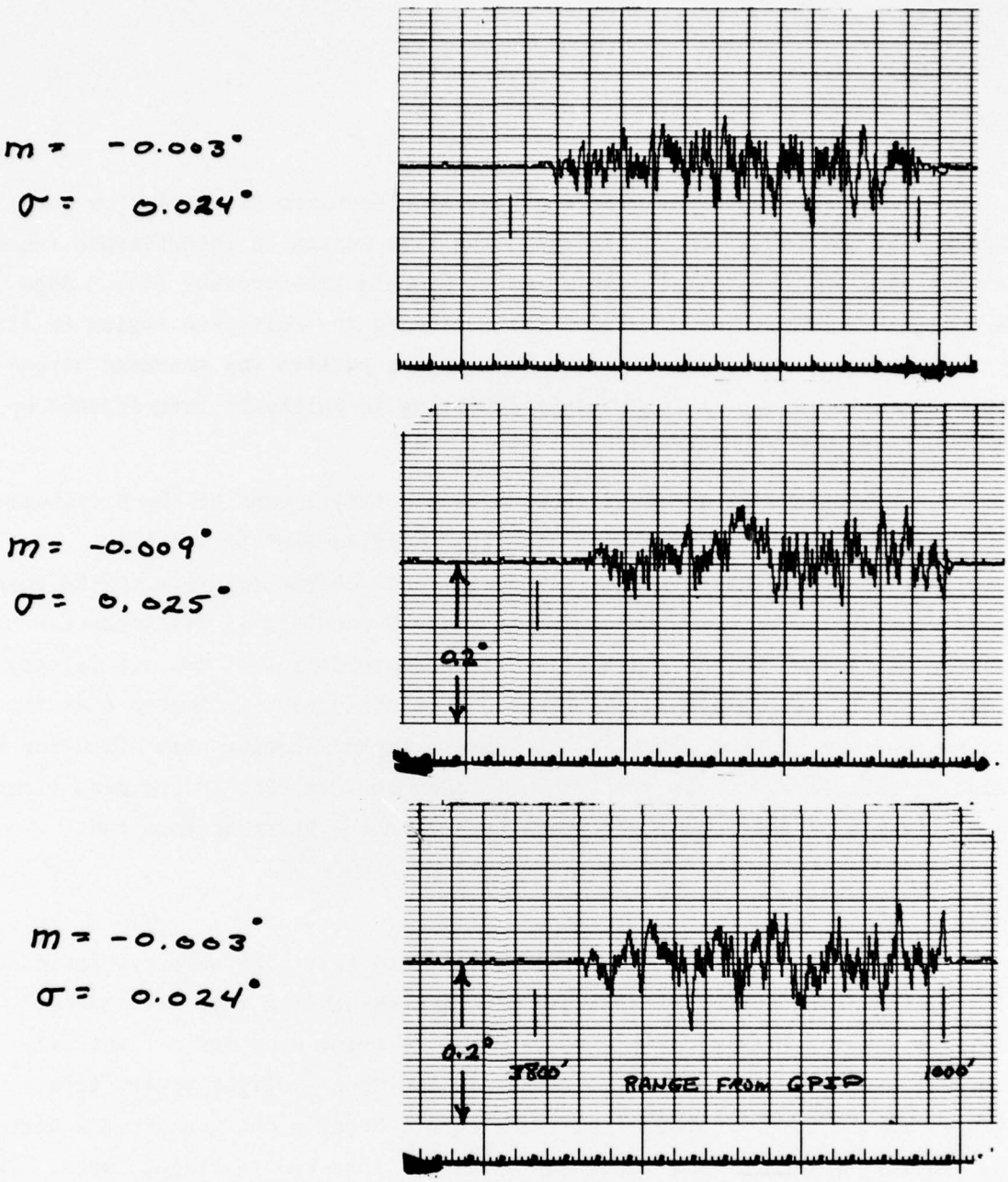

Figure 4-61 SCENARIO AWOP B-2 (MODIFIED)
BREADBOARD RECEIVER
220 FT/SEC, 20:1 GLIDE SLOPE

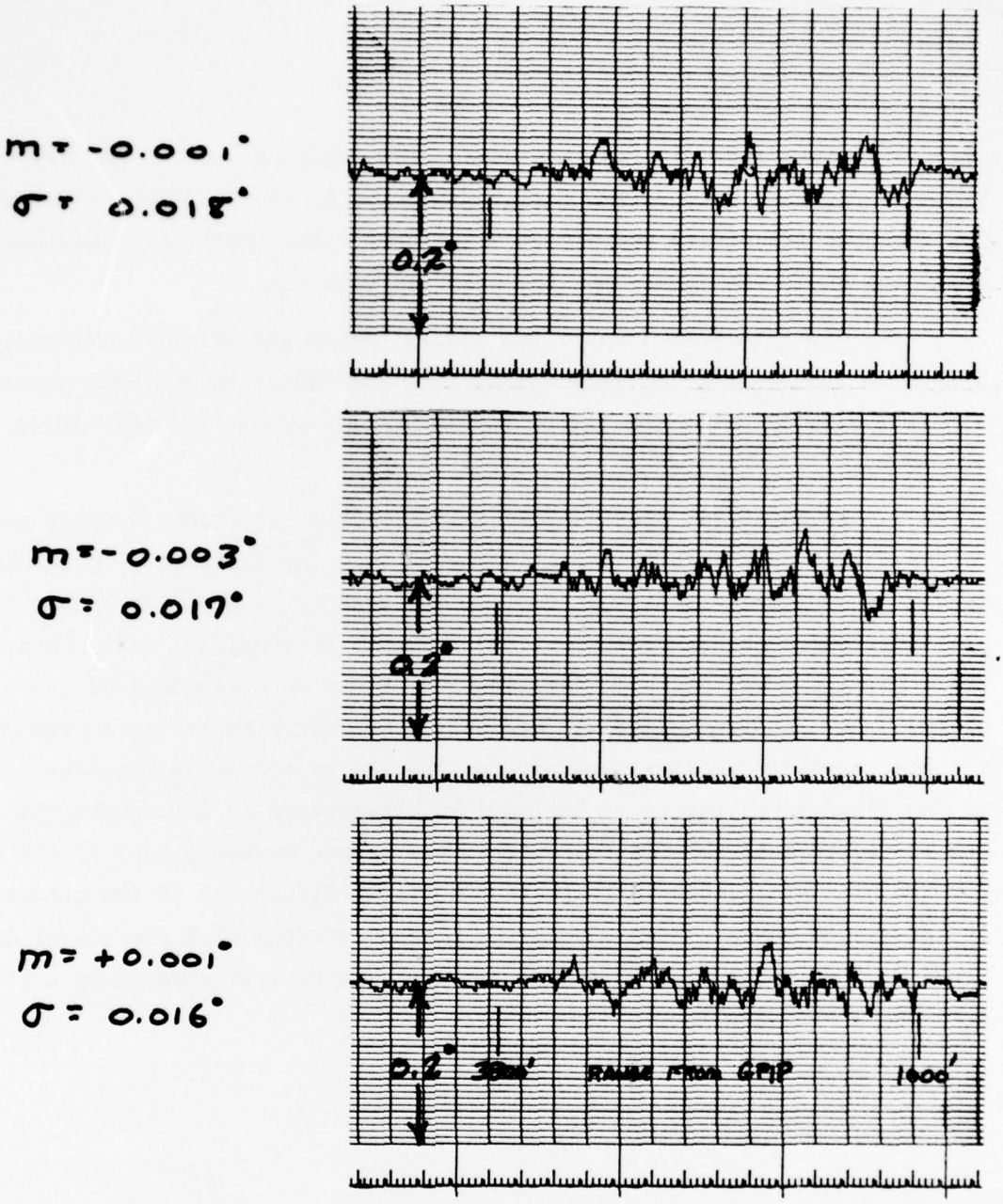

Figure 4-62 SCENARIO 1, AWOP B-2 (MODIFIED), ELEVATION
PHASE 3 RECEIVER P101
3 REPLICATIONS
220 FT/SEC, 20:1 GLIDE SLOPE

with sufficient tilt to produce a separation angle of 0.6°. Time histories shown in Figure 4-63 were run for an M/D ratio of -5 dB. Three replications are shown to illustrate the effect of different multipath phase angles. The multipath phase was random for the start of each run.

The slew rate limiter was placed before and after the 10 radian/second filter in the Phase 2 1/2 receiver to show the effect on the mean error. Placing the rate limiter after the filter significantly reduces the mean shift for this scenario.

If the first time history from filter F_1 of Figure 4-63 is compared to the flight test results shown in Figure 4-64 the similarity in the two error traces is apparent. A higher level of M/D such as -4 dB would result in very close agreement between the error magnitudes. It should be noted that the range scale for the error plots of the simulator tests were expanded by about a factor of two. Also, there appears to be considerably more filtering in the photo reduced, merged tape data plotted from the flight tests. A "smoothed curve" of the first time history is included in Figure 4-64 to illustrate the similarity. The multipath interference region from the screen occurs closer to the GPIP than for the simulator scenario indicating a slight difference in the geometry used in the flight tests. Even though the screen is not a flat surface it does produce error traces for this scenario that can be approximated by a flat screen in a multipath simulator.

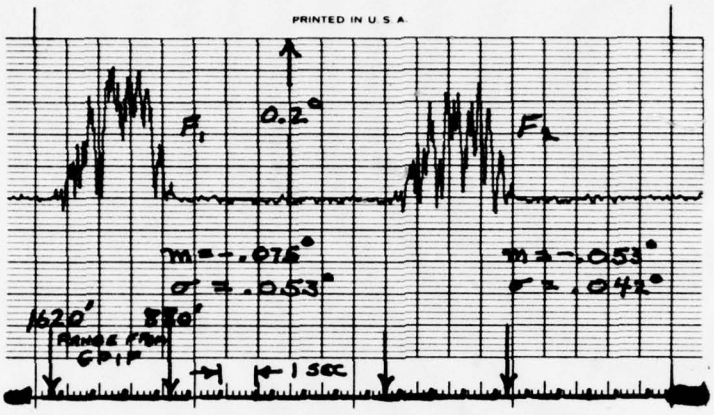

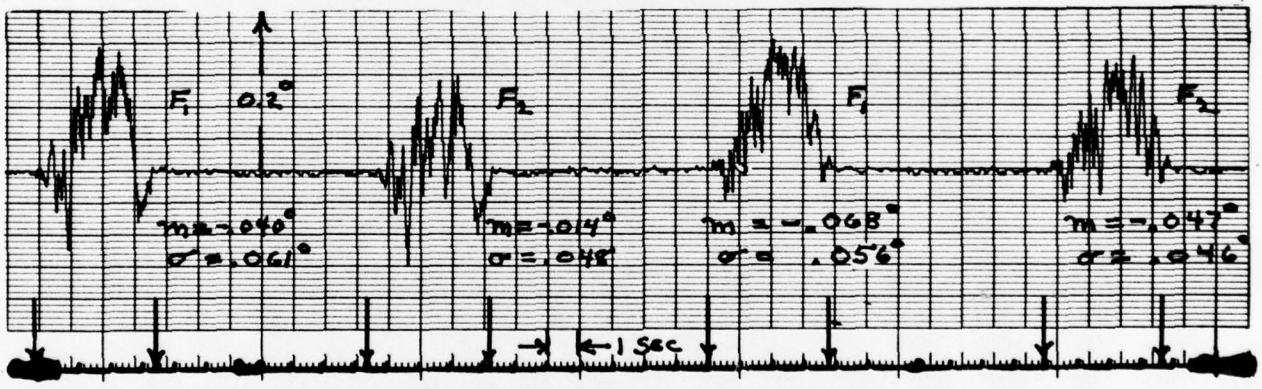

F_1 = limiter before filter

F_2 = limiter after filter

Figure 4-63 SCREEN A THRESHOLD MULTIPATH - THREE REPLICATIONS (BENDIX RECEIVER E-104, PHASE 2 1/2)

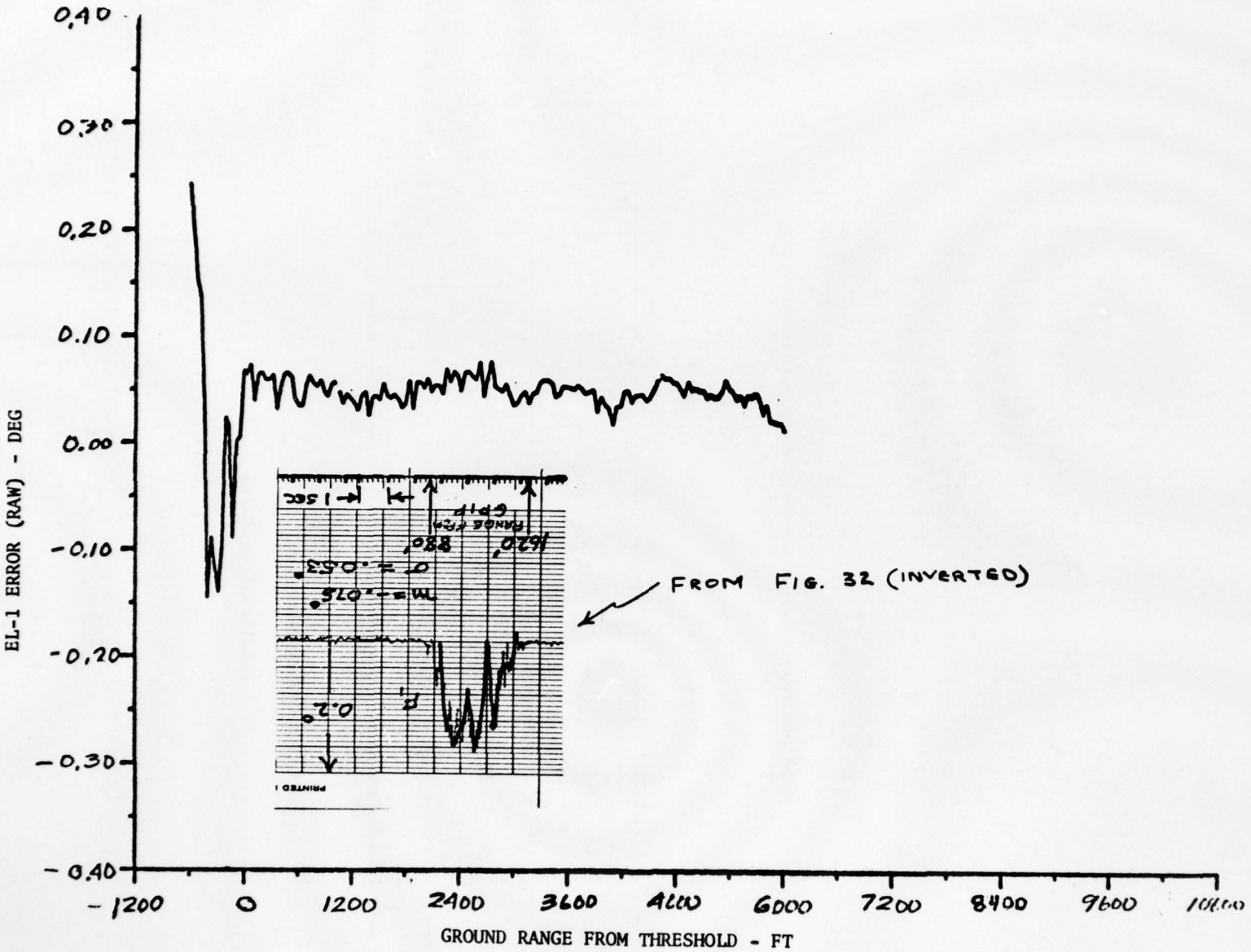

Figure 4-64 SCREEM A MULTIPATH FILM CORRECTED ERROR PLOT

Section 5.0
SINGLE EDGE PROCESSOR (SEP)

The SEP has been proposed as the airborne processing technique for flare data in the TRSB. In this section the performance characteristics of the SEP will be presented and are based upon simulation tests of the breadboard processor. In addition to processing flare data it is shown in Section 5.3 that the multipath errors in elevation data can be greatly reduced and SEP can complement the dwell gate processor for elevation data.

5.1 Description of Breadboard SEP

When multipath occurs, the beams may be distorted and errors are introduced. In the case of elevation, the distortion occurs principally on the inside beam edges for typical reflectors; vertical hangars for elevation and the surface in front of the antenna for flare. It is possible to reduce the effects of elevation multipath by making use of this characteristic and process the outside edges of the DOWN-UP scans. This technique is referred to as single edge processing.

A delay and compare technique was implemented that is similar to the processor under evaluation for flare. On the DOWN scan, the video signal is attenuated and compared with the unattenuated but delayed video signal. Equality of these signals starts the counter. During the UP scan, it is the delayed signal that is attenuated and compared with the undelayed, unattenuated signal. Equality then stops the counter. A bias determined by an average beamwidth measurement is subtracted from the count to produce the angle indication.

The operation of the Calspan breadboard delay and compare receiver is depicted in Figure 5-1 and the signals involved are shown in Figure 5-2. The threshold points to start and stop the angle indication count are adjustable by means of the analog delay line (to 30 μseconds) and the attenuation bias level (attenuation is proportional to bias for a log video signal). The values currently being used are 12.5 microseconds and -10 dB. The comparator output is high when

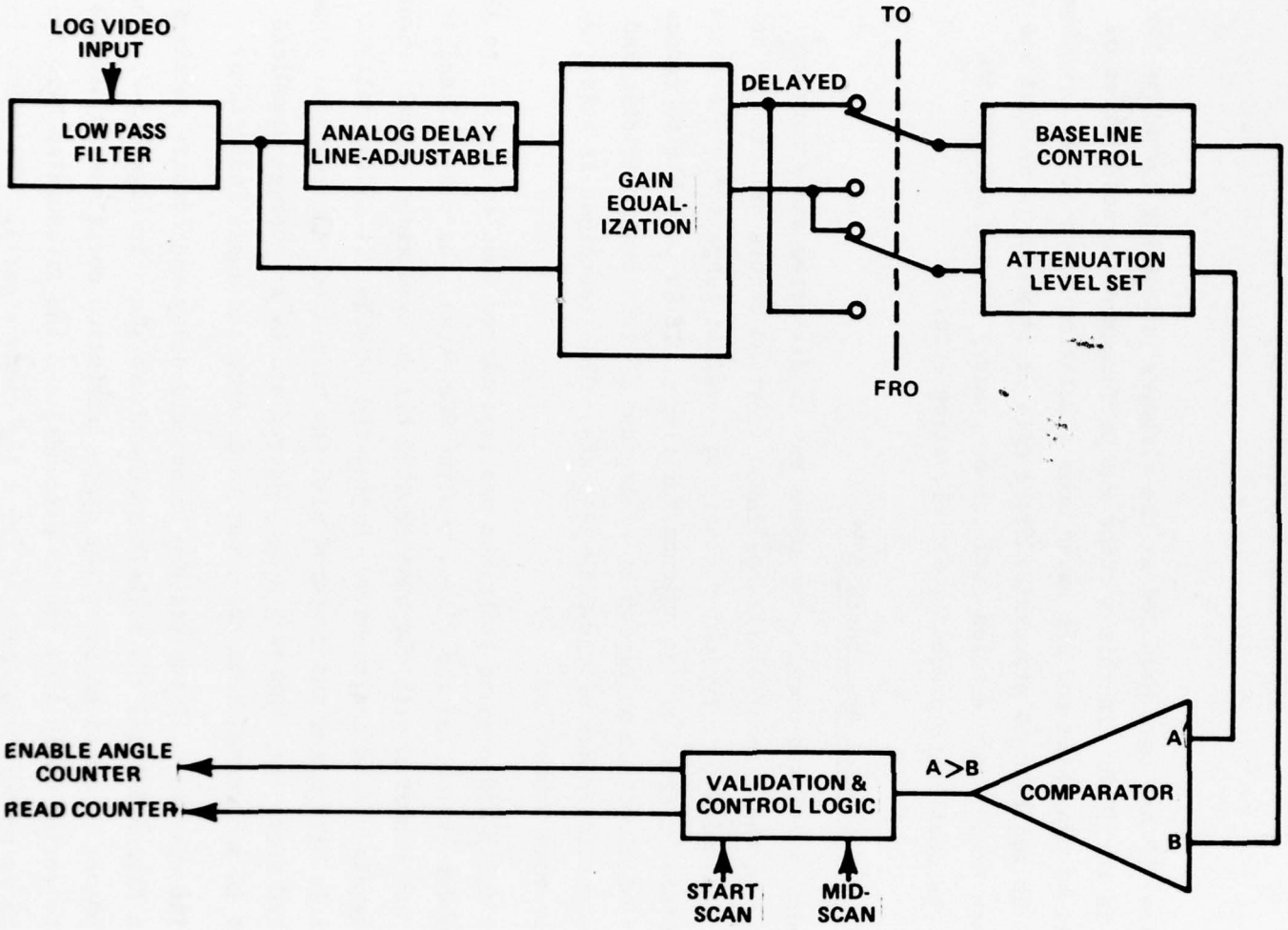

Figure 5-1 CALSPAN BREADBOARD DELAY AND COMPARE RECEIVER

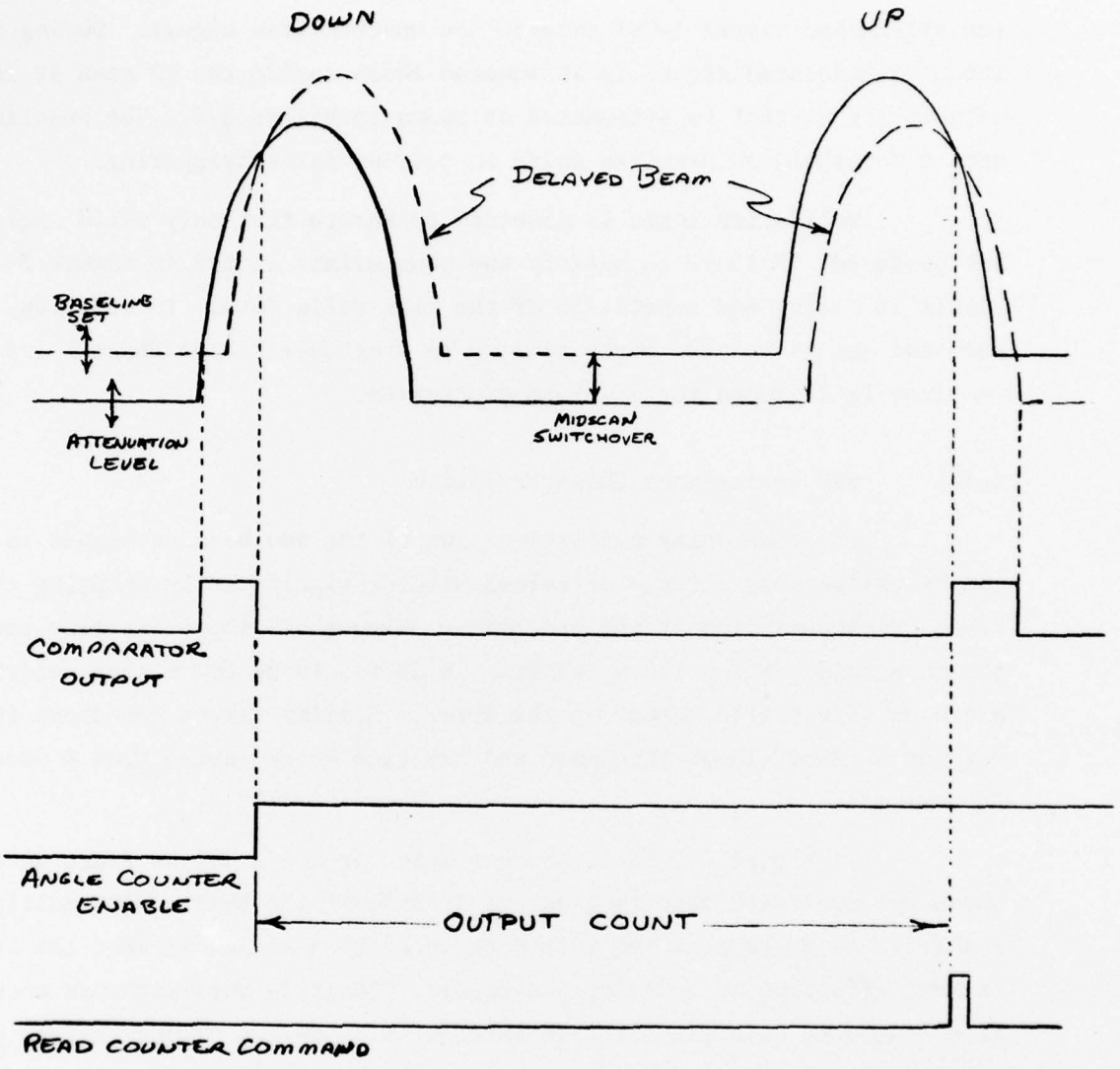

Figure 5-2 DELAY & COMPARE RECEIVER WAVESHAPES

Validation & Control Logic Functions

1) "Angle Counter Enable" may be set high only during the "DOWN Scan."

2) "Read Counter" command is issued only during the "UP Scan" when angle counter enable is high.

3) "Angle Counter Enable" is set high by the first trailing edge out of the comparator; succeeding comparator outputs will not affect it.

4) A "Read Counter" command is issued for every comparator leading edge in the UP scan and the final read counter is the actual count that is put out.

the attenuated signal level exceeds the unattenuated signal. During the DOWN scan the undelayed signal is attenuated while during the UP scan it is the delayed signal that is attenuated as shown in Figure 5-2. The baseline control sets a threshold on baseline noise to prevent false triggering.

Validation logic is provided to ensure that only valid angle counts are produced. Failure to satisfy the constraints listed in Figure 5-2 will result in a flag and repetition of the last valid data. In addition, a peak detector and associated logic similar to that used in the Phase 2 1/2 threshold receiver is included for sidelobe protection.

5.1.1 SEP Performance Characteristics

The time delay and attenuation of the two beam envelopes in the SEP can be varied over a range of values without significantly changing the multipath error characteristics of the processor. Figure 5-3 shows baseline tests in which the threshold setting is varied from -6 dB to -10 dB for a time delay of 12.5 μseconds with little affect on the error. Similar curves are shown in Figure 5-4 for a fixed -10 dB threshold and the time delay varied from 8 μseconds to 20 μseconds.

In Figure 5-5 baseline test data for a 1/2 degree flare antenna are shown for multipath occurring on either side of the beam. Most multipath scenarios generate negative multipath separation angles so that the SEP technique is very effective in reducing the errors. Positive multipath can occur in the flare maneuver when the aircraft antenna is below the ground antenna phase center height. Roof edge diffractions from tall hangars can also generate positive separation angles. The error curves of Figure 5-5 shows that significant errors can occur unless the multipath level is low and the positive separation angles are small. This is the case for realistic situations as will be shown in Section 5.2.4.1.

Motion averaging is still effective at positive multipath separation angles in reducing the standard deviation of the errors as is shown in Figure 5-6 for tests out to a scalloping frequency of 200 Hz. The higher scalloping frequencies have little affect on the mean errors.

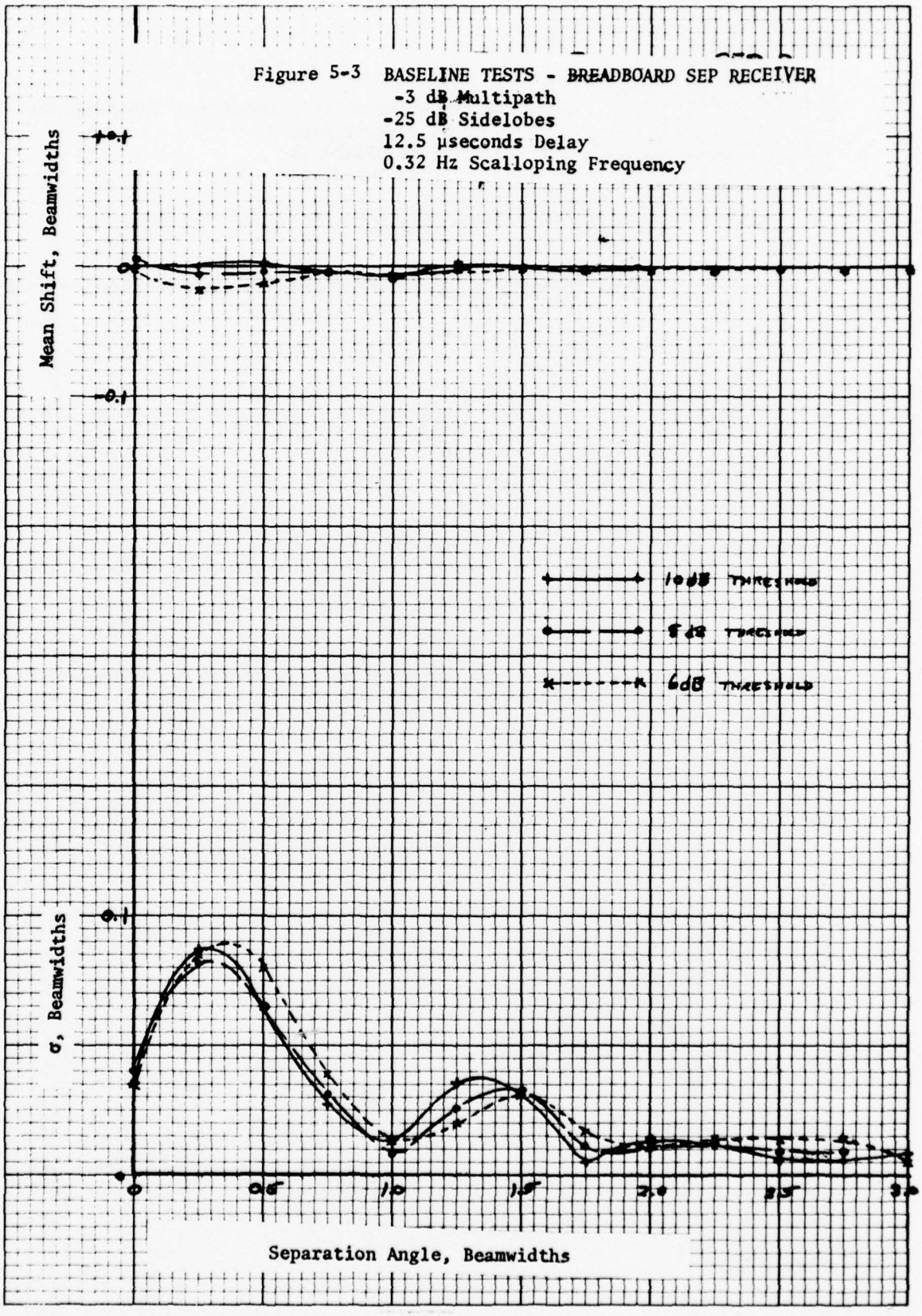
Figure 5-3 BASELINE TESTS - BREADBOARD SEP RECEIVER
-3 dB Multipath
-25 dB Sidelobes
12.5 μseconds Delay
0.32 Hz Scalloping Frequency
Mean Shift, Beamwidths
+0.1
0
-0.1
10dB THRESHOLD
8 dB THRESHOLD
6dB THRESHOLD
σ, Beamwidths
0.1
0
.05
.10
.15
.20
.25
.30
Separation Angle, Beamwidths

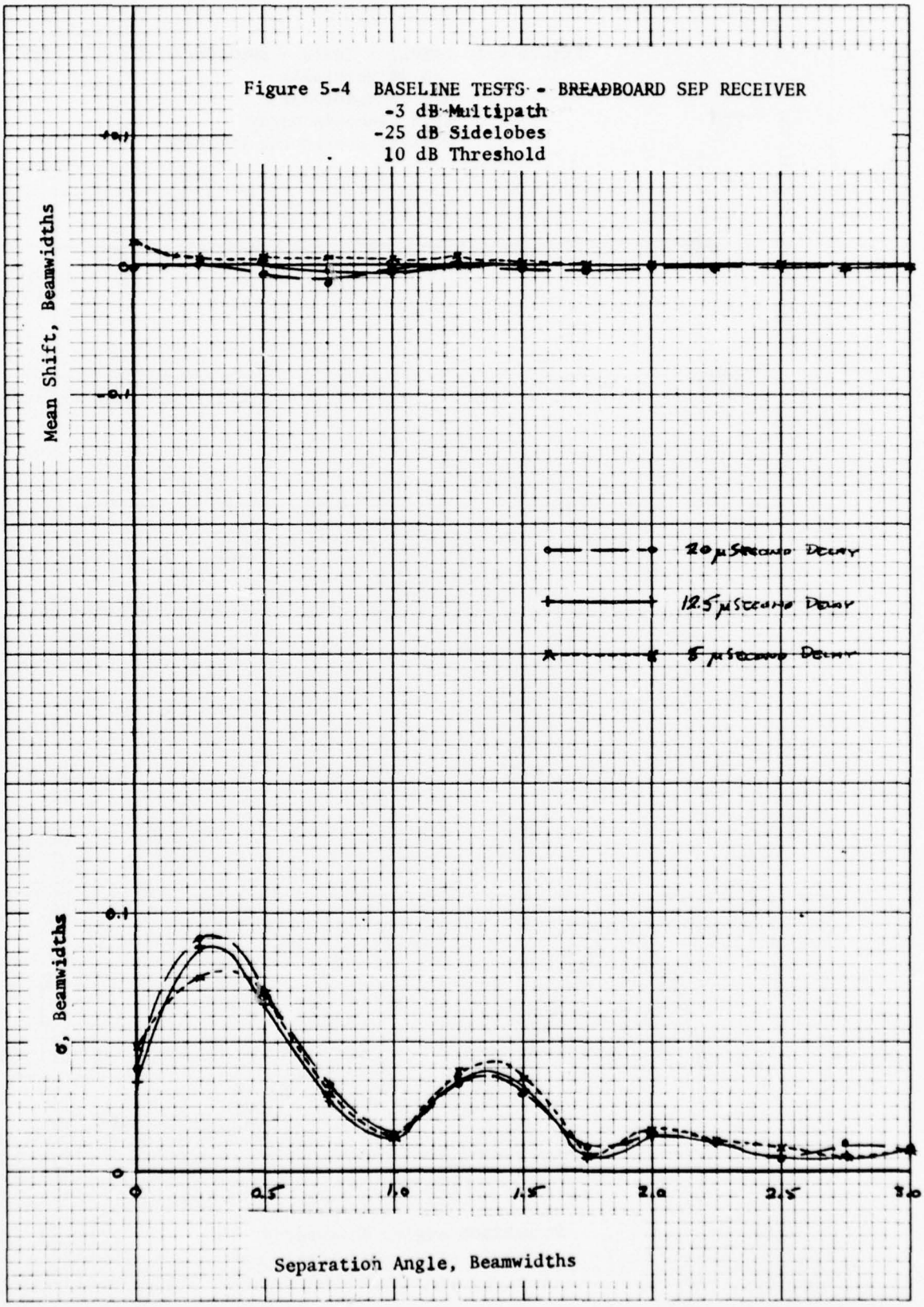
Figure 5-4 BASELINE TESTS - BREADBOARD SEP RECEIVER
-3 dB Multipath
-25 dB Sidelobes
10 dB Threshold
Mean Shift, Beamwidths
+0.1
0
-0.1
20 μ Second Delay
12.5 μ Second Delay
5 μ Second Delay
σ, Beamwidths
0.1
0
0.5
1.0
1.5
2.0
2.5
3.0
Separation Angle, Beamwidths

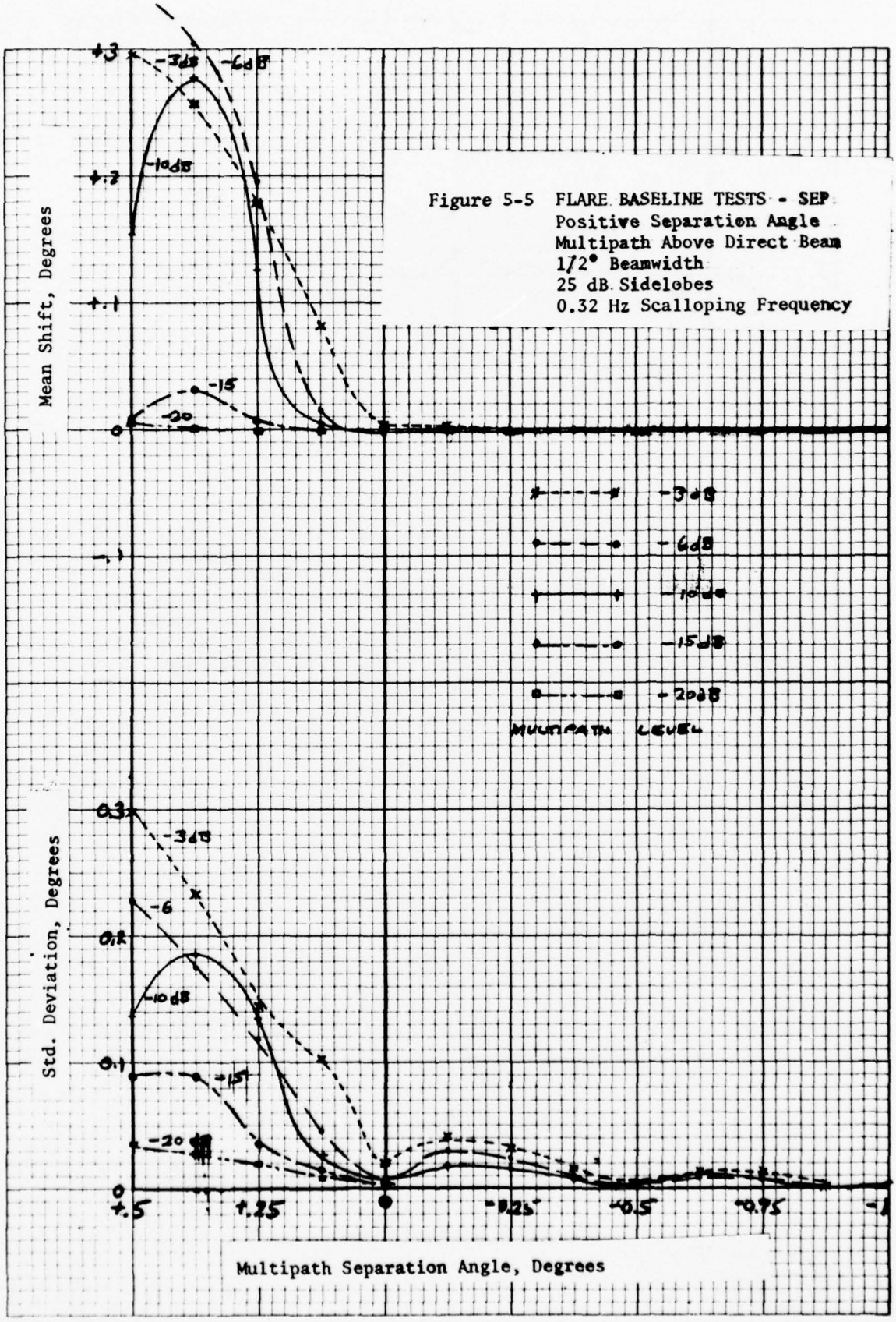

Figure 5-5 FLARE BASELINE TESTS - SEP
Positive Separation Angle
Multipath Above Direct Beam
1/2° Beamwidth
25 dB Sidelobes
0.32 Hz Scalloping Frequency

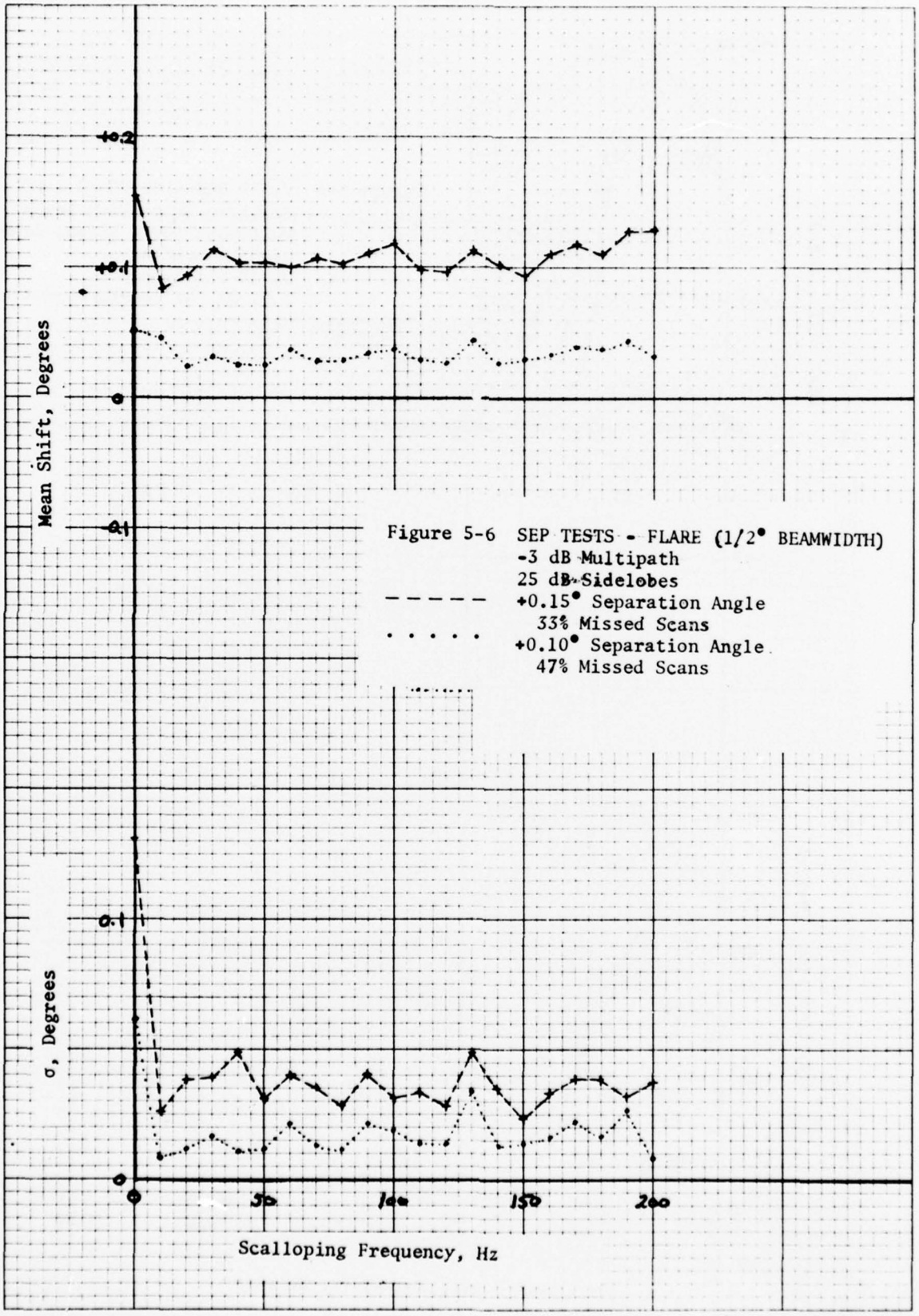

Figure 5-6 SEP TESTS - FLARE (1/2° BEAMWIDTH)
-3 dB Multipath
25 dB Sidelobes
– – – – – +0.15° Separation Angle
33% Missed Scans
. . . . . +0.10° Separation Angle
47% Missed Scans

5.1.2 Linearity Effects

The SEP accuracy is sensitive to any beam shape distortions in the receiver processing. Nonlinearities in the log IF amplifiers can cause shifts in the decoded angle that vary for different signal levels. Tests were run on the log IF in the Calspan breadboard over the useable range of signal levels. Figure 5-7 shows the mean shift and standard deviation of the decoded angle for a 10 second test period at various signal levels. The mean shifts fall within about 1% of the correct value down to signal levels of -73 dBm. At -82 dBm the beam shape distortion is sufficient to cause system flags. The linearity specification on this log IF was ±1 dB over the 80 dB input range of the amplifier.

For single edge processing it would be desirable to have a log IF with better linearity. With a digital processor these mean shifts can be calibrated out and used as a correction factor in the angle decoding. These correction factors could be determined in the initial bench checks on the receiver and then stored in the computer memory. Further test data are required on the log IF nonlinearities before the need for a calibration factor can be determined.

The sensitivity of the SEP to nonlinearities should be considerably reduced in a digital processor that can utilize averaging techniques in determining the threshold point. Thus, the nonlinearities in the log IF may not be very significant for subsequent SEP designs.

5.1.3 Beamwidth Measurements

The SEP angle measurements must be corrected by a quantity proportional to the beamwidth of the signal. This quantity is approximately constant for ranges in the far-field (beyond D^2/λ) antenna pattern for elevation data. For flare data with the antenna focused at 1500 feet the beam will become broader in the far field. The beamwidth correction can be determined from a dwell-gate width measurement using averaging and outlier criteria to minimize the effects of multipath and noise.

The dwell gate measurement should be carried out as soon as the beam is acquired. This will avoid the principal effects of multipath that occur at lower altitudes. Receiver noise at low signal level causes the standard

Figure 5-7 SEP PERFORMANCE VS. SIGNAL LEVEL

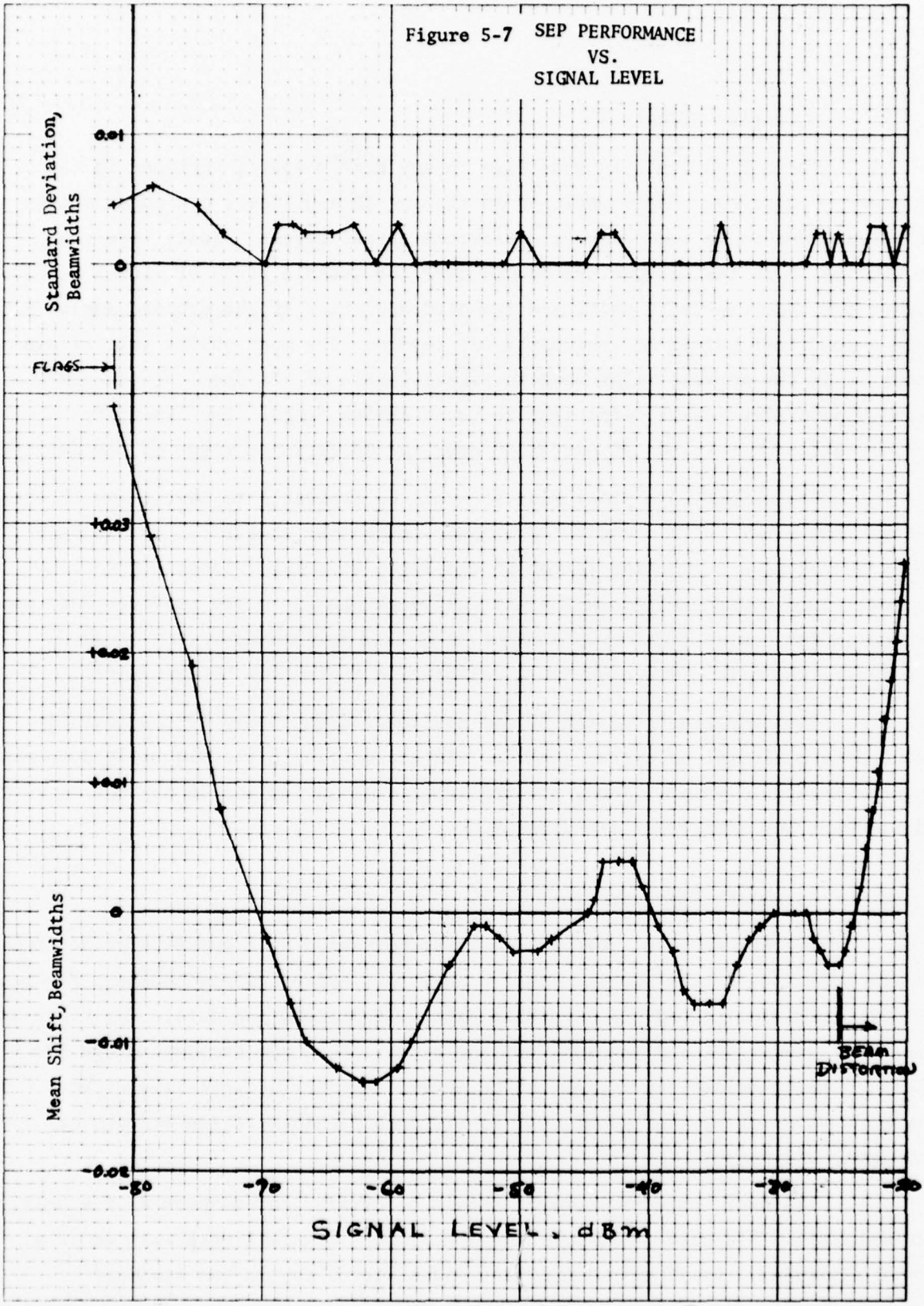

deviation of beamwidth measurement illustrated in Figure 5-8. The sum of the DOWN and UP dwell gates for each scan was used for this measurement. The standard deviation of an average dwell gate measurement can be reduced by the square root of the number of measurements in the average. For example, 5 seconds of averaging (at 40.5 scans/second) will reduce the average dwell gate standard deviation to about 0.002° at a -100 dBm signal level. At higher signal levels shorter averaging times will provide even more stable measurements.

It is necessary to maintain linearity in the signal processor so that the dwell gate threshold retains its level as the signal input is varied. In the breadboard receiver (implementation is similar to Phase 2 1/2 receivers) this was not the case, with the result that the measured dwell gate width varied with signal level. This is illustrated in Figure 5-9 where the threshold was set at -7 dB (average of the SEP comparison points, -4 dB and -10 dB) in the middle of the range.

The breadboard receiver uses an analog delay line (ITT type TCA 350) or bucket brigade device to provide the delayed log video signal to the threshold comparator. Most of the system nonlinearity appeared to be in this delay circuitry. No attempt was made to linearize this circuit or to try some of the newer bucket brigade devices now on the market. It is apparent that a great improvement in linearity or compensation is necessary if an analog circuit is to be used for beamwidth measurement. The use of digital circuitry such as is used in the Phase 3 receivers (analog to digital converter and digital shift registers for delay) would provide good linearity and permit accurate beamwidth measurements.

5.1.3.1 Effects of Multipath

Beamwidth measurements can be affected by multipath signals distorting the beams. Simulations were run to determine how much averaging is required in the beamwidth measurement to make the effects of multipath insignificant. A series of tests were run with the AWOP B-2 elevation hangar reflections using different averaging times before the beam is distorted by the multipath. Figure 5-10 shows the results of these tests. These data show that beamwidth measure-

Figure 5-8 STANDARD DEVIATION OF DWELL GATE WIDTH MEASUREMENTS AS-A FUNCTION OF INPUT SIGNAL LEVEL BREADBOARD RECEIVER

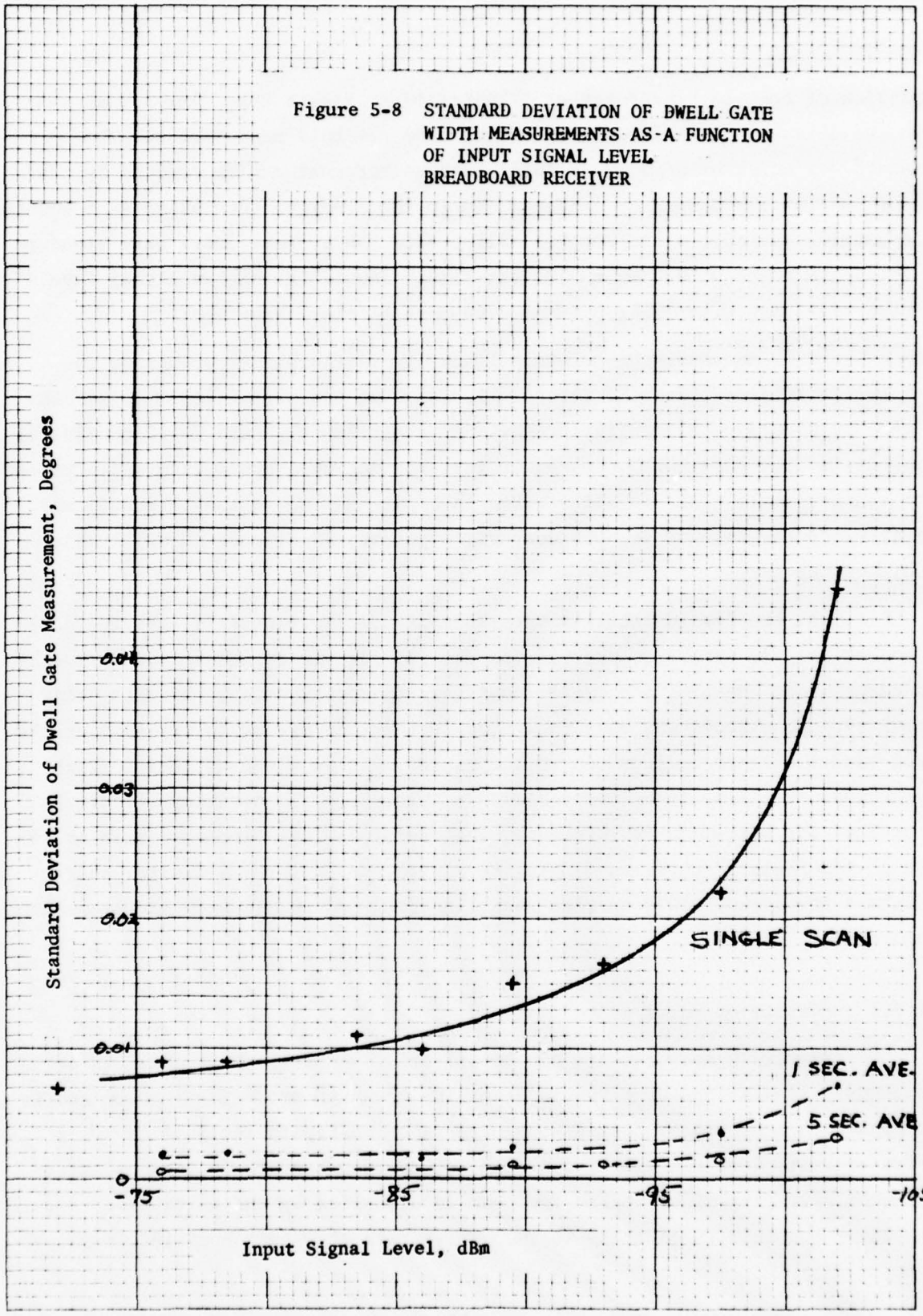

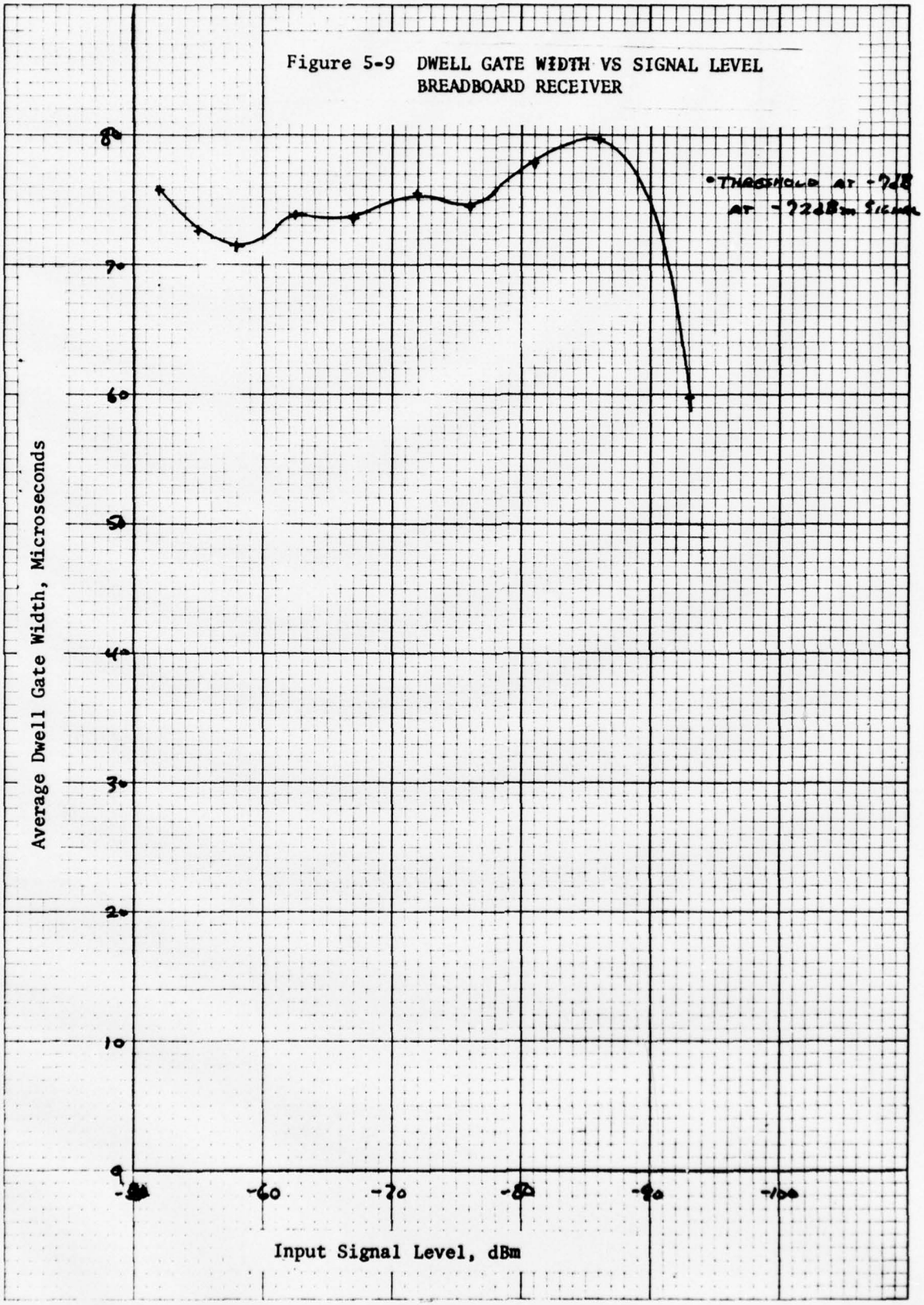
Figure 5-9 DWELL GATE WIDTH VS SIGNAL LEVEL
BREADBOARD RECEIVER
*THRESHOLD AT -92
AT -92dBm SIGNAL
Average Dwell Gate Width, Microseconds
80
70
60
50
40
30
20
10
0
-50
-60
-70
-80
-90
-100
Input Signal Level, dBm

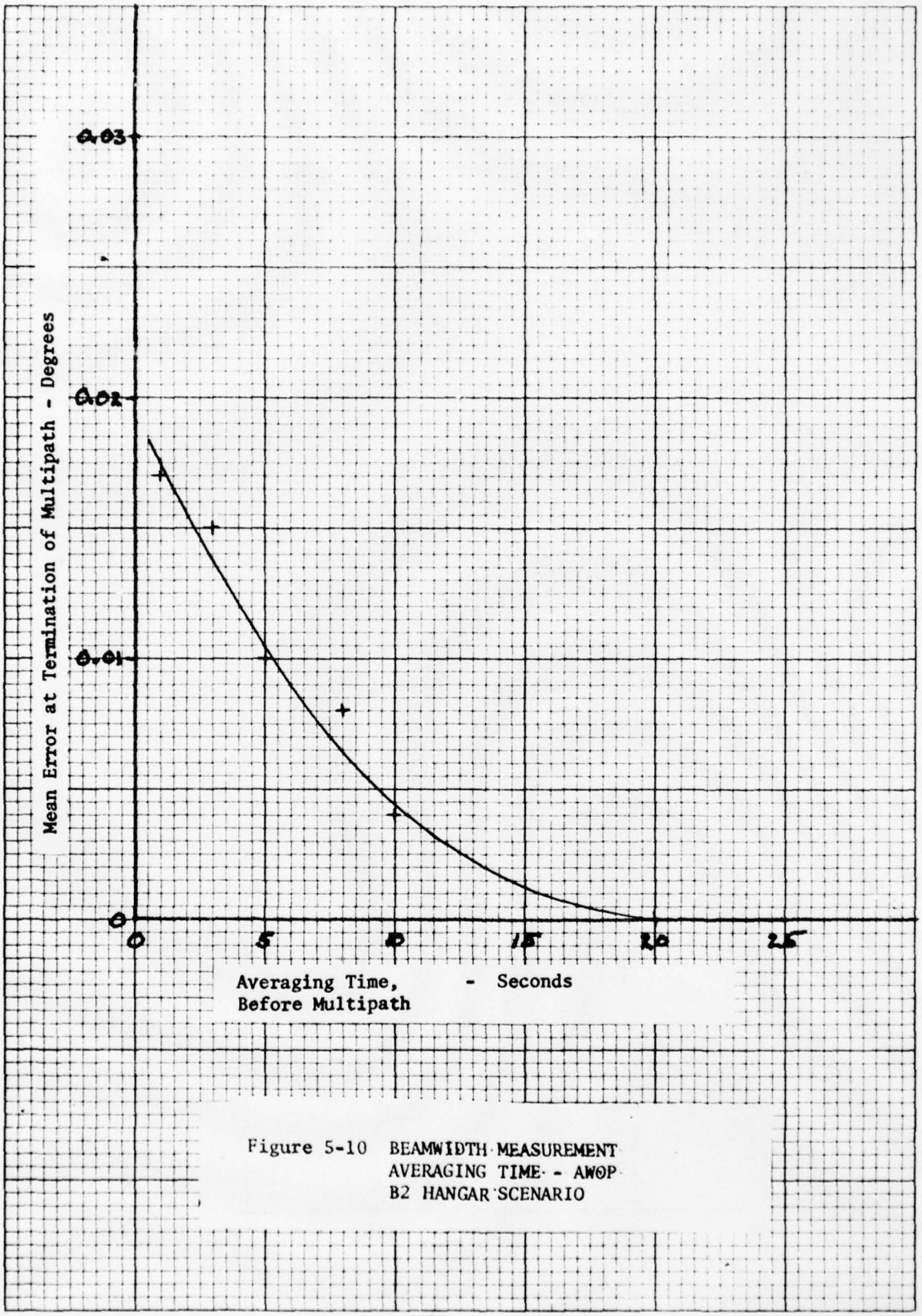

Figure 5-10 BEAMWIDTH MEASUREMENT AVERAGING TIME - AWOP B2 HANGAR SCENARIO

ments averaged 10 seconds before the multipath region would result in an increase in the mean error of 0.004 degrees. Zero error results for a 20 second averaging period. Averaging times of 10-20 seconds are short enough to make insignificant the error from beam broadening due to the scan angle in elevation and the focussed flare antenna.

If the SEP is used in the flare processor sufficient averaging must be used in the beamwidth measurement to make the effects of ground reflections insignificant. It was found from flare simulations that for a touchdown at threshold and a 0 dB ground reflection if the beamwidth average measurements are started at 26 seconds before touchdown the error in the elevation angle measurement will be less than 0.004 degrees.

Beam broadening due to near field effects can also affect beamwidth measurements. These effects should be insignificant since they only occur for long touchdowns near the antenna. The long touchdown flight paths have very small beam distortions from ground reflections and are in the broadened beam of a focussed antenna for about 3 seconds. The beamwidth for an antenna focussed at 2500 ft does not increase significantly until within about 1500 feet from the antenna. The averaging time of 26 seconds is too long to permit the beamwidth measurements to follow the near field beam broadening. However, the increased error that does occur close to the antenna can be accommodated in the angular error budget that increases as the touchdown distance from the antenna decreases. In the far field the beamwidth will change slowly with range so that long averaging times may be acceptable. The optimum averaging time for flare data can only be selected from a computer simulation of the antenna pattern variations as a function of the range from its focal point.

5.2 Flare Tests with SEP

Flare scenarios were run to measure the peak errors expected with the SEP technique. Some comparison tests were run using a multipath control technique (MCT) requiring power programing of the ground antenna and an airborne correction in the processor. Several hangar scenarios were run including a tilted hangar to determine the significance of hangar reflection on the SEP for flare data.

5.2.1 Flare Scenarios

All of these scenarios are based on an exponential flare with fixed parameters, e.g. a preprogramed flare path. These parameters are:

Initial Aircraft Antenna Height	60	Feet
Initial Glide Slope	3	Degrees
Horizontal Aircraft Velocity	200	Feet/Second
Initial Descent Rate	10.5	Feet/Second
Descent Rate at Touchdown	2	Feet/Second

The range at touchdown (from a point on centerline opposite the flare antenna) was varied from 4000 feet to 1000 feet in 1000 foot increments*. The height of the aircraft antenna at touchdown was set at 8 feet and 12 feet. Twelve feet is typical of a transport type aircraft considering the antenna to wheel height and angle of attack. Eight feet is the specified minimum guidance height for flare and represents the worst case multipath beam separation angle.

A horizontal reflecting ground was assumed throughout the tests. Reflectivity was taken as 70% (-3 dB) and 100% (0 dB). (Zero dB results are reported here. Typically, a 25% reduction in peak error was found for -3 dB multipath.) The antenna phase center height was 15 feet for a 1/2° beamwidth and 11 feet for 3/4° beamwidth. These heights allow approximately 3 feet clearance for snow. The multipath phase was computed for the geometrical path length difference with an added 180° phase shift at reflection. This would be typical for near grazing incidence.

Figure 5-11 illustrates the geometry of these flare scenarios. The multipath separation angle is $(\theta_D + \theta_M)$ from this diagram. As the aircraft descends, the multipath separation angle becomes small and the effect of the multipath increases. Plots of the extreme cases of separation angle variation with time are shown in Figure 5-12. The smallest separation angles occur for touchdowns at 4000 feet from the antenna. The separation angles for a touchdown at 1000 feet remain large and the multipath errors for this case are correspondly

*The simulator does not include the effects of beamwidth variations with range.

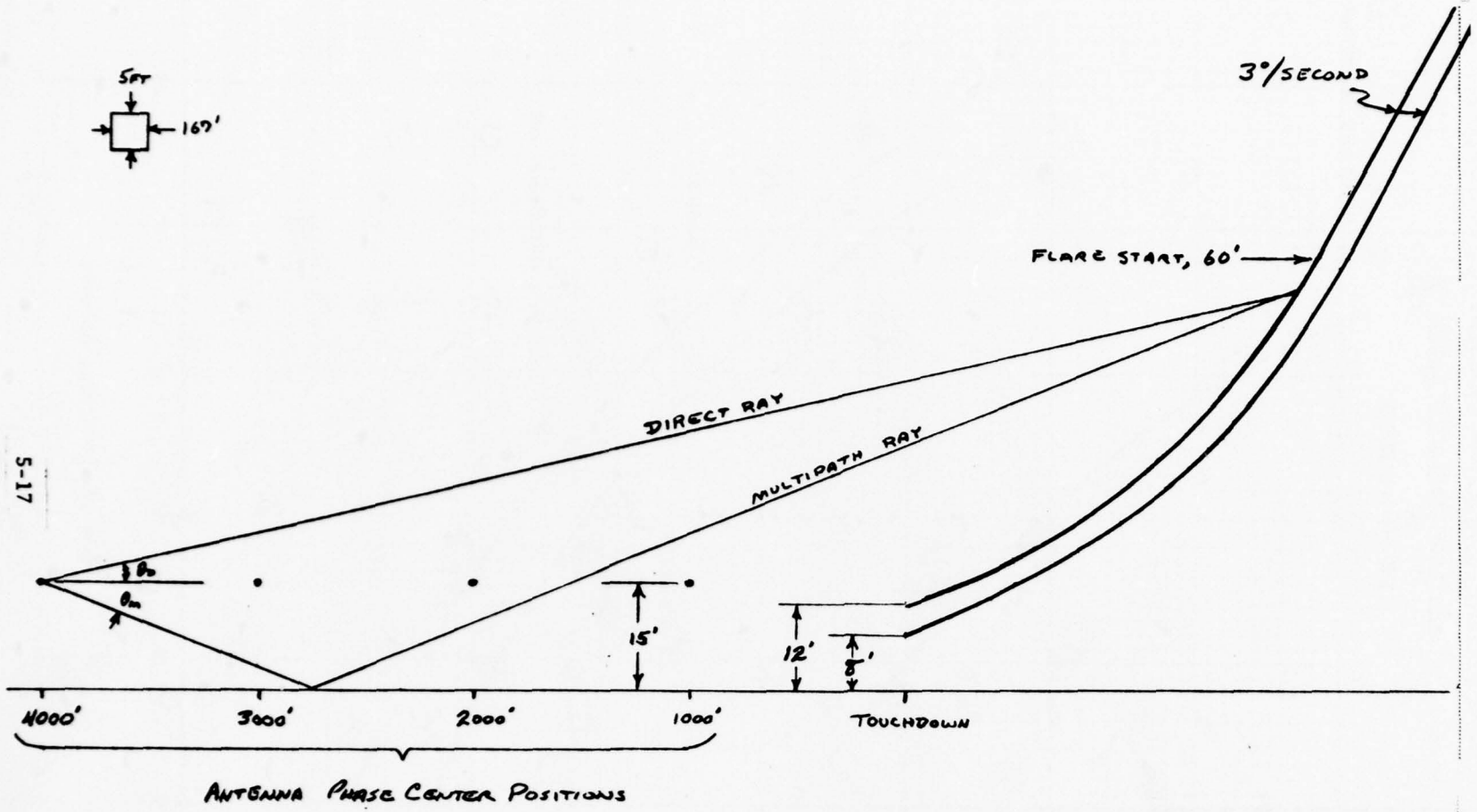

θ_D - Direct Angle

θ_M - Multipath Angle

Aircraft Antenna Path Shown

1/2° Antenna Beamwidth

Note: The multipath separation angle is $\theta_D + \theta_M$

Figure 5-11 FLARE SCENARIO GEOMETRY

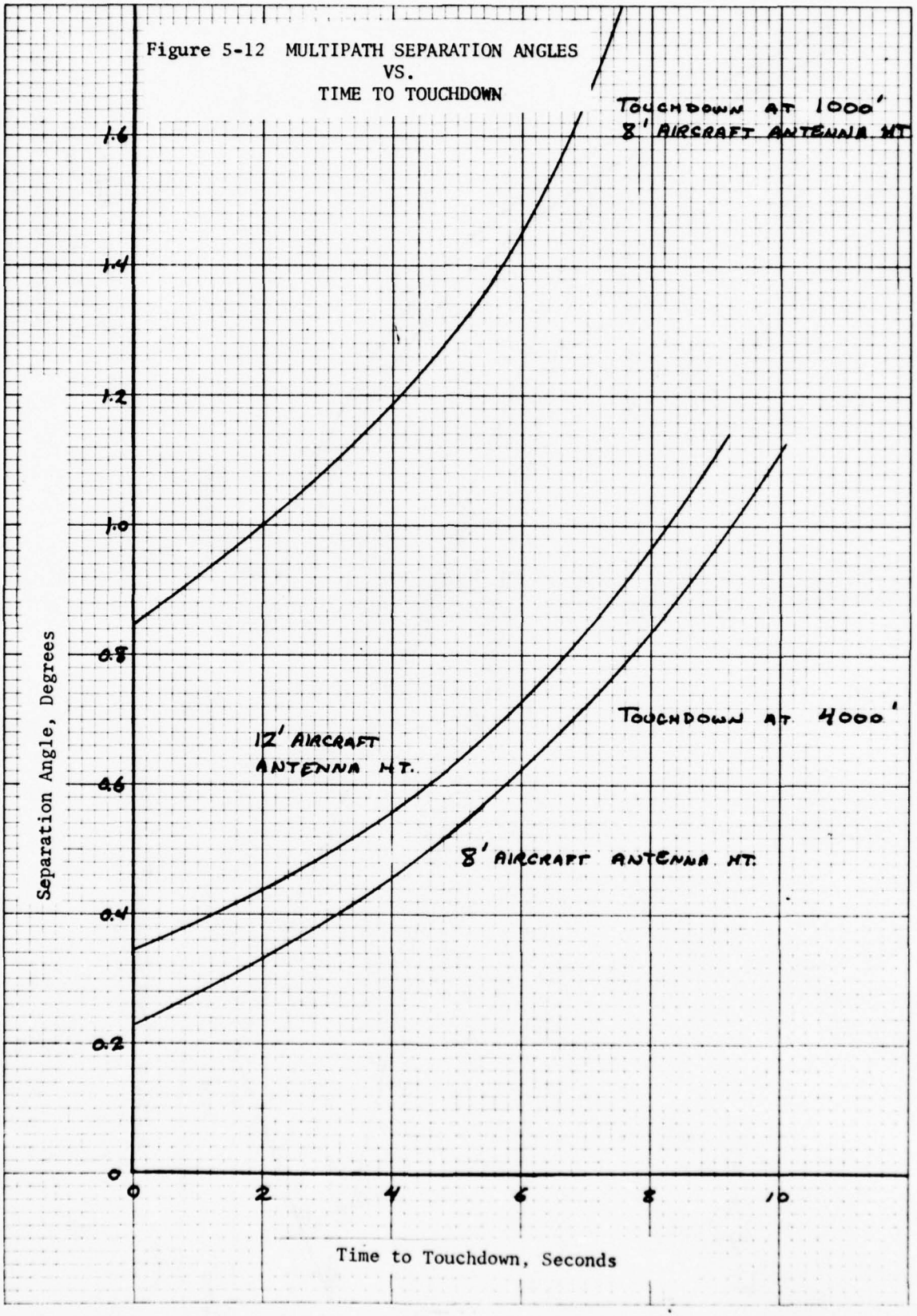
Figure 5-12 MULTIPATH SEPARATION ANGLES VS. TIME TO TOUCHDOWN
TOUCHDOWN AT 1000'
8' AIRCRAFT ANTENNA HT
TOUCHDOWN AT 4000'
12' AIRCRAFT ANTENNA HT.
8' AIRCRAFT ANTENNA HT.
Separation Angle, Degrees
1.6
1.4
1.2
1.0
0.8
0.6
0.4
0.2
0
0
2
4
6
8
10
Time to Touchdown, Seconds

small. The relative multipath phase for these same extreme cases is presented in Figure 5-13.

The TRSB simulator provides control of the multipath scalloping frequency. For most scenarios frequency control is adequate but for flare simulations the differential multipath phase must be controlled directly. A future modification of the simulator will implement phase control as this is necessary for closed loop flare tests.

At present, an approximate flare simulation is made possible by initiating a fixed scalloping frequency at the desired phase and varying the separation angle linearly with time. The correct phases and separation angles are obtained throughout the test as they are linearly related. Both are proportional to aircraft height divided by range in the small angle approximation. The relationship is shown in Figure 5-14. Since phase does not really advance linearly with time for these scenarios, the time scale becomes nonlinear as is evident from the error plots.

These scenarios are based on specific flight path geometries. However, variations of an aircraft from the flight path change the multipath phase and separation angle proportionately as indicated above. The effect is not to change the error magnitude but to introduce a further distortion into the time scale. The multipath errors presented here are, therefore, representative of all flares within the range of parameters covered. Likewise, raising the reflecting surface by snow cover has the same effect on the separation angle and multipath phase as an aircraft height deviation. The results reported are also representative of this condition.

5.2.2 Flare Processing with MCT and SEP

An alternate flare processing technique modifies the ground transmissions so that the multipath signal is reduced and a dwell gate processor can be used in the aircraft. In this multipath control technique (MCT) the beam scan is stopped before the ground is significantly illuminated so that a large multipath signal is not produced.

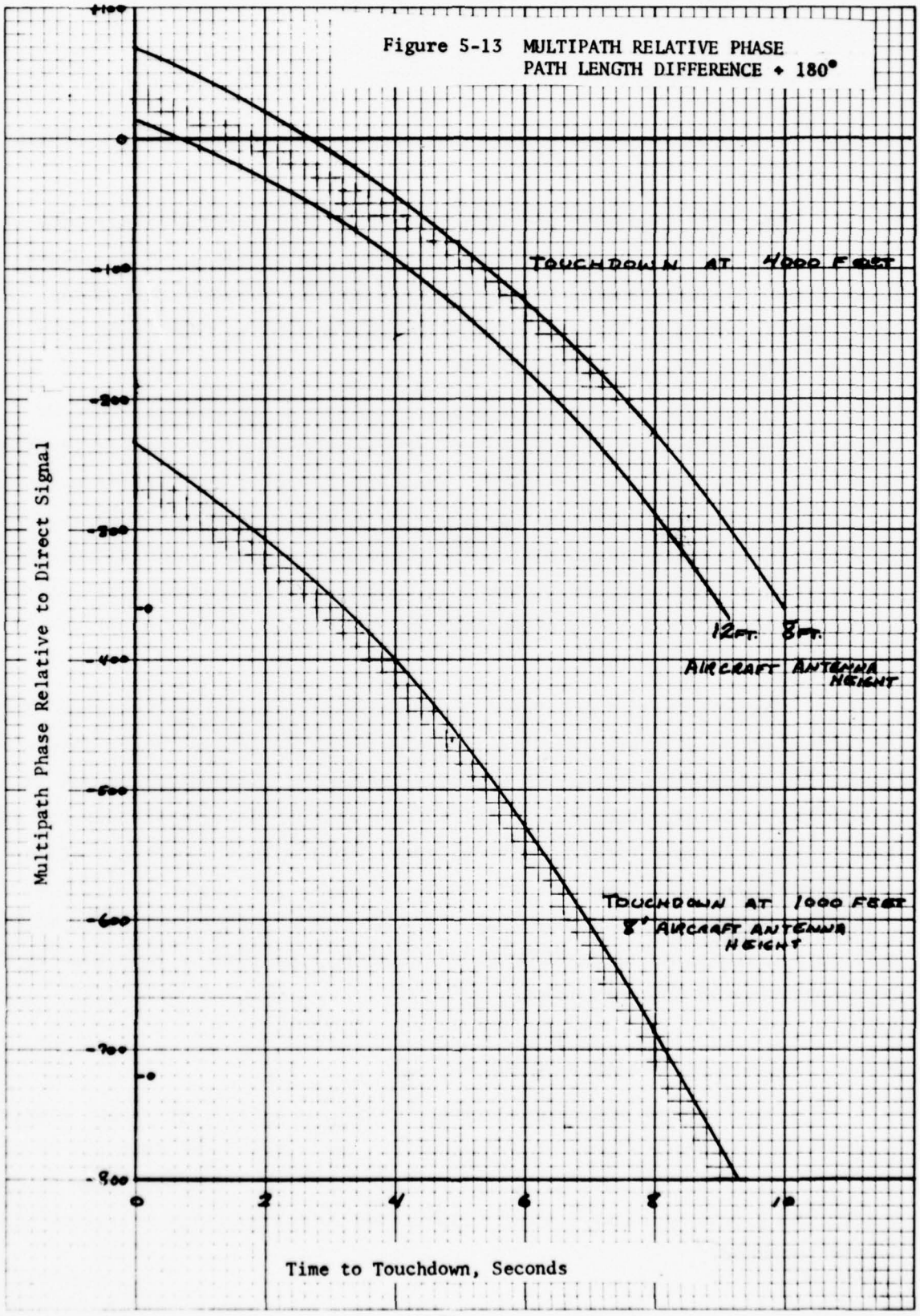
Figure 5-13 MULTIPATH RELATIVE PHASE
PATH LENGTH DIFFERENCE ÷ 180°
TOUCHDOWN AT 4000 FEET
12FT. 8FT.
AIRCRAFT ANTENNA HEIGHT
TOUCHDOWN AT 1000 FEET
8' AIRCRAFT ANTENNA HEIGHT
Multipath Phase Relative to Direct Signal
Time to Touchdown, Seconds
0
2
4
6
8
10

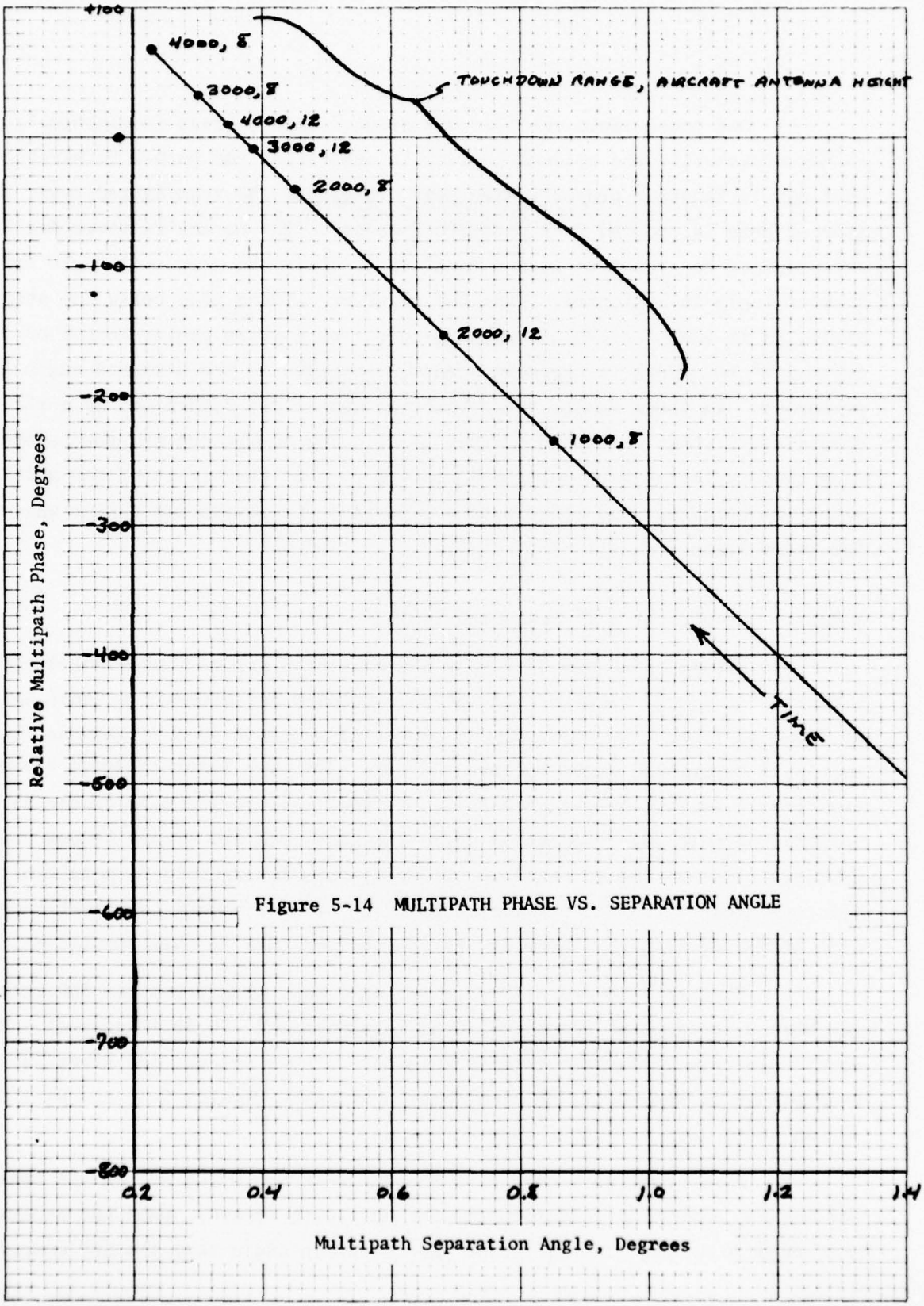

Figure 5-14 MULTIPATH PHASE VS. SEPARATION ANGLE

For these tests the beam was stopped at 0 degrees (horizontal). This is not necessarily the optimum angle. In order that the normal receiver can continue to function properly when near 0 degrees, the transmitted power in the stopped beam is reduced in a prescribed manner. The normal receiver dwell gates are produced for receiver angles equal to or above the stop scan angle and the correct angle is indicated. When the receiver antenna goes below the stop scan angle, as it must for C-band transmissions from a phase center height of 15 feet for a 1/2° beamwidth, a correction must be applied to the measured angle in the processor. In these tests, the correction was simply determined by a flare simulation without multipath (Figure 5-15). The correction was then subtracted from the simulation with multipath applied so that the effect of the multipath alone was obtained. In other words, a perfect MCT correction factor was used for these tests.

5.2.2.1 Results of 1/2° Beamwidth Tests

Figures 5-16 and 5-17 show the multipath errors from simulations using MCT with the normal receiver and -30 dB sidelobes for aircraft antenna heights of 8 and 12 feet. The worst errors appear at the 4000 foot touchdowns where the multipath separation angle becomes minimum. The peak error exceeded 4 feet with an aircraft antenna height of 8 feet. As the landings are made closer to the antenna the multipath separation angle increases and the errors become very small. Landings close to the antenna are, however, more susceptible to possible discrepancies in the MCT correction factor. Beam broadening at short range can also introduce errors. These errors are not included in this simulation.

Figures 5-18 and 5-19 give the multipath errors for the SEP receiver (no MCT) with the same scenarios (0 dB multipath and -30 dB sidelobes). The errors are very well controlled in this case. However, the SEP error is susceptible to the multipath sidelobes as shown by Figures 5-20 and 5-21 for -25 dB sidelobes.

A few runs were made with the SEP receiver using MCT on the transmitter. The MCT had almost no effect on the SEP multipath errors. When the aircraft descended to an angle so far below the stop scan angle that the SEP comparison

Figure 5-15 MCT CORRECTION FACTOR
- 1/2° Beamwidth, Stop Scan at 0°
- Measured on Simulator
- Correction at 0° is required as receiver threshold was -3 dB but simulator MCT program was designed for -4 dB

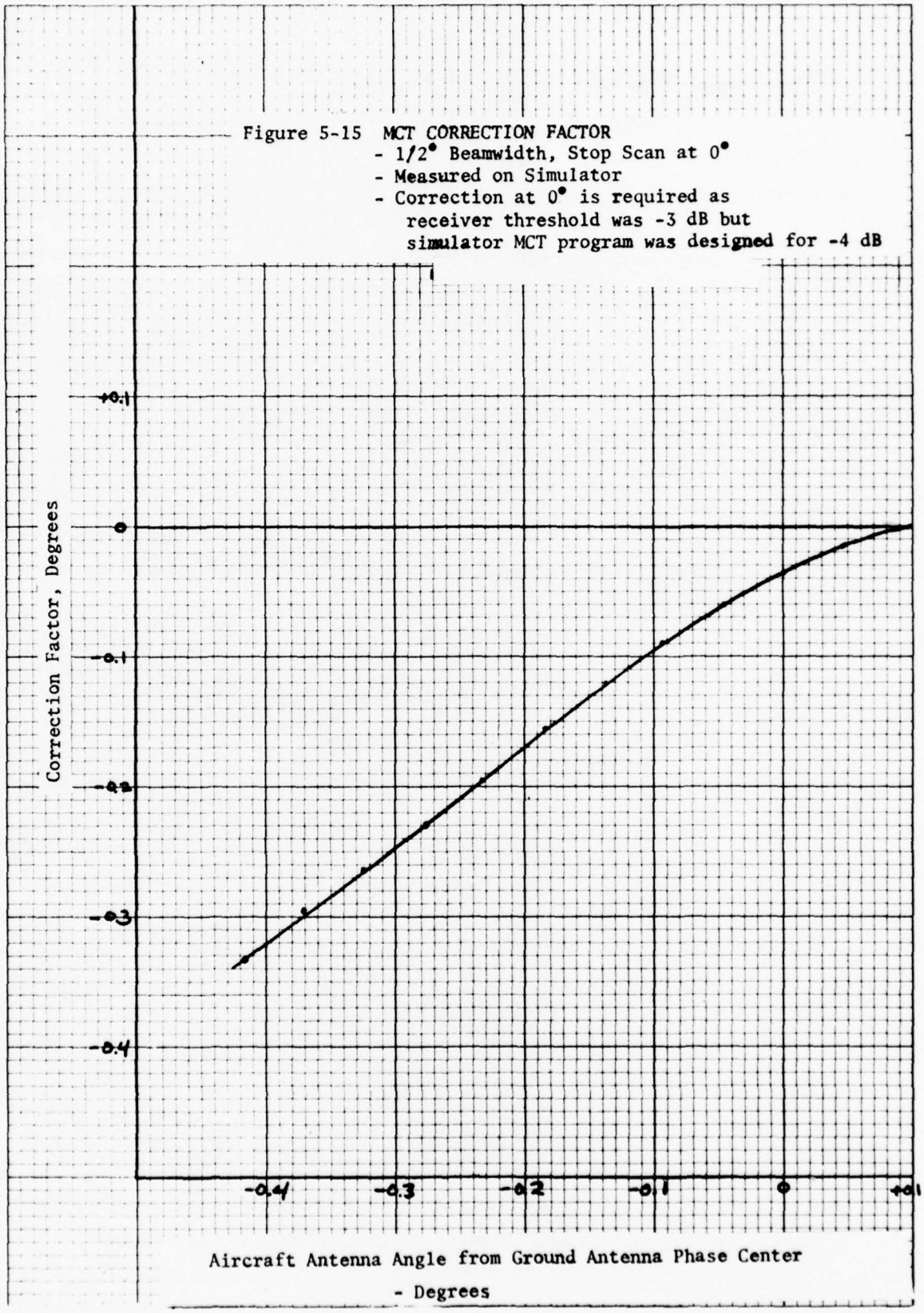

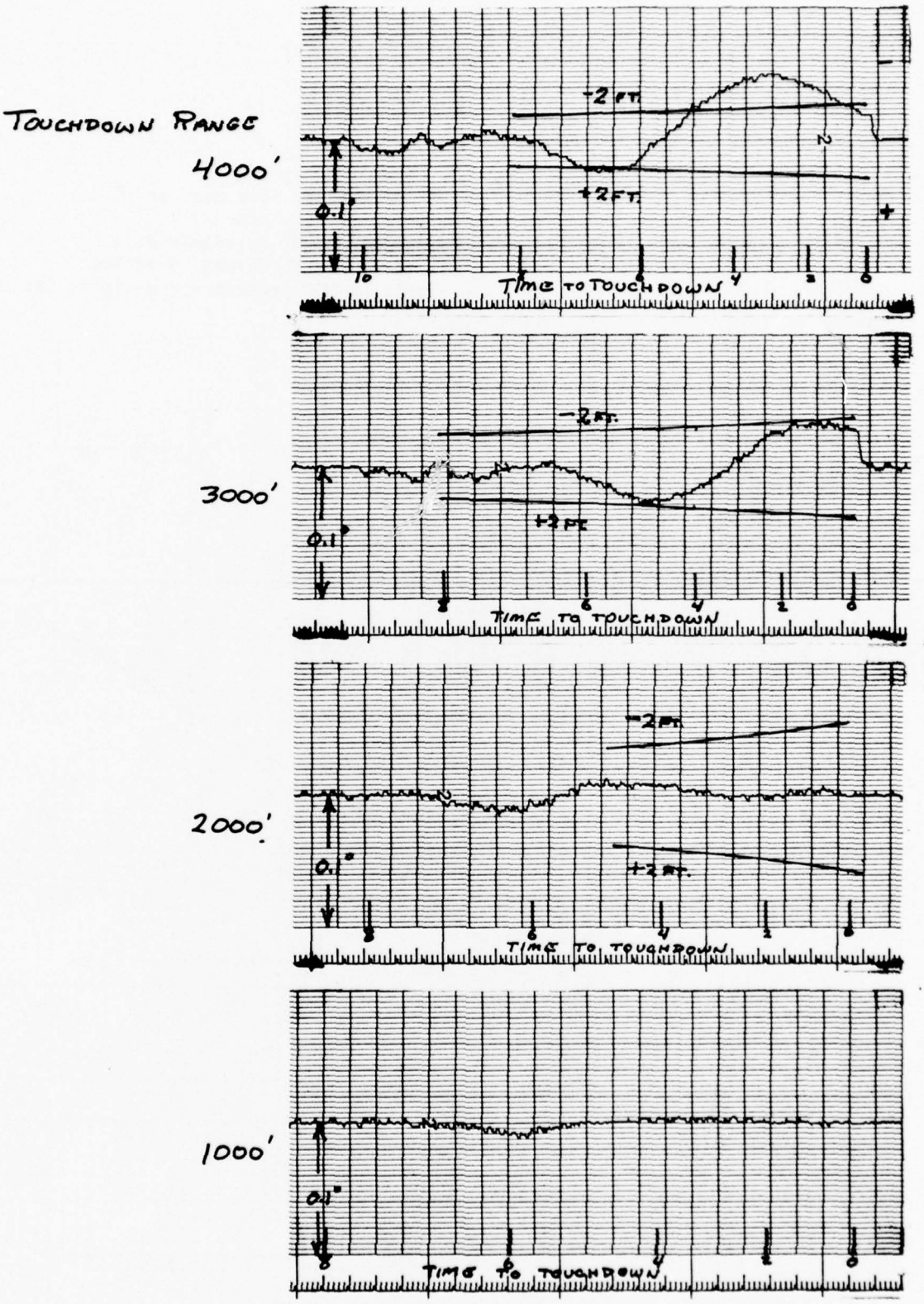

Figure 5-16 FLARE SCENARIO. - NORMAL RECEIVER WITH MCT 8 FT. AIRCRAFT ANTENNA HT., 0 dB MULTIPATH, -30 dB SIDELOBES

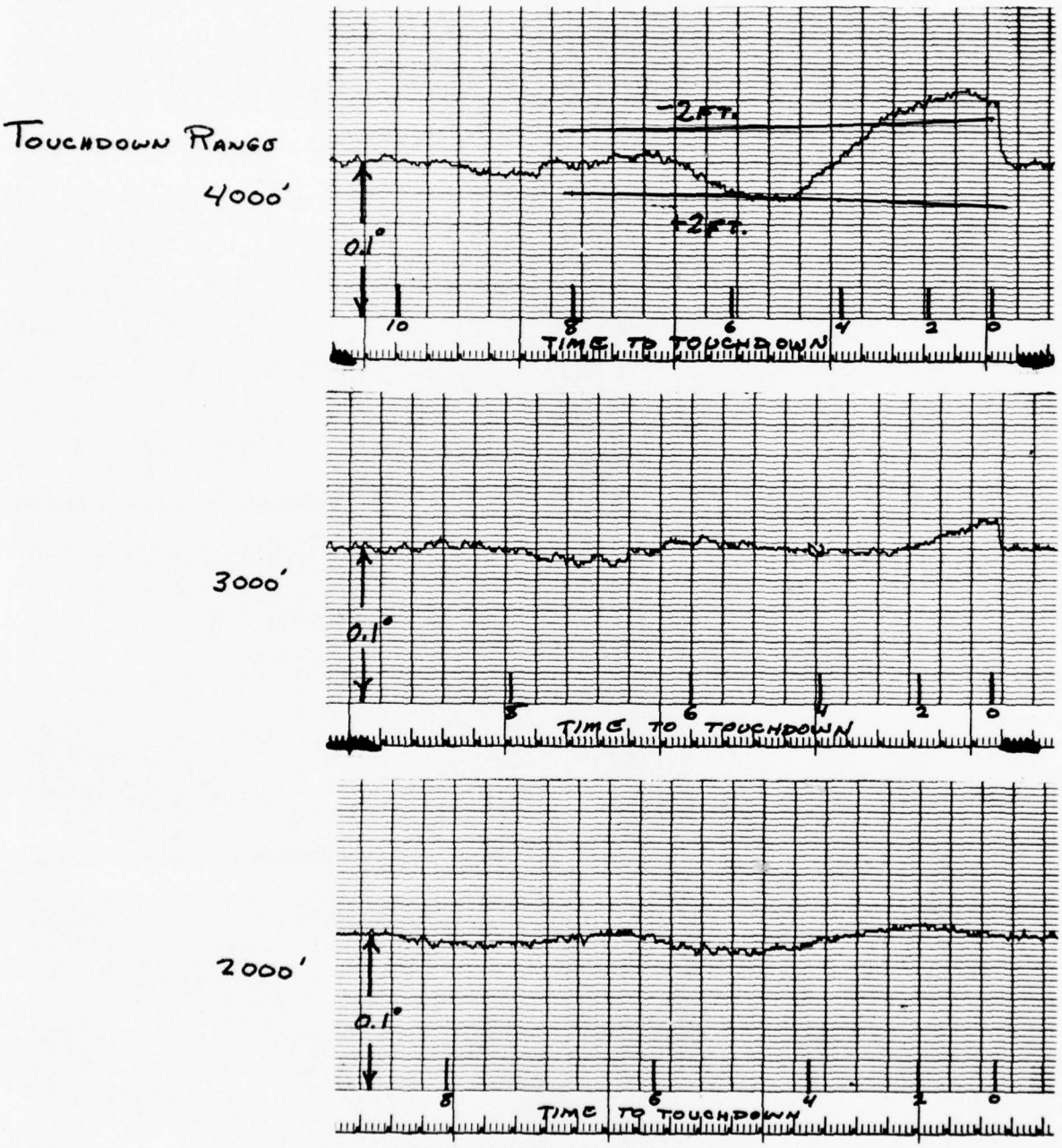

Figure 5-17 FLARE SCENARIO - NORMAL RECEIVER WITH MCT 12 FT. AIRCRAFT ANTENNA HT., 0 dB MULTIPATH, -30 dB SIDELOBES

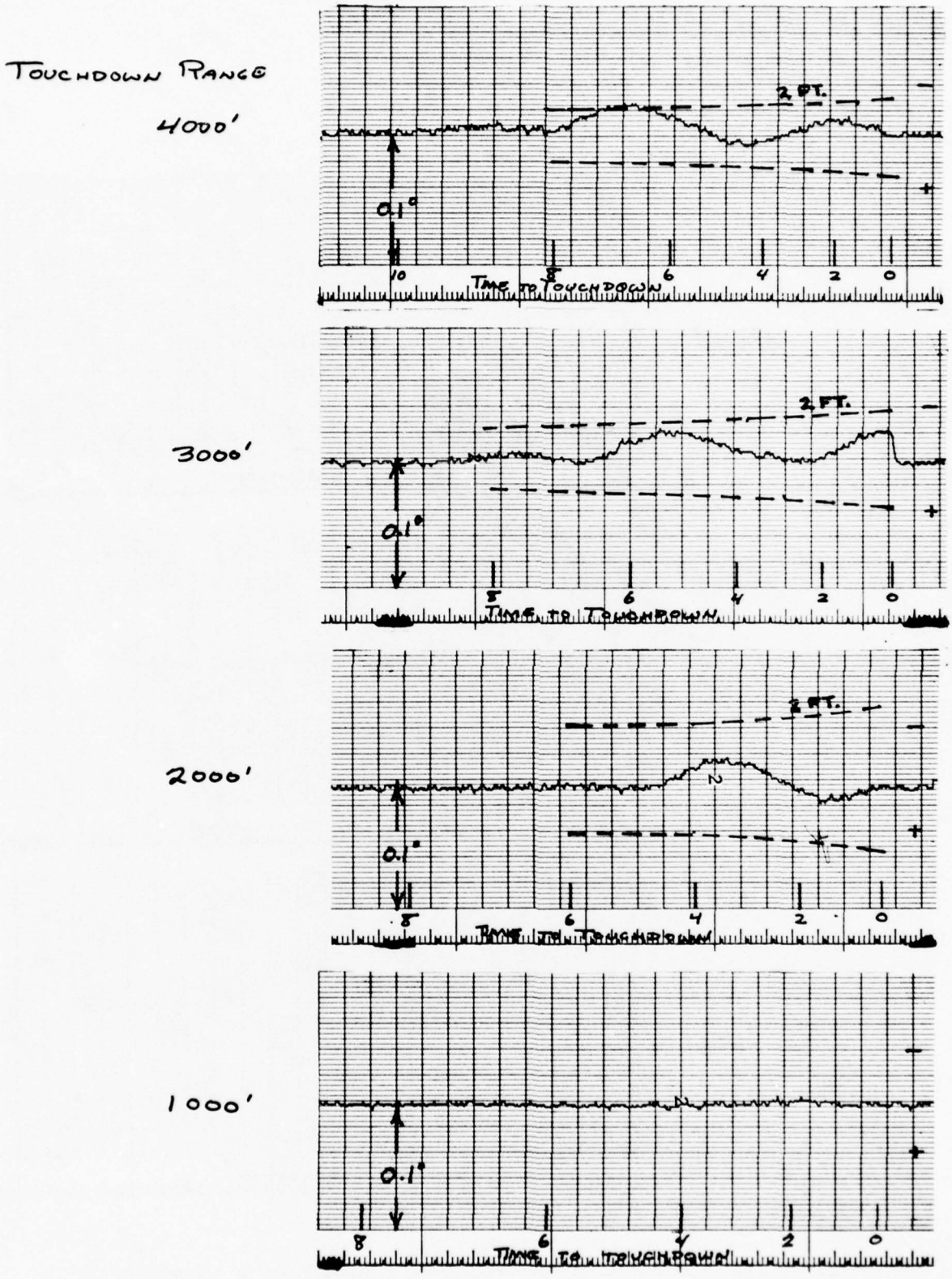

Figure 5-18 FLARE SECNEARIO - SEP RECEIVER (DELAY & COMPARE) 8 FT. AIRCRAFT ANTENNA HT.,0 dB MULTIPATH, 30 dB SIDELOBES

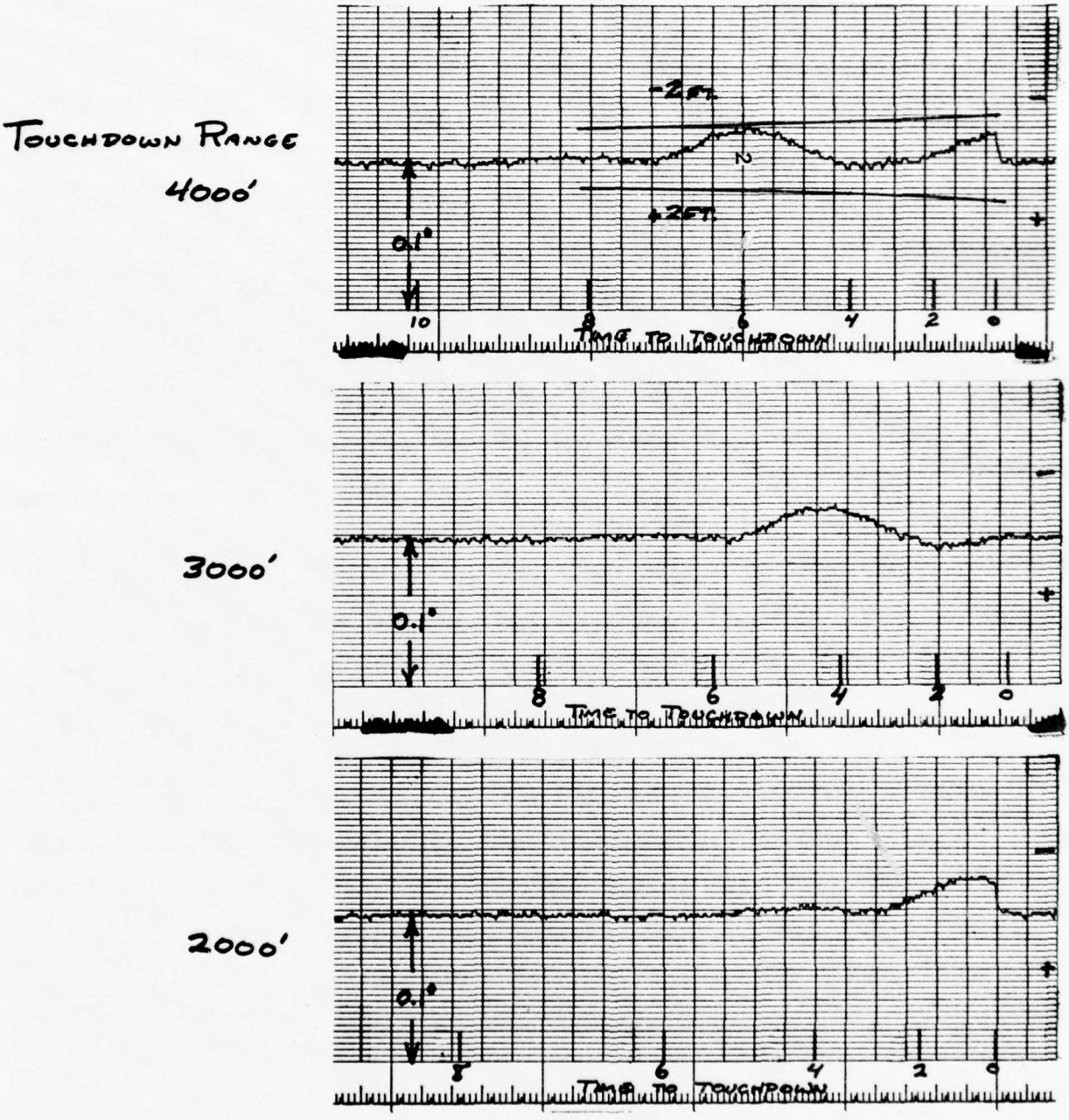

Figure 5-19 FLARE SCENARIO - SEP RECEIVER (DELAY & COMPARE) 12 FT.. ANTENNA HT., 0 dB MULTIPATH, 30 dB SIDELOBES

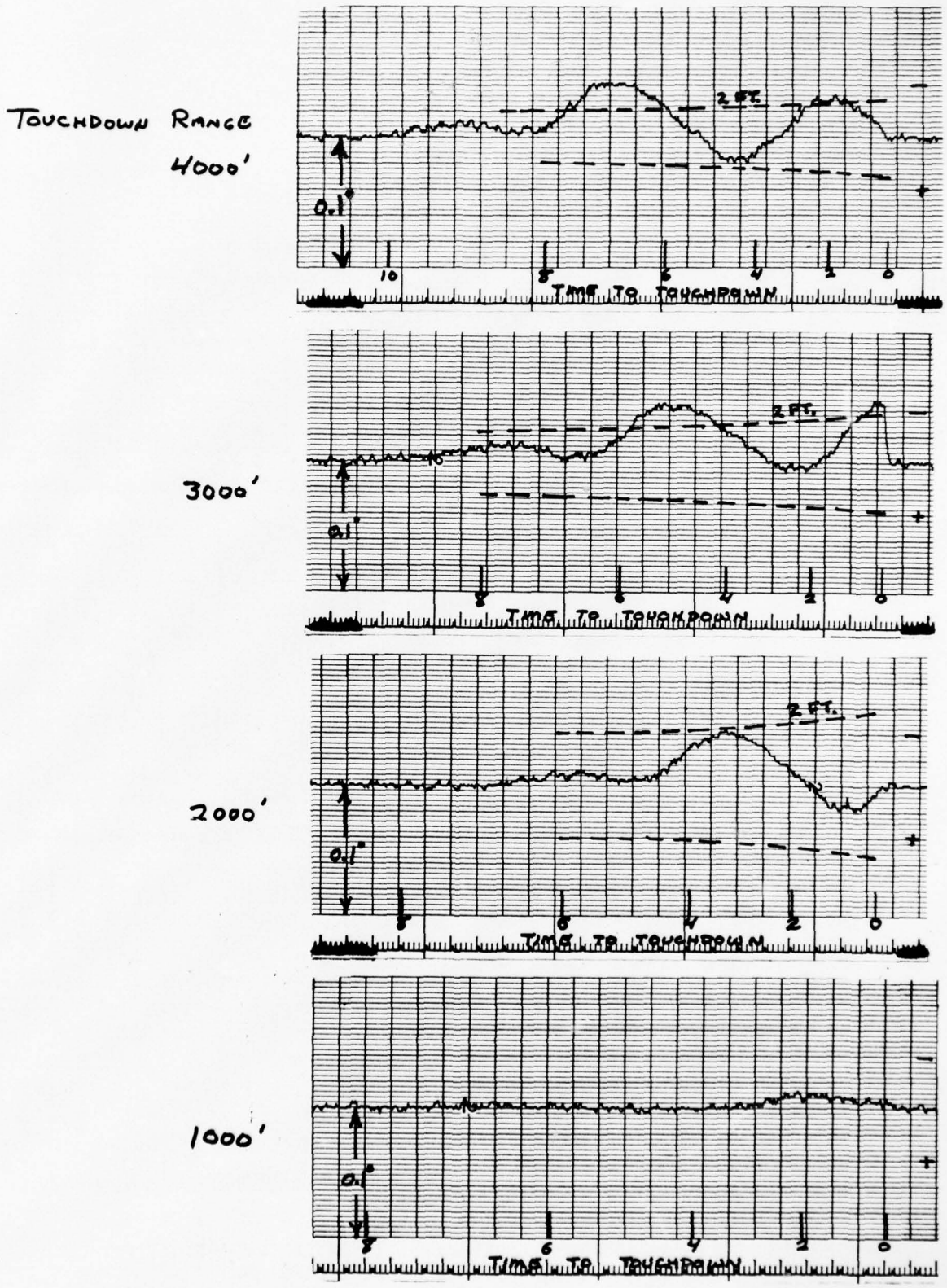

Figure 5-20 FLARE SCENARIO - SEP RECEIVER (DELAY & COMPARE) 8 FT.AIRCRAFT ANTENNA HT., 0 dB MULTIPATH,-25 dB SIDELOBES

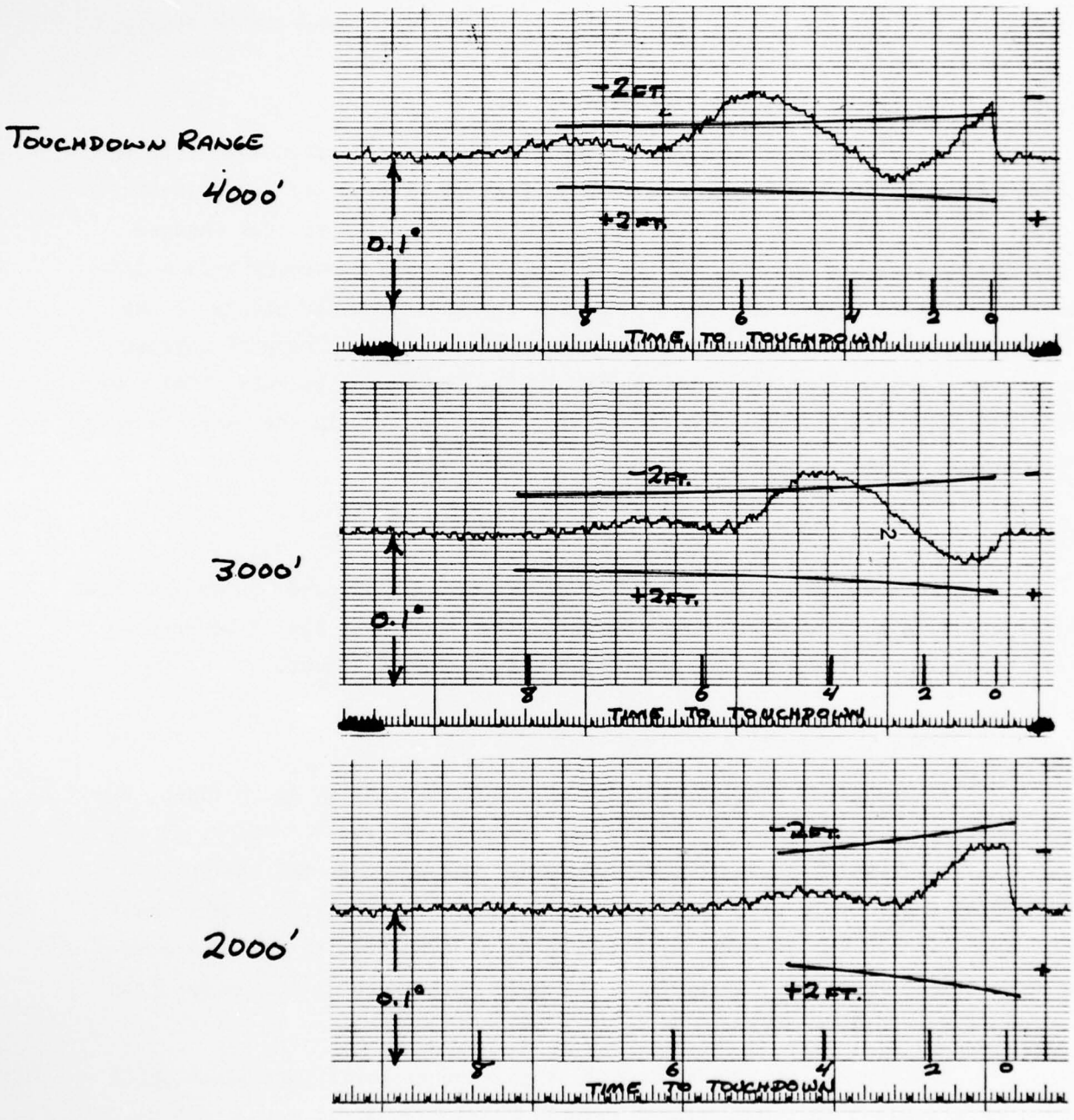

Figure 5-21 FLARE SCENARIO - SEP RECEIVER (DELAY & COMPARE) 12 FT. AIRCRAFT ANTENNA HT., 0 dB MULTIPATH, 25 dB SIDELOBES

points were disturbed by the power programming, large errors occurred. Although these errors may be correctable, in the same way as the dwell gate receiver was corrected, MCT and SEP are not presently considered to be compatible techniques.

5.2.2.2 Results of 3/4° Beamwidth Tests

A 3/4° beamwidth antenna is smaller than a 1/2° antenna so that the phase center height can be lowered from 15 feet to 11 feet for C-band (with 3 foot ground clearance). The multipath separation angles are not changed. Only SEP results are shown since the errors for the MCT processor with a 1/2 degree beamwidth were about twice those for the SEP. The SEP errors in the 3/4° beamwidth scenarios appear in Figures 5-22 and 5-23. The peak angular errors are increased about in proportion to the beamwidth increase (50%) over the 1/2° beamwidth errors. The errors also start earlier in the flare because of the wider beam.

5.2.2.3 Sidelobe Effects

The peak errors for sidelobes of -20 dB, -25 dB, and -30 dB are shown in Figure 5-24 for the SEP. These indicate that sidelobes should be keep to less than -25 dB if the height errors are not to exceed 2 feet.

5.2.3 Error Correction Algorithms for SEP

As described previously, at small elevation angles as in flare, the multipath phase and separation angles are linearly related. In fact, as was shown in Figure 5-14, a single flare scenario that provides the smallest separation angle of interest will pass through all the other applicable multipath conditions. The scenario with touchdown at 4000 feet range and 8 feet antenna height meets this criterion. A simple correction algorithm has been developed for this scenario.

The correction is based on the variation in dwell gate width which provides a measure of the multipath effect. A plot of dwell gate width vs. SEP angle error for the 4000 ft/8 ft scenario is shown in Figure 5-25. Time is increasing in the direction of the arrows. It is seen that the function may be

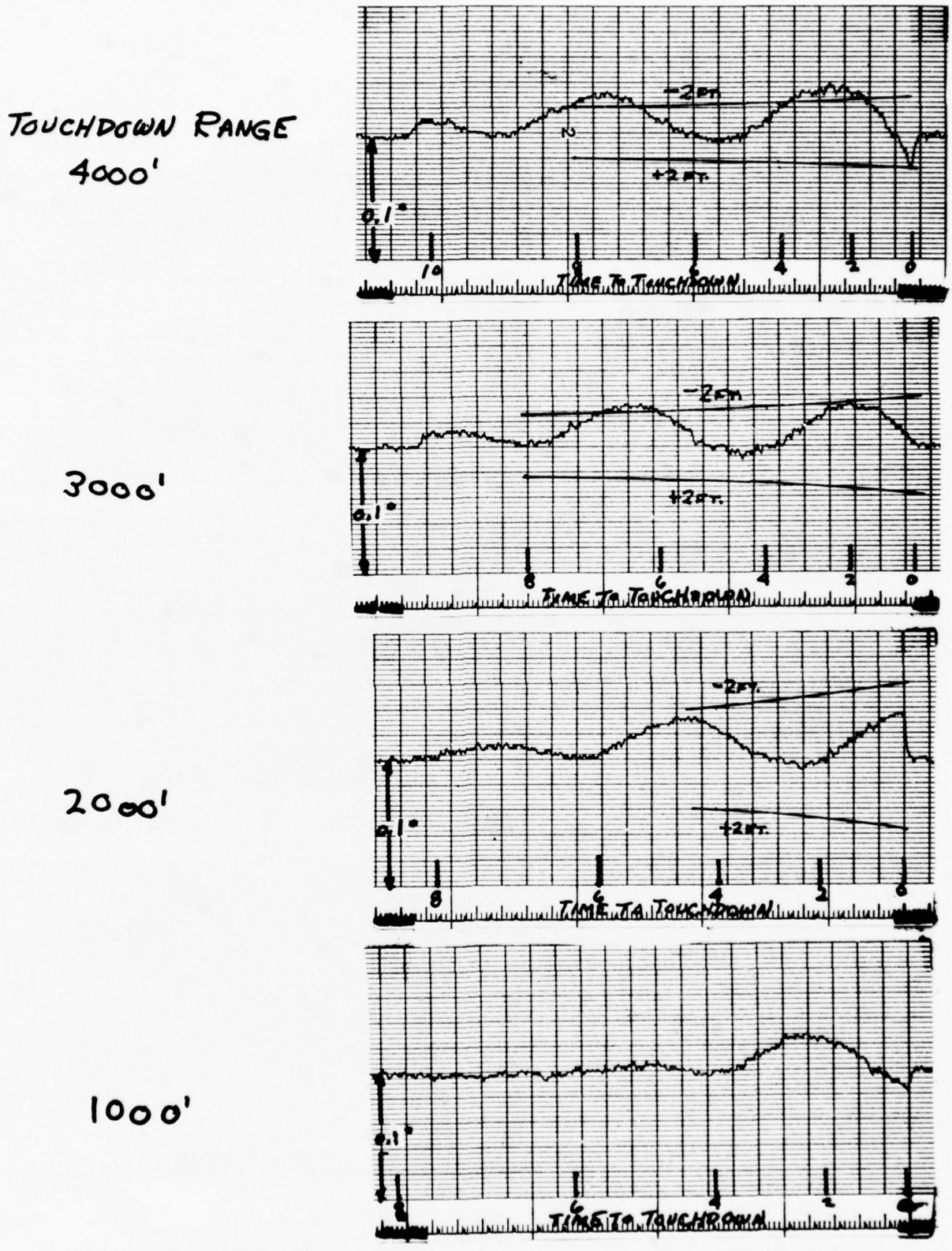

Figure 5-22 FLARE SCENARIO - SEP RECEIVER, .75° BEAMWIDTH
8 FT AIRCRAFT ANTENNA HT., 0 dB MULTIPATH, -30 dB
SIDELOBES

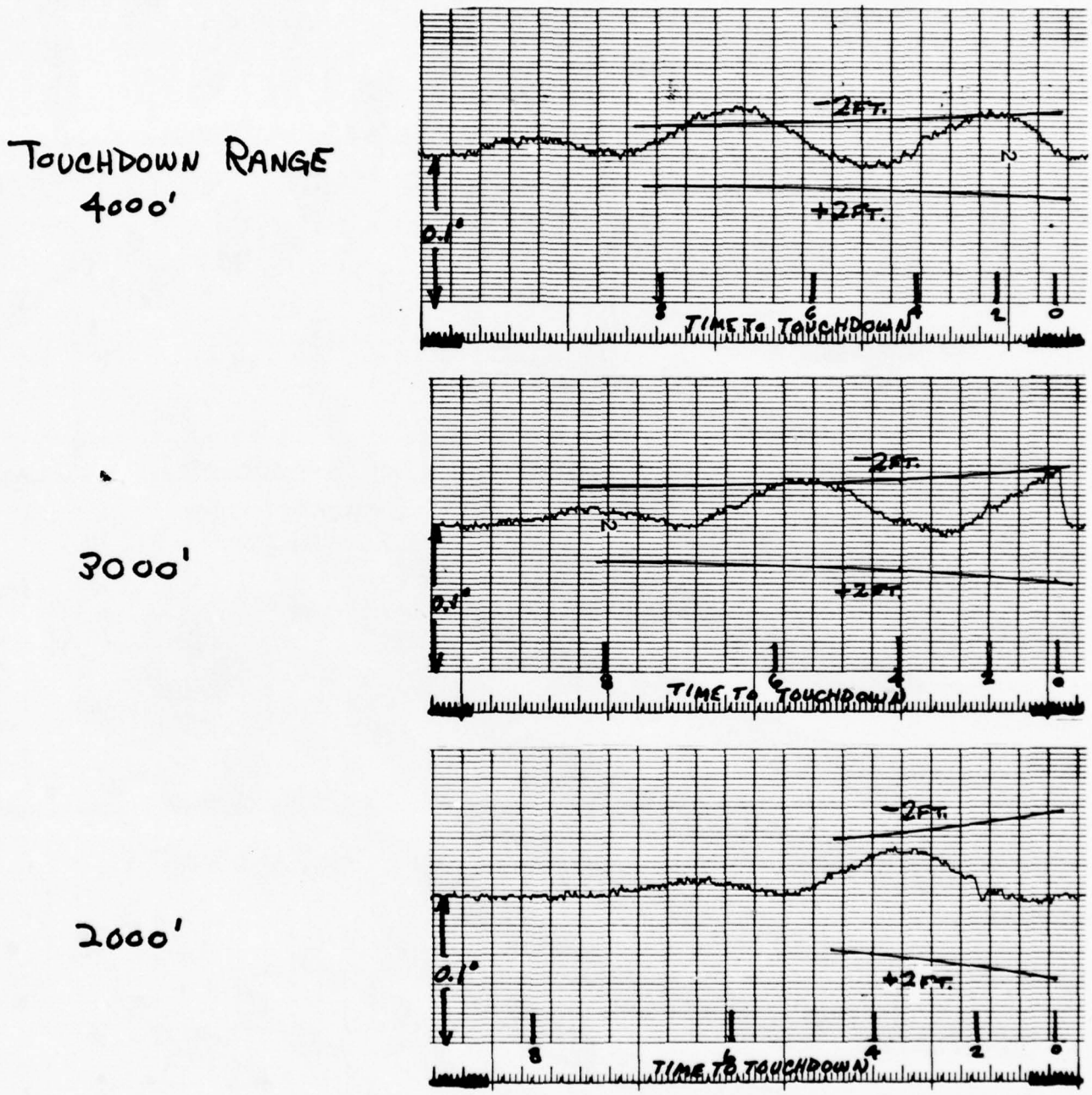

Figure 5-23 FLARE SCENARIO - SEP RECEIVER, .75° BEAMWIDTH, 12 FT. AIRCRAFT ANTENNA HT., 0 dB MULTIPATH, 30 dB SIDELOBES

Figure 5-24 PEAK ERRORS IN FLARE SCENARIOS
SEP, 12.5 sec & 10 dB DELAY &
COMPARE 0.5° BEAMWIDTH

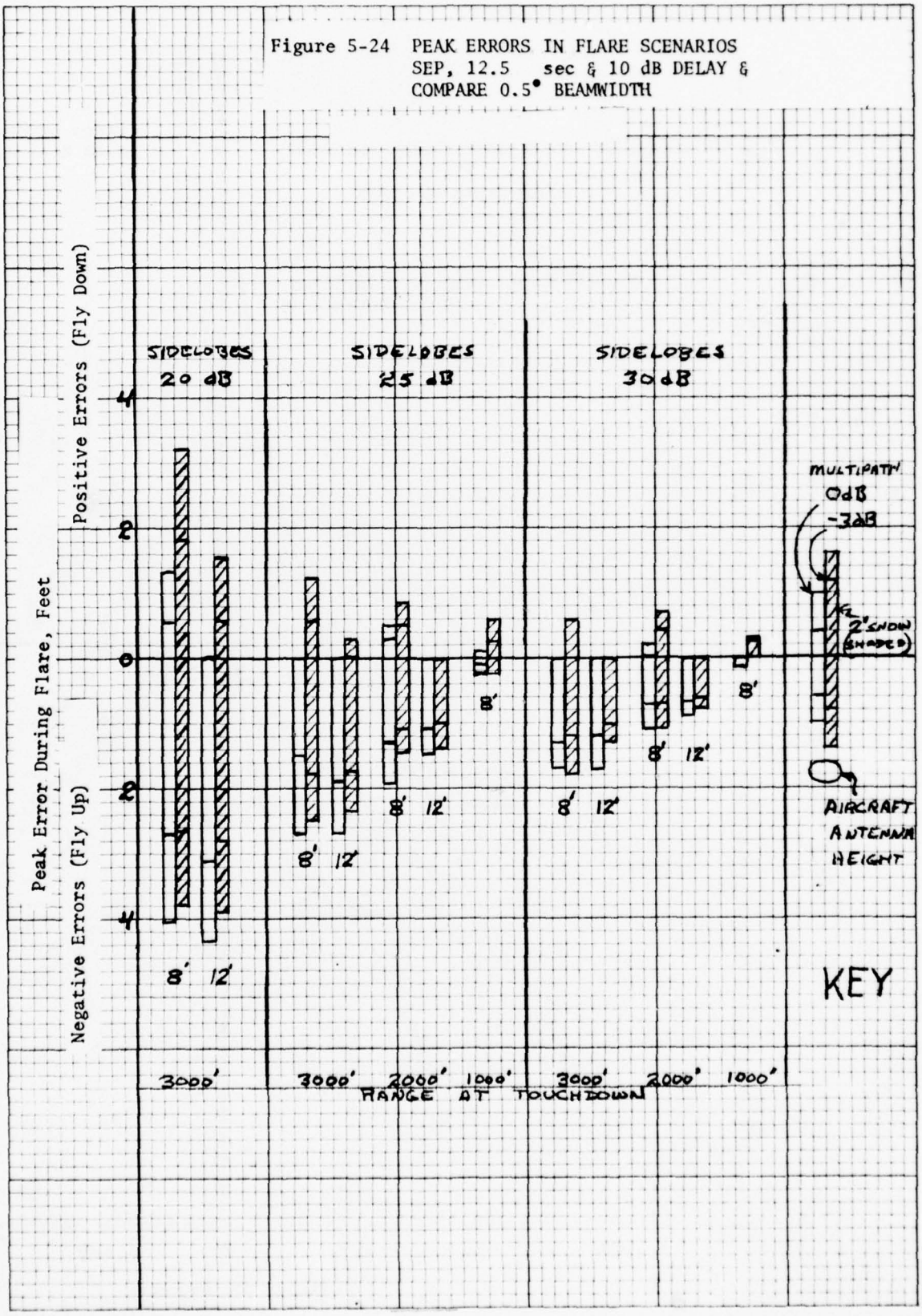

Figure 5-25 DWELL GATE WIDTH VARIATION
VS.
ANGLE ERROR IN FLARE

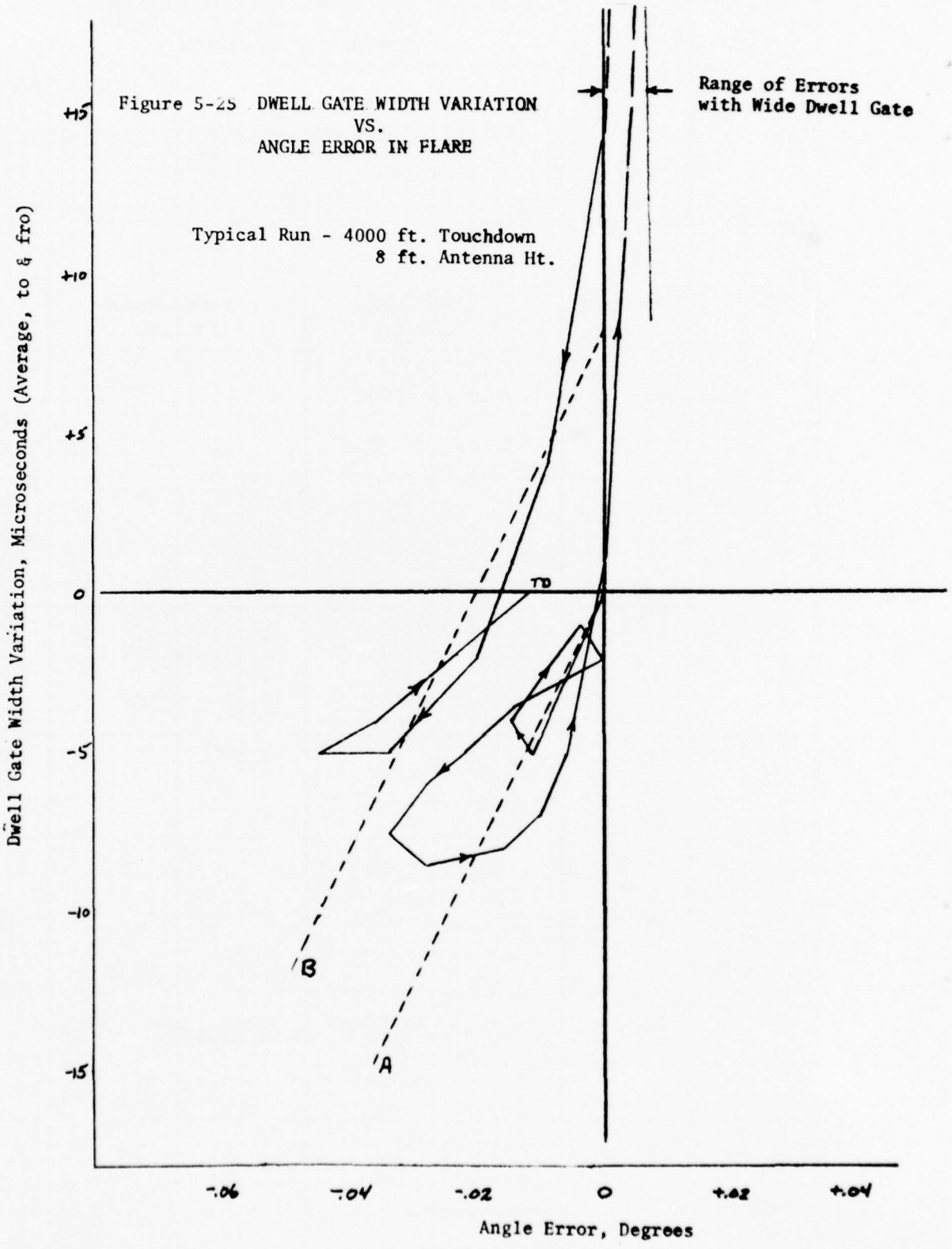

separated into 2 regions. Early in the flare, the dwell gates are shortened and the errors are negative as the multipath sidelobes influence the measurement. Late in the flare, after the multipath and direct beams have joined to give a very wide dwell gate, the error again becomes negative and the dwell gate varies through its average value.

A correction algorithm was prepared that follows the two straight lines indicated in Figure 5-25. Until the dwell gate deviation exceeds a large positive value, correction line A is used. The dwell gate deviation (negative) is multiplied by a constant (0.0025 degrees/microsecond) and subtracted from the angle. Deviations from line A then represent the residual error.

No correction is attempted when the dwell gate is very large as the error is relatively small and the gate width is varying rapidly. However, when the gate width deviation decreases (to 8 microseconds), correction curve B is implemented. The slope is the same as curve A but a constant 8 microseconds is subtracted from the width deviation.

Figure 5-26 illustrates the dwell gate width, the error without correction and the corrected error for zero dB multipath. The corrected error is always less than 2 feet in magnitude even for the 4000 foot touchdown case. Figure 5-27 illustrates the correction effect when the multipath level is reduced. At -3 dB multipath the error becomes very small. Even when the multipath is reduced after having been large the error is small as illustrated by the 10 dB reduction in multipath level. The "glitch" in this error curve is the result of suddenly switching a 10 dB attenuator into the multipath signal.

There is a possibility that if the multipath is very low up to the final 3 or 4 seconds of flare, a wide dwell gate will not occur. Then the switch between correction curves A and B may not occur. The error would correspond to deviations from line A as indicated in Figure 5-25 (using line A where B is more appropriate). As with the other error curves above, the effect of this error remains to be determined.

During flare, the output of the SEP would be used to determine aircraft control signals, in particular, descent rate. The errors shown thus far, although small in magnitude, have a significant high frequency noise component that would

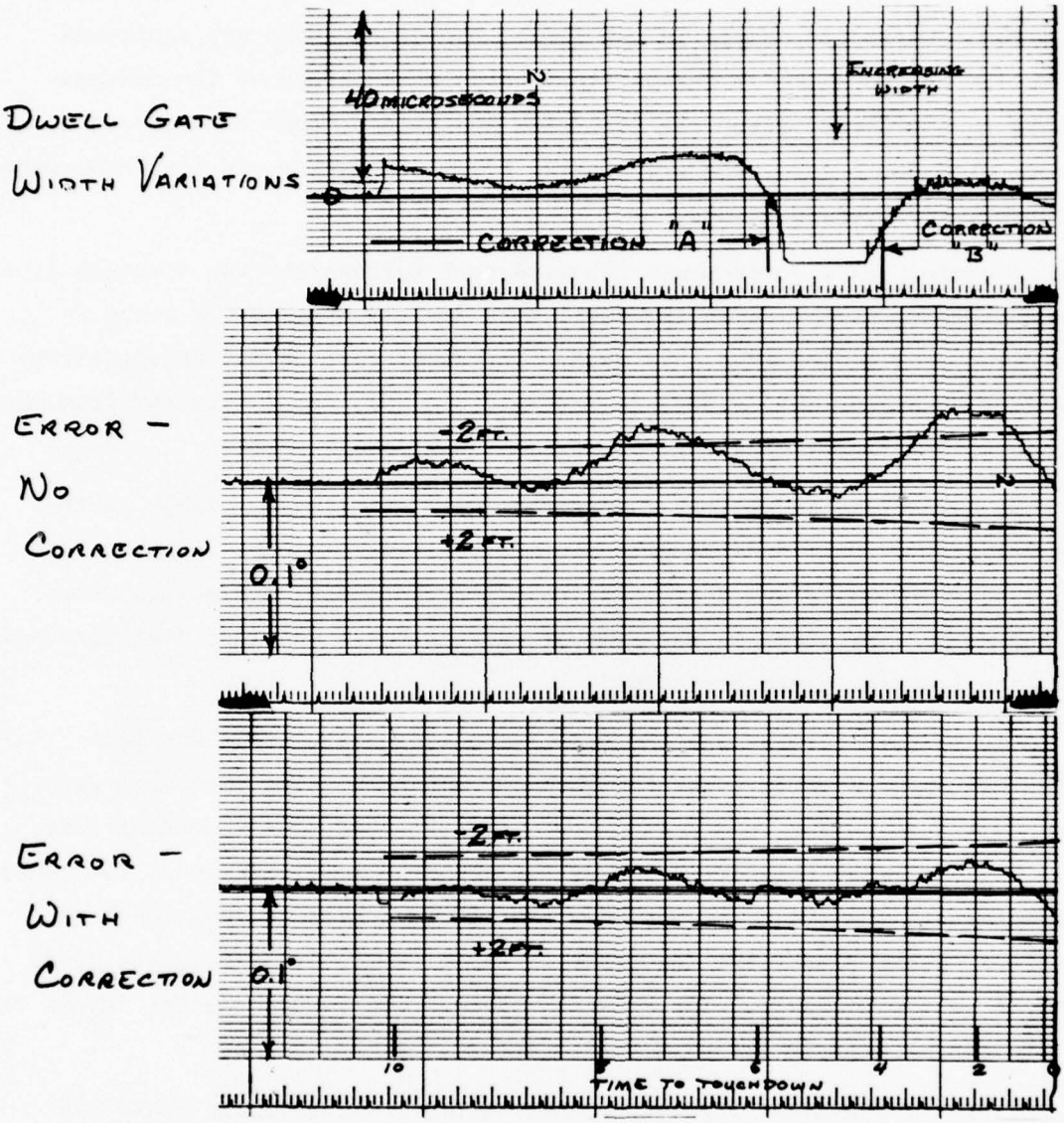

Figure 5-26 FLARE SCENARIO - TOUCHDOWN AT 4000 FT.
AIRCRAFT ANTENNA HT. 8 FT.
0 dB MULTIPATH, 1/2° BEAMWIDTH, -25 dB SIDELOBES
200 FT/SEC

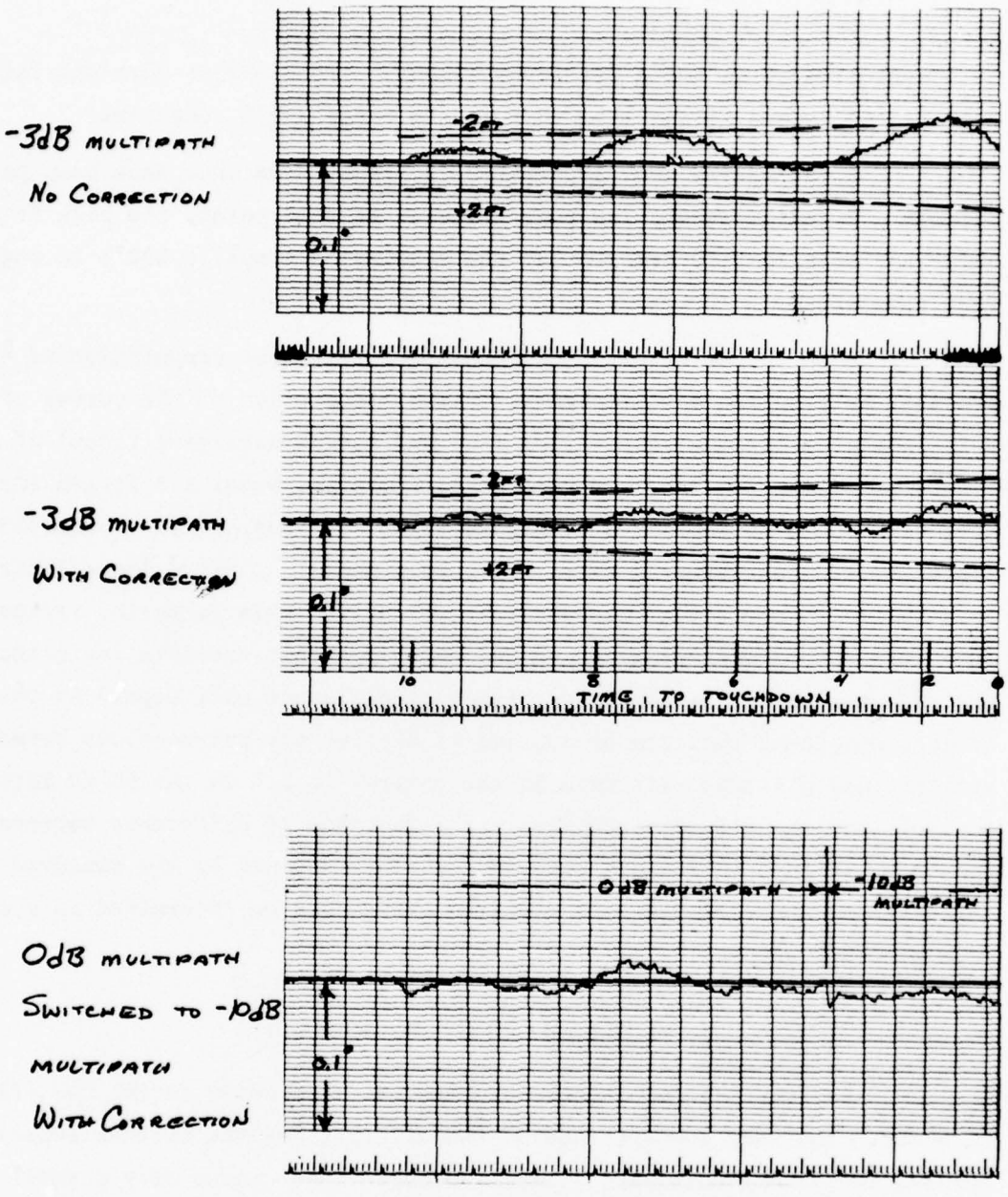

Figure 5-27 FLARE SCENARIO - TOUCHDOWN AT 4000 FT.
AIRCRAFT ANTENNA HT. 8 FT.
1/2° BEAMWIDTH, 200 FT/SEC, -25 dB SIDELOBES

be accentuated by an angle rate measurement. These errors were all filtered by a 10 radian/second filter like that in the Phase 2 1/2 receivers.

Error curves are illustrated in Figure 5-28 that have been passed through a 2 radian/second low pass filter. At this point, the high frequency noise has been largely removed but the resolution steps (0.002°) in angle are very apparent.

Both the error magnitude and error rate (for computation of $\dot{h}$) will probably be required for autolands. Visual inspection of the curves of Figure 5-28 indicates maximum rate errors (for one second averaging times) of about 2.1 ft/sec exist for the receiver output angle and about 1.3 ft/sec for the corrected angle as indicated in Figure 5-29. In general, the correction algorithm reduces the peak rate errors by a modest amount. These errors may be compared to the actual descent rate which, for this scenario, varies from 10.5 ft/sec to 2 ft/sec at touchdown. Although this estimate indicates that the rate errors may be too large, their significance will depend on the degree of data smoothing that can be applied as well as any interactions between the attitude and altitude rate data in the control loop. In the DC-10 autoland control loop the elevator commands are a function of difference between the measured altitude rate and a programed rate determined by the measured altitude. The altitude and altitude rate requirements should be determined in a closed loop aircraft simulation.

5.2.4 Flare Hangar Scenarios

Reflections from nearby hangars can also occur during the flare maneuver. The very low altitude of the aircraft and the antenna location results in a small multipath separation angle that causes only a small error. The scalloping frequency can be high so that the error is reduced further by motion averaging.

Three flare hangar scenarios illustrated in Figure 5-30 were defined using JFK Buildings B2 and B3 from AWOP Scenario 5 (Reference 14). The elevation antenna pattern shaping was used which is much broader than required for the flare system coverage. The simulation parameters used in these tests are given in Table 3.

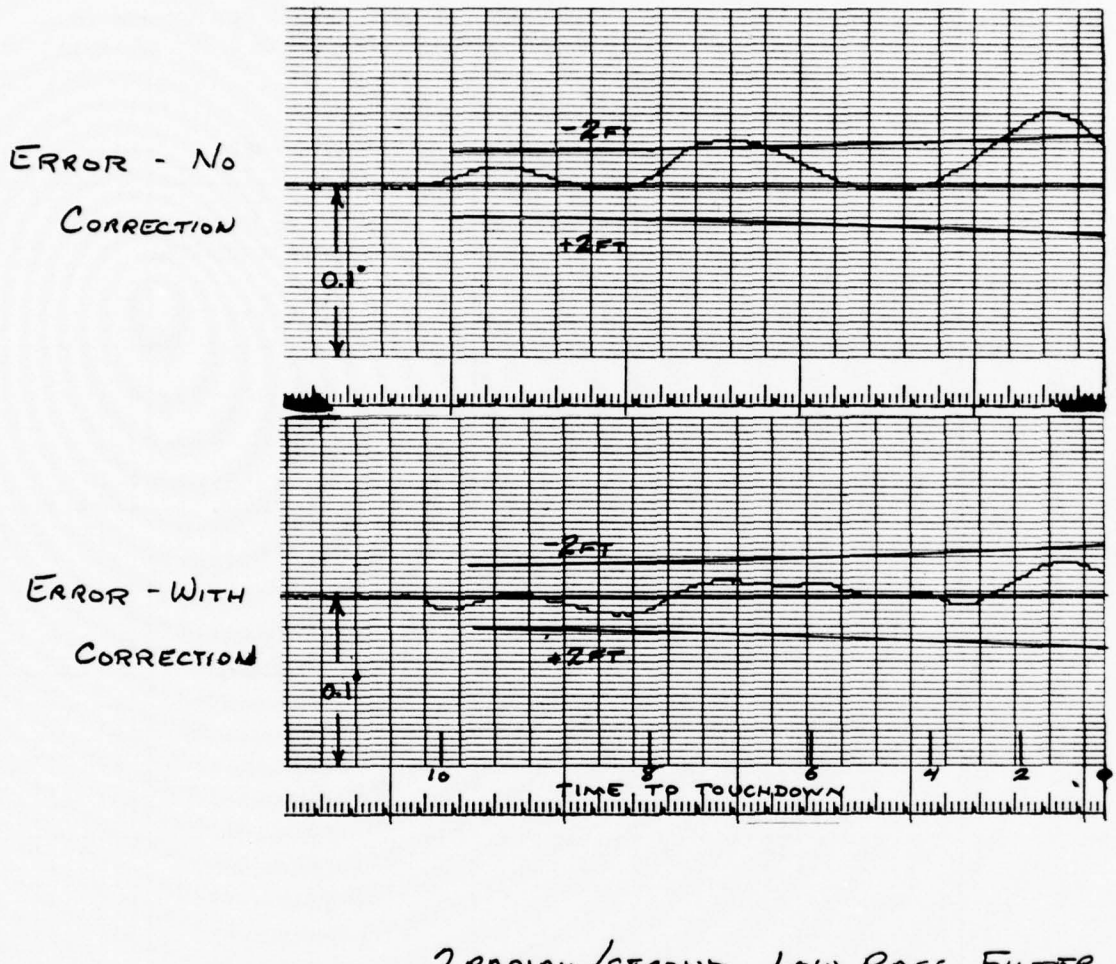

Figure 5-28 FLARE SCENARIO - TOUCHDOWN AT 4000 FT.
AIRCRAFT ANTENNA HT. 8 FT.
1/2° BEAMWIDTH, 200 FT/SEC, -25 dB SIDELOBES
0 dB MULTIPATH

Figure 5-29 FLARE ERROR RATE

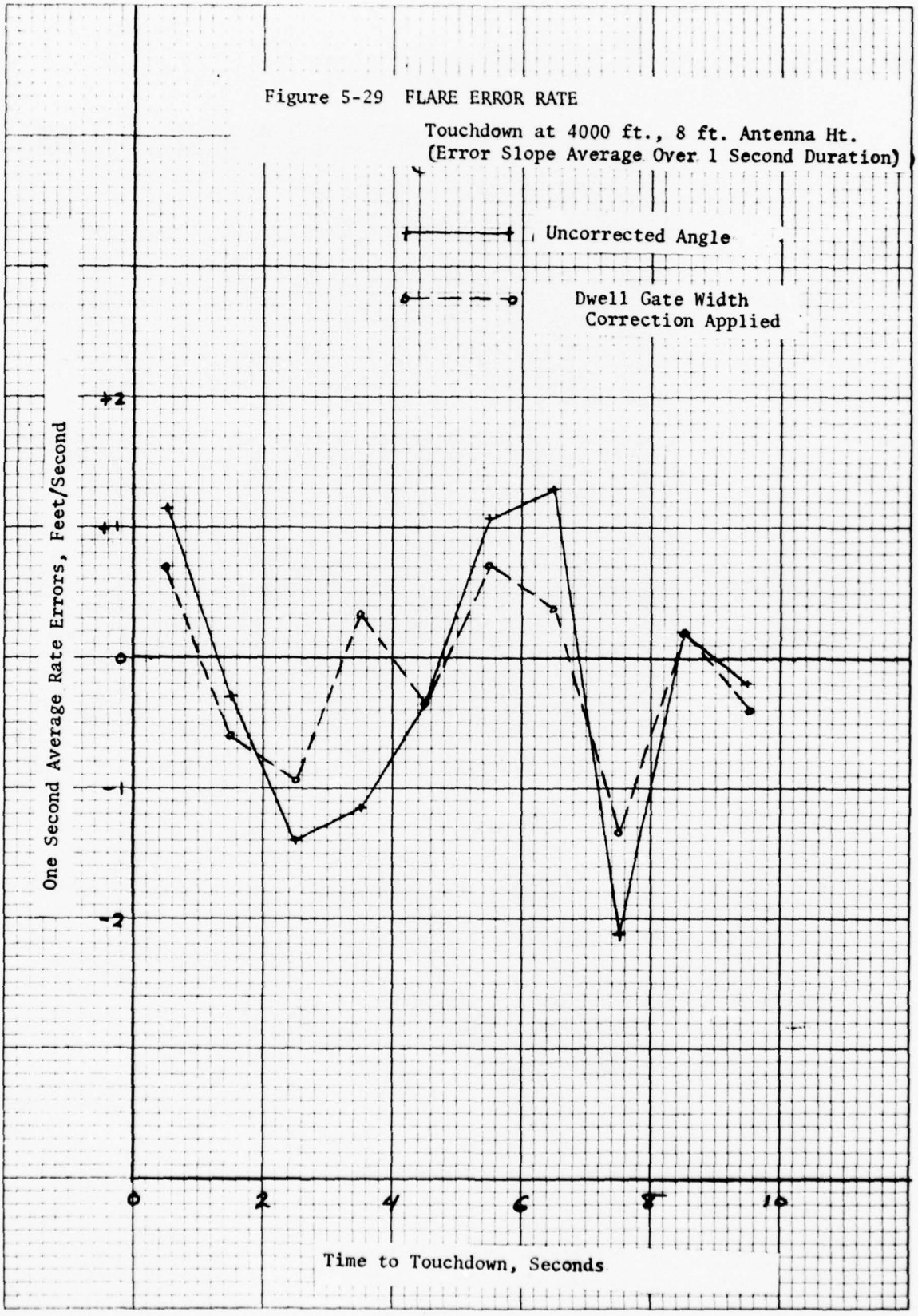

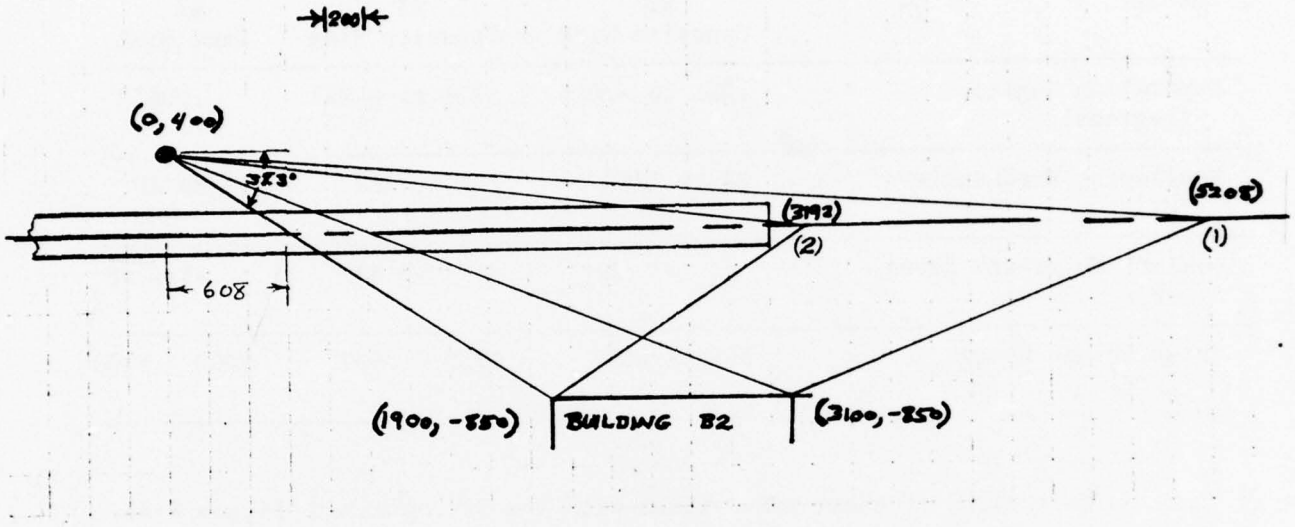

Flare Scenario, AWOP B2, Opposite Side

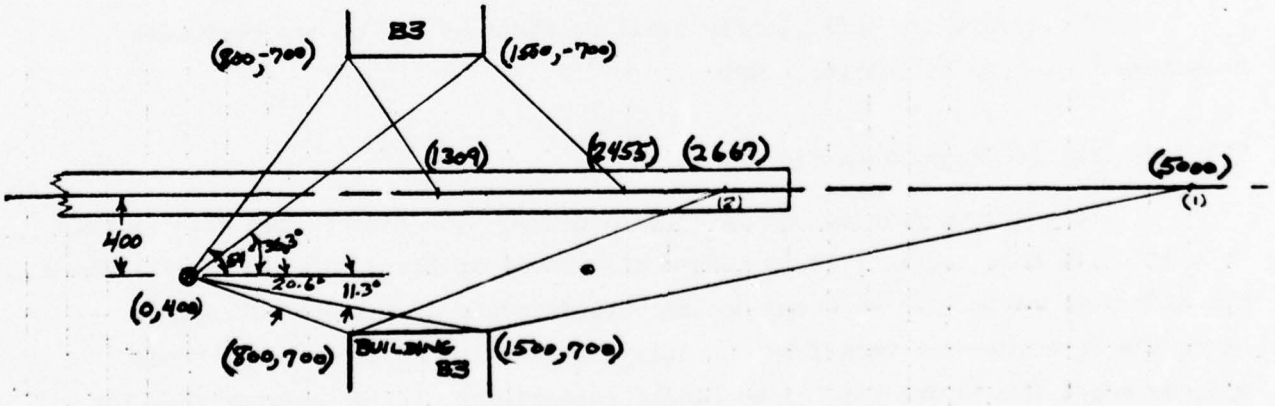

Flare Scenario, AWOP B3, Same & Opposite Side

Figure 5-30 HANGAR SCENARIOS FOR FLARE
Antenna Gain: 0 dB within ±10°, 4 dB at 20°, -7 dB at 60°
Building Reflectivity: 0.9 to 20°, 0.7 beyond 20°
Antenna is located 3000 ft. from threshold

Table 3

Scenario	JFK Buildings B2 Opposite Side	B3 Opposite Side	B3 Same Side
Separation Angles (Degrees)	.051 to -.016	.116 to -.054	.006°
Scalloping Frequencies (Hz)	62 to 171	181 to 381	14 to 48
Maximum Multipath Level (dB)	-7 dB	-8 dB	-1.5 dB
Interference Ranges (Feet)	3150 - 5300	1230 - 2500	3000 - 5400

The results of these simulations with the SEP appear in Figure 5-31. The errors are quite small and do not appear likely to cause any aircraft disturbance.

The errors are sufficiently small so their effect on the beamwidth measurements should be insignificant.

5.2.4.1 Tilted Hangar Scenario

It has been pointed out in Reference (15) that hangars can tilt as much as 0.10°. If this hangar tilt is toward the runway or flare antenna it will cause the multipath reflection to occur on the outside edges of the DOWN-UP scans. Since the threshold determined by the delay and compare technique uses these outside edges the errors for tilted hangar reflections will be greater than for vertical hangars.

In order to measure the effects of a tilted hangar a flare scenario was simulated with parameters selected to be a worst case situation. The simulation parameters were based upon the JFK hangar B3 that has been elongated and tilted 0.20°. The airport geometry and multipath levels were prepared by the Lincoln Laboratory propagation program.

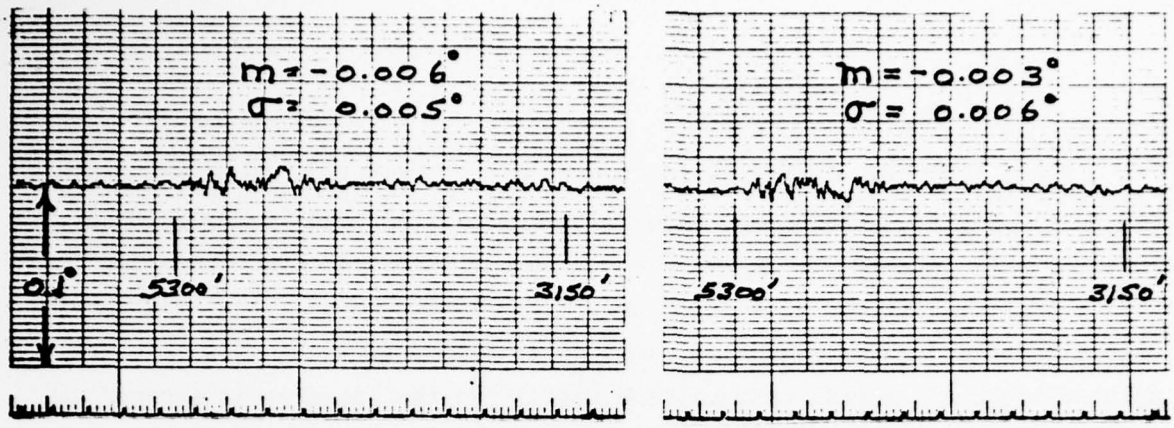

AWOP B-3 Opposite Side of Runway, Touchdown at 1000 ft.

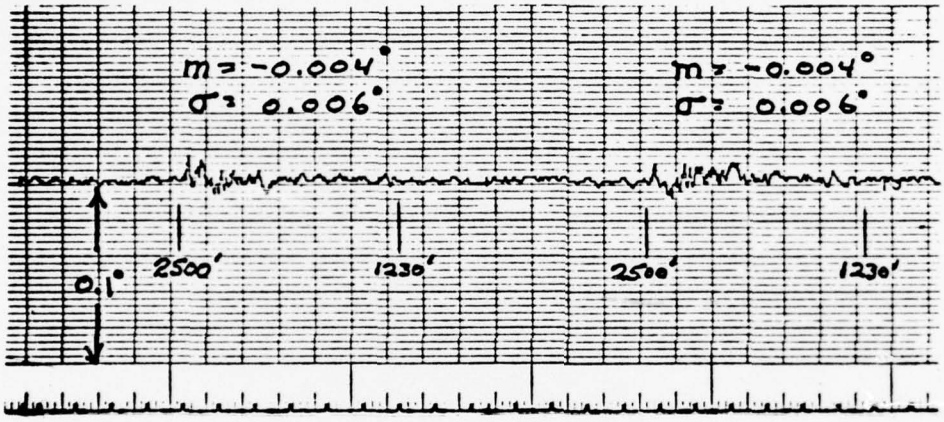

AWOP B-2 Opposite Side of Runway, Touchdown at 3000 ft.

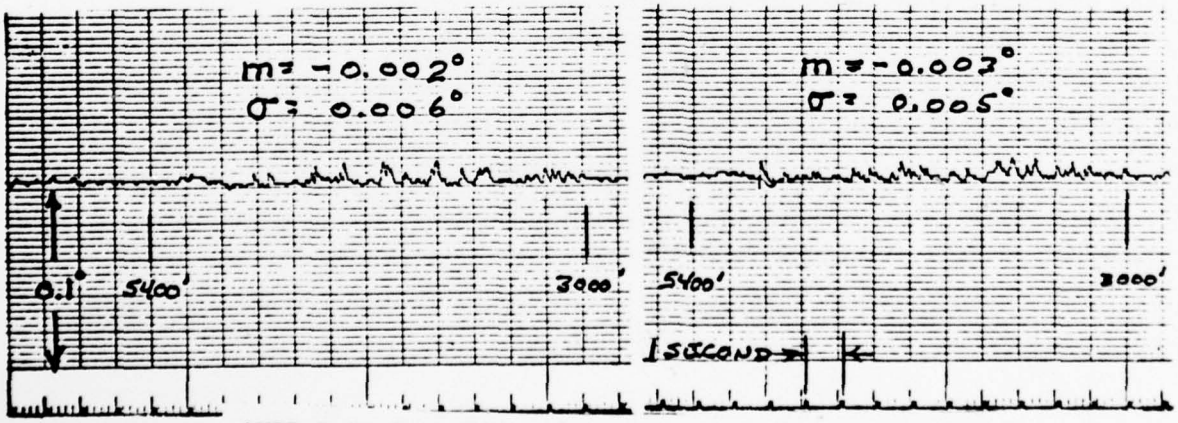

AWOP B-3 Same Side of Runway, Touchdown at 3000 ft.

Figure 5-31 FLARE HANGAR SCENARIOS - 2 RUNS EACH SEP RECEIVER

A straight line approximation to the actual computed values was used for the scalloping frequencies and separation angles programed in the Calspan hybrid simulator. Figures 5-32a and 5-32b show the scalloping frequency and separation angle variations as a function of time to touchdown. A flared path with the aircraft touching down at a range of 8550 feet from the azimuth antenna, the point where the aircraft antenna is 8 feet above the runway, was assumed in the Lincoln Laboratory computations.

The actual multipath levels at the aircraft receiver are determined by the relative multipath amplitude and the horizontal (azimuth) pattern of the flare antenna. The antenna pattern for the K_u-band flare unit was used in computing the multipath levels for this scenario. Figure 5-33 shows the antenna pattern proposed for the flare system. Since flare guidance is only required over a very limited area a very narrow pattern can be used. The flare antenna pattern is compared to the elevation pattern in Figure 5-33. The resulting multipath levels for this scenario are shown in Figure 5-34.

The results of three replications of this test appear in Figure 5-35. The raw data shown corresponds to the first α, β tilted run. It can be noted that the multipath errors from this hangar scenario with a 0.20° hangar tilt are insignificant.

The effectiveness of antenna pattern shaping can be illustrated by running the same scenario with the wider elevation pattern. Figure 5-36 shows three replications of this scenario with the resulting increase in error as the aircraft approaches touchdown, the point where the separation angle is about 0.20°. For this antenna pattern the peak multipath level is -5 dB and at touchdown is -10 dB. It should be noted that modifications to the SEP could be made, such as envelop averaging, that would reduce its sensitivity to multipath interference occurring on the outside edges.

5.3 SEP For Elevation

Although the TRSB receivers have demonstrated suitable performance for elevation data in all the ICAO multipath scenarios, there may be special situations for VTOL type aircraft and helicopters in which the very slow final

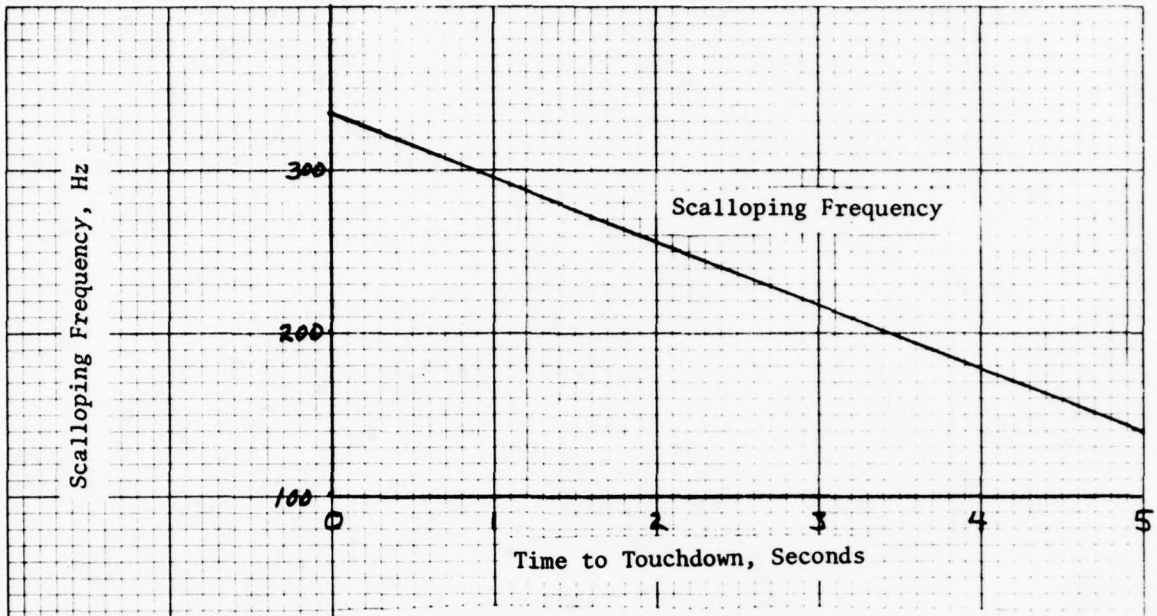

Figure 5-32 SCALLOPING FREQUENCY-FLARE SCENARIO JFK B3 (TILTED 0.2°)

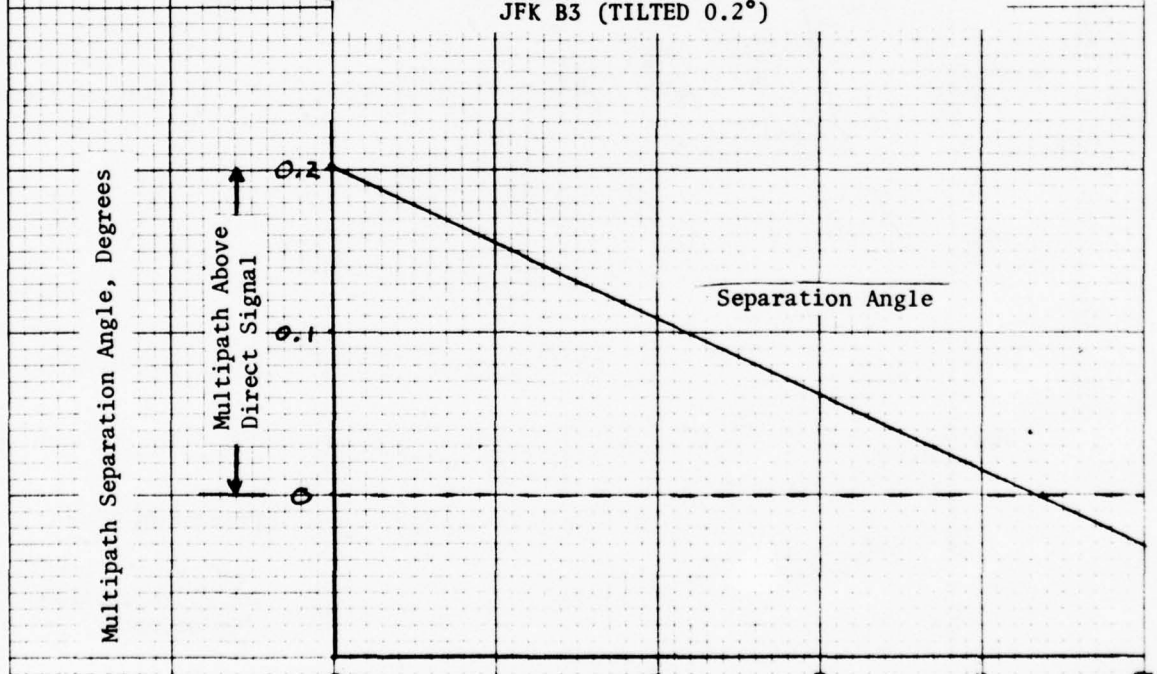

Figure 3b SEPARATION ANGLE - FLARE SCENARIO JFK B3 (TILTED 0.20°)

Figure 5-33 ANTENNA AZIMUTH PATTERNS

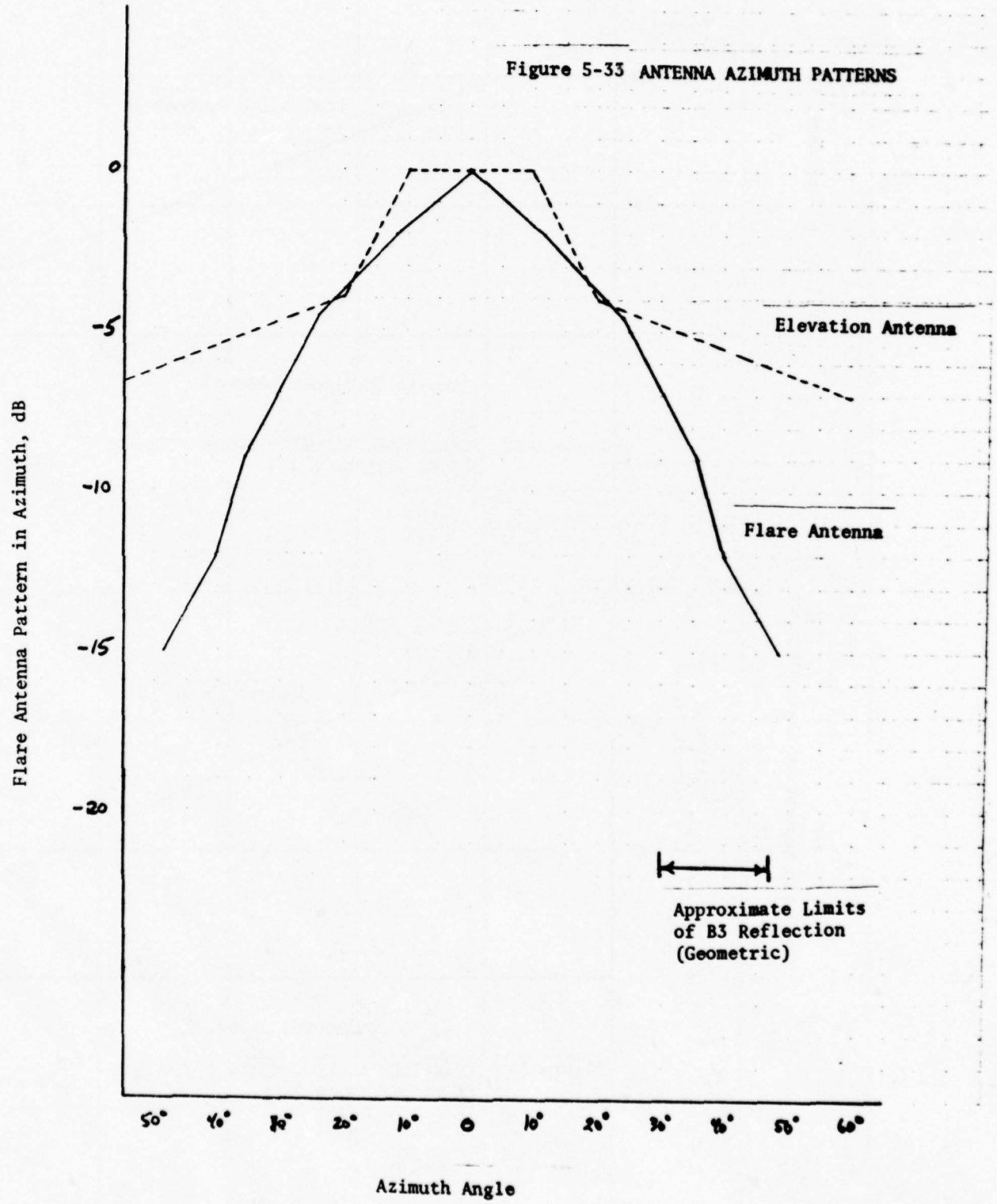

Figure 5-34 APPROXIMATE MULTIPATH AMPLITUDE RELATIVE TO DIRECT SIGNAL
FLARE SCENARIO JFK B3, TILTED 0.2°
NARROW PATTERN (AZIMUTH) ANTENNA

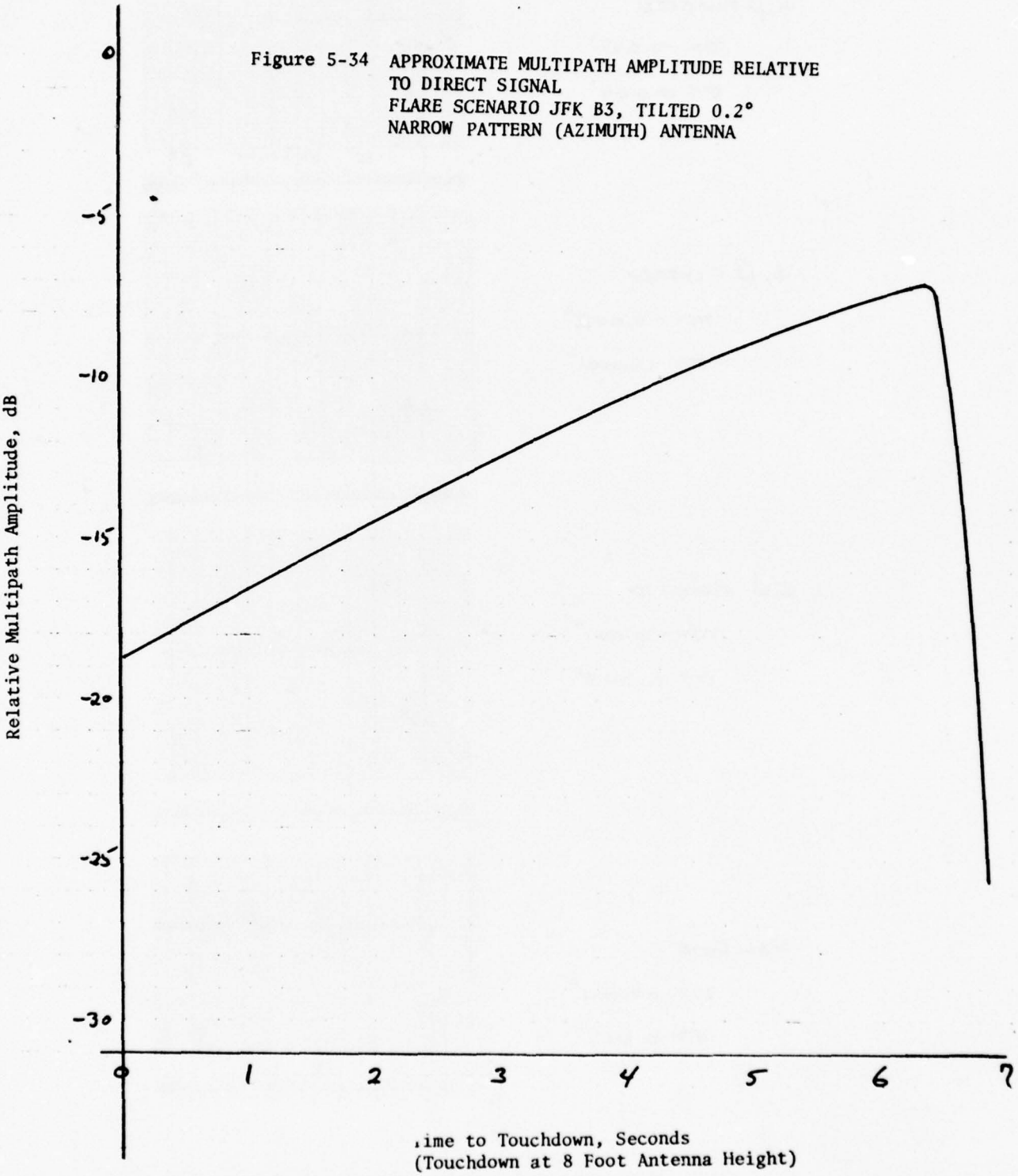

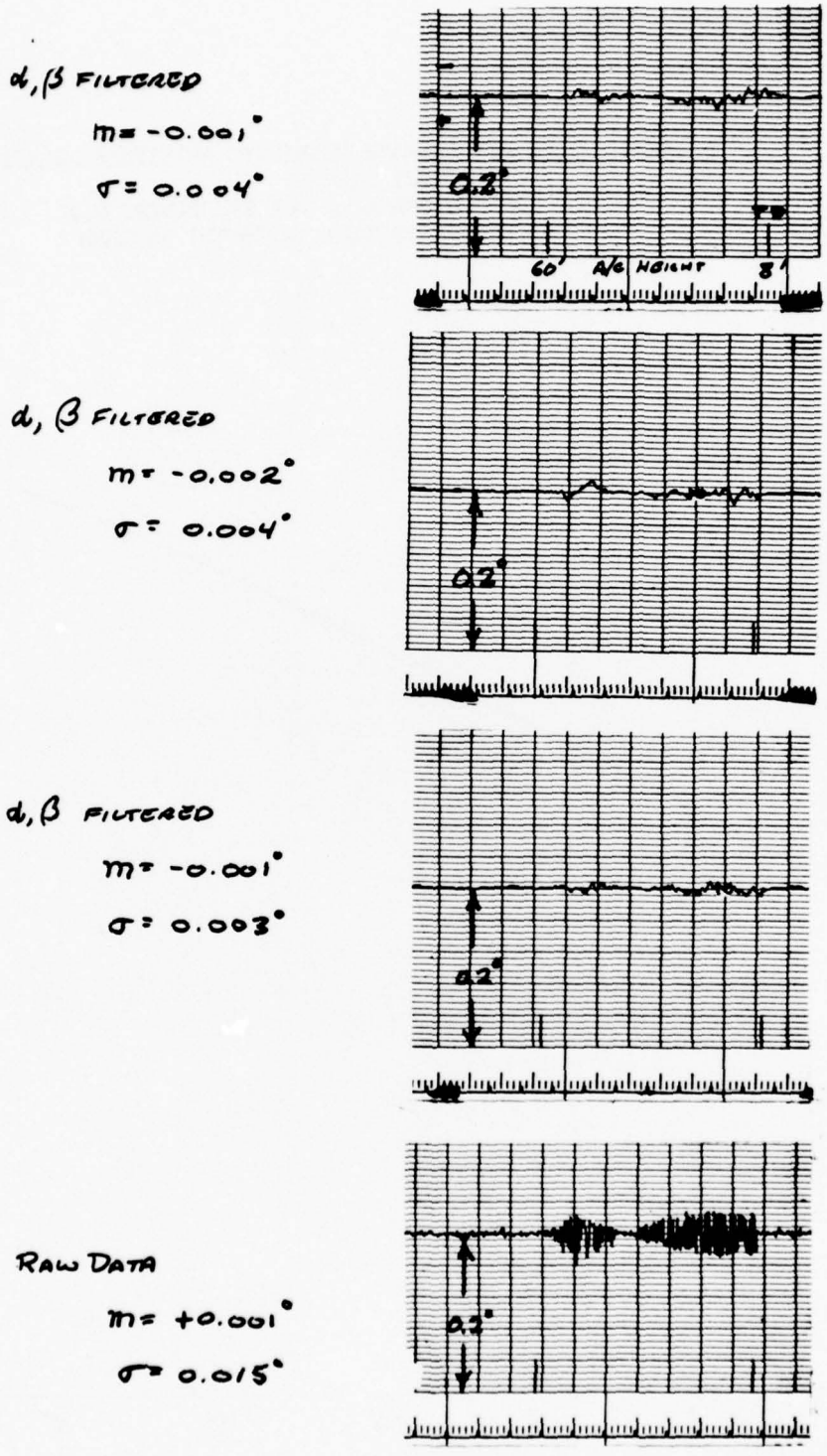

Figure 5-35 - SEP -
FLARE HANGAR SCENARIO, JFK B3 TILTED 0.2°
1/2° BEAMWIDTH, -25 dB SIDELOBES [NARROW AZIMUTH PATTERN]

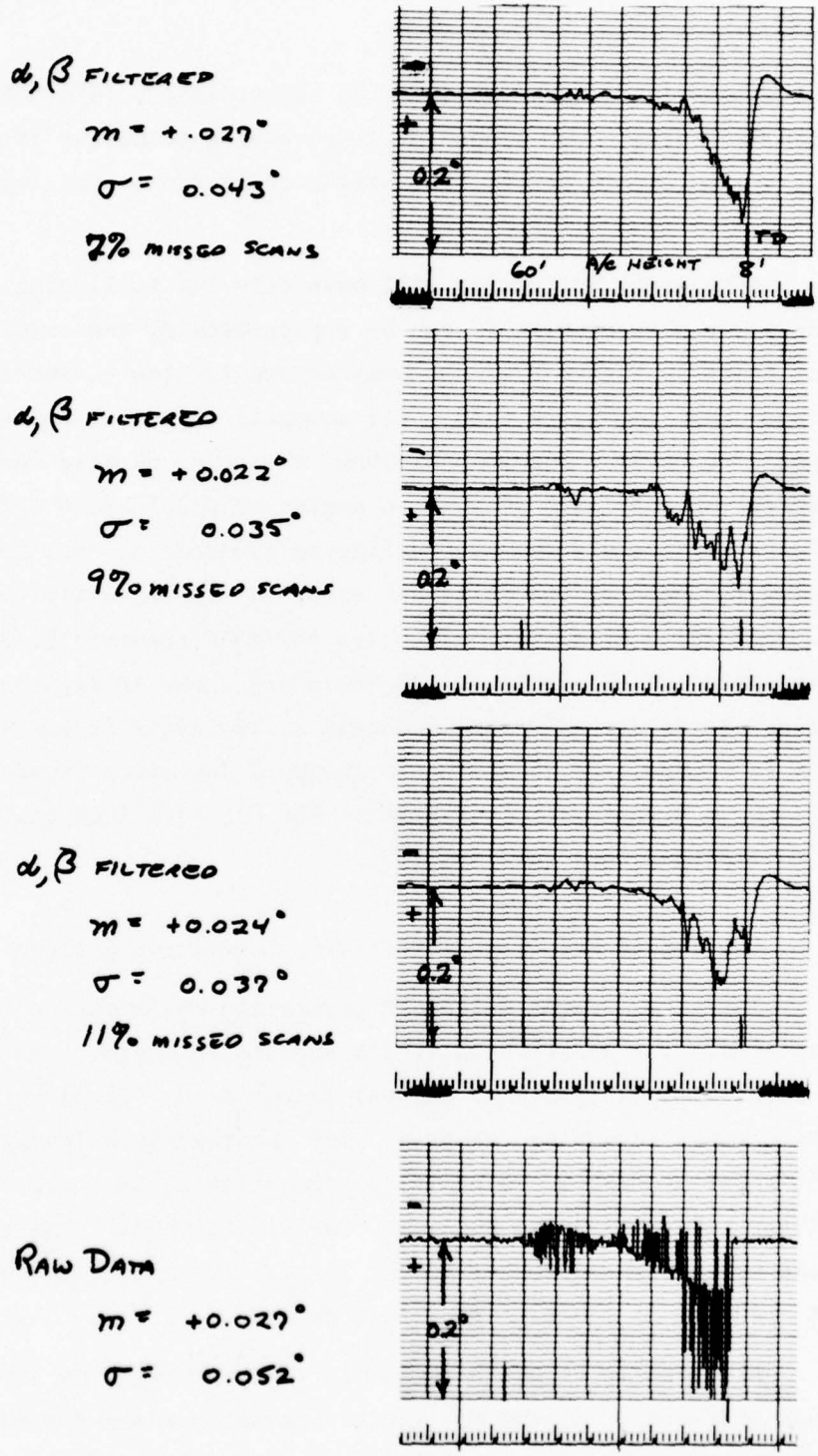

Figure 5-36 - SEP - FLARE HANGAR SCENARIO, JFK B3 TILTED 0.2°
1/2° BEAMWIDTH, -25 dB SIDELOBES, [EL-1 ANTENNA AZIMUTH PATTERN]

approach speeds (near zero velocity) do not provide sufficient error reductions by motion averaging. The single edge processing technique is very effective in reducing the multipath errors from hangar reflections even for a hovering helicopter.

A hovering helicopter will have very low scalloping frequencies so that the error characteristics can be represented by the error curves from the baseline tests in Figure 5-37 and peak errors for the in-and-out of phase conditions shown in Figure 5-38. For comparison similar curves are shown for the Phase 3 receiver. Figure 5-39 shows the error plotted versus scalloping frequencies for multipath separation angles of 0.25° and 0.75°. The errors with the SEP are quite small even at scalloping frequencies near zero. At the higher scalloping frequencies the multipath error is significantly smaller than the Phase 3 receiver. Error time histories for AWOP scenario 1, hangar B2 with approach speeds of 130 knots and 40 knots are shown in Figures 5-40 and 5-41 for the SEP receiver. The same scenario at 130 knots is shown for the Phase 3 receiver in Figure 4-62 in which the standard deviation increases to about 0.017° with no significant mean error. The SEP technique can make elevation hangar multipath errors very small.

5.3.1 Effects of Multipath at Positive Separation Angles

The error versus multipath separation angle curves in Figure 5-37 show the errors for positive multipath separation angles. Multipath interference on the outside edges (positive angles) cannot occur for elevation data in realistic hangar scenarios except at very low multipath levels as a result of edge diffraction effects. A positive separation angle could occur if a hangar has a large tilt toward the antenna. For elevation data the aircraft never flys below the antenna phase center height so positive multipath separation angles can not occur as is the case for flare data.

As shown in Figure 9 of the Lincoln Laboratories ATC Working Paper 44WP-5040 (Reference 14) the multipath separation angle for building B2 scenario 1 (JFK) starts out at a positive 1.5 degrees. At these positive values the multipath level is very low, less than -32 dB, as would be expected for edge diffraction

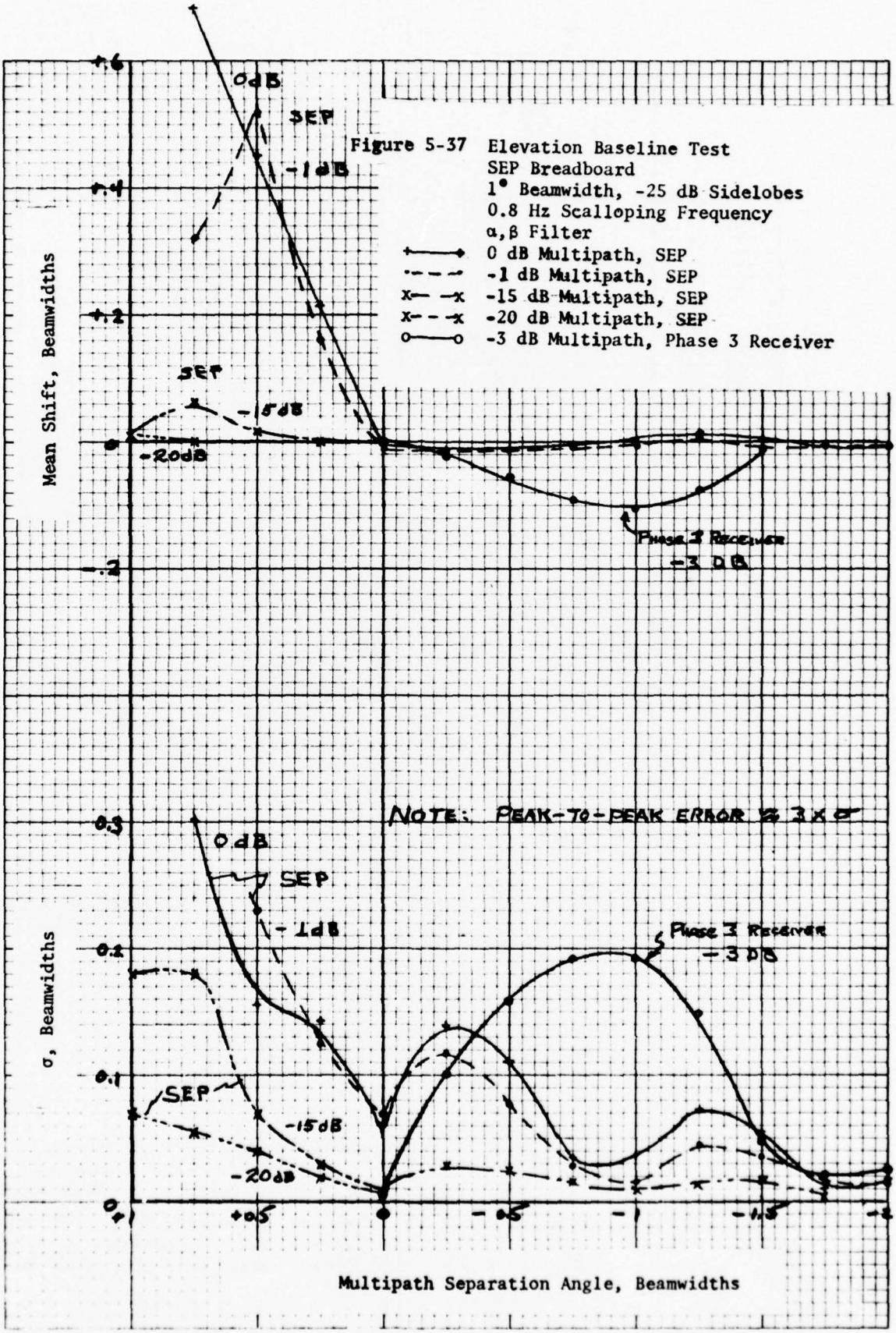

Figure 5-37 Elevation Baseline Test
SEP Breadboard
1° Beamwidth, -25 dB Sidelobes
0.8 Hz Scalloping Frequency
α,β Filter
0 dB Multipath, SEP
-1 dB Multipath, SEP
-15 dB Multipath, SEP
-20 dB Multipath, SEP
-3 dB Multipath, Phase 3 Receiver

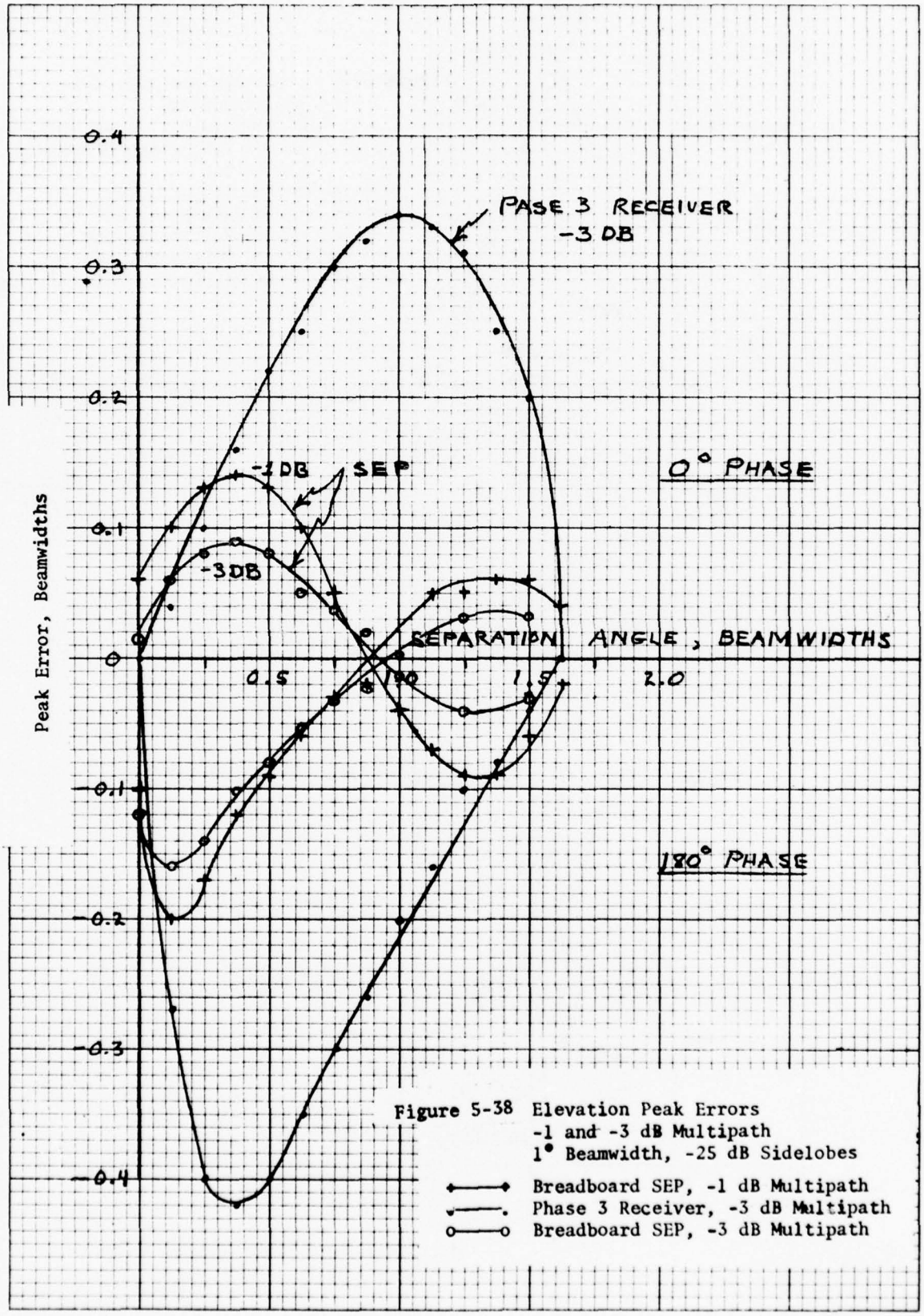

Figure 5-38 Elevation Peak Errors
-1 and -3 dB Multipath
1° Beamwidth, -25 dB Sidelobes

- Breadboard SEP, -1 dB Multipath
- Phase 3 Receiver, -3 dB Multipath
- Breadboard SEP, -3 dB Multipath

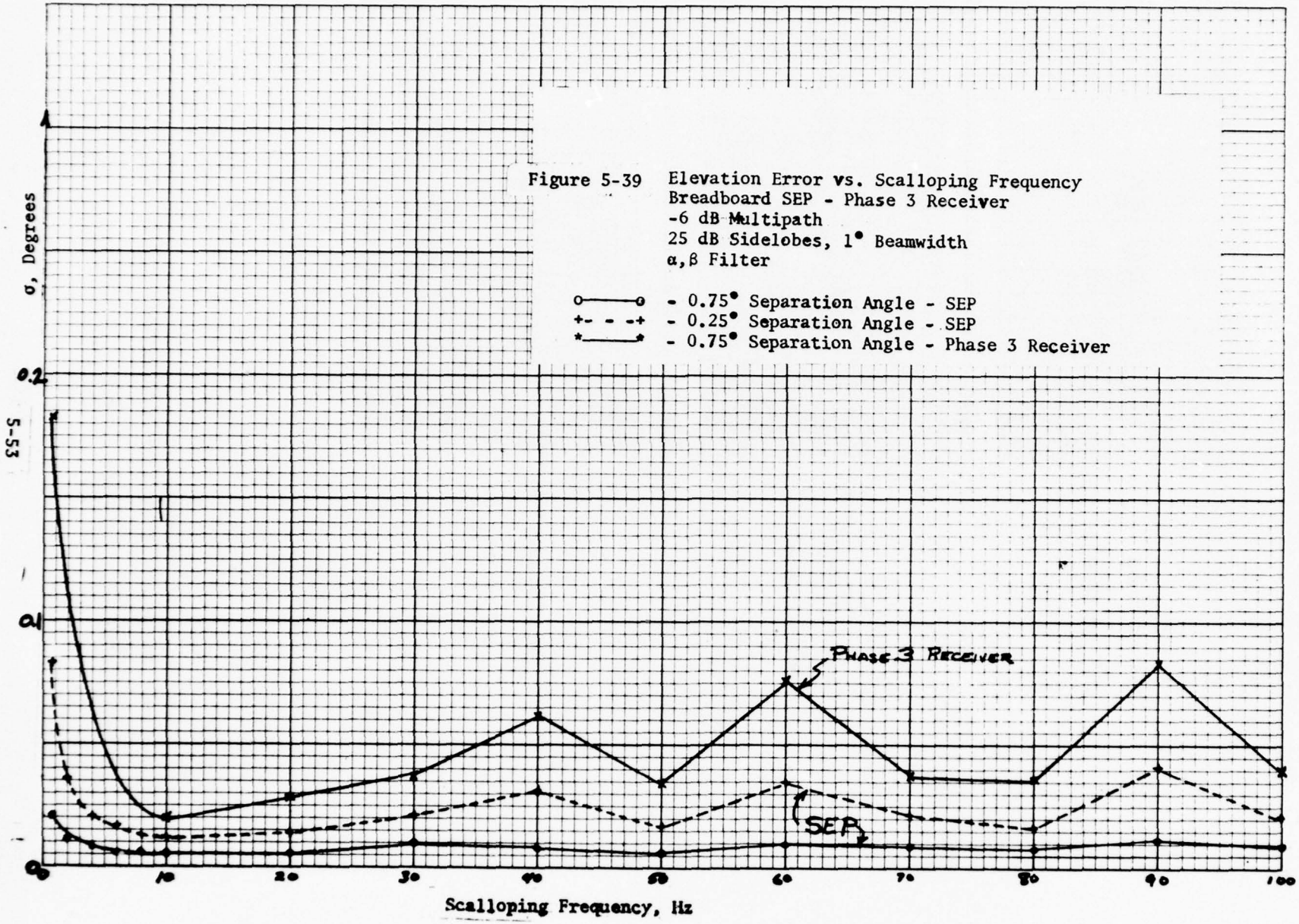

Figure 5-39 Elevation Error vs. Scalloping Frequency
Breadboard SEP - Phase 3 Receiver
-6 dB Multipath
25 dB Sidelobes, 1° Beamwidth
α,β Filter

o——o - 0.75° Separation Angle - SEP
+- - -+ - 0.25° Separation Angle - SEP
—— - 0.75° Separation Angle - Phase 3 Receiver

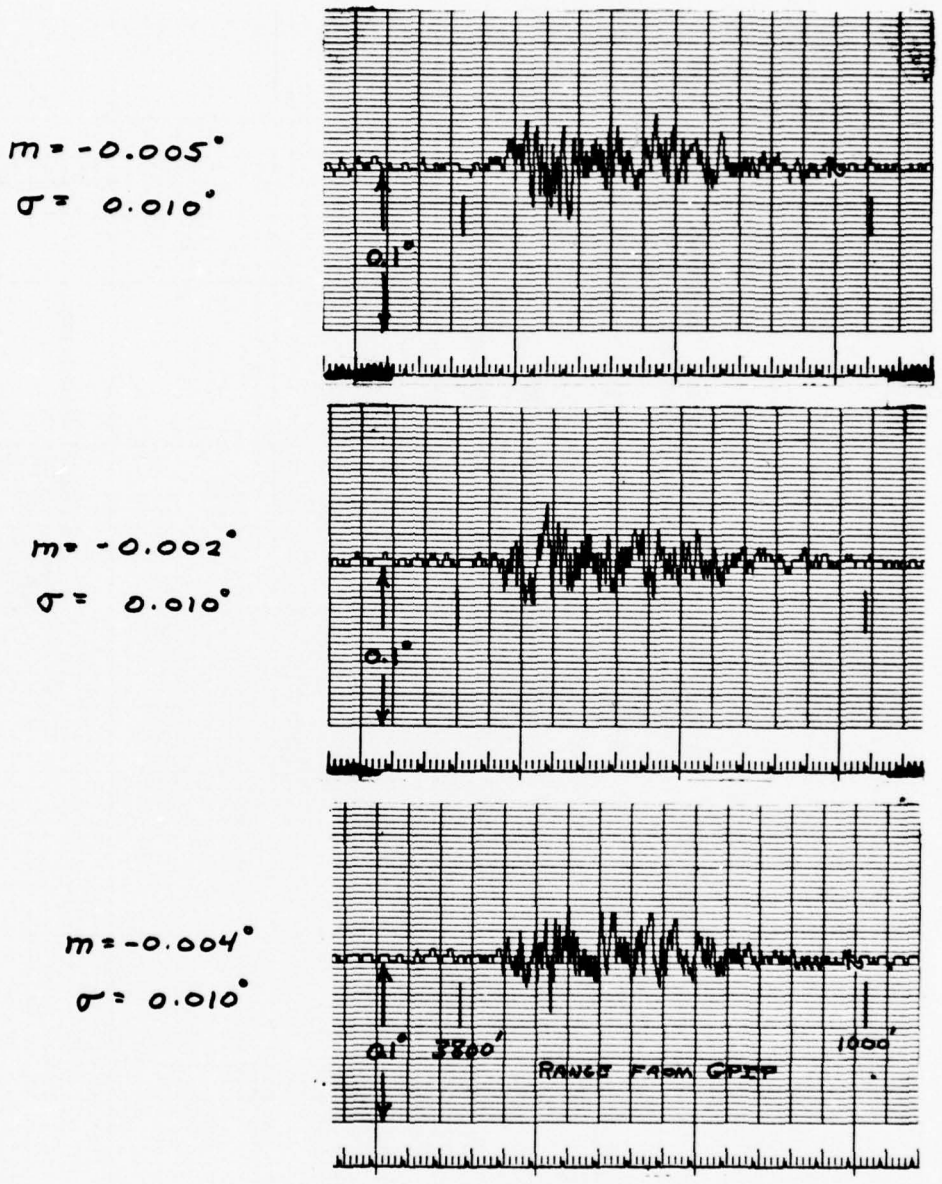

Figure 5-40 Breadboard SEP Receiver
AWOP B2 Scenario 1 (Modified), Elevation
3 Replications
220 Ft/Second, 20:1 Glide Slope

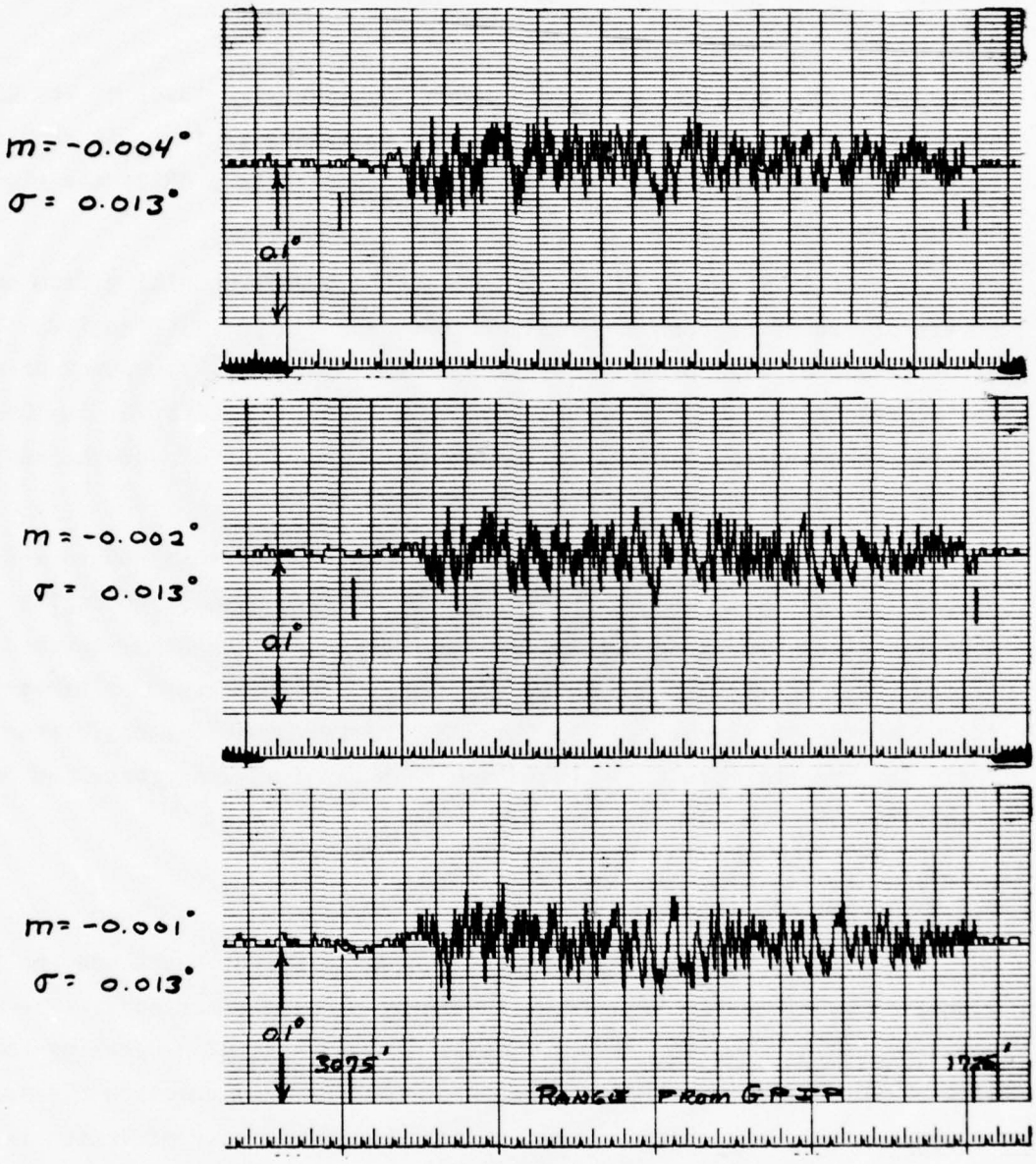

Figure 5-41 Breadboard SEP Receiver
40 Knot Version of AWOP-B2 Scenario 1 (Modified)
(Multipath Truncated to 20 Seconds)
3 Replications
68 Ft/Sec, 20:1 Glide Slope

multipath. The separation angle becomes negative at a level of -24 dB and approaches -1.5 degrees at the end of the multipath region. It should be noted that these levels would be reduced an additional 4 to 5 dB by the elevation antenna pattern shaping.

It is shown in Figure 5-37 that the errors resulting from multipath levels of -20 dB or less are insignificant for all positive angles. Since the error curves of Figure 5-37 are based upon a scalloping frequency of 0.8 Hz they are representative of the errors seen by a hovering helicopter in the multipath interference region. If the helicopter is approaching at several knots the motion averaging would make the multipath quite small.

Averaging techniques can be used in the SEP that should reduce the errors for multipath at both positive and negative separation angles. A dual mode elevation processor utilizing both the SEP and the beam centroid processor of the Phase 3 receiver should provide optimum performance for elevation data in any multipath scenario. The Phase 3 receiver processor has better low S/N ratio performance than the SEP and should be used at long range and for signal acquisition.

5.3.2 Implementation of SEP

The SEP concept has been evaluated in flight tests and the hybrid MLS simulator using analog techniques in the breadboard processors. The Phase 3 receiver and all subsequent models will utilize digital processing techniques with microprocessors. Implementation of the SEP only requires the addition of appropriate computer programs. Since the SEP is very effective in reducing elevation multipath errors it could be included in all future processing algorithms.

The concept of dual SEP and centroid processing for elevation data is very attractive. The incoming beam shapes would be digitized and then processed in the two separate computer programs. Data outputs would utilize the centroid processor until the SEP output has smaller noise errors at which time the SEP data would be the output. This and other algorithms based upon the time separation of multipath signals should be evaluated to determine the best technique for utilizing the SEP multipath reduction capabilities in future processors.

Section 6.0
AIRCRAFT CLOSED LOOP TESTS

An aircraft simulation was added to the MLS simulator so that closed loop tests could be conducted to determine the effects of multipath on an aircraft making an approach under autopilot control. In addition, the closed loop simulation was used to determine the effectiveness of MLS beam rate data in compensating for wind shears during an autopilot approach with the MLS elevation channel.

6.1 Description of Closed Loop Simulation

The aircraft used in the closed loop simulation was the Boeing 707-300 that is representative of a medium weight transport aircraft and had been programed on the analog computer for other simulation analyses. Aircraft dynamics were computed for a gross weight of 200,000 lbs, glide slope of 2.7 degrees and a trim velocity in the landing approach configuration of 162 knots. This aircraft simulation is connected to the MLS simulator for the closed loop tests with the MLS breadboard processor.

Two autopilot configurations were implemented for these evaluations. A baseline autopilot that is a simplified version of system B specified in Reference (16) in which MLS angle displacement was used with a longitudinal accelerometer and altitude rate data for stabilizing the control loop.

A simplified autopilot was synthesized that only used rate data derived from the MLS signal in the control loop. This configuration was evolved to provide tighter beam following in the presence of wind shears. In addition the design represents a rather simple autopilot implementation.

Both autopilots can be divided into two basic blocks, an outer loop to track the MLS received angle and an inner loop, also known as a Stability Augmentation System (SAS), to provide stability to the basic airframe and help eliminate short term environmental disturbances. The performance of the baseline autopilot in the presence of multipath and wind shears will be the reference for comparing the performance of the derived rate autopilot.

The outer loop of the baseline autopilot uses MLS received glide slope angle and rate of descent ($\dot{h}$) from a rate sensor. Figure 6-1 shows how these elements fit together. The MLS received angle deviation is limited to 0.2 degrees and converted to altitude offset from the glide slope using altitude (h) or range as the programing variable. The error from the glide slope is now independent of range. This offset and its integral are the position correcting elements of the outer loop and when combined with a complementary filtered rate of descent ($\dot{h}$), become the commanded pitch angle. Commanded elevator angle (δ_{eo}) is obtained by combining pitch angle with aircraft pitch rate ($\dot{\theta}$) and normal acceleration ($\ddot{h}$). These combined elements form the Stability Augmentation System (inner loop).

The derived rate autopilot only uses aircraft pitch rate ($\dot{\theta}$) and MLS received glide slope angle. The other element, change in rate of descent ($\Delta\dot{h}$), is derived from the glide slope angle by a rate circuit within the autopilot. Figure 6-2 shows a block diagram for these elements. The MLS received angle is again limited to 0.2 degrees and converted to an altitude offset before further processing. The angle-to-offset conversion could use signal level as the programing variable or a crude range measurement. Range to the antenna is inversely related to signal amplitude. The filtered aircraft offset and its integral become the position error for the outer loop. The damping term for the outer loop is obtained from a band limited differentiator and low pass filter which operates on the MLS received angle. The combined result of these three elements is the change in commanded pitch angle. The inner loop subtracts the pitch angle rate damping term from the commanded pitch angle to arrive at a commanded elevator angle.

The closed loop frequency response curves for these two autopilots to glide slope angle errors are shown in Figures 6-3 and 6-4. The rate system is very underdamped indicating a need for accelerometer data to complement the angle rate data in order to improve the system performance. However, because of the limited scope of this investigation no attempt was made to optimize the rate derived system.

This AWOP B2 scenario (modified) described in Figure 4-56 was run with both autopilots and the dwell gate and single edge processors.

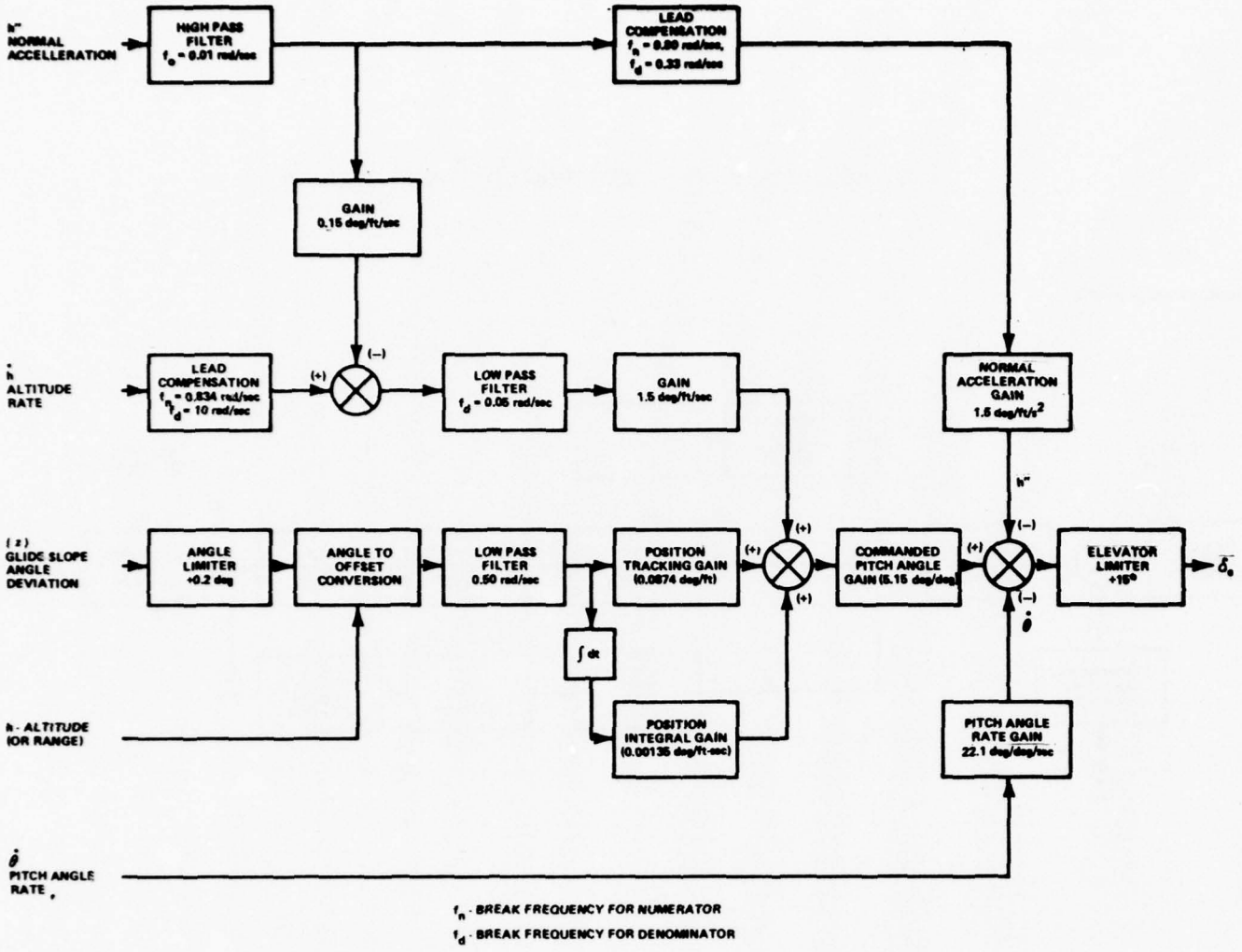

Figure 6-1 LONGITUDINAL AUTOPILOT – BASELINE SYSTEM

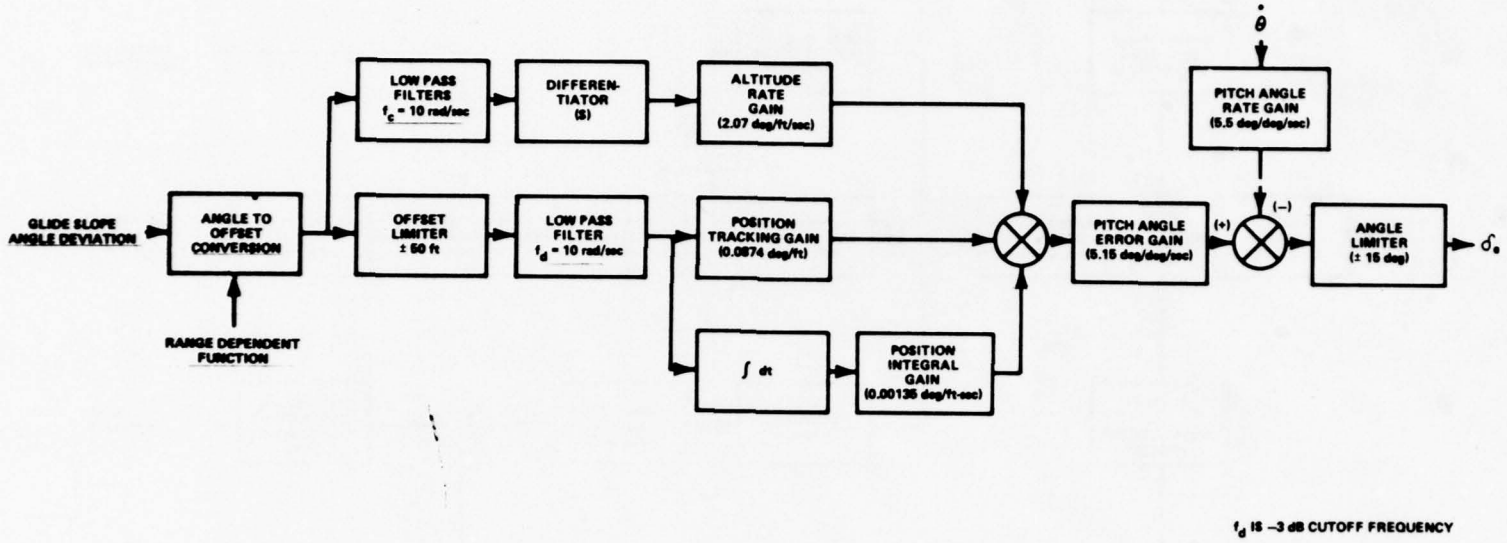

Figure 6-2 LONGITUDINAL DERIVED RATE AUTOPILOT

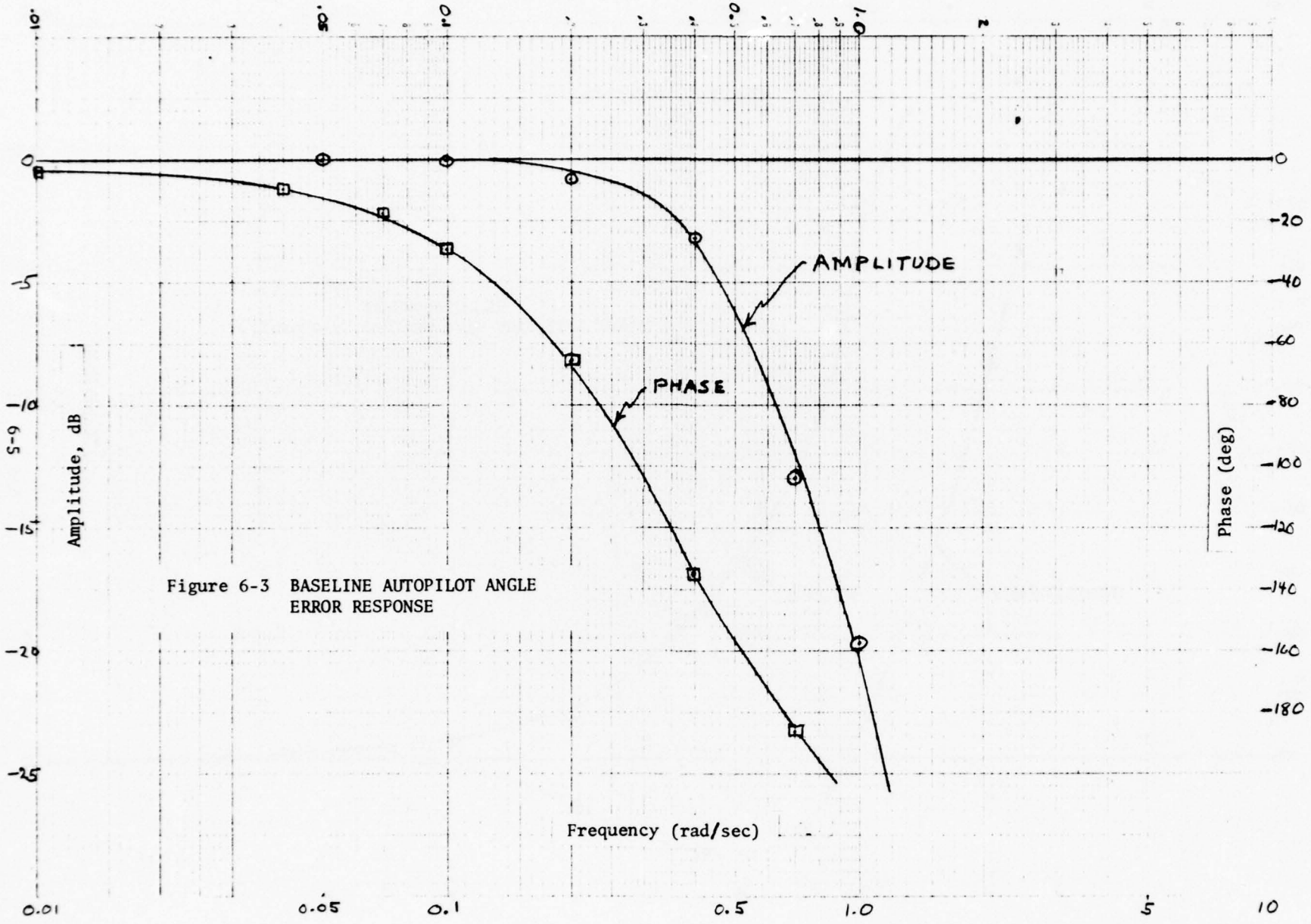

Figure 6-3 BASELINE AUTOPILOT ANGLE ERROR RESPONSE

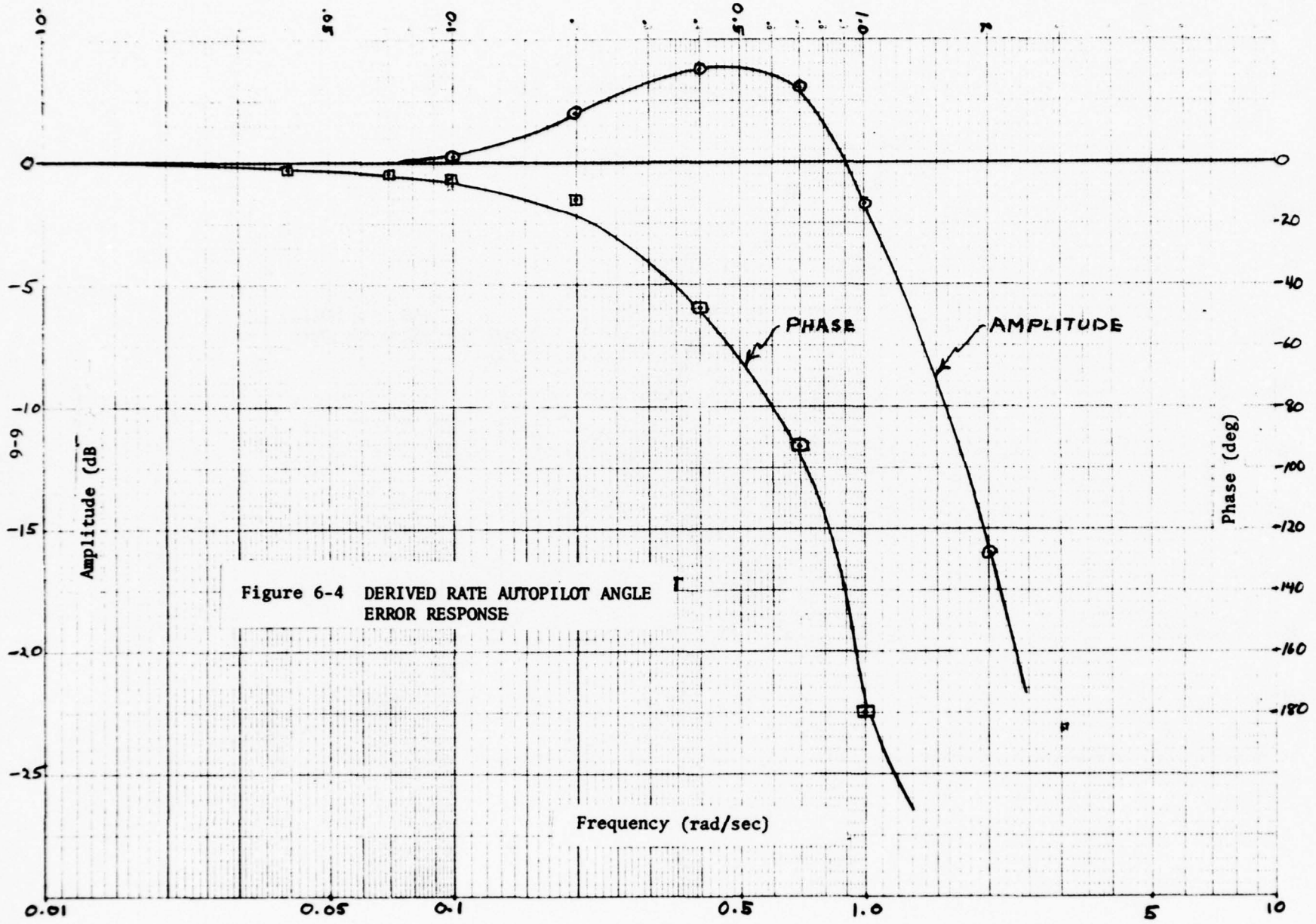

Figure 6-4 DERIVED RATE AUTOPILOT ANGLE ERROR RESPONSE

The simulated multipath level was equivalent to a hangar with a reflection coefficient of -3 dB in the AWOP scenario after applying the elevation antenna pattern shaping. A ramp angle error input was introduced in a later test to simulate the effect of a wind shear in order to evaluate the relative performance of the two autopilots. The multipath scenarios were initiated by starting the aircraft down the glide path for approximately 5 seconds before initiating the multipath signal. Two seconds after passing through the multipath interference region the simulation is terminated. At the end of the simulation the aircraft has reached the flare initiation point but has not returned to the glide path. The aircraft has a delay of about 2 seconds from the time the multipath signal is applied until aircraft path deviations occur.

6.2 Test Results

The aircraft perturbations resulting from the multipath errors in the AWOP B2 scenario are shown in Figure 6-5 and 6-6 with the dwell gate processor for the two autopilots. The baseline autopilot held the aircraft displacement to about 1 foot with peak-to-peak elevator control motions of 0.25°. With the rate derived autopilot the flight deviations we kept to about 0.5 feet but the control motions were extremely large, about 10° peak-to-peak. These large control motions indicate the need for better damping data such as accelerations and a reduced loop gain. It should be noted that these runs are terminated before the aircraft can return to the glide path.

Responses for the control motion and aircraft motion approximating filters specified in Reference (17) are also shown. The poor agreement in the simulated aircraft responses and filter responses is apparent. Modifications in the filter transfer functions could be made that should provide more realistic outputs.

Figure 6-7 shows the same multipath scenario run with the SEP and the baseline autopilot. The resulting flight path deviations and control motions are insignificant with the SEP. Similar SEP tests with the derived rate autopilot resulted in control motions of about half amplitude of those with the dwell gate processor.

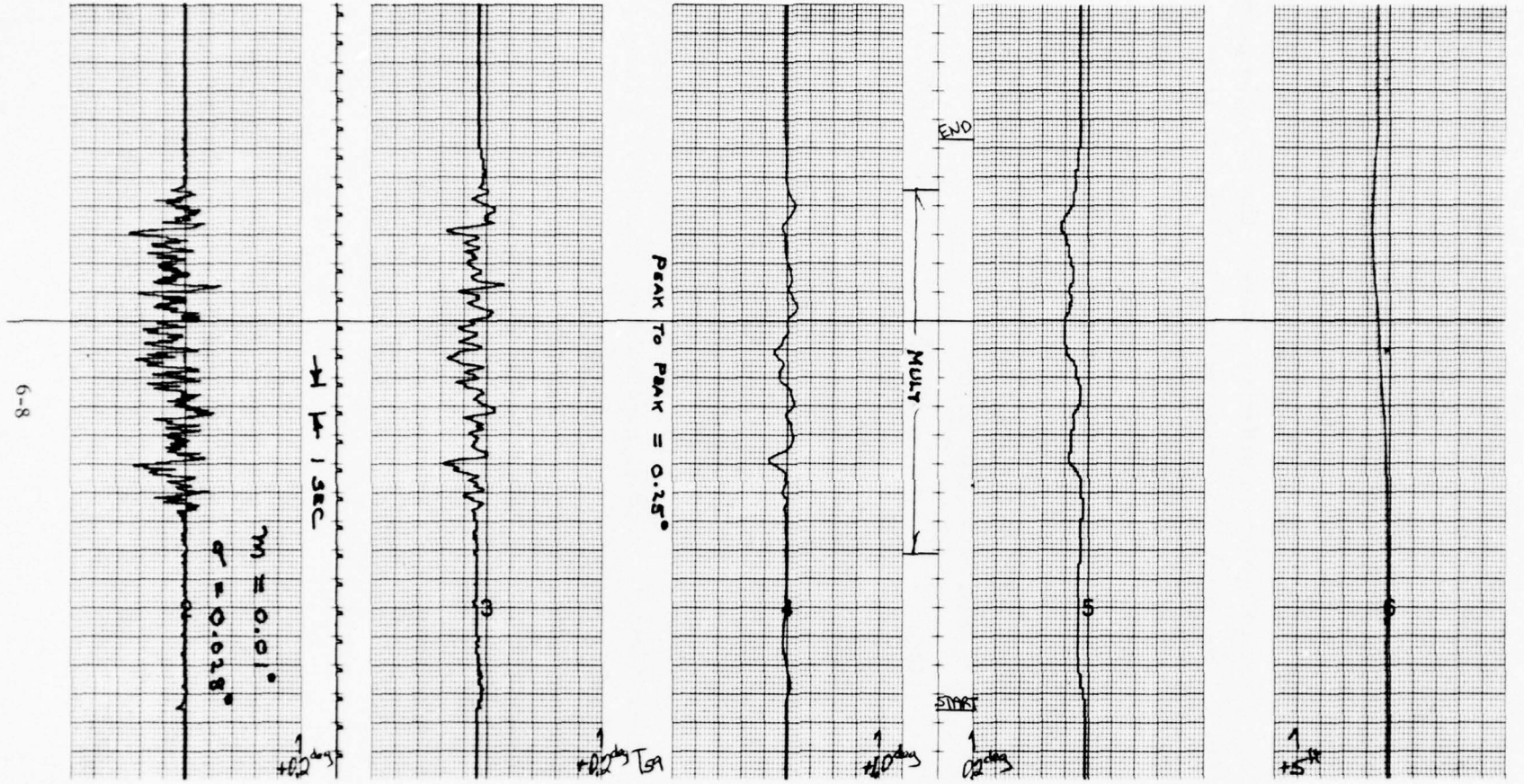

Figure 6-5 DWELL GATE PROCESSOR - Baseline Autopilot, AWOP-B2 Scenario

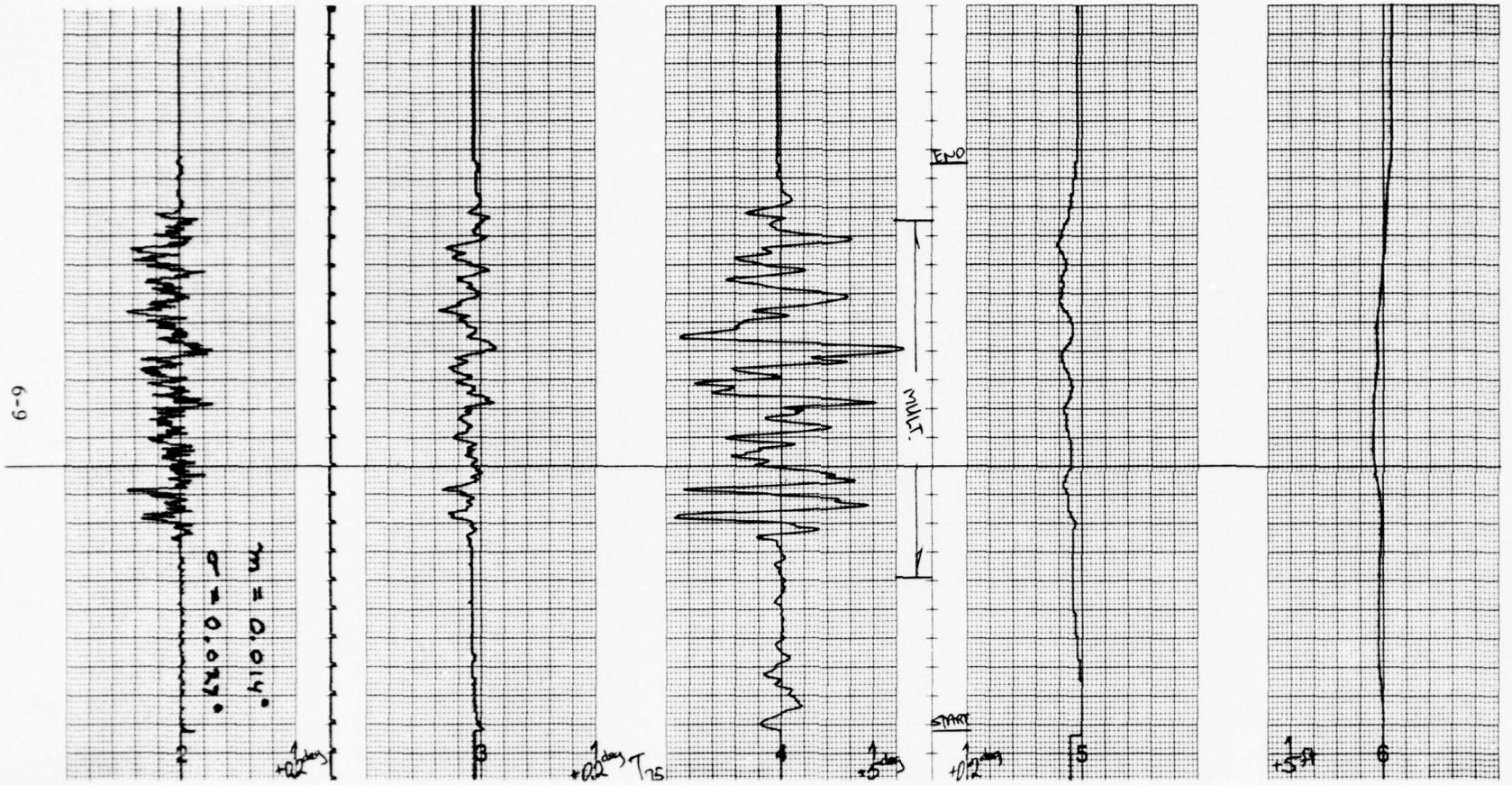

Figure 6-6 DWELL GATE PROCESSOR - Derived Rate Autopilot, AWOP-B2 Scenario

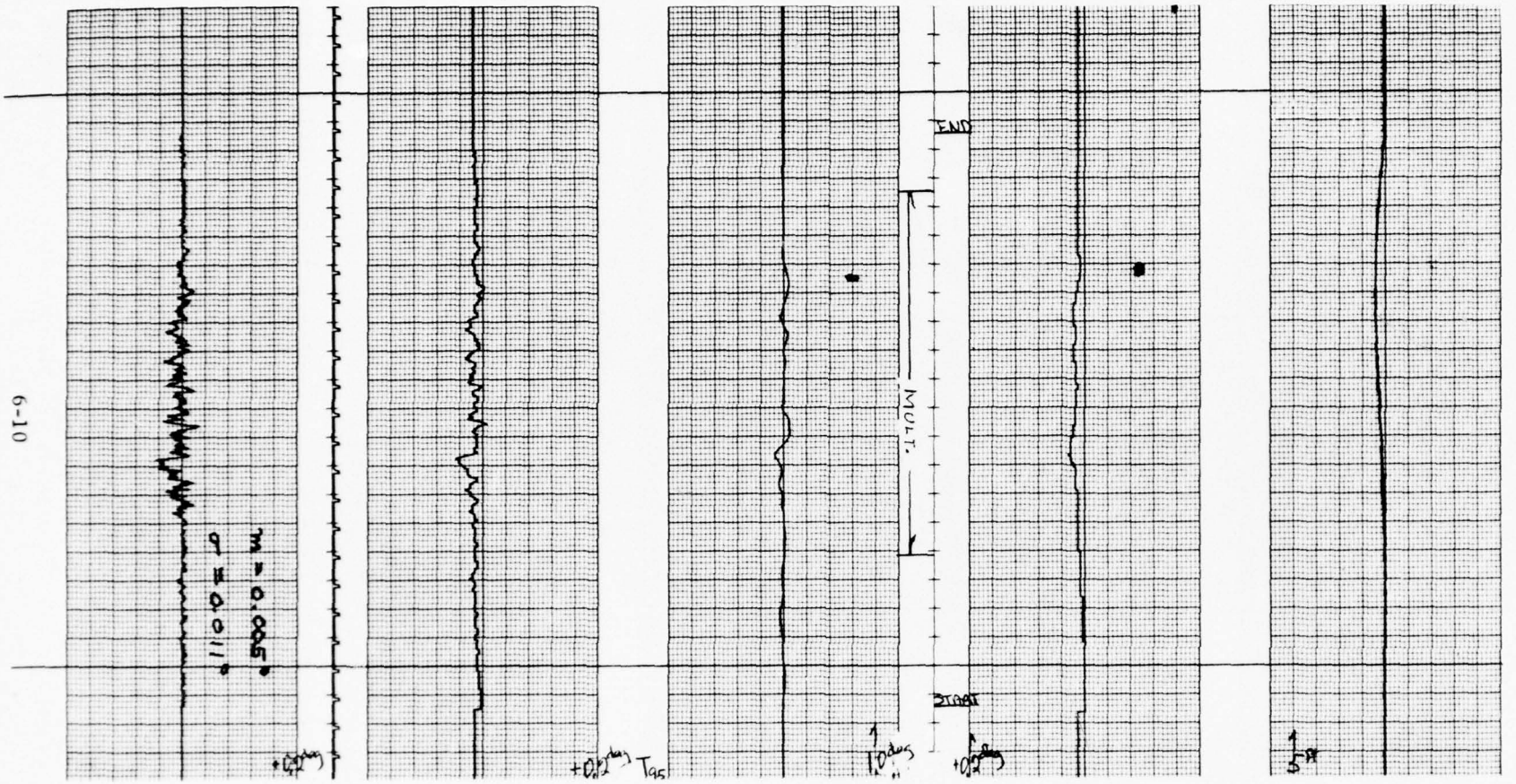

Received Angle Error | Control Motion (filter model) | Control Motion (analog simulation) | Aircraft Motion (filter Model) | Aircraft Motion (analog simulation)

Figure 6-7 SEP - Baseline Autopilot, AWOP B-2 Scenario

Figures 6-8 and 6-9 show the aircraft response to a ramp error of 0.05 degree per second assumed to be a crude approximation to the effects of wind shears experienced by an aircraft following the glide slope. The advantage of using rate data derived from the MLS angle signals is apparent from a comparison of the aircraft motion resulting with these two autopilots. The derived rate autopilot follows the ramp error with very little lag and steady state error. A significant steady state lag, equivalent to about 20 feet in altitude, occurs with the baseline autopilot.

It appears that MLS rate data could be effective in reducing the effect of wind shears for an aircraft on an autopilot approach. However increased control motions will result from multipath disturbances. A SEP may be required with a rate type autopilot to minimize the control motions.

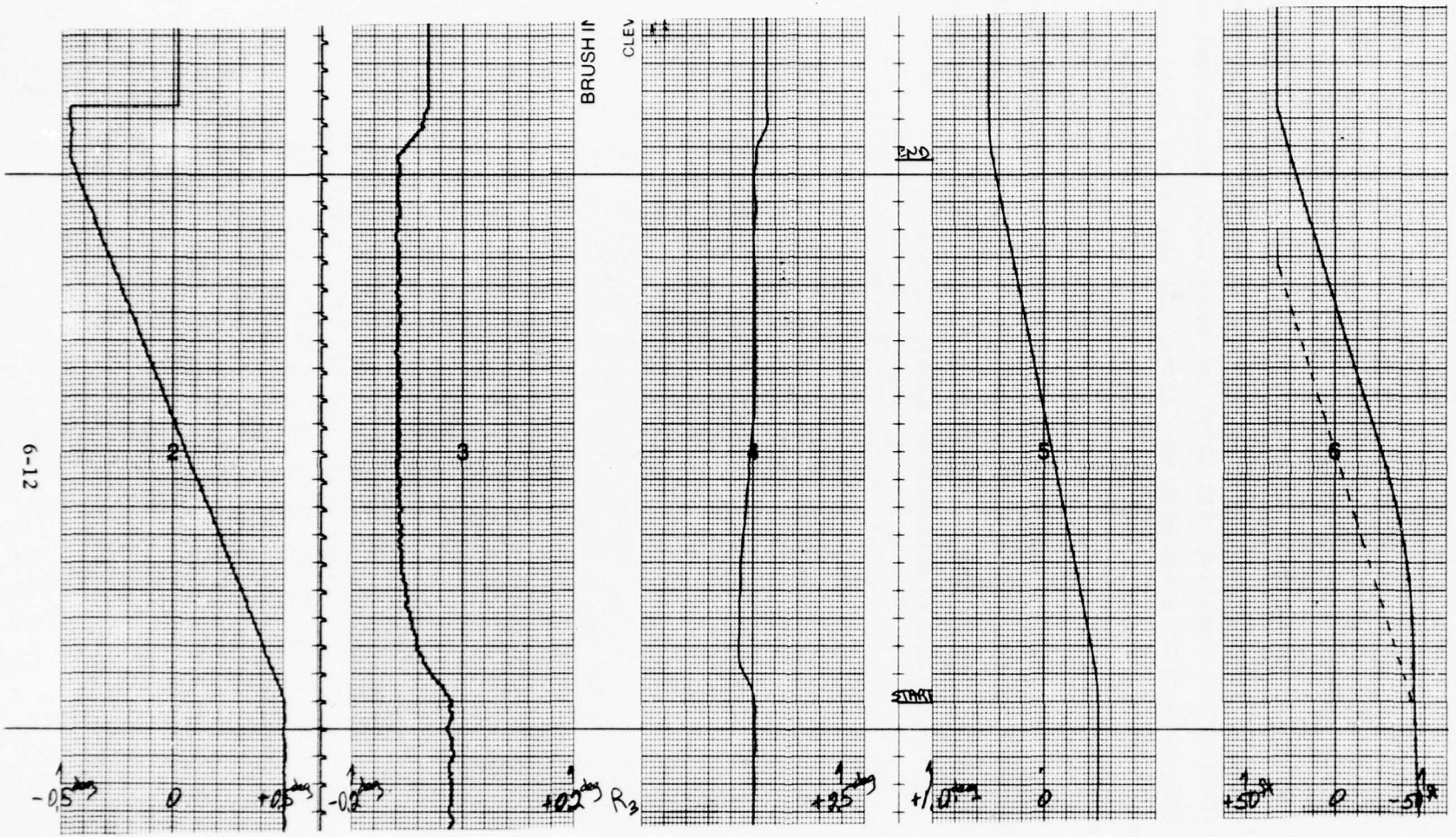

Figure 6-8 BASELINE AUTOPILOT - Ramp Response

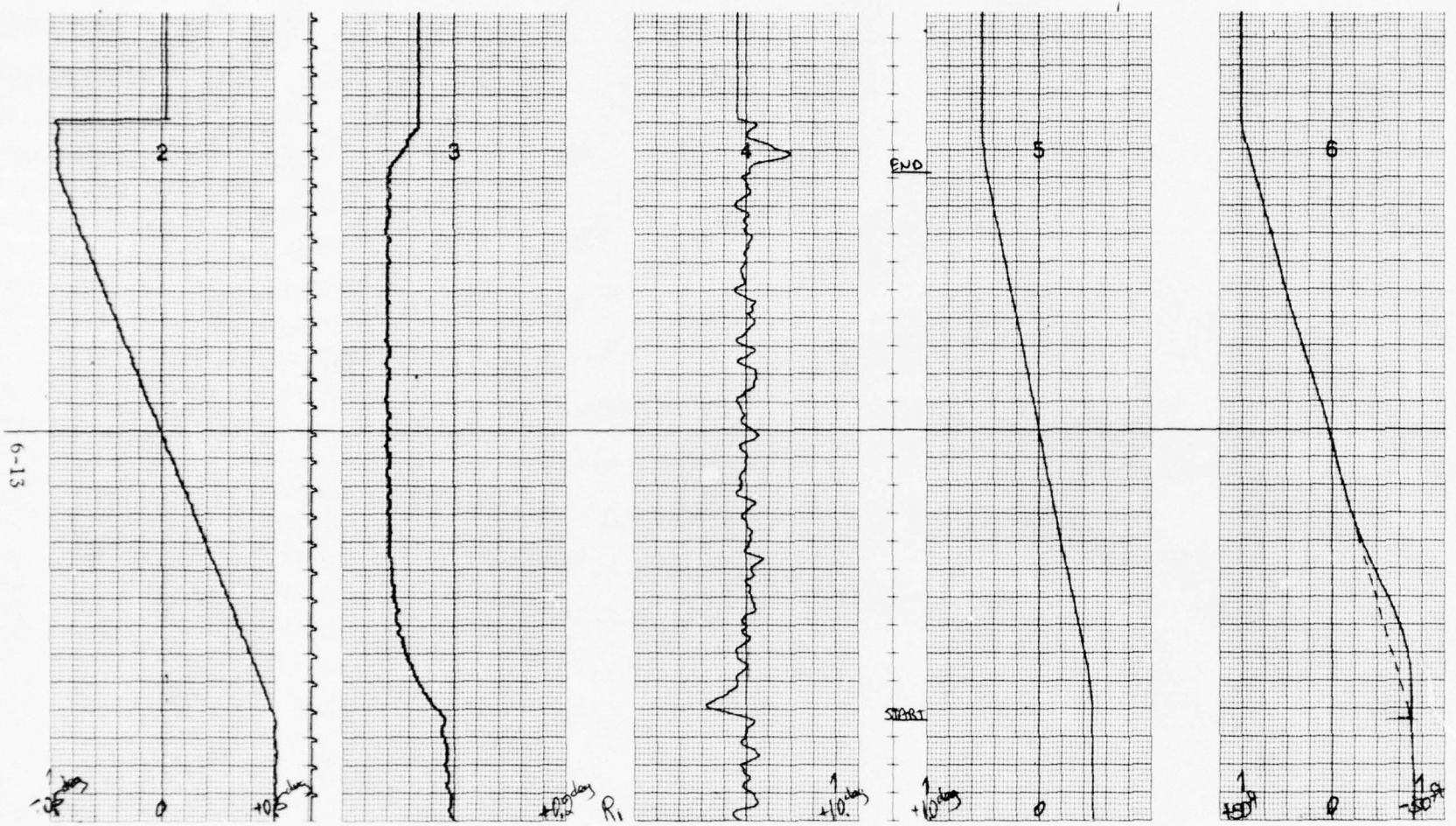

Figure 6-9 DERIVED RATE AUTOPILOT - Ramp Response

Appendix A
PROPELLER MODULATION

The TRSB signal format includes a variable time between function repetitions so that it is not possible for propeller shadowing to become synchronized with the angle scans. This jitter is incorporated into the simulator signal. Propeller modulation was simulated by introducing trapezoidal waveform pulses into the gain controls of the signal amplifiers. The pulse width used was 1.87 milliseconds at the mid-amplitude points with 0.5 millisecond rise and fall times. At the rotational speeds used for these tests, this pulse width corresponds to a duty cycle of 11.7% or a propeller width of 21° (6" width at 16.4" radius). The pulse amplitude was adjusted to provide 4, 8 or 12 dB maximum attenuation.

"Worst case" propeller modulation tests were carried out using 37 propeller passes per signal repeat period of 592 milliseconds[18]. This corresponds to 1875 rpm for a two-bladed propeller. The propeller modulation repetition frequency was locked to the signal frequency and the phase was adjusted for a maximum number of signal eclipses. As a result, 8 DOWN scans and 3 UP scans were fully attenuated and 1 DOWN scan was partially attenuated during the 24 DOWN-UP scans of one elevation frame. The same propeller frequency with a different phase adjustment resulted in 4 fully (almost) eclipsed TO scans and 1 fully eclipsed FRO pulse during an azimuth frame of 8 TO-FRO scans.

Some tests were run with the propeller modulation unlocked and offset from the worst case condition to provide an indication of average propeller modulation effects. The offset frequency corresponded to about 1850 rpm with a two-bladed propeller.

A.1 Propeller Modulation Effects at Low Signal Levels*

Propeller modulation tests were run at high (-60 dBm) signal levels with very little effect. Eclipsing by as much as 12 dB caused a slight increase

*All of the low signal level tests were run on the Phase 2 1/2 receiver.

in noise but the standard deviation of the filtered data remained about 0.003°.

At low signal levels, the propeller modulation can cause additional errors and missed scans. Figures A-1 and A-2 illustrate the increased angle errors and missed scans for an azimuth test with synchronized worst case modulation. Propeller modulation is seen to result in only minor increases in angle error but it does cause earlier drop out (system flag) with low signal level. In the average case, however, shown in Figure A-2, the actual signal level required for acquisition is only 1 to 2 dB greater for normal propeller modulation levels of 4 to 8 dB.

The elevation case is illustrated in Figures A-3 and A-4. The angle errors in this case are not greatly different than the case with no propeller modulation so separate curves were not drawn for these cases. The number of missed scans was nearly constant over a range of signal levels as indicated by the plateau on the plot of missed scans. Here, each signal eclipse results in a missed scan, the previous data is held and the error is minimized. Elevation differs from azimuth because of the much higher probability that both scans in a frame are eclipsed. Elevation tests were carried out at 3° or about 700 microseconds beam separation while azimuth tests were at 0° or about 6600 microseconds separation. The angle filter at 10 radians/second cutoff is also more effective for elevation because of the higher data rate. Even for the worst case (modulation synchronized) the propeller modulation had an insignificant effect on acquisition range.

Propeller modulation can also affect the DPSK signal. The results of a test are shown in Figure A-5. The system flag point is little changed because this test was carried out at the elevation data rate where there are insufficient eclipses to actually cause dropout (plateau in Figure A-4).

A.2 Effects of Propeller Modulation in Multipath

During final approach, the direct MLS signal to the aircraft will always be eclipsed if the airborne antenna is on the centerline behind the propeller and the propeller modulation occurs simultaneously with the signal. Multipath from hangars will arrive from angles farther from the flight path and

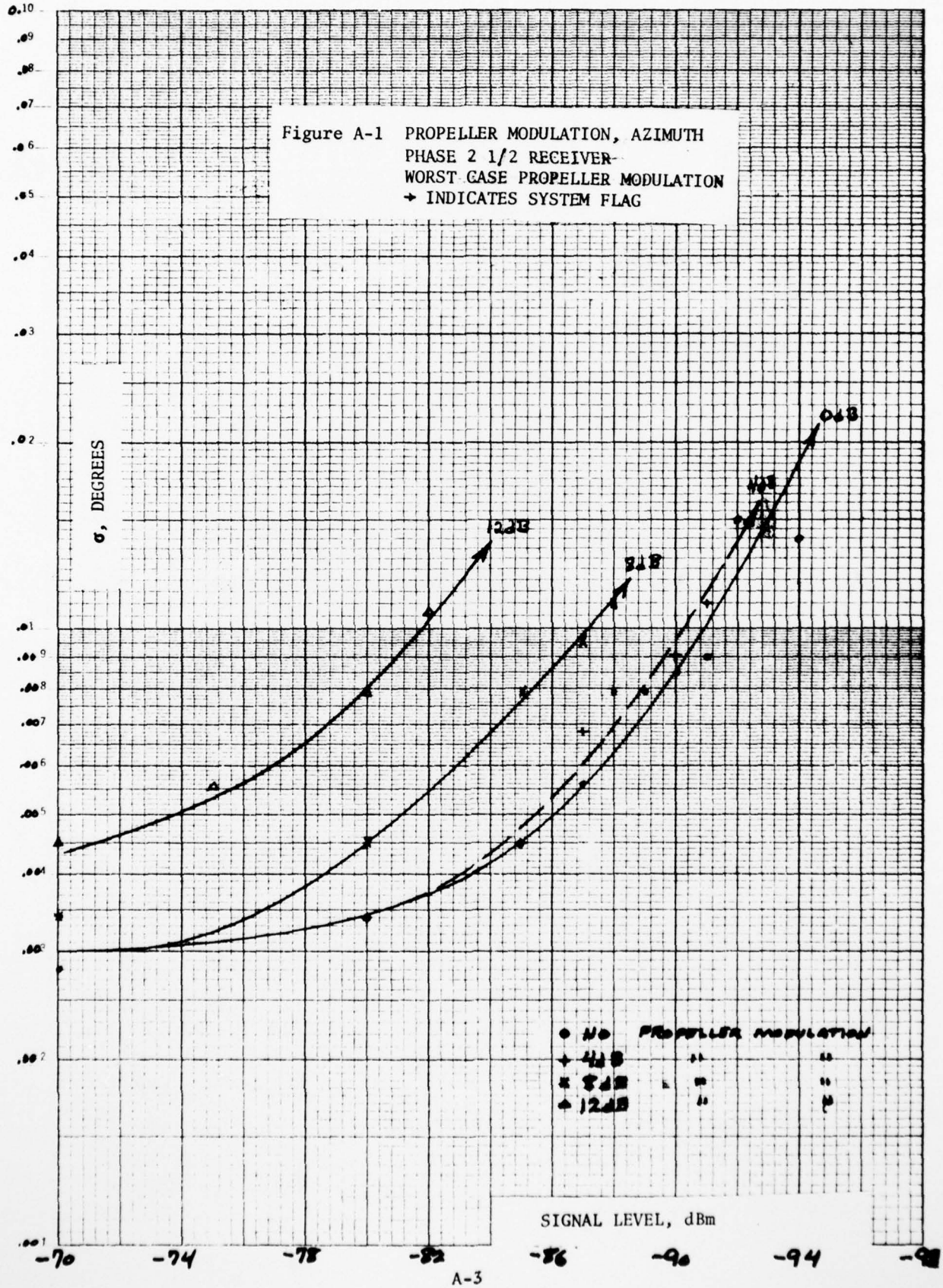

Figure A-1 PROPELLER MODULATION, AZIMUTH
PHASE 2 1/2 RECEIVER-
WORST CASE PROPELLER MODULATION
→ INDICATES SYSTEM FLAG

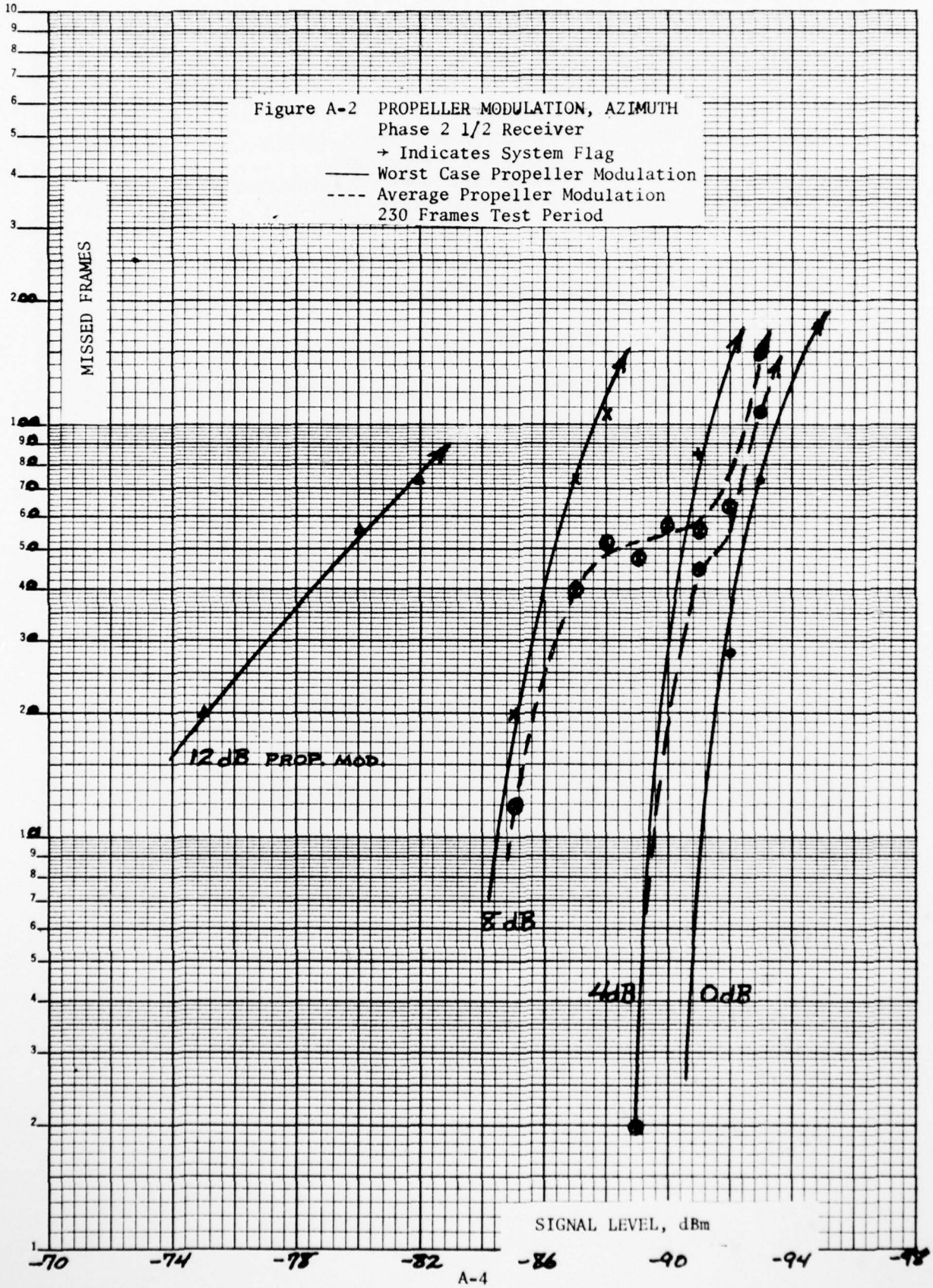

Figure A-2 PROPELLER MODULATION, AZIMUTH
Phase 2 1/2 Receiver
→ Indicates System Flag
—— Worst Case Propeller Modulation
---- Average Propeller Modulation
230 Frames Test Period

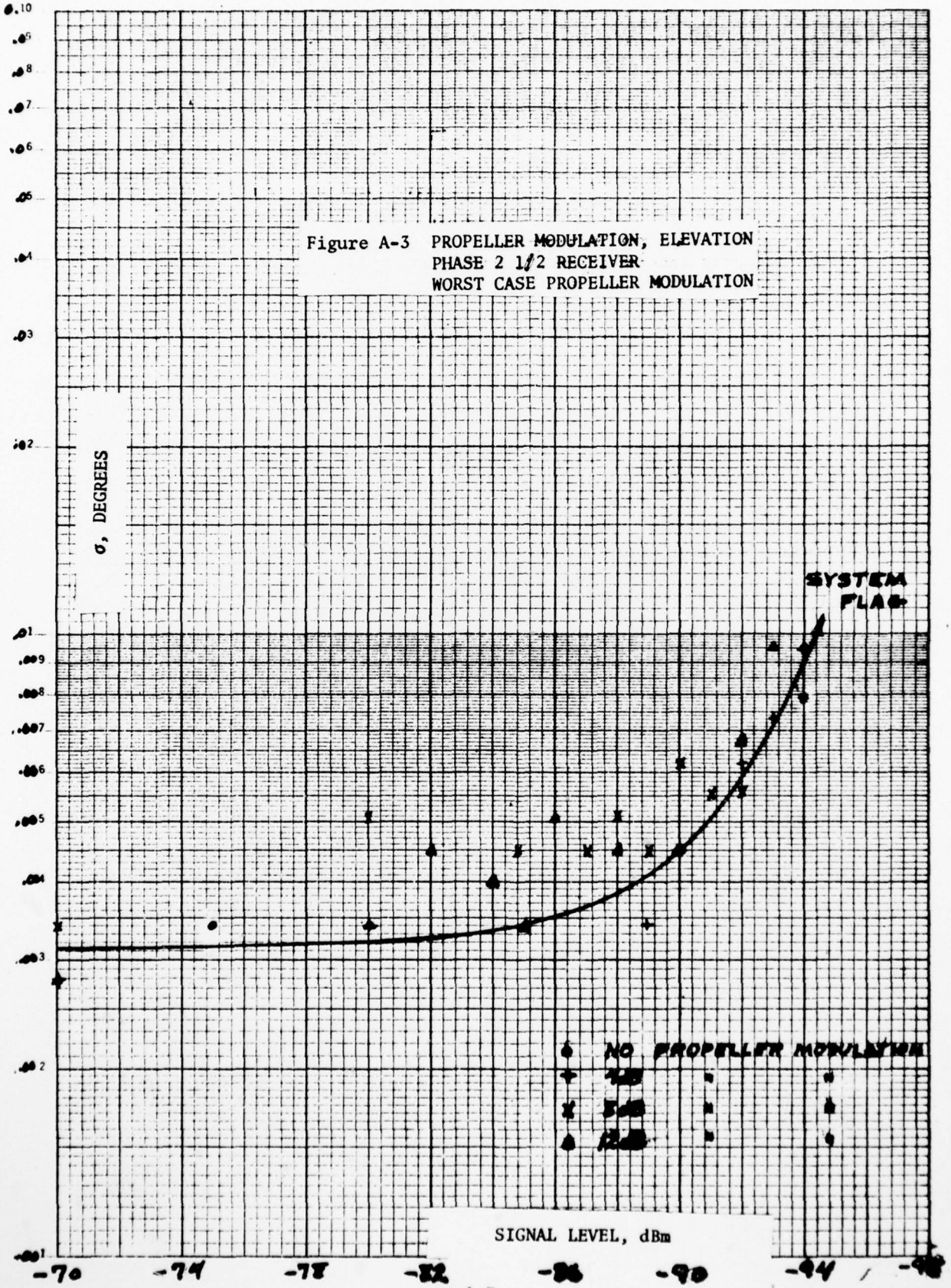

Figure A-3 PROPELLER MODULATION, ELEVATION
PHASE 2 1/2 RECEIVER
WORST CASE PROPELLER MODULATION

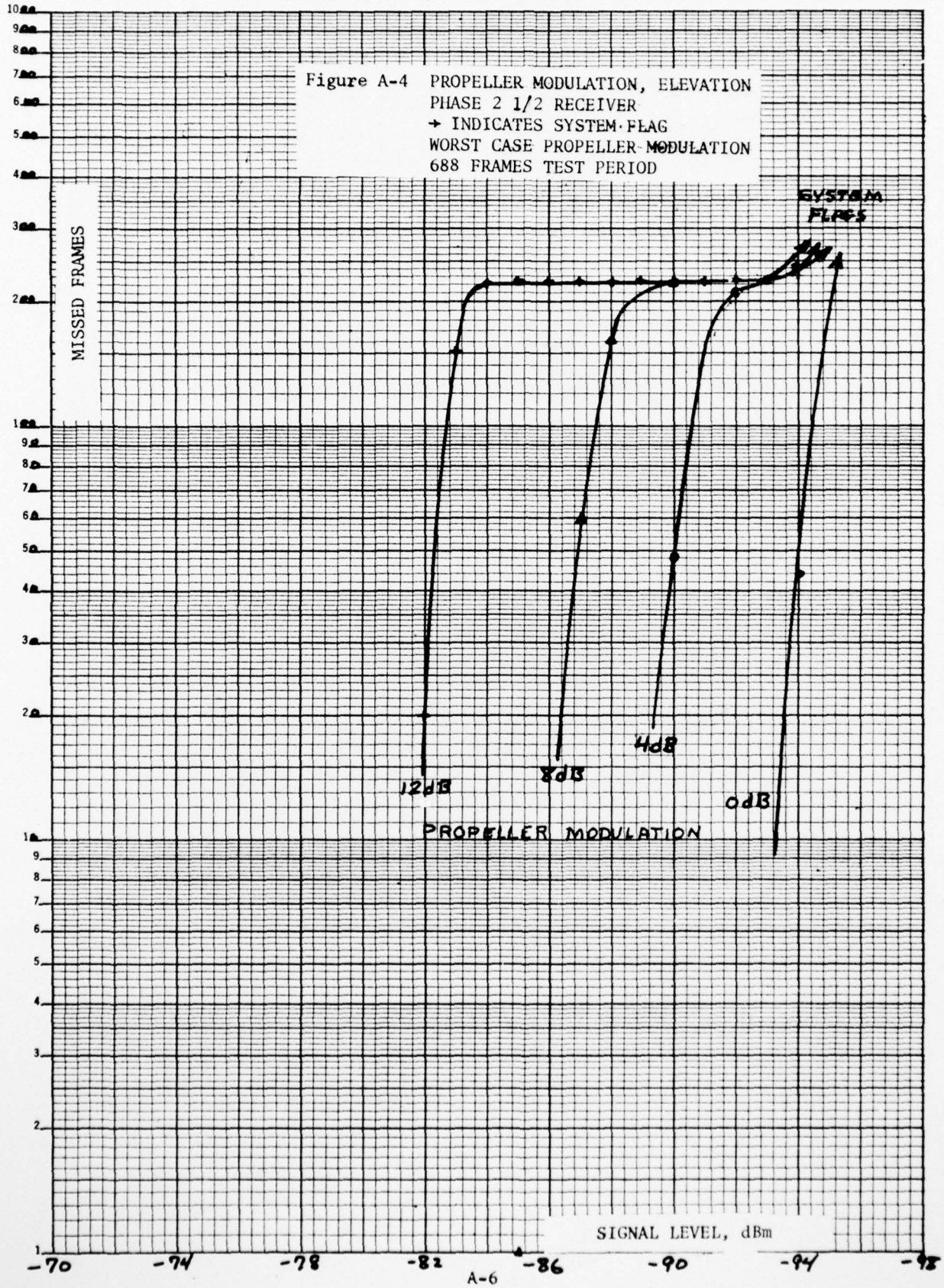
Figure A-4 PROPELLER MODULATION, ELEVATION
PHASE 2 1/2 RECEIVER
→ INDICATES SYSTEM FLAG
WORST CASE PROPELLER MODULATION
688 FRAMES TEST PERIOD
MISSED FRAMES
SYSTEM FLAGS
12dB
8dB
4dB
0dB
PROPELLER MODULATION
SIGNAL LEVEL, dBm
-70
-74
-78
-82
-86
-90
-94
-98

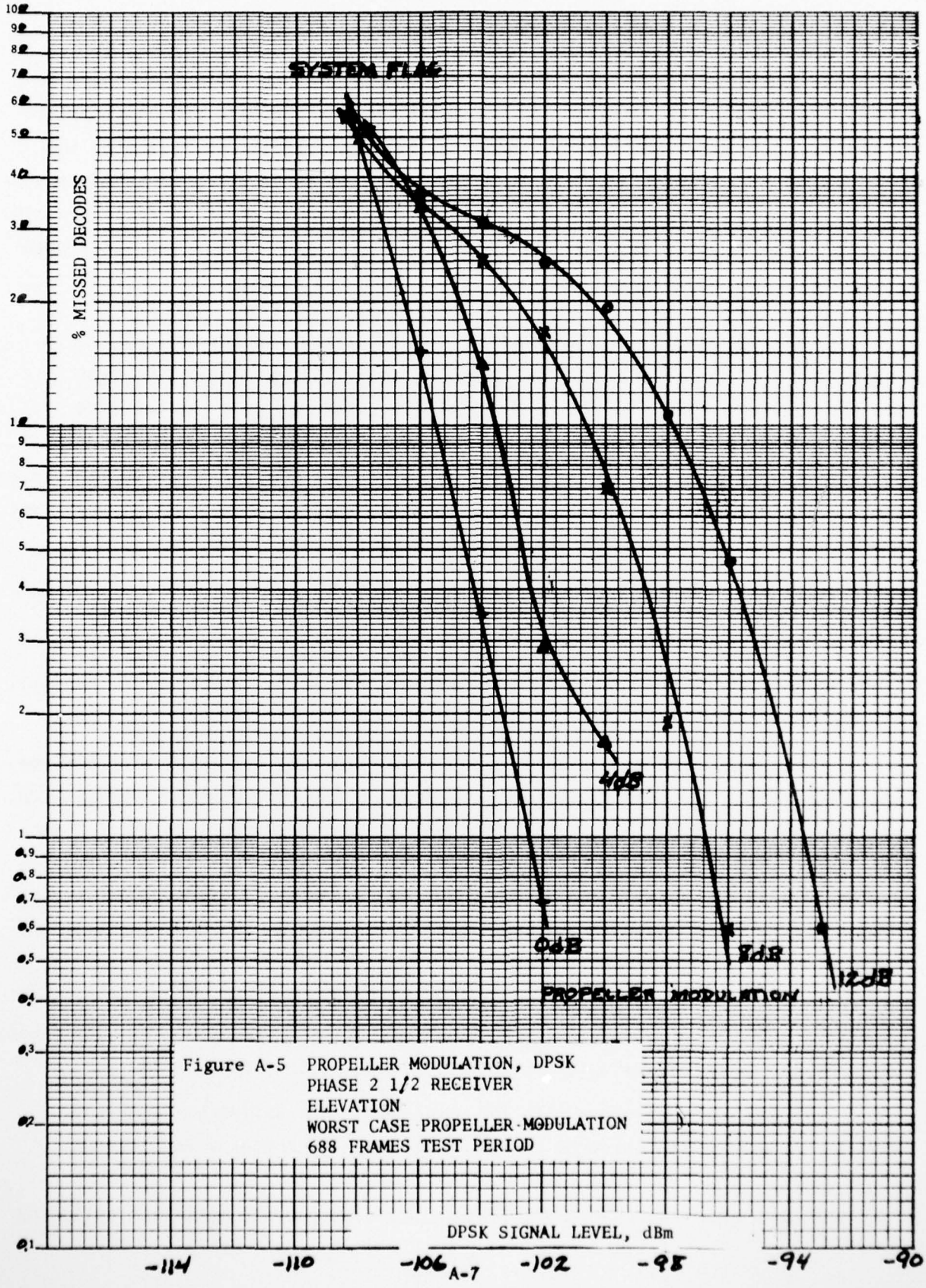

Figure A-5 PROPELLER MODULATION, DPSK
PHASE 2 1/2 RECEIVER
ELEVATION
WORST CASE PROPELLER MODULATION
688 FRAMES TEST PERIOD

may or may not be eclipsed, depending on the geometry of the situation. If the geometry does allow the multipath beam to pass through the disc of the propeller, the eclipsing of this path will be separated in time from the eclipsing of the direct signal. Multipath that is not eclipsed at all or is eclipsed separately from the direct beam results in the largest errors because it is at full strength when the direct beam is reduced. Therefore, the propeller modulation tests were run with only the direct beam eclipsed as a worst case condition.*

The multipath scenarios used in the first test series are; A2, a hangar 1200 feet from the runway and parallel to it, B1, a hangar 1000 feet from the runway and rotated 12° to bring the interference into the decision region, and B3, a hangar 850 feet from the runway similar to a hangar at JFK 13L. The hangars were on the same side of the runway as the elevation transmitter in each case. A fixed multipath level of -6 dB was used (antenna pattern shaping was not considered in these scenarios). These scenarios are more fully described in Calspan TN-4.

Subsequent tests were run with the AWOP B-2 scenario described in Figure 4-56. These were run with the breadboard processor operating in the dwell gate and SEP modes.

The multipath scenario tests were run with varying depths of propeller modulation added. As shown in Figures A-6 through A-8, the errors increase with propeller modulation but not drastically for typical modulation depths of 4 to 6 dB. Note that these tests were run with worst case eclipsing as described previously. At the greater depths of eclipsing, the Phase 2 1/2 receiver shows a reduction in the standard deviation of error as compared to the breadboard receiver. This is apparently the effect of the rate limiter incorporated into the Phase 2 1/2 receiver. The tests with the AWOP B-2 scenario shown in Figure A-9 were run for both average and worst case propeller modulation. No significant change in the errors occur until the depth of modulation exceeds 8 dB.

A few tests were run with the propeller phase varied but with the propeller frequency still locked to the 37th harmonic of the overall format

---

*TN-4 contains more complete test results, including partial multipath eclipsing.

Figure A-6 SCENARIO A-2 WITH PROPELLER MODULATION
PARALLEL HANGAR ELEVATION
-6 dB MULTIPATH
WORST CASE PROPELLER MODULATION
60 dBm SIGNAL LEVEL

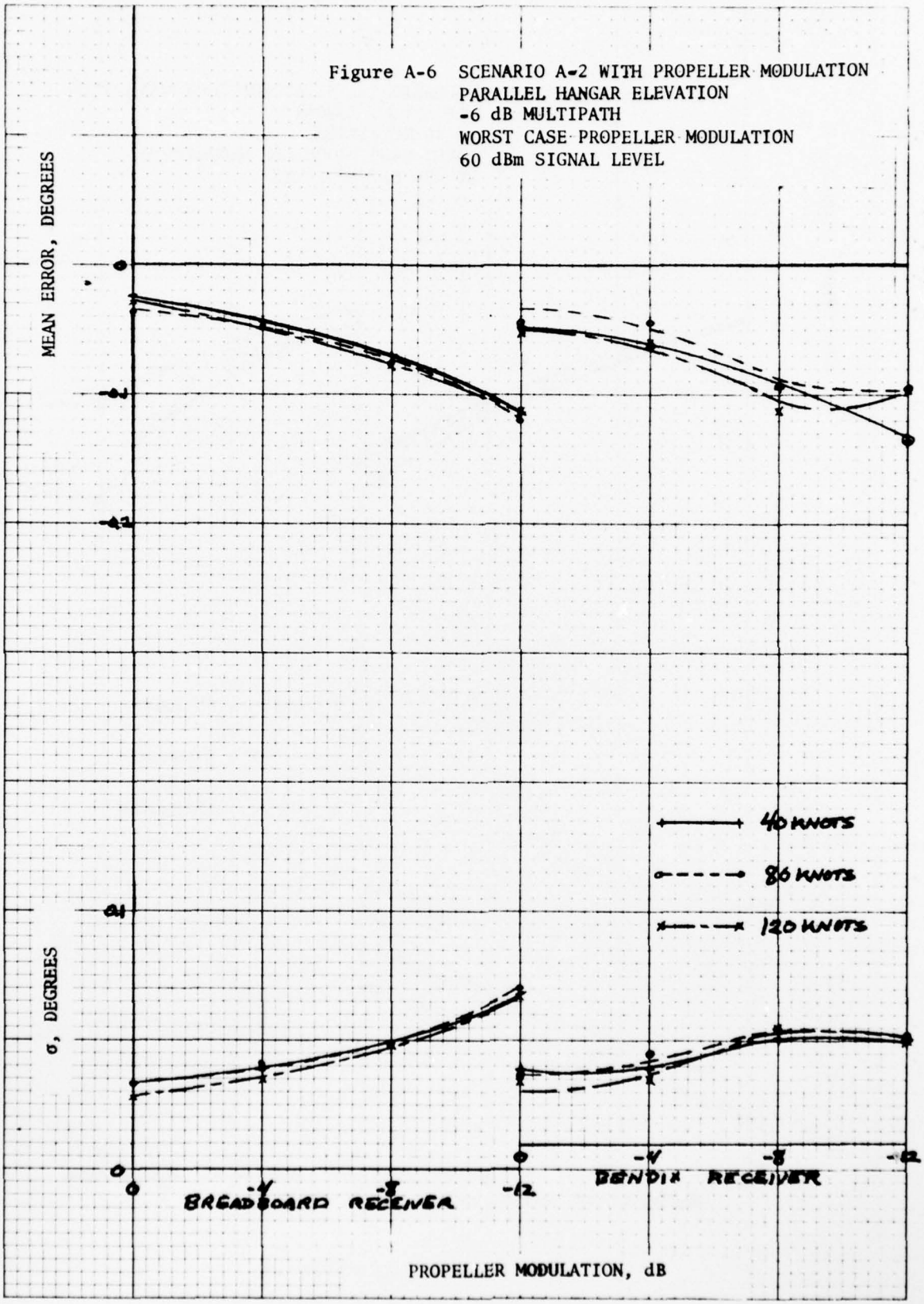

Figure A-7 SCENARIO B-1 WITH PROPELLER MODULATION
ELEVATION, HANGAR
-6 dB MULTIPATH
WORST CASE PROPELLER MODULATION
60 dBm SIGNAL LEVEL

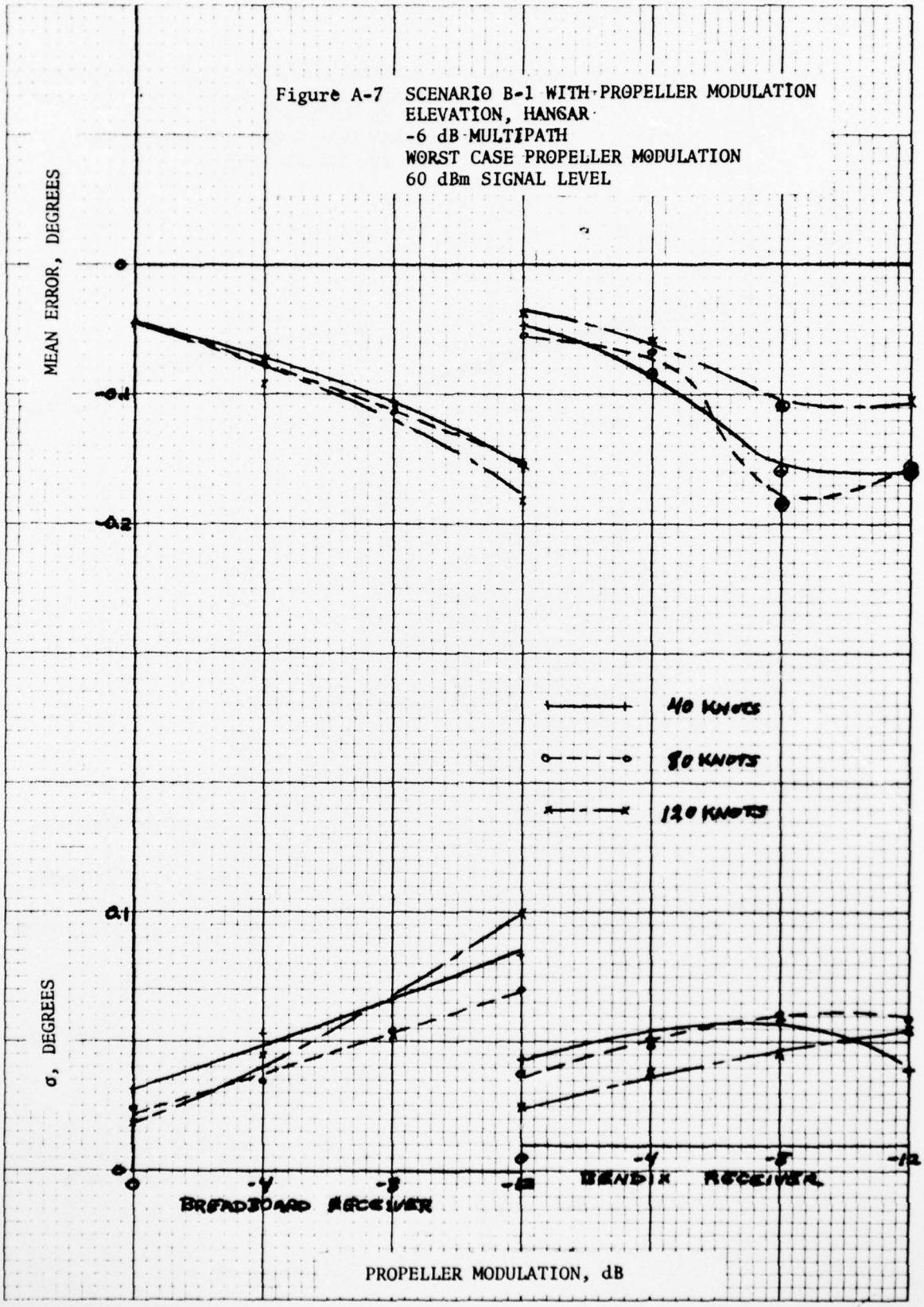

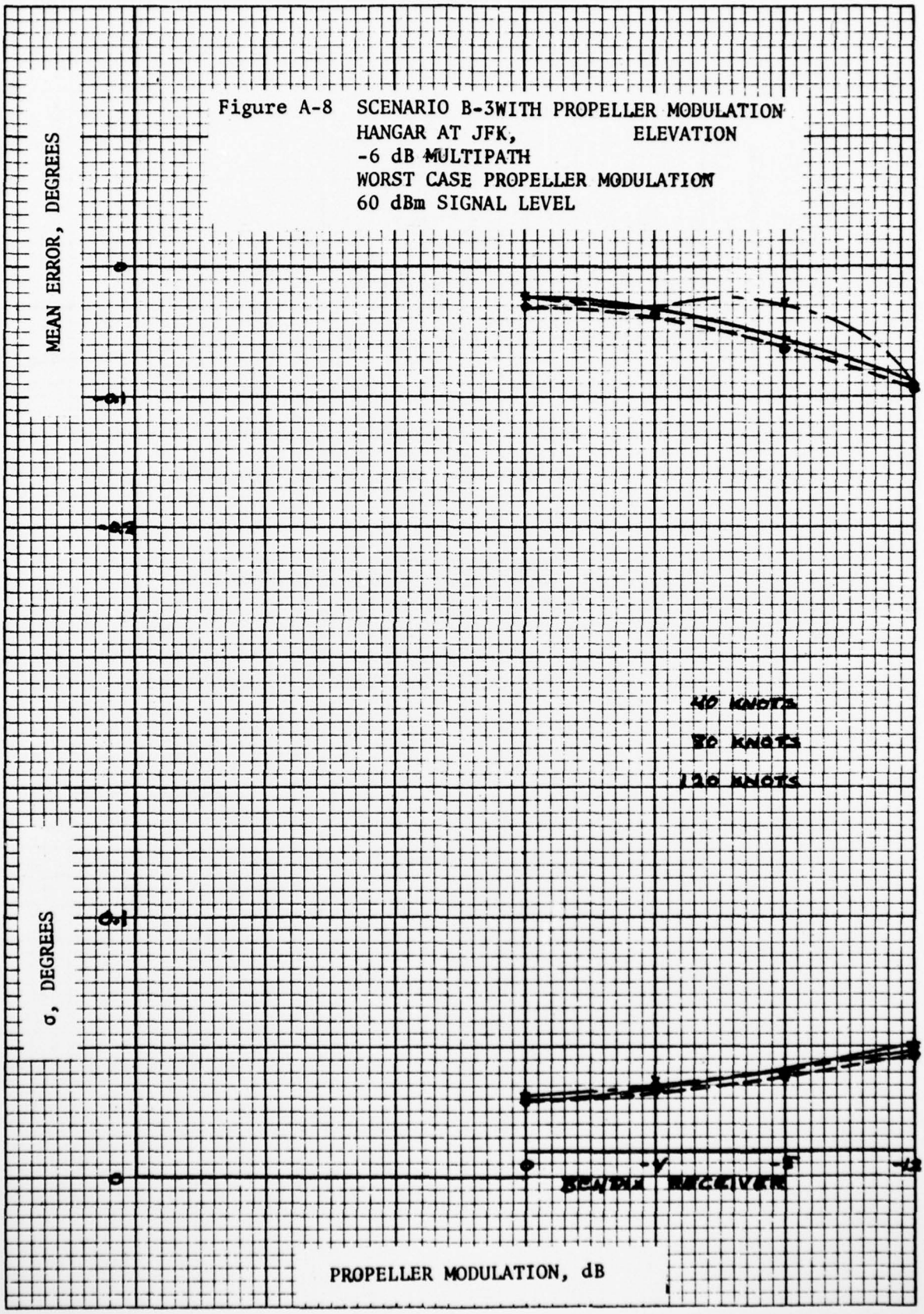

Figure A-8 SCENARIO B-3WITH PROPELLER MODULATION
HANGAR AT JFK, ELEVATION
-6 dB MULTIPATH
WORST CASE PROPELLER MODULATION
60 dBm SIGNAL LEVEL

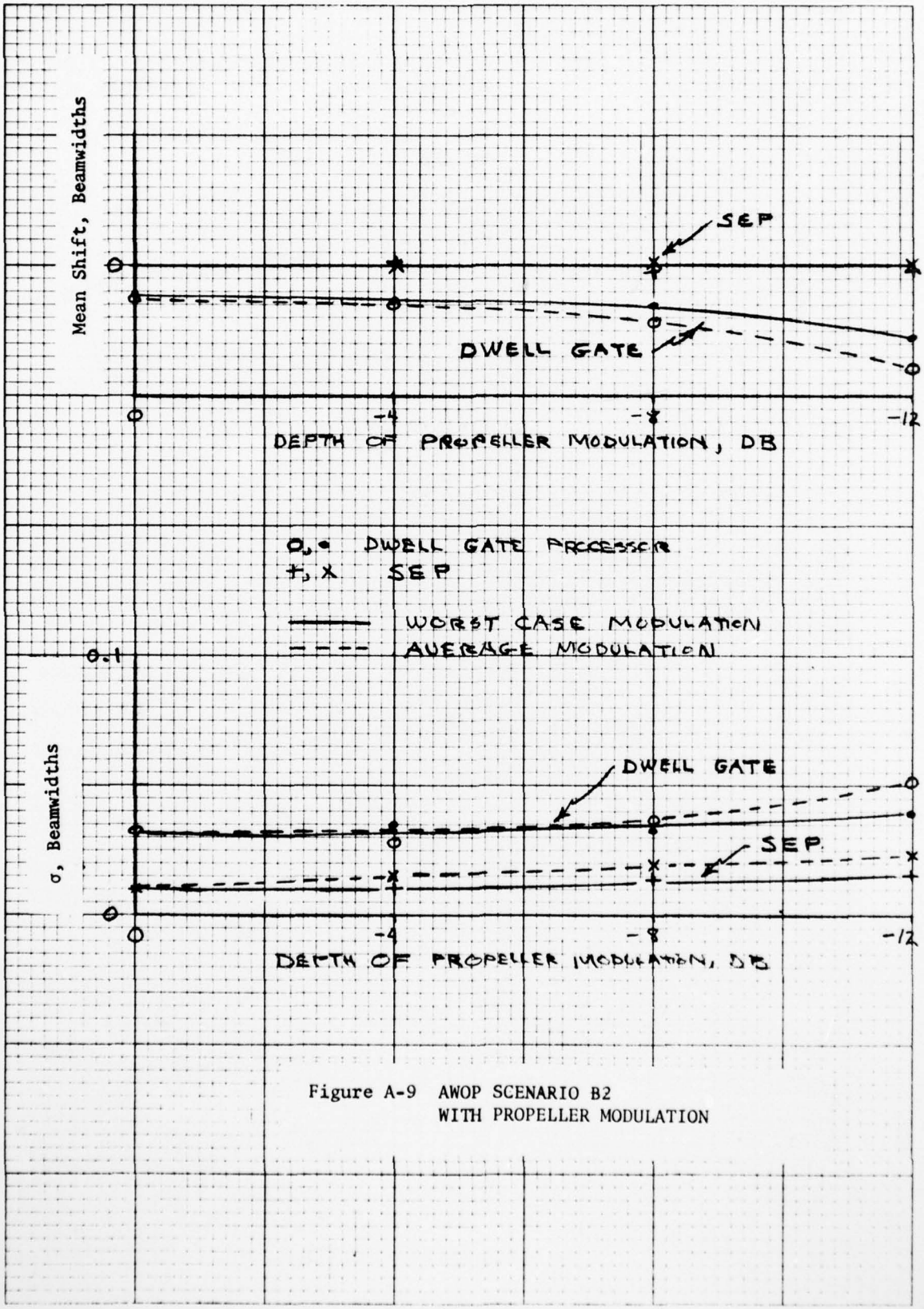

Figure A-9 AWOP SCENARIO B2
WITH PROPELLER MODULATION

repetition frequency (0.592 second period). The results appear in Figure A-10. Also appearing on this plot are averages of several tests taken with a free running frequency for random phase results. The random phase tests were taken with the propeller modulation free running at nearly 1 Hz (25 rpm) lower frequency than the worst case 37th harmonic. Even for the average case, it is seen that, in the presence of multipath, propeller modulation causes a significant error increase when the multipath separation angle approaches one beamwidth as occurs in scenario B-1.

The one case where direct and multipath eclipsing are virtually simultaneous is for ground reflections in azimuth. This case is illustrated in Figures A-11 and A-12 for scenario E-1 (5° transverse ground slope). The additional error attributable to propeller modulation is quite small in this case.

Figure A-10 SCENARIO B-1 WITH PROPELLER MODULATION
VARIABLE PROPELLER PHASE
ELEVATION, HANGAR
BREADBOARD RECEIVER
-6 dB MULTIPATH
80 KNOTS APPROACH SPEED
WORST CASE PROPELLER FREQUENCY

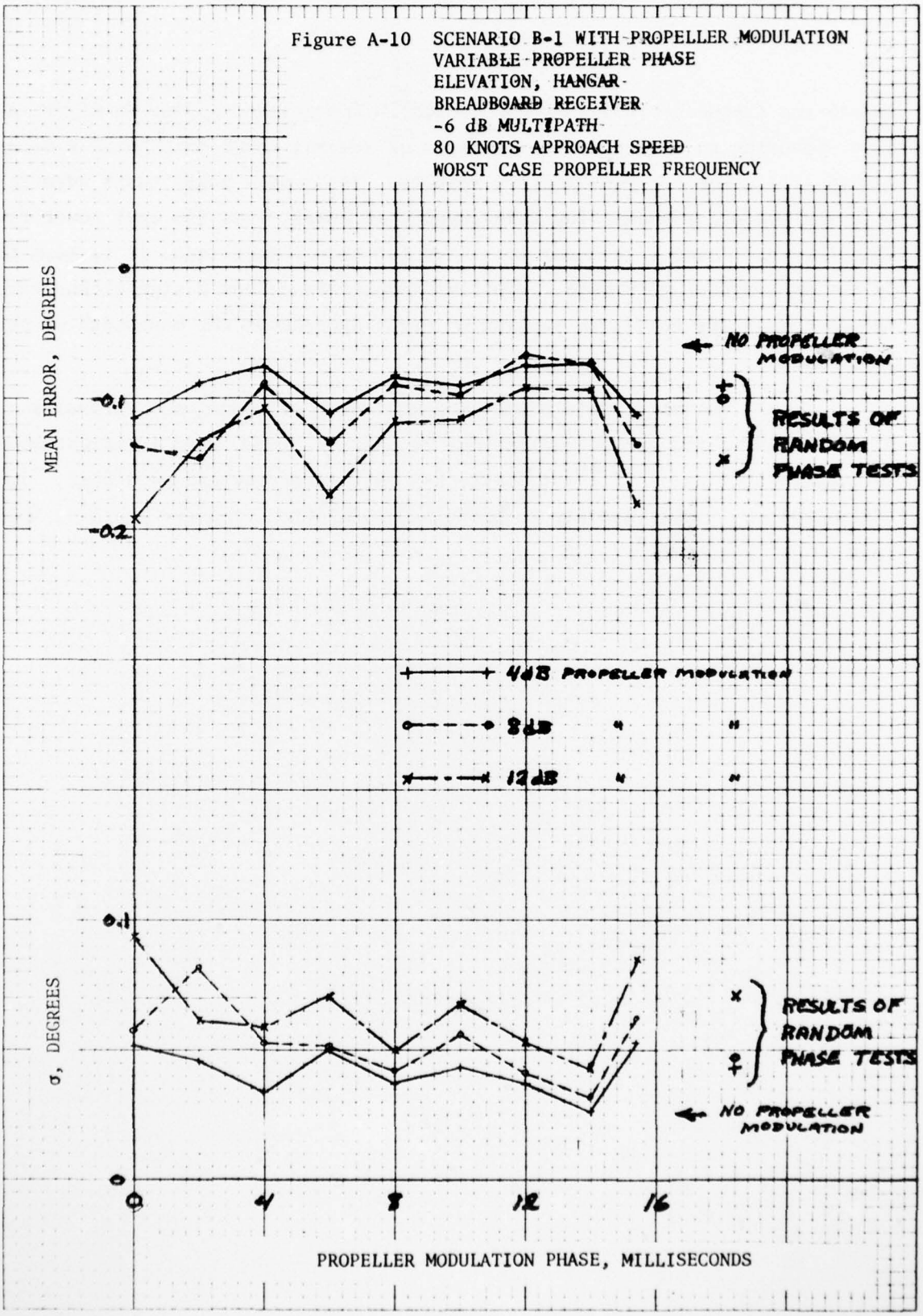

Figure A-11 SCENARIO E-1 WITH PROPELLER MODULATION
AZIMUTH, SURFACE
BREADBOARD RECEIVER
120 KNOTS

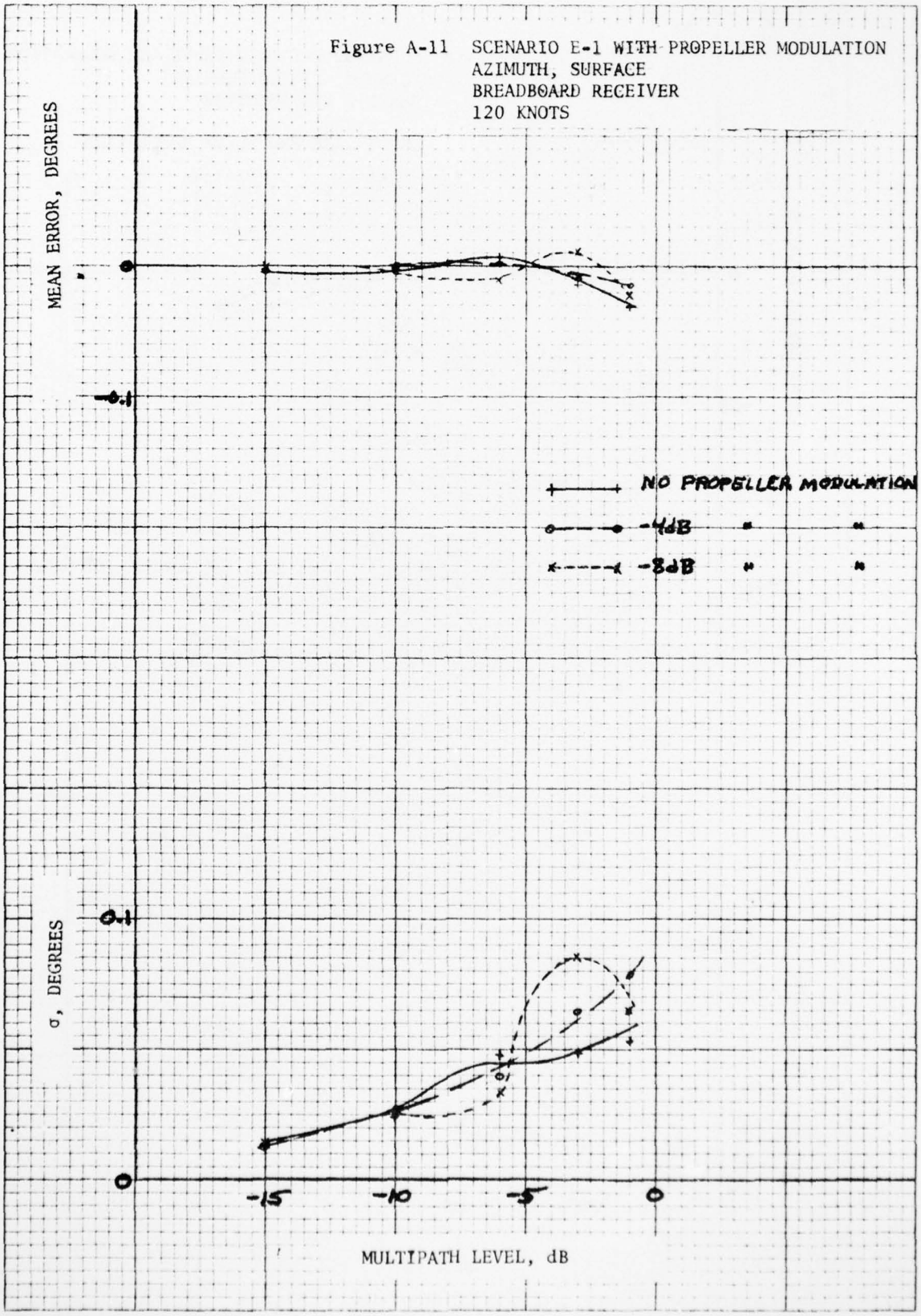

AD-A041 891 CALSPAN CORP BUFFALO N Y F/G 17/7
MULTIPATH AND PERFORMANCE TESTS OF TRSB RECEIVERS.(U)
MAR 77 J BENEKE, C W WIGHTMAN, C B VALLONE DOT-FA74WA-3445
UNCLASSIFIED CALSPAN-AG-5580-E-1 FAA-RD-77-66 NL

3 OF 3
ADA041891

END

DATE
FILMED
8 - 77

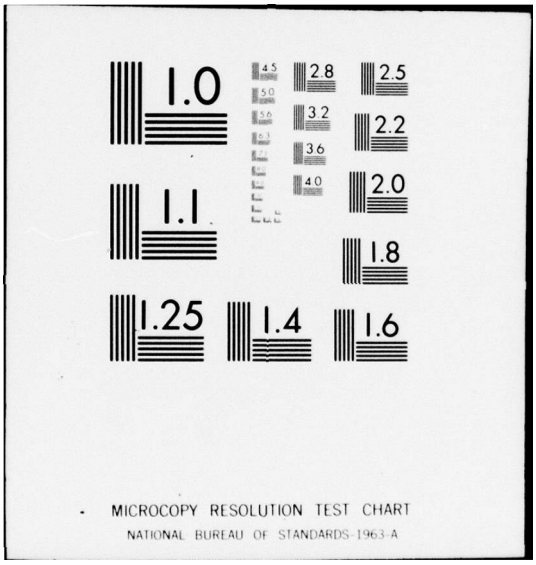
1.0
1.1
1.25
1.4
1.6
1.8
2.0
2.2
2.5
2.8
3.2
3.6
4.0
4.5
5.0
5.6
MICROCOPY RESOLUTION TEST CHART
NATIONAL BUREAU OF STANDARDS-1963-A

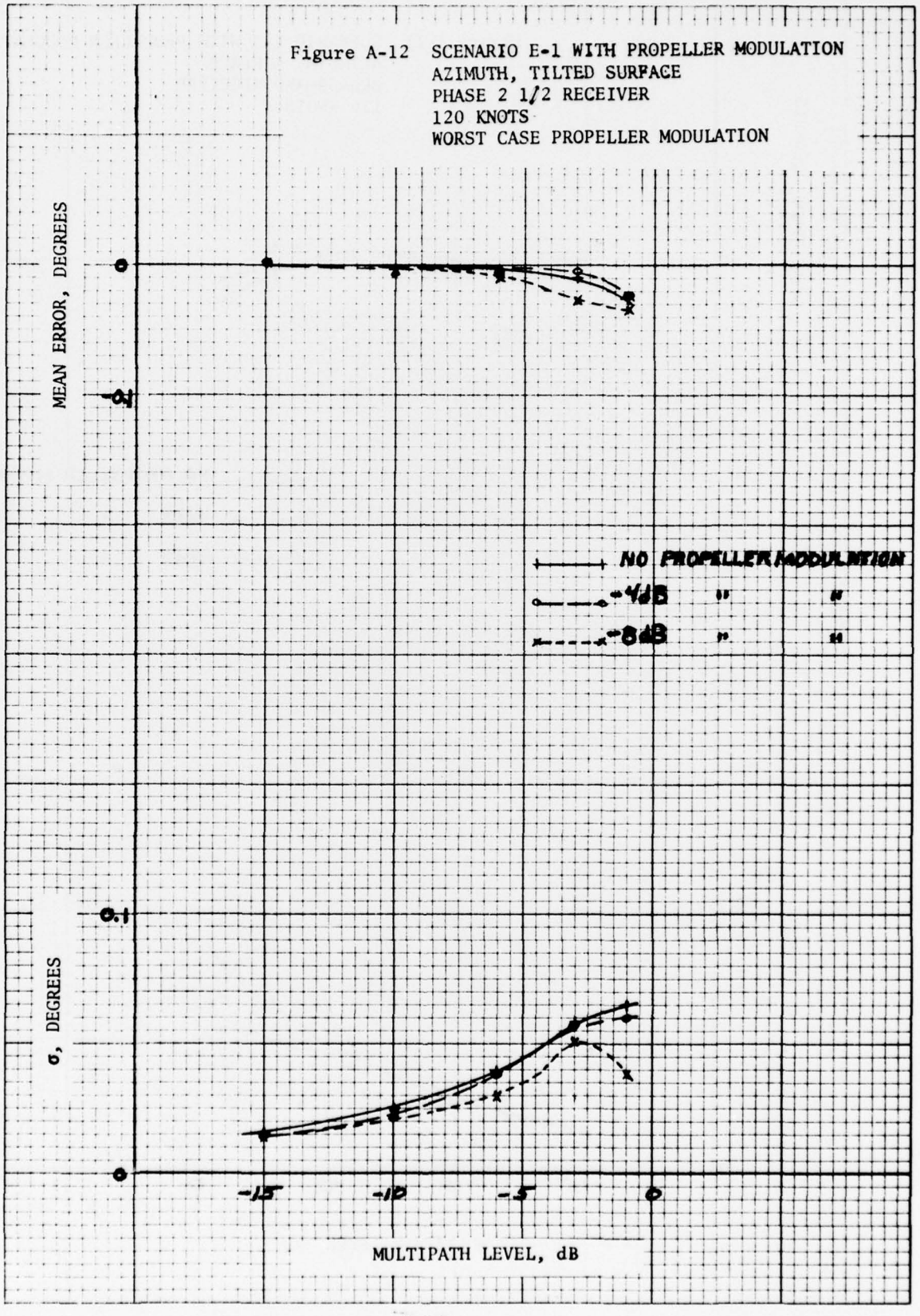

Figure A-12 SCENARIO E-1 WITH PROPELLER MODULATION
AZIMUTH, TILTED SURFACE
PHASE 2 1/2 RECEIVER
120 KNOTS
WORST CASE PROPELLER MODULATION

Appendix B
WEATHER RADAR AND CW INTERFERENCE TESTS

Both pulse and CW interference tests have been run on the TRSB receivers. The pulse tests have simulated the interference effects in the MLS band of the C-band weather radars. A limited number of tests were conducted with CW interference that are representative of possible AEROSAT interference and any unauthorized spurious emissions in the MLS band.

B.1 Weather Radar Interference Tests

Pulse interference tests were run on the TRSB processors to measure the sensitivity of the processing techniques to interference from weather radars. An MLS antenna located in a radome adjacent to a C-band weather radar will be subject to some level of interference from the radar transmissions.

Two unsychronized pulse trains were used in these tests to simulate the interference level in the MLS band from the weather radars.

2 microseconds, 400 PPS pulses typical of the AVQ-10 and RDR-1C radars
6 microseconds, 200 PPS pulses typical of the AVQ-30 radar

The C-band pulses, at the MLS frequency were added to the receiver inputs and varied in level relative to the DPSK or scanning beam signals. The proportion of missed scans (for the DPSK) and frame flags (for angle data) in a ten second period were recorded as a measure of the interference effect. Since the receivers hold the previous output when a missed scan or frame flag occurs, there was very little increase in angle noise even at the point of angle drop out (50% missed data). Several DPSK and angle signal levels were used as well as with no DPSK signals.

Four different processors were used in these tests. These were the Phase 3 receiver P101, Phase 2 1/2 receiver E103, Phase 2 1/2 breadboard receiver and the single edge processor (SEP) breadboard. The main differences in the interference rejection of receivers P101 and E 103 for these tests were the narrow adaptive tracking gates in the P101 receiver instead of the wide

(about 250 microseconds) tracking gates of receiver E103. Both receivers have 12 microsecond pulse slicers designed to eliminate the first 12 microseconds of rapidly rising signals as protection against pulse interference. These receivers also shave the leading edge of the dwell gates by 12 microseconds for receiver P101 and 20 microseconds for receiver E103. The processing logic in the breadboard processor was similar to receiver E103 except it has no pulse slicer or confidence counter for out-of-beam multipath. The single edge processor used the tracking gates of the breadboard processor.

In interpreting the results of these tests it should be noted that C-band radars typically rotate 360° every 4 seconds. The transmitter is emitting pulses only while the antenna is pointing within ±120 degrees of the aircraft heading. Thus, the interference can occur only 2 2/3 seconds out of every 4 second period. The TRSB antenna is located in the near field of the radar antenna and will receive interfering pulses that are amplitude modulated as the radar dish rotates.

Interference level tests at NAFEC* with the RDR-1C radar show two peak lobes with several sidelobes that are down 5 to 10 dB during the time the radar is radiating. The test data showed the duration of the peak lobes were less than 0.4 seconds with a peak interference level of about -70 dBm at a frequency of 5189 MHz (Phase 2 1/2 receiver). The simulated interference tests were run with a continuous, constant amplitude pulse train and indicate the effects at the peak interference levels. The short duration of the main interference lobes must be considered in evaluating these simulation test results.

B.1.1 Phase 3 Receiver Tests

The results of these tests are shown in Figures B-1 to B-5. Figures B-1 and B-2 show the percentage of missed data plotted versus the level of pulse interference in dBm for the 2 microsecond, 400 PPS pulses and 6 microsecond, 200 pps pulses. Several levels of DPSK and angle signals have been used. Both azimuth and elevation tests were run at a level of -95 dBm for DPSK and -85 dBm

*NAFEC Weather Radar Interference Test Report.

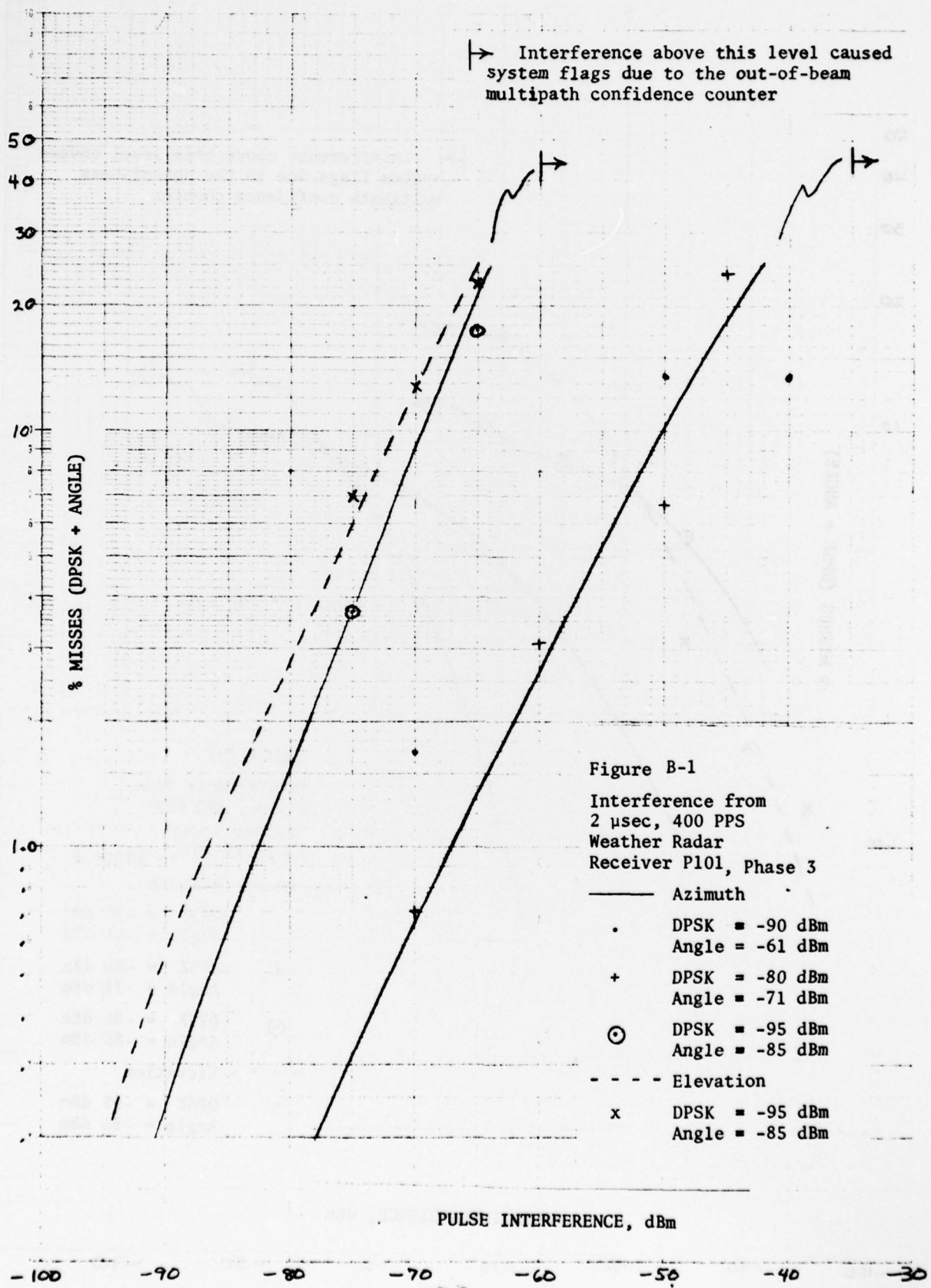

Figure B-1

Interference from
2 μsec, 400 PPS
Weather Radar
Receiver P101, Phase 3

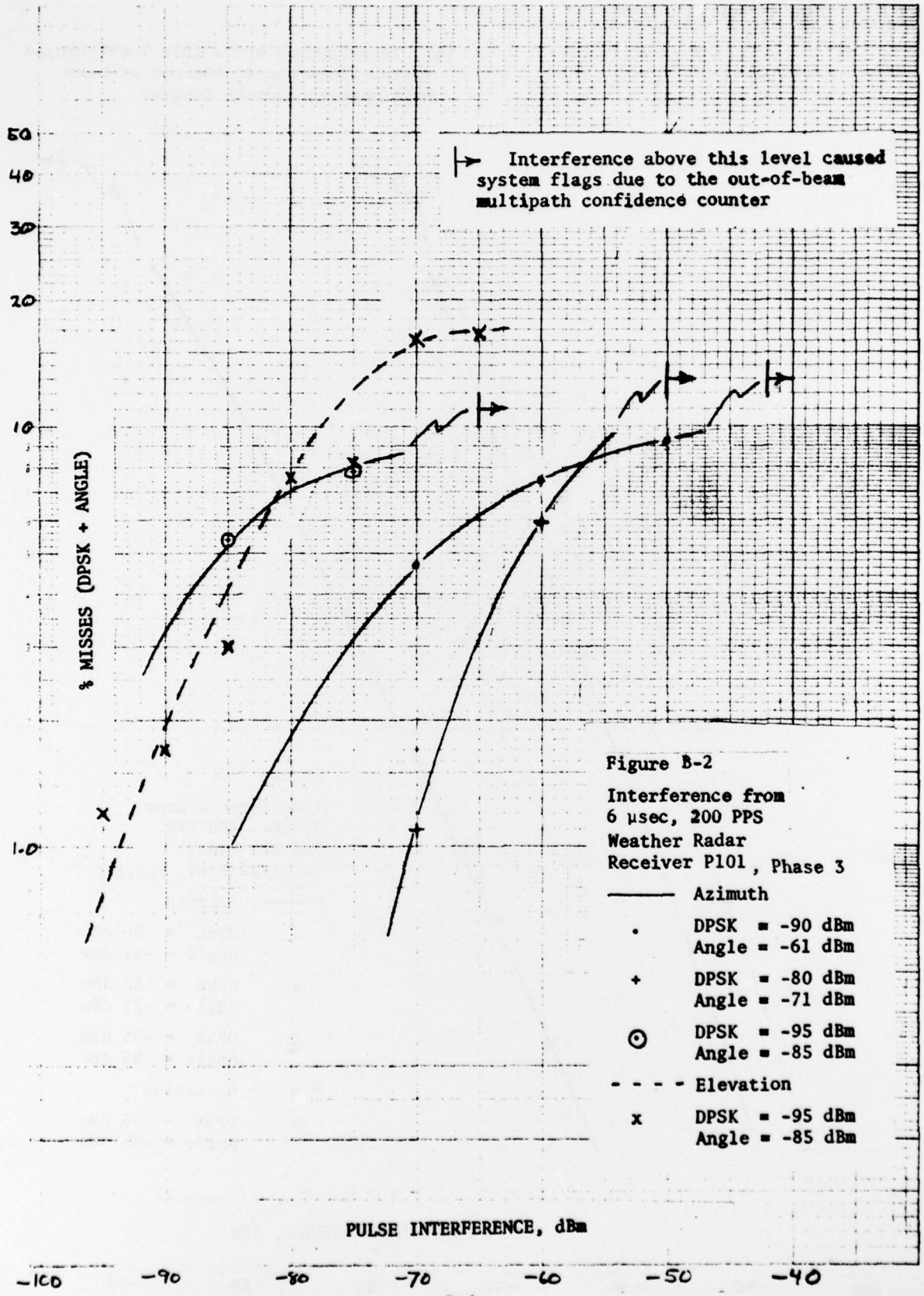
Interference above this level caused system flags due to the out-of-beam multipath confidence counter
% MISSES (DPSK + ANGLE)
50
40
30
20
10
1.0
PULSE INTERFERENCE, dBm
-100
-90
-80
-70
-60
-50
-40
Figure B-2
Interference from 6 μsec, 200 PPS Weather Radar Receiver P101, Phase 3
Azimuth
DPSK = -90 dBm
Angle = -61 dBm
DPSK = -80 dBm
Angle = -71 dBm
DPSK = -95 dBm
Angle = -85 dBm
Elevation
DPSK = -95 dBm
Angle = -85 dBm

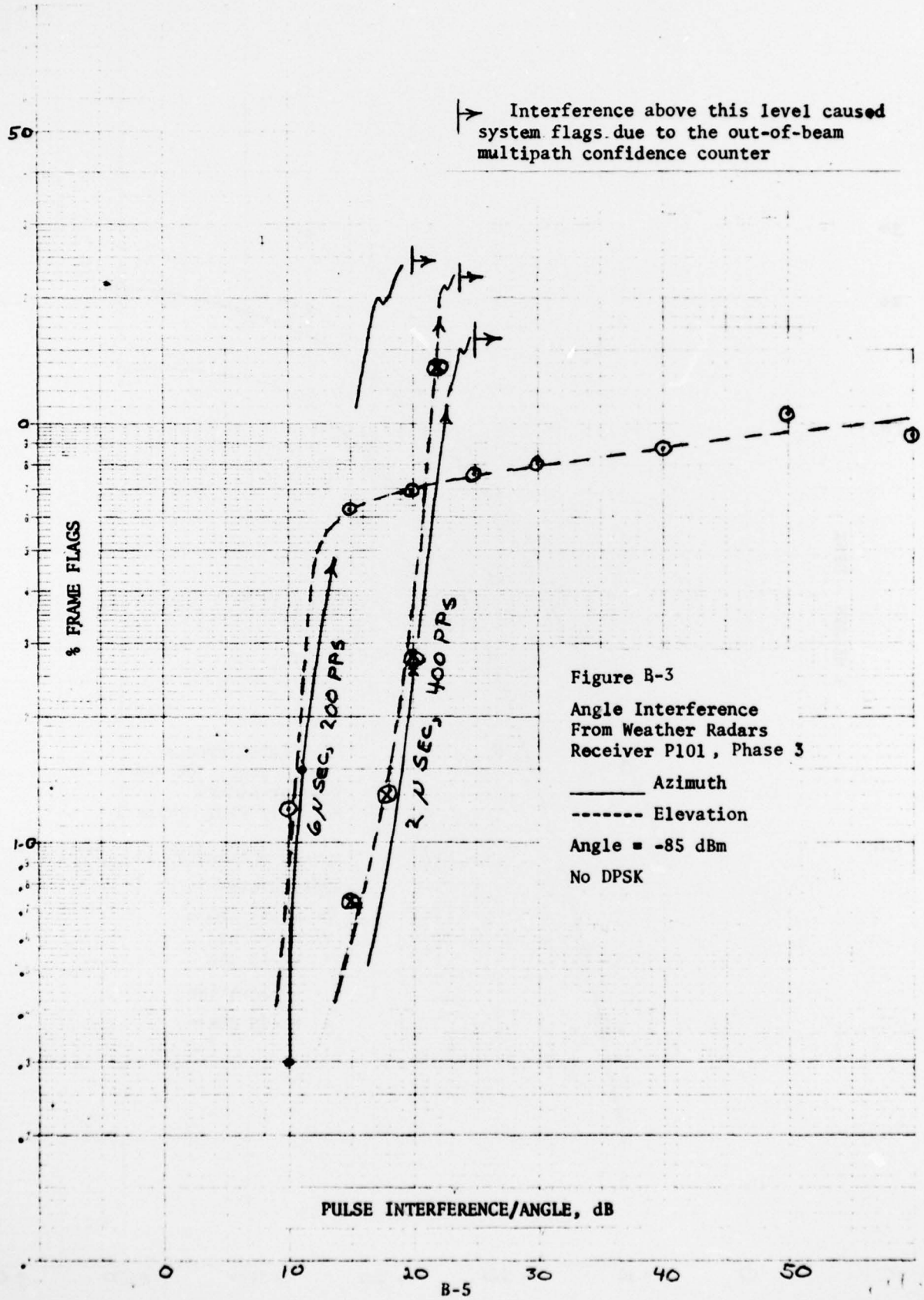

Figure B-3

Angle Interference
From Weather Radars
Receiver P101, Phase 3

_____ Azimuth

------- Elevation

Angle = -85 dBm

No DPSK

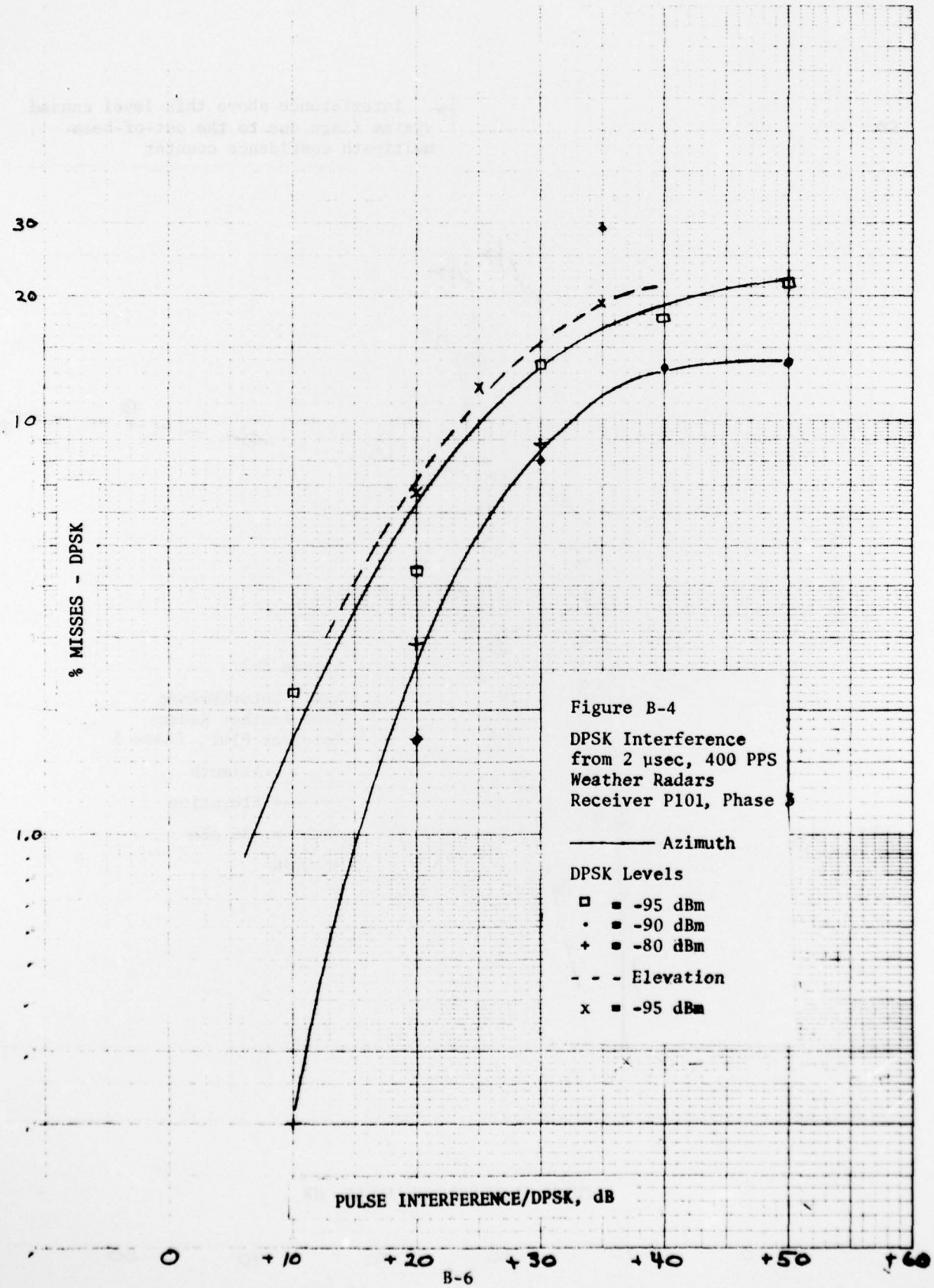
30
20
10
1.0
% MISSES - DPSK
0
+10
+20
+30
+40
+50
+60
PULSE INTERFERENCE/DPSK, dB
Figure B-4
DPSK Interference
from 2 µsec, 400 PPS
Weather Radars
Receiver P101, Phase
Azimuth
DPSK Levels
-95 dBm
-90 dBm
-80 dBm
Elevation
-95 dBm

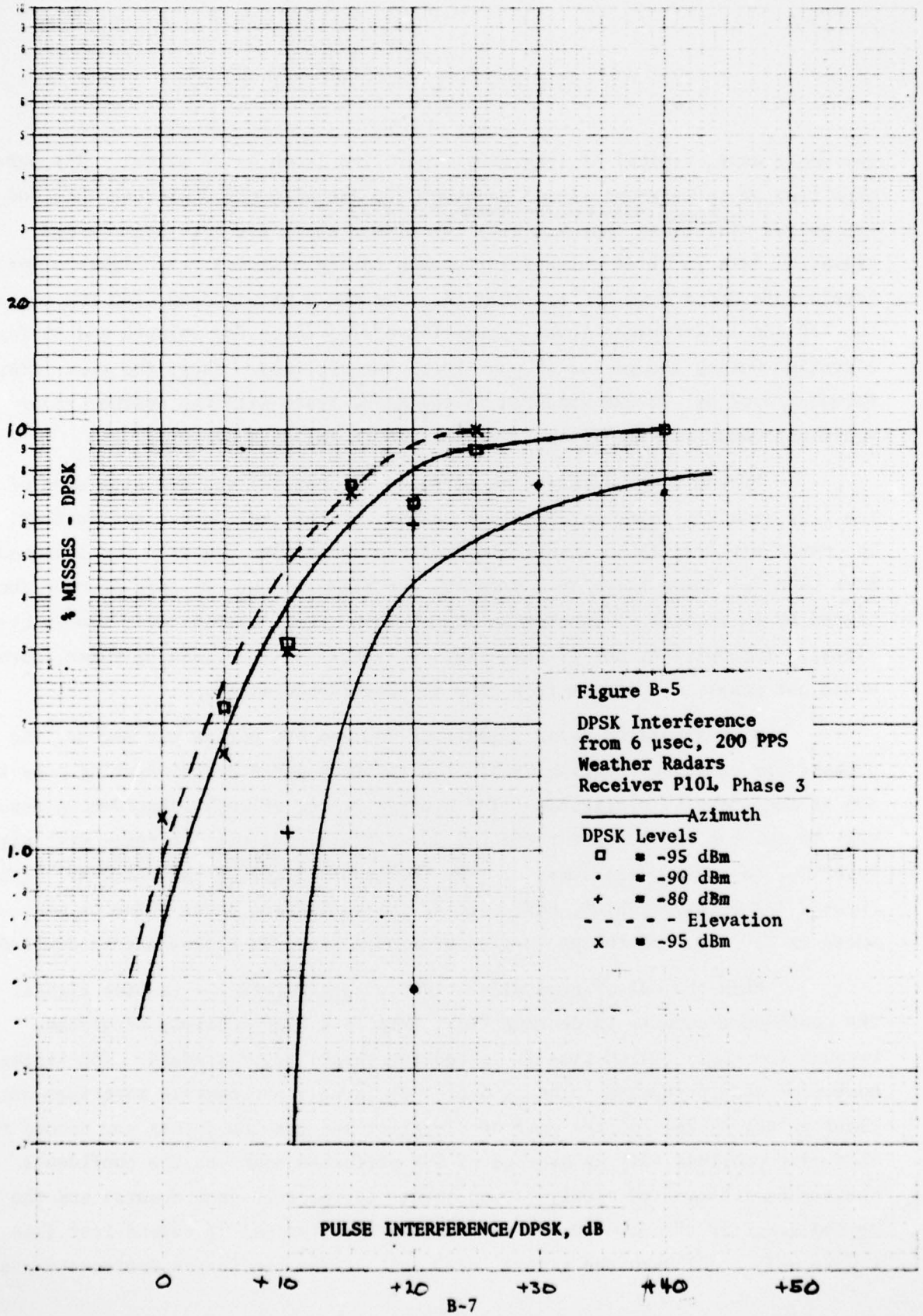

Figure B-5

DPSK Interference
from 6 μsec, 200 PPS
Weather Radars
Receiver P101, Phase 3

———— Azimuth
DPSK Levels
□ = -95 dBm
• = -90 dBm
+ = -80 dBm
- - - - - Elevation
x = -95 dBm

for angle data, typical of long range operation (such as 20 miles). The curves show that an interference level of about -70 dBm with the 2 microsecond, 400 PPS pulses will cause approximately 10% missed scans for both azimuth and elevation data (a 17 dB pulse-interference to angle ratio). At higher signal levels this drops down to less than 1%. For the 6 microsecond, 200 PPS pulses, the -70 dBm interference level causes 16% missed scans for azimuth and 9% for elevation during the period of peak level interference. Thus, the peak interference level of -70 dBm measured in the NAFEC tests with the weather radar would not cause any significant degradation in the data accuracy.

System flags occurred as noted on Figures B-1 and B-2 with some of the P101 receiver pulse interference tests. In this receiver a system flag indicates either; 1) an insufficient rate of good data (no data for 1 second or more than 50% frame flags in 2 seconds, for example), or 2) lack of confidence caused by 15 seconds of continuous out-of-beam signal that exceeds the in-beam signal. Intermittent out-of-beam signals typical of the scanning radar, normally would not generate a system flag from the confidence count.

With simulated radar signals of 200 and 400 pulses per second, the probability of pulses falling within the tracking gates and disrupting more than 50% of the scans is negligible. The average number of such coincidences should only be about 6 and 12% for these two pulse trains but will increase with signal level due to radar pulse stretching in the input filter of the receiver. (The Phase 2 1/2 receiver, E103, has tracking gates that are about twice as wide as those in P101 so that the proportion of missed scans is approximately doubled.)

When the out-of-beam radar video pulses exceed the in-beam signal, the confidence counter is decremented. This is a highly likely occurrence because the whole TO-FRO time is tested for these larger signals. The average number of such perturbed scans is over 100% (some scans contain more than one radar pulse) except for the case of elevation and the 200 pulses per second radar. This case provides only an average of 60% perturbed scans so the confidence counter is decremented slowly (40 up counts for each 60 down counts) and the 15 second range of the counter was not reached in a typical 17 second test (see Figure B-3). Although the signal level that caused confidence decrements was not

measured precisely, comparison of the system flag points indicate that a pulse to scanning-beam ratio of +20 dB for 6 μsecond pulses and +24 dB for 2 μsecond pulses is sufficient. It should be noted that for the intermittent weather-radar pulse-interference, system flags would not occur at these interference levels.

Further tests were run to measure the sensitivity of the DPSK and angle data separately. Figure B-3 illustrates the interference effect on angle only data. For azimuth and elevation data about 6% missed scans occur when the pulse interference level is about 15 dB above the angle signal or -70 dBm for the 6 microsecond, 200 PPS pulses. For the 2 microsecond, 400 PPS pulses an interference level of -70 dBm caused less than 1% missed scans.

Figures B-4 and B-5 show the percentage of missed scans as a function of pulse interference level for several DPSK signal levels. For very high interference levels the 6 microsecond, 200 PPS pulses can cause about 10% missed DPSK decodes. The 2 microsecond, 400 PPS pulses can reach about 20% missed decodes. These tests show that at low signal levels the missed DPSK decodes are the major effect of pulse interference from weather radars and missed frames due to angle interference become significant only after the interference level exceeds the angle signal by about 15 dB. It should be noted that the interference levels causing these missed decodes may vary with different decoder implementations.

B.1.2 Phase 2 1/2 Receiver Tests

The results of tests on the Phase 2 1/2 receiver for elevation data are shown in Figure B-6. These tests were run with the scanning beam signal at -80 dBm and the DPSK at -92 dBm. Pulse interference levels of -65 dBm and -70 dBm caused 10% missed scans for 2 microsecond, 400 PPS pulses and 6 microsecond, 200 PPS pulses. These interference levels are higher than shown for the Phase 3 receiver, probably due to a DPSK level of -92 dBm compared to -95 dBm.

Additional tests were run on the breadboard receiver which is similar to the Phase 2 1/2 receiver E103 except it does not have the pulse slicer, confidence counter and DPSK decoder. These results are shown in Figure B-7. The 10% interference level occurs at pulse interference levels 10 dB and 15 dB above the angle data for these two pulse trains, which shows a greater angle sensitivity to pulse interference than the Phase 3 receiver. Receiver P101 requires the 50 dB

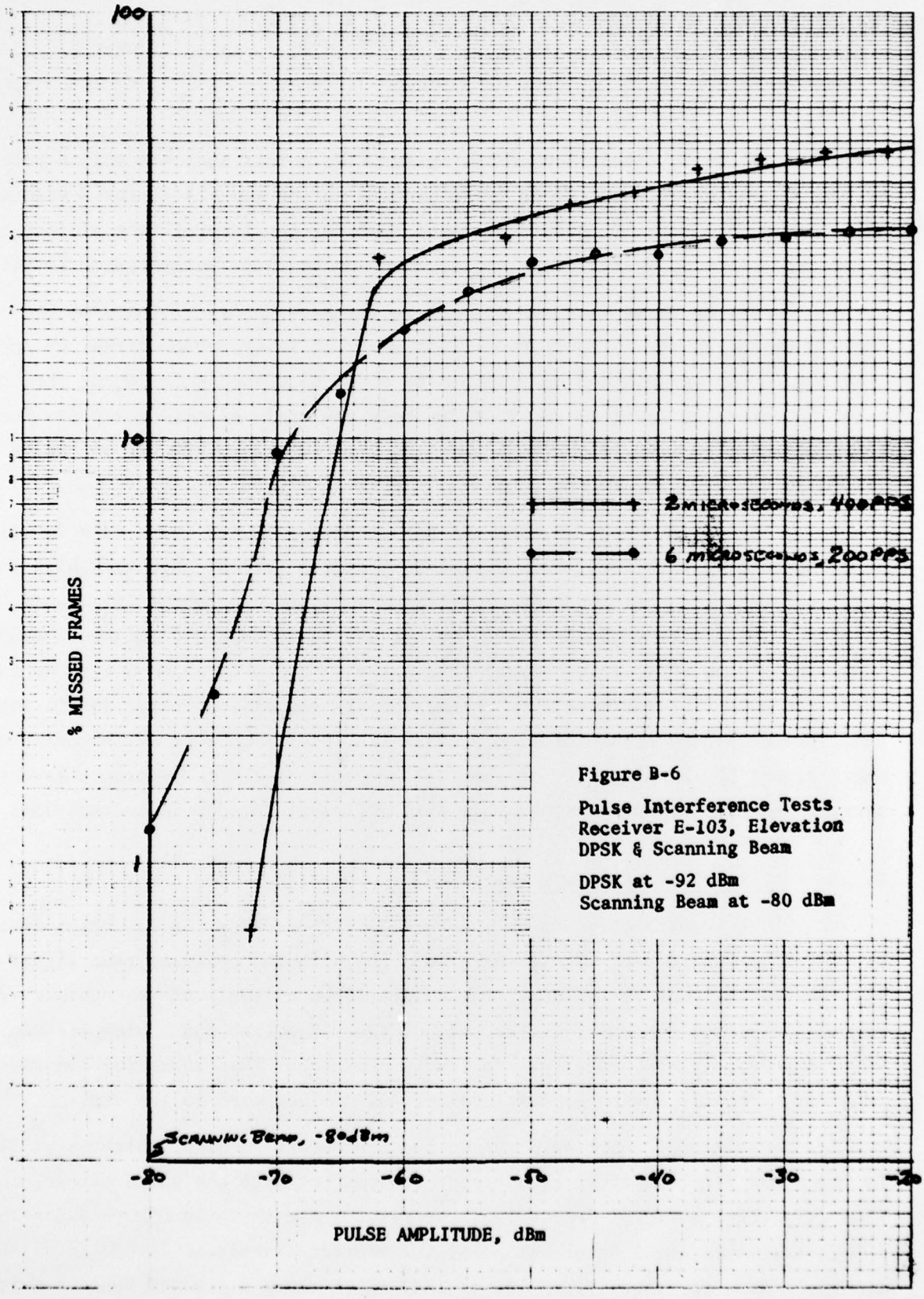

Figure B-6

Pulse Interference Tests
Receiver E-103, Elevation
DPSK & Scanning Beam

DPSK at -92 dBm
Scanning Beam at -80 dBm

and 20 dB interference levels shown in Figure B-3. The pulse slicer and narrow tracking gates probably account for this difference.

In Figure B-7 the percentage of misses for the 2 microsecond, 400 PPS pulses are very close to those for receiver E103 shown in Figure B-6. The 6 microsecond, 200 PPS pulses produce significantly fewer misses at high pulse-to-signal ratios than were found for receiver E103. It appears that many of the misses in the E103 receiver tests must have been caused by interference with the DPSK. A change of 20 dB in signal level did not affect the test results.

B.1.3 SEP Pulse Interference Tests

The interference tests on the breadboard processor were repeated on the single edge processor. Figure B-8 shows the results of these tests. In general, the same characteristic curve is produced by both receivers. Again, the results appear relatively independent of signal level.

The results for the breadboard and SEP receivers are compared in Figure B-9. Although the differences are not great, the SEP receiver seems slightly more sensitive to relatively low pulse levels. At higher pulse interference levels, the SEP saturates at a somewhat lower level of missed scans, indicating a narrower region of sensitivity.

B.1.4 Acquisition Tests, P101 Receiver

Azimuth angle acquisition tests were carried out by first supplying the receiver with a solid DPSK signal (-95 dBm). Pulse interference was then introduced and the scanning beam was turned on at a level of -85 dBm. Acquisition was achieved within one second when the interfering pulses were below a well defined threshold. Above this threshold, acquisition did not occur. The relative pulse amplitudes for this threshold are as follows:

	Relative Pulse Amplitude	
	Acquisition	No Acquisition
2 Microsecond Pulses 400 PPS	+21 dB	+22 dB
6 Microsecond Pulses 200 PPS	+12 dB	+13 dB

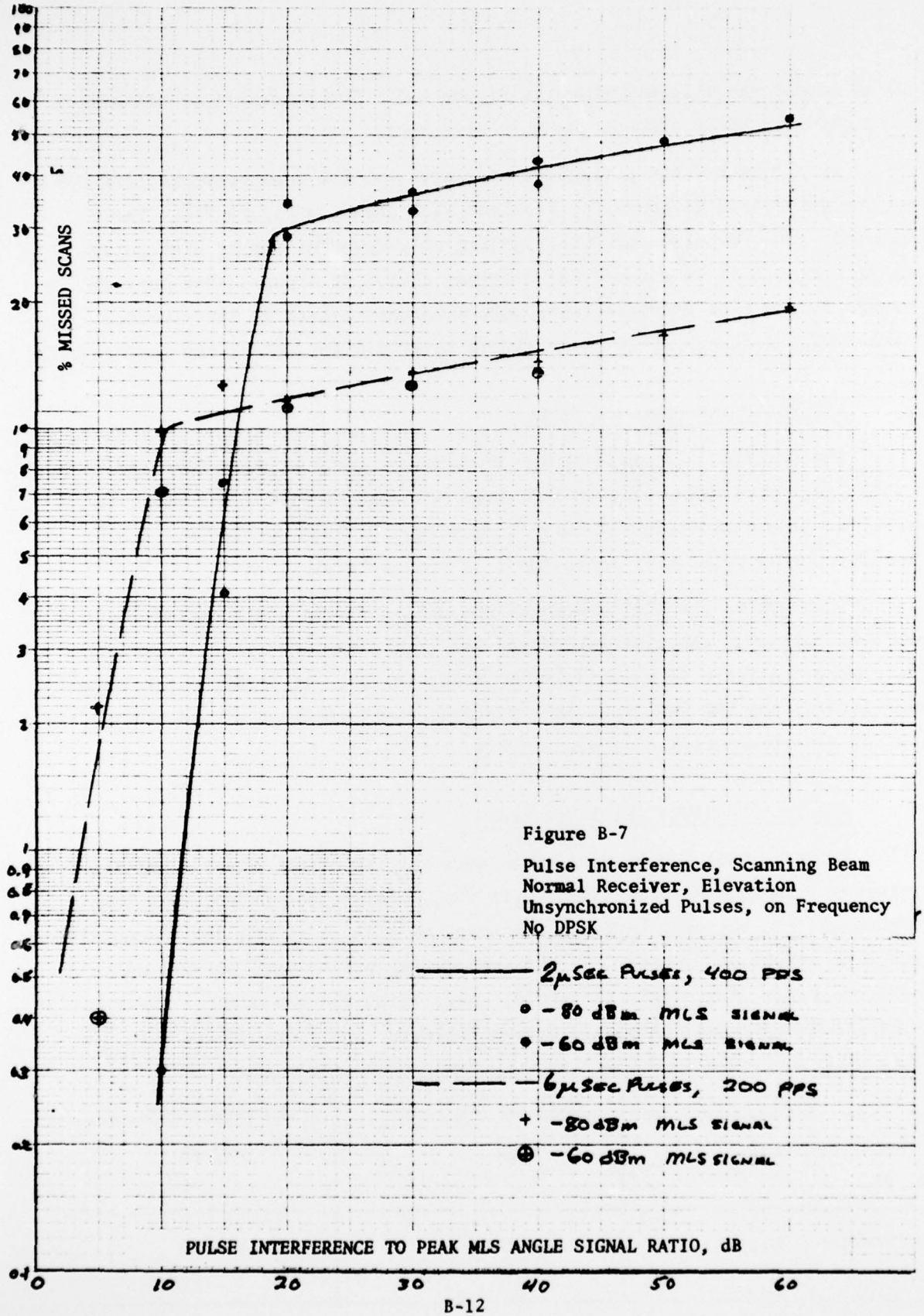

Figure B-7

Pulse Interference, Scanning Beam
Normal Receiver, Elevation
Unsynchronized Pulses, on Frequency
No DPSK

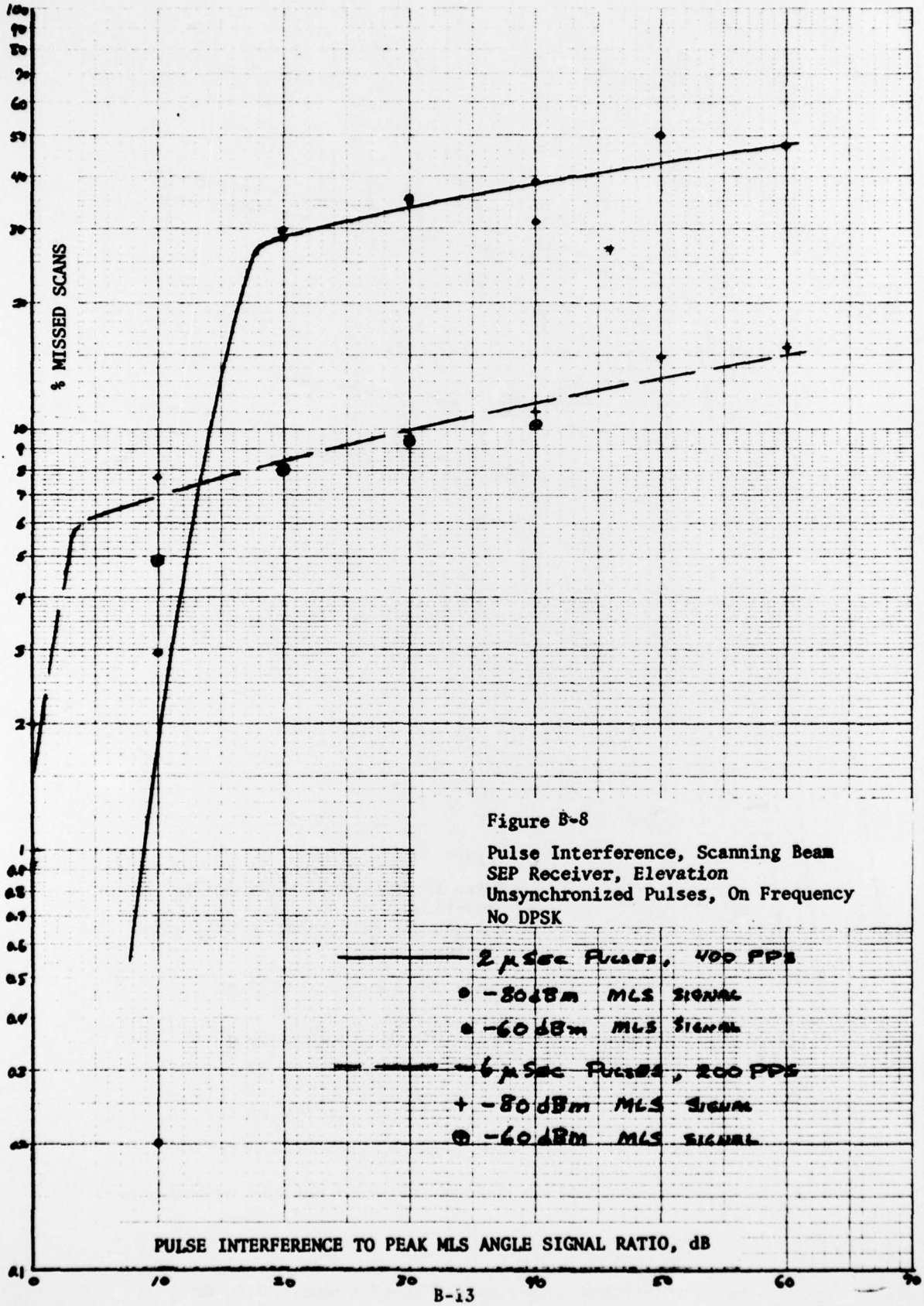

Figure B-8

Pulse Interference, Scanning Beam
SEP Receiver, Elevation
Unsynchronized Pulses, On Frequency
No DPSK

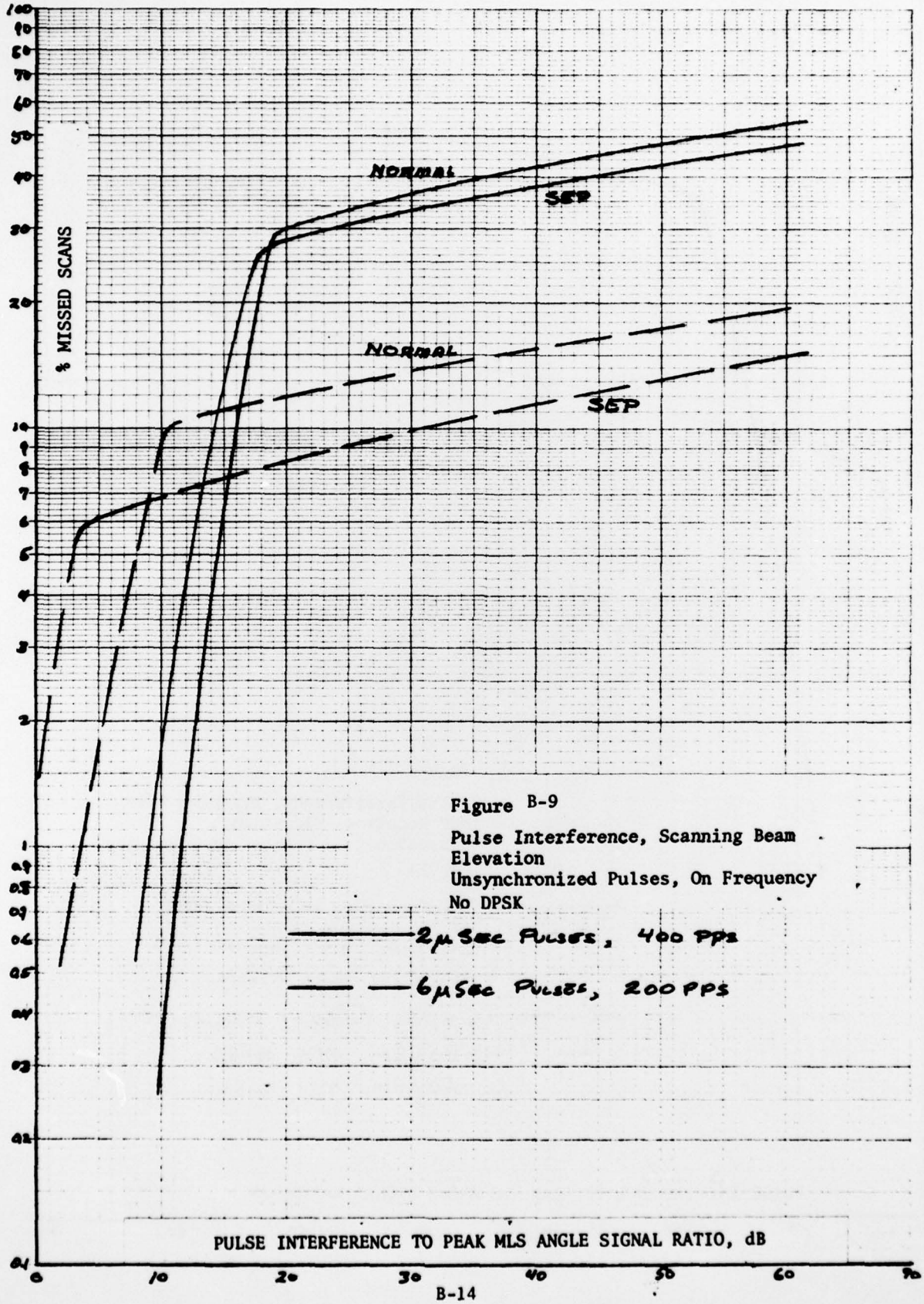

Figure B-9

Pulse Interference, Scanning Beam Elevation
Unsynchronized Pulses, On Frequency
No DPSK

In comparing these thresholds with the data in Figures B-1 and B-2 it is noted that system flags occur at higher pulse amplitudes of +25 dB and +20 dB when the signal is being tracked. Since no radar interference occurs when the radar dish is point aft (transmitter is off) for a period of over one second during each 4 second scan period the signal would always be acquired until the interference level reaches +20 dB or +25 dB. Acquisition for this receiver occurs in one second with no interference.

B.2 CW Interference Tests

Tests were run to determine the effects of continuous wave (CW) signals on the TRSB receiver. The Phase 3 receiver P101 was used in these tests. Figure B-10 shows the results of in-band CW interference on the TRSB signals. The two curves show the percent of missed scans as a result of interference with the angle and DPSK data separately. Both signals show a large number of missed scans when the CW signal level is -10 dB. It was observed in these tests that CW interference causes the DPSK signal and the scanning beam to break up.

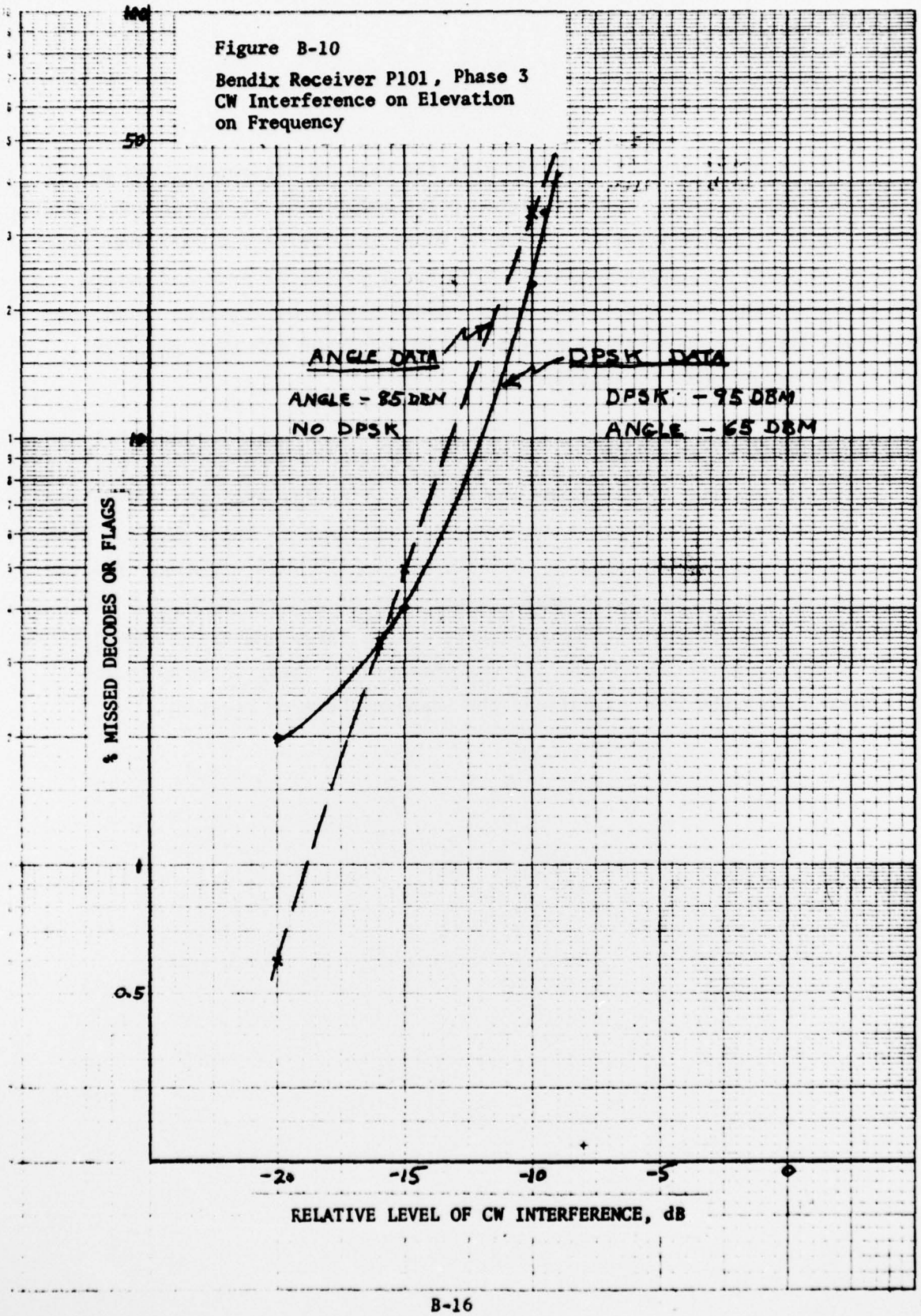
Figure B-10
Bendix Receiver P101, Phase 3
CW Interference on Elevation
on Frequency
ANGLE DATA
ANGLE - 85 DBM
NO DPSK
DPSK DATA
DPSK - 95 DBM
ANGLE - 65 DBM
% MISSED DECODES OR FLAGS
50
1
0.5
-20
-15
-10
-5
0
RELATIVE LEVEL OF CW INTERFERENCE, dB

Appendix C

REFERENCES

1. Calspan TN-1, "MLS Baseline Functional Requirements", 15 April 1974.

2. Calspan TN-2, "MLS Baseline Functional Requirements", 25 July 1974, Addendum 1, 16 August 1974.

3. Calspan TN-3, "Dynamic Multipath Performance of Airborne Processors", 6 December 1974.

4. Calspan TN-4, "Performance Characteristics of MLS Phase II Receiver-Processors", November 1975 (Revised May 1976).

5. Calspan TN-5, "Performance Tests of the Phase 2 1/2 and Phase 3 TRSB Receivers", June 1976.

6. Calspan TN-6, "Multipath Performance Tests of TRSB Receivers", September 1976.

7. Calspan TN-7, "Azimuth Multipath Tests of the Doppler System", June 1976

8. Calspan TN-8, "Weather Radar and CW Interference Tests on TRSB and Doppler Processors", October 1976.

9. Calspan TN-9, "SEP in Tilted Hangar Flare Scenario", December 1976.

10. Calspan TN-10, "AGC Performance Tests of DMLS", January 1977.

11. Calspan TN-11, "Additional Tests on Phase 3 Receivers", January 1977 (Revision 1).

12. Calspan TN-12, "SEP for TRSB Elevation", February 1977 (Revision 1).

13. "Analytical Study of MLS Operations with L-Band DME", Flight Systems Division, Bendix Corp., September 26, 1975.

14. Shnidman, D.A., Evans, J.E., "Multipath Characteristics of AWOP WG-A Multipath Scenarios", MIL Lincoln Laboratory, ATC Working Paper No. 44WP-5040, 25 June 1976.

15. "Danger of Single Edge Processing as Used in TRSB", Background Information Paper 53, London AWOP ICAO Meetings, November 1976.

16. Bleeg, R.J., Tisdale, H.F., Vircks, R.M., "Inertially Augmented Automatic Landing System", Boeing Co., Report No. FAA RD-72-22, April 1972.

17. ICAO Test Plan for U.S. Microwave Landing System", FAA Report, March 31, 1975.

18. Perper, L.J. and Hoehn, A.J., "Propeller Modulation, Final Report", 31 May 1975, Prepared for DOT, Federal Aviation Administration.

☆ U.S. GOVERNMENT PRINTING OFFICE 1977— 727-753/1124